UNIVERSITY OF CALGARY

Synthesis and Glutathione Peroxidase-Like Activity of Aromatic Derivatives and

Tellurium Analogues of Cyclic Seleninate Esters and Spirodioxyselenuranes

by

Dušan Kuzma

A THESIS

SUBMITTED TO THE FACULTY OF GRADUATE STUDIES

IN PARTIAL FULFILMENT OF THE REQUIREMENTS FOR THE

DEGREE OF MASTER OF SCIENCE

DEPARTMENT OF CHEMISTRY

CALGARY, ALBERTA

JANUARY, 2007

Canada

Abstract

This Thesis describes the synthesis of novel organoselenium and organotellurium compounds and their evaluation as mimetics of glutathione peroxidase (GPx), the selenoenzyme that protects cells from oxidative stress by reducing harmful peroxides with the thiol glutathione. Novel aromatic derivatives of the previously reported 1,2-oxaselenolane *Se*-oxide and 1,6-dioxa-5λ^4-selena-spiro[4.4]nonane (a spirodioxyselenurane) displayed significantly lower catalytic activity in the reduction of hydrogen peroxide and *tert*-butyl hydroperoxide with the sacrificial thiol benzyl thiol, compared to their parent compounds. Conversely, aliphatic tellurium analogues proved to be extraordinary GPx mimetics, providing the fastest reaction rates by far of all of the compounds investigated to date in our laboratory. Our study was expanded with the evaluation of the effect of substitution on the catalytic activity of the aromatic cyclic seleninates and spirodioxyselenuranes. In general, electron-donating groups in the *para* position relative to the selenium atom increased their GPx activity, while catalysts with electron-withdrawing groups proved to be inferior in catalytic activity when compared to the unsubstituted compounds. Additionally, a highly unusual tellurium dimer, containing an ether and a peroxy bridge was discovered along with an unstable spirodiazaselenurane and its acylaminoselenonium salts.

Acknowledgements

For my Family

Table of Contents

List of Tables

List of Figures

List of Symbols, Abbreviations and Nomenclature

Å	Ångström
Anal.	Elemental analysis
Ar	aryl
ATP	adenosine triphosphate
Bn	benzyl
br	broad
Bu	butyl
°C	degrees Celsius
c	concentration
calcd	calculated
cm^{-1}	reciprocal centimetres-wavenumbers
^{13}C NMR	carbon-13 nuclear magnetic resonance
d	doublet or days
dd	doublet of doublets
dt	doublet of triplets
δ	chemical shift in ppm
DMSO	dimethyl sulfoxide
DNA	deoxyribonucleic acid
equiv.	equivalents
Enz	enzyme
ESI	electrospray ionization
Et	ethyl
g	grams
GPx	glutathione peroxidase
H^+	acid
h	hours
^1H NMR	proton nuclear magnetic resonance
HMPA	hexamethylphosphoric triamide
HPLC	high performance liquid chromatography

Hz	Hertz
i	iso
IR	infrared
J	coupling constant
LAH	lithium aluminum hydride
lit	literature
M	molar
m	multiplet
M^+	molecular ion
Me	methyl
MOM	2-methoxymethyl
mg	milligrams
MHz	megahertz
min	minutes
mL	millilitres
μL	microlitres
mm	millimetres
mmol	millimoles
mol	moles
mp	melting point
MS	mass spectrometry
M.Sc.	Master of Science
m/z	mass to charge ratio
n-	straight chain
NADPH	nicotineamide adenine diphosphate
nm	nanometres
NMR	nuclear magnetic resonance
N.R.	no reaction
Nu	nucleophile
ox.	oxidation
p.	page

p-	*para*
Ph	phenyl
ppm	parts per million
psi	pounds/square inch
q	quartet
R	generalized alkyl group
ref.	reference
r.t.	room temperature
s	singlet
t	triplet
t-	tertiary
TBHP	*tert*-butyl hydroperoxide
THF	tetrahydrofuran
TLC	thin layer chromatography

Chapter One

Introduction

1.1 History of Organoselenium and Organotellurium Compounds

The first historical reference to the element selenium appeared in 1818, when it was discovered by two Swedish chemists J. J. Berzelius and J. G. Gahn.[1] It was named after the Greek goddess of the moon, Selene. Tellurium was first found in a gold ore from Transylvania in 1782 by Mueller von Reichenstein.[2] Initial problems with its identification resulted in the name *metallum problematicum*, which persisted for almost 15 years. Its true identity as an element was finally confirmed by von Reichenstein's student Michael Klaproth, who named it tellurium, derived from the Latin *tellus* (earth). In 1836, only a few years after the discovery of selenium, Loewig[3] prepared the first organoselenium compound, diethyl selenide. The first organotellurium compound, diethyl telluride, was reported in 1840 by Woehler.[4] Other organic Se and Te compounds were then made within a short period of time: ethaneselenol (1847),[5] diethyl telluroxide (1853),[6] dimethyl telluride and dimethyl diselenide (1857),[7] followed by many others. Organoselenium and tellurium chemistry advanced very slowly in its early stages due to the lack of appropriate modern methods and equipment for handling these compounds. These simple aliphatic organoselenium and tellurium compounds are infamous for their sensitivity to air and light, and unpleasant odours. After many years of little activity in this field, renewed interest was awakened by the discovery of the biological importance of selenium compounds. In the 1930s, it was observed that animals in South Dakota exhibited a variety of injuries to the nervous system and liver, which were attributed to the toxicity caused by selenium incorporated into the plants they were fed.[8] Other areas with high concentrations of selenium were identified elsewhere in the world and selenium was recognized as a naturally occurring toxicant. On the other hand, in 1954, traces of selenium were shown to be required by bacteria[9] and, three years later, also by mammals.[10] Furthermore, it was discovered that dietary liver necrosis in animals can be prevented by the addition of vitamin E and sulfur amino acids into the diet. This baffling observation led to the concept of a mysterious "factor 3", which was later identified as

selenium that had contaminated the sulfur amino acids.[11] In the 1960s, selenium supplementation in animal feeds in low-selenium areas decreased the occurrence of associated disease states. Since then, selenium was accepted as an essential nutrient. In 1973, an article published in *Science* by Rotruck and colleagues[12] suggested that selenium is an essential part of the enzyme glutathione peroxidase, the function of which was not entirely clear at that time. Later, other selenium-containing enzymes were found, such as glycine reductase, formate dehydrogenase, tetraiodothyronine 5`-deiodinase and plasma protein P.

Driven by the biological interest in selenium, the modern era of organic Se and Te chemistry commenced. The first extensive review on organoselenium chemistry was a text edited by Klayman and Günther,[13] which appeared in 1973. At around that time, the synthetic utility of selenium compounds began to be appreciated and eventually resulted in several reviews and books.[14]   Among the most widely used synthetic organoselenium reactions today are the selenoxide *syn* elimination, which is a convenient method for the preparation of olefins, the [2,3]sigmatropic rearrangement of allylic selenoxides, leading to allylic alcohols, electrophilic selenenylation reactions, radical cyclizations triggered by homolytic C-Se bond cleavage, and oxidations of various substrates using selenium dioxide or benzeneseleninic acid or anhydride.[14] Organotellurium compounds were considered rather exotic and the development of their synthetic utility took even longer than that of their selenium counterparts. Tellurium reagents have found use in selective oxidations, selective reductions, the removal of protecting groups, and as sources of carbon radicals.[15]

During the last few years, a tremendous effort has been directed toward the synthesis of stable organoselenium and organotellurium compounds that could be used as antioxidants, enzyme mimetics, antitumor, antimicrobial, and antihypertensive agents, as well as antivirals and cytokine inducers, and these topics will be part of the discussion in Chapter 1.2 of this Thesis. The main emphasis will be focused on the enzyme glutathione peroxidase and its important role in mammalian organisms as a natural defense against

oxidative damage caused by peroxides. Organoselenium and organotellurium compounds that minimize oxidative damage by mimicking the activity of this enzyme will be reviewed in detail, with emphasis on the mechanism of their catalytic activity and the subtle factors that affect this activity. Chapters 2 and 3 will describe our research in the area of glutathione peroxidase mimetics.

1.2. Biological Significance of Organoselenium and Organotellurium Compounds

1.2.1 Oxidative Stress and Antioxidant Defense

In the past two decades, it has become apparent that peroxides and related reduced oxygen species are critical mediators of many degenerative diseases and conditions. These short-lived intermediates have been termed reactive oxygen species (ROS) and are generated mainly in mitochondria during the normal course of oxidative phosphorylation.[16] Throughout this process, energy released by electron transfer in the respiratory chain is conserved in the form of ATP.[17] The mitochondrial respiratory chain employs a series of enzyme complexes (complex I, III, IV) embedded in the lipid bilayer of the inner mitochondrial membrane. During normal oxidative phosphorylation, O_2 is successively reduced by four electrons to form H_2O as shown on Scheme 1.1.[18]

Scheme 1.1 Four Electron Reduction of Oxygen to Water

$$O_2 \xrightarrow{1\,e^-} O_2^- \xrightarrow[2\,H^+]{1\,e^-} H_2O_2 \xrightarrow[-OH^-]{1\,e^-} HO^\bullet \xrightarrow[H^+]{1\,e^-} H_2O$$
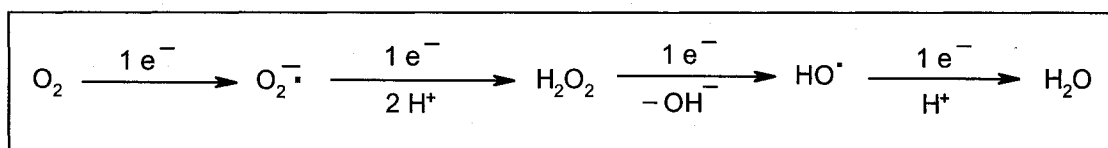
Throughout this process, electrons derived from the oxidation of metabolic substrates in the mitochondrial matrix flow through a series of redox carriers from NADH to molecular oxygen to form O_2^-, which is followed by stepwise reduction to water catalyzed by cytochrome oxidase. Leakage of these reactive oxygen species and their reaction with biomolecules is referred to as "oxidative stress" and is implicated in a

variety of serious diseases such as oncogenesis and tumor promotion,[19] inflammation, myocardial infarction, lung damage in adult respiratory distress syndrome,[20] renal damage in acute tubular necrosis, hepatic damage, ischemic and postischemic reperfusion cell damage,[21] as well as dysfunction of pancreatic β-cells, inducing type II diabetes,[22] aging and degenerative neuromuscular disorders, including Alzheimer's disease. There is also a recently discovered link between oxidative stress and the manifestation of AIDS in HIV infected patients.[23] Free radical generation is enhanced when mitochondrial respiration is stimulated by increased availability of ADP,[24] under conditions of hyperoxia and hyperbaric oxygen exposure,[25] postischemic reperfusion and mostly by decreased activity of radical-scavenging enzymes. All previously mentioned intermediates in the respiratory chain can further create ROS via several pathways. Superoxide, $O_2^{\cdot-}$, is additionally produced by the enzyme NADPH oxidase on the plasma membrane during the "respiratory burst" (a sudden increase in oxygen consumption during ingestion of microorganisms by phagocytic cells[26]) of neutrophils in order to kill invading microorganisms, by xanthine oxidase, and via nonenzymatic ways such as exposure to cigarette smoke, toxins, and transition metals.[27] Superoxide can be converted to hydrogen peroxide[28] via a disproportionation reaction catalyzed by the enzyme superoxide dismutase (SOD). Production of hydrogen peroxide is estimated to account for ca. 2% of oxygen consumed by mitochondria under normal conditions.[29] Additionally, it is formed during the oxidative deamination of catecholamines (e.g. dopamine) with monoamine oxygenase enzyme (MAO) and is involved in the progress of neurodegenerative disorders such as Parkinson's disease.[30] Hydroxyl radical HO$^{\cdot}$, one of the most reactive free radicals formed in biological systems, is generated by transition metals which induce homolytic decomposition of hydrogen peroxide (the Fenton reaction, equation 1) or from superoxide and hydrogen peroxide via the iron-catalyzed Haber-Weiss reaction (equation 2).[31]

Fenton reaction $\qquad H_2O_2 + Fe^{2+} \longrightarrow HO^- + HO^{\cdot} + Fe^{3+}$ $\qquad$ (1)

Haber-Weiss reaction $\quad O_2^{\cdot-} + H_2O_2 \longrightarrow HO^- + HO^{\cdot} + O_2$ $\qquad$ (2)
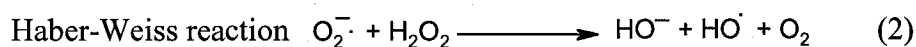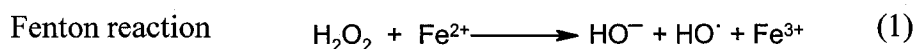
Even though hydroxyl radical reacts with all known biomolecules at diffusion-limited rates (ca. 10^8-10^{10} M^{-1} s^{-1}), it does not significantly contribute to oxidative stress. It is very short-lived and the estimated diffusion distance is only 3 nm, which is about the average diameter of a typical protein.[32]

In addition to reactive oxygen species, strong oxidants such as hypochlorous acid (HOCl), peroxynitrite (ONOO⁻) and singlet oxygen ($^1O_2$) contribute to oxidative stress.[33] Hypochlorous acid is generated from H_2O_2 by myeloperoxidase (MPO) in neutrophils, while peroxynitrite is formed from superoxide ($O_2^{·-}$) and nitric oxide (·NO). Formation of these biological oxidants is depicted in Scheme 1.2.

Scheme 1.2 Formation of Reactive Oxygen and Reactive Nitrogen Species[34]
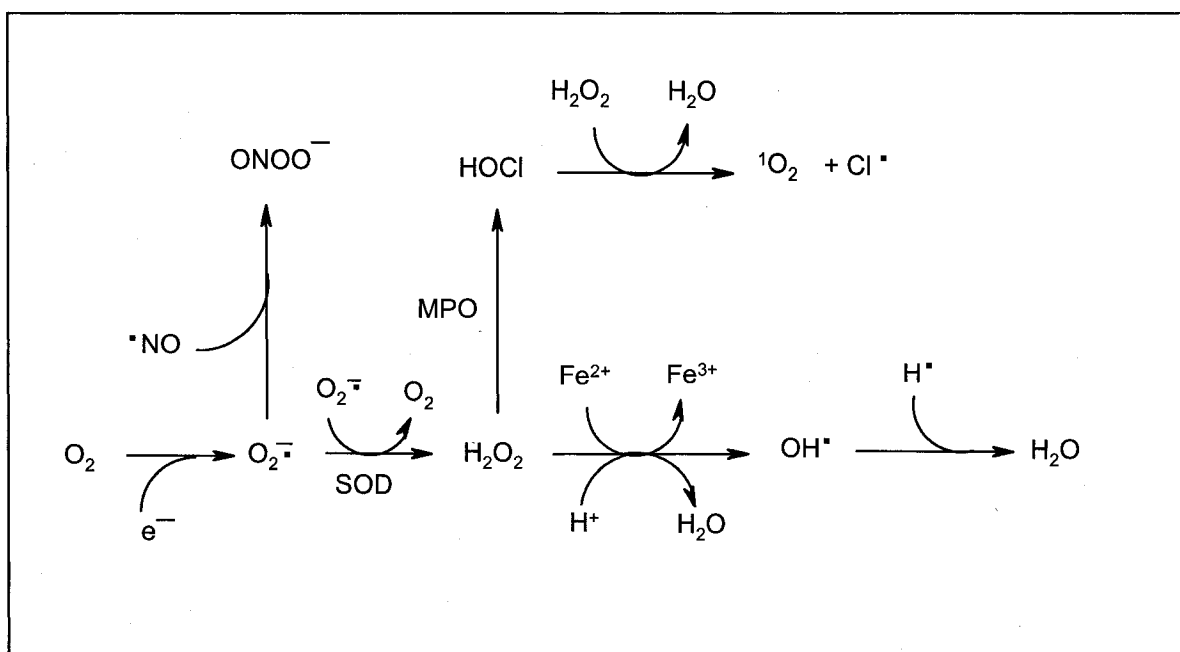
The major targets of both reactive oxygen (ROS) and reactive nitrogen species (RNS) are lipids (mainly polyunsaturated lipids) in the mitochondrial membrane, resulting in its increased permeability, as well as proteins and DNA. Modification of individual amino acids in binding sites may lead to the loss of function of proteins. ROS can react with

DNA either at the sugar-phosphate backbone or at a base.[27] In particular, mammalian mitochondrial DNA (mtDNA) is very susceptible to attack by ROS.[35] Even though it is not very abundant, it possesses high information density and mutates much faster than nuclear DNA. Damage to mtDNA leads to damage to the polypeptides encoded by mtDNA in the respiratory complexes with consequent impairment of mitochondrial energy generation and increased production of ROS. This premise was formulated in 1972 by Denham Harman as part of the mitochondrial theory of aging.[36]

Mammalian cells have developed complicated defense mechanisms against biological oxidants, as presented in Scheme 1.3.[37,38,39] The "first row" scavenging mechanisms present in the cell are endogenous enzymes such as the previously mentioned superoxide dismutase (SOD), glutathione peroxidase (GPx), and catalases. In addition to the endogenous enzymes, vitamins C and E, polyphenolic antioxidants, and transport proteins (e.g. ferritin, transferrin, lactoferrin), which bind redox-active metals (iron, copper) responsible for catalyzing formation of ROS, help destroy the latter or suppress their formation.

Scheme 1.3 Protection Against the Reactive Oxygen Species[34]
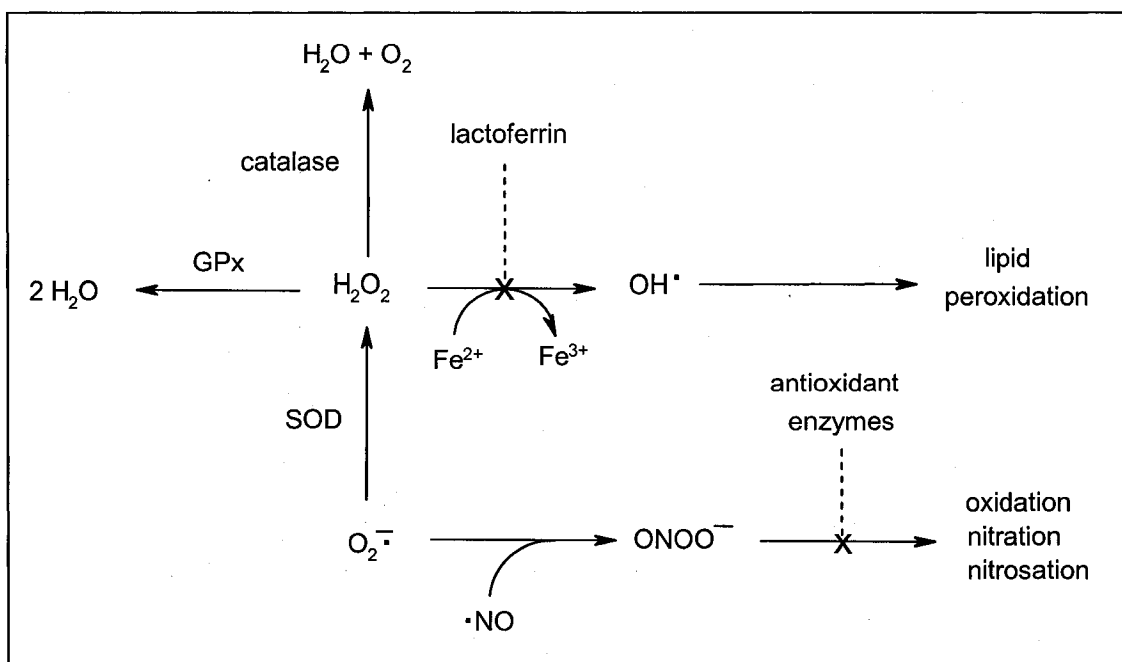
Superoxide dismutase (SOD) comprises a family of enzymes with different protein structures and different metal cofactors. The predominant one is copper zinc SOD located in the cytosol of almost all cells.[40] It catalyzes dismutation of superoxide to H_2O_2[41] via the reaction in equations 3 and 4.

$$Cu^{2+} + O_2^{-} \longrightarrow Cu^{+} + O_2 \qquad (3)$$

$$Cu^{+} + O_2^{-} + 2\,H^{+} \longrightarrow Cu^{2+} + H_2O_2 \qquad (4)$$
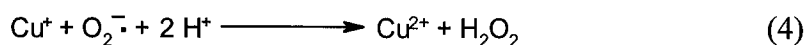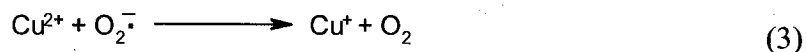
Hydrogen peroxide is then further reduced to H_2O by glutathione peroxidase (GPx)[42] or to O_2 and H_2O by catalase. Catalases have a heme-iron active site[43] and are primarily located in peroxisomes, which are a major site of intracellular H_2O_2 production.

1.2.2 Glutathione Peroxidase - Its Structure and Catalytic Mechanism

Glutathione peroxidase plays an important role in the defense mechanism of mammals, birds and fish against oxidative stress. It catalyzes the reduction of a variety of hydroperoxides (ROOH) and H_2O_2 using as a stoichiometric reductant glutathione (GSH) (1), a tripeptide thiol that is ubiquitous in the cells of higher organisms.[44] Hitherto, there have been identified four isoenzymes of glutathione peroxidase in mammals.[45] Their levels vary and are dependent on the type of tissue.[46] In Table 1.1 are summarized types of glutathione peroxidase, their location and reducing activity.

glutathione

1
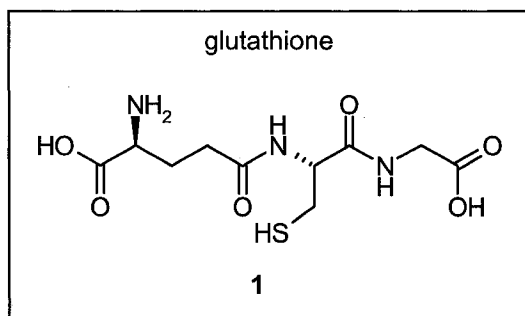
Table 1.1 Types of Glutathione Peroxidase and Their Activities

isoenzyme	abbreviation	reducing substrate	activity	location
Classical GPx	cGPx	GSH	hydrogen peroxide	cytosol
Phospholipid hydroperoxide GPx	PHGPx	GSH	phospholipid hydroperoxides, fatty acid hydroperoxides, cholesterol hydroperoxides, hydrogen peroxide	membrane
Plasma GPx	pGPx	thioredoxin, glutaredoxin	hydrogen peroxide	plasma
Gastrointestinal GPx	giGPx	GSH	hydrogen peroxide	liver, gastrointestinal tract

Classical GPx (cGPx) is the most active type of glutathione peroxidase and is located in the cytosol. Phospholipid hydroperoxide GPx (PHGPx) is a membrane-bound enzyme and exists as a monomer. It reduces phospholipid and cholesterol hydroperoxides in biological membranes.[47] Plasma GPx (pGPx) is approximately 10 times less active than the cytosolic GPx. Because the concentration of GSH in human plasma is very low, thioredoxin or glutaredoxin serve as reducing substrates for this enzyme. Gastrointestinal GPx (giGPx) functions as a barrier against the absorption of dietary hydroperoxides.

A crystal structure of the human plasma GPx was obtained by Ladenstein and his coworkers at 2.9 Å resolution,[48] providing a closer look into the structure and function of this enzyme. Human plasma GPx is a tetramer in both crystalline form and solution. It has a flat shape and dimensions of 77 Å x 75 Å x 43 Å. The centre of the enzyme is vacant with size of 12 to 15 Å. The active sites contain selenocysteine (2) residues[49] in a tetradic arrangement and are located on two opposite surfaces of the tetramer (Figure

1.1). GSH and inhibitor binding studies on the bovine cellular enzyme performed by Epp and his colleagues[50] showed that only two glutathione molecules bind to each tetramer, which suggests a half-site reactivity of this enzyme.

Figure1.1 Structure of Human Plasma Glutathione Peroxidase
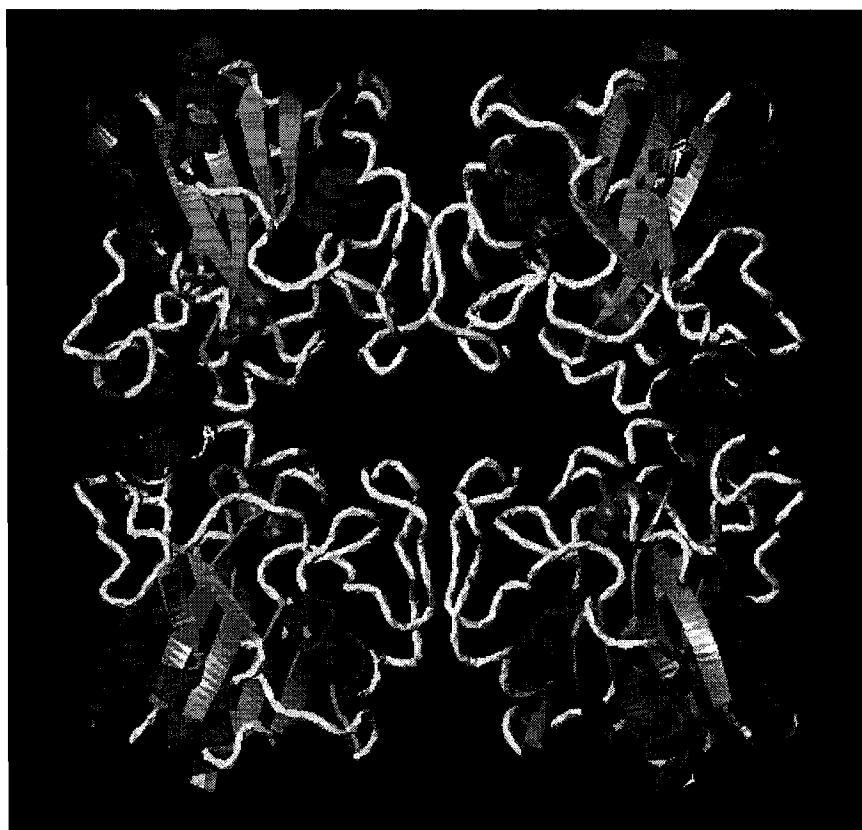
The selenocysteine moieties **2** in the active sites of the enzyme are in the form of selenols (EnzSeH), in which the selenium atom acts as a strong nucleophile[51] under normal physiological conditions. Additionally, low redox potential of selenocysteine allows for favourable conversion of EnzSeH to EnzSeOH in the GPx catalytic cycle. Flohe et al.,[52] after detailed kinetic studies, proposed a mechanism by which the selenoprotein reduces hydroperoxides in the presence of the thiol glutathione. It is depicted in Scheme 1.4.

selenocysteine

$HSe\diagdown\diagup^{NH_2}_{}COOH$

2
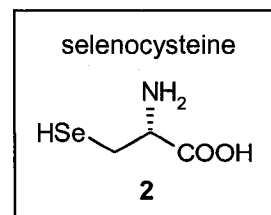
Scheme 1.4 Catalytic Mechanism of Glutathione Peroxidase

EnzSeH = glutathione peroxidase
GSH = glutathione
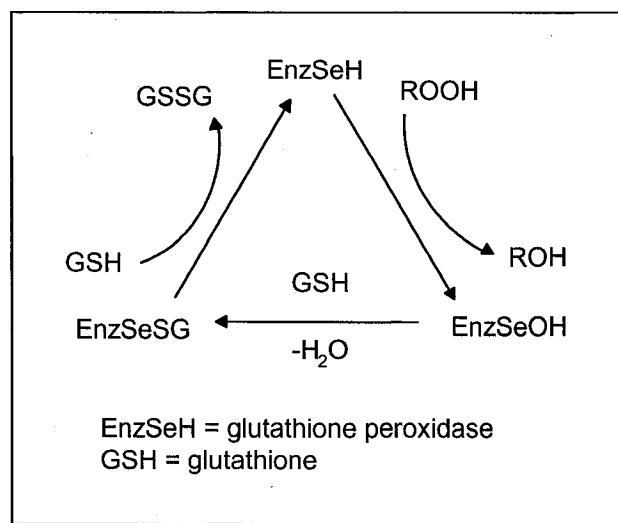
In this catalytic cycle, the selenol (EnzSeH) form of the enzyme reacts with organic peroxides to generate the corresponding selenenic acid (EnzSeOH), which further reacts with the reduced form of glutathione (GSH), resulting in the corresponding selenenyl sulfide (EnzSeSG) and water. Subsequently, a second molecule of glutathione attacks the sulfur atom in the selenenyl sulfide intermediate, yielding glutathione disulfide and regenerating the selenol to complete the catalytic cycle. In the overall process, two equivalents of the thiol are oxidized to the disulfide and water, while the hydroperoxide is reduced to the corresponding alcohol. At high concentrations of the organic peroxides, the corresponding seleninic acid (EnzSe(=O)OH) was proposed to be formed, even though it is believed to play a negligible role in the catalytic cycle under physiological conditions.

Several studies indicated that the amino acid residues tryptophan and glutamine play important roles in the stabilization and activation of the selenol moiety towards oxidation via hydrogen bonding and salt bridges (Figure 1.2)

Figure 1.2 Interaction of the Selenol Group with Amino Acid Residues in GPx[48, 53]
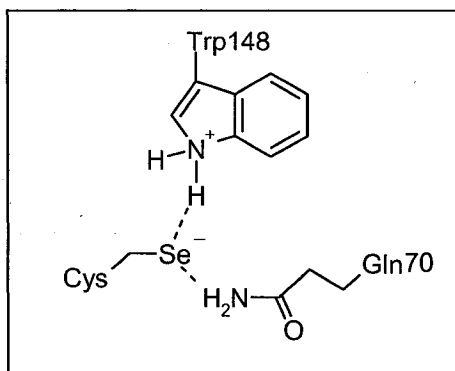
In the second step of the catalytic cycle, there are two important aspects influencing the catalytic activity of GPx; the relative stability of EnzSeOH against further oxidation and its fast reaction with glutathione. Binding interactions of the selenenic acid of GPx with GSH and stabilization of the EnzSeOH.GSH complex by additional hydrogen bonds and salt bridges from proximate amino acids help the sulfur atom of GSH form the selenenyl sulfide with ease (Figure 1.3).

Figure 1.3 Several Key Binding Interactions of the Selenenic Acid of GPx with GSH[53, 54]
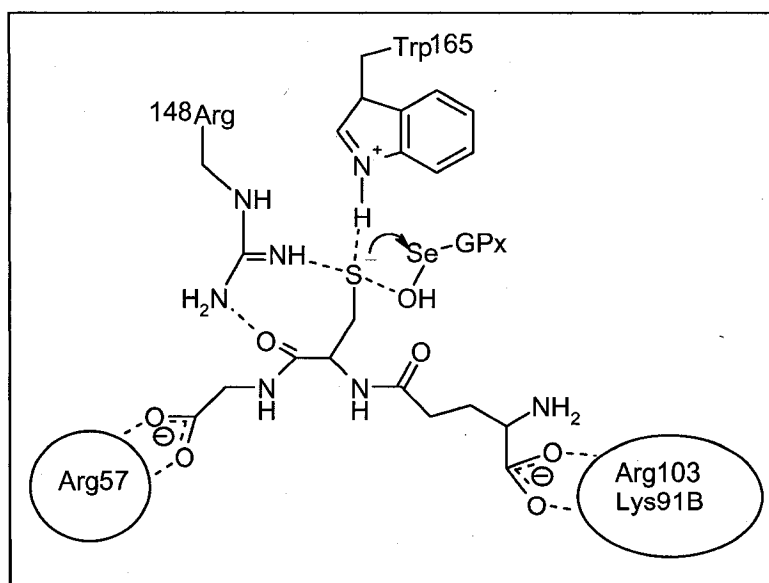
The last step in the catalytic mechanism is the reaction of the selenenyl sulfide with a second molecule of glutathione, which is guided by binding interactions with amino acid residues as well. The most important is the coordination of the amido nitrogen atom of a threonine residue to the sulfur atom, which polarizes the selenium-sulfur bond in the EnzSeSG (Figure 1.4)

Figure 1.4 Binding Interactions in the Selenenyl Sulfide Form of GPx[54, 53]
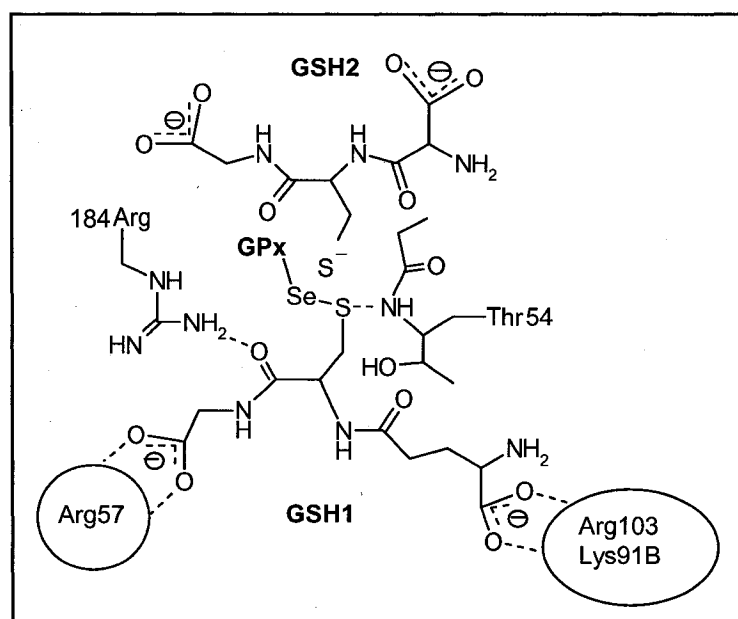
1.2.3 Organoselenium Compounds as GPx Mimetics

Glutathione peroxidase (GPx) mimetics are an important class of small molecule selenium-containing antioxidants that catalyze the reduction of biologically harmful peroxides in the presence of stoichiometric amounts of glutathione (GSH) or other thiols.[11,49] They are of special interest as anti-inflammatory and neuroprotective agents. One such compound, ebselen (PZ 51) (3), is currently in Phase III clinical trials as a neuroprotective agent (Daiichi Pharmaceutical Co., Japan). Ebselen, through its glutathione peroxidase-like action, significantly reduces damage done by oxidants accumulated during post-acute ischemic stroke, when administered within 48 hours.

Even though aliphatic organoselenium compounds are toxic, ebselen does not display significant toxicity at pharmacologically active concentrations. The reason is that it is an aromatic selenium compound which is not readily metabolized to more toxic inorganic species. In addition, it does not oxidize GSH in the presence of oxygen, which would lead to uncontrolled production of superoxide and other free radical species (so called glutathione oxidase activity, which will be discussed in Chapter 1.2.7 in detail).[55] It has been found that in vivo, **3** becomes bound to proteins in the form of its selenenyl sulfide **4**[56,57] and is metabolized predominantly into relatively non-toxic glucuronidated metabolites.[58,59,60]

ebselen

3

ebselen derived
selenenyl sulfide

4
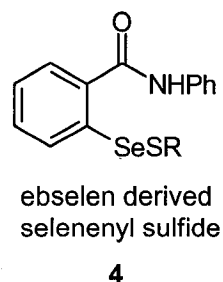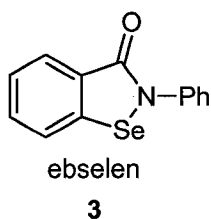
Several catalytic mechanisms for the reduction of peroxides with ebselen were reported depending on the concentration of peroxide and thiol. As shown on Scheme 1.5, the catalytic mechanism proposed by Fischer and Dereu[61] indicates that in the presence of high peroxide concentration ebselen (**3**) itself is the key catalytic species. It is readily oxidized to the corresponding seleninamide **5**, which undergoes rapid reaction with a thiol such as glutathione to form the thioseleninate intermediate **6**. This is followed by reaction of the latter with a second equivalent of thiol to generate selenenic acid **7** and one mole of the corresponding disulfide. The catalytic cycle is completed by dehydration of **7** and regeneration of the active catalyst **3**.

Scheme 1.5 Catalytic Cycle of Ebselen at High Peroxide Concentration[61]
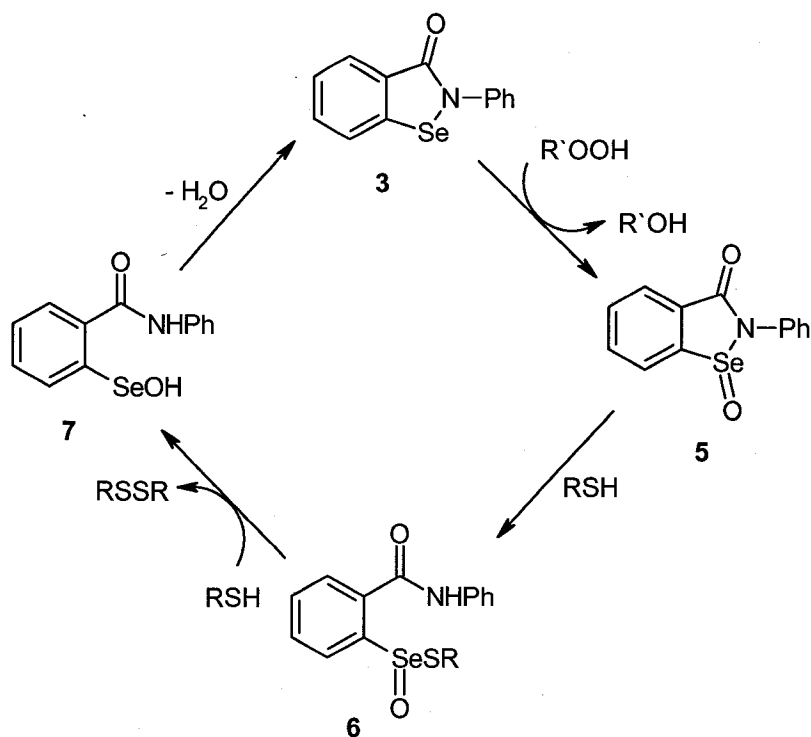
On the other hand, when ebselen exerts its catalytic activity under conditions of excess thiol, it reacts first with the thiol to form the corresponding selenenyl sulfide **4**, which undergoes a very slow disproportionation reaction to produce the diselenide **8** and the disulfide. Oxidation of diselenide **8** with peroxide regenerates ebselen **3** via a selenenic anhydride **9** (Scheme 1.6).

Scheme 1.6 Catalytic Cycle of Ebselen at High Thiol Concentration
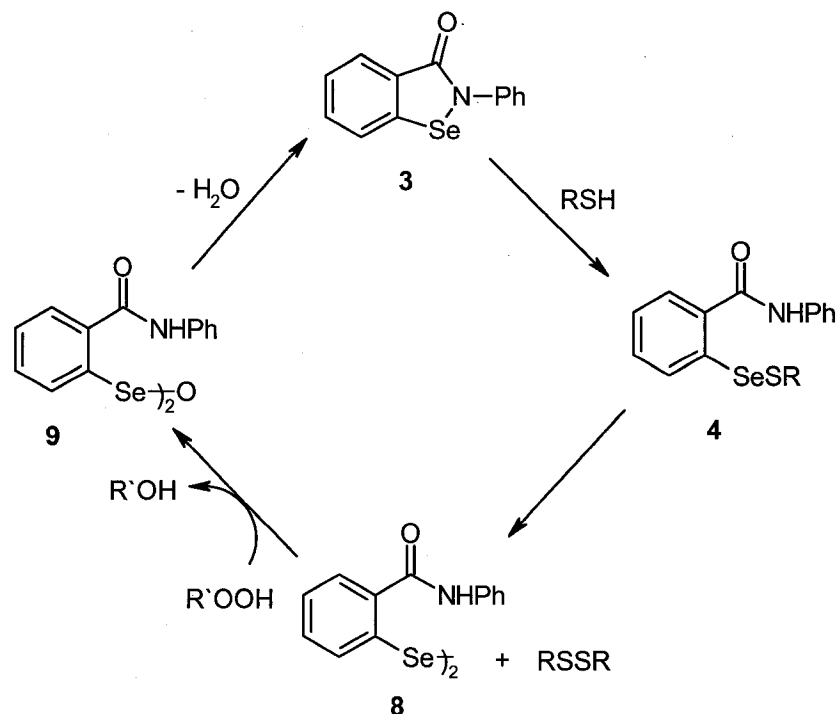
Engman[62] and Haenen[63] independently proposed alternative catalytic cycles for ebselen, which vary from the one mentioned in Scheme 1.6 with respect to the intermediates playing key roles in the mechanism. Engman suggested that the selenenyl sulfide intermediate **4** does not disproportionate but rather undergoes a slow oxidation with peroxide to thioseleninate **6** followed by a rapid reaction with the thiol to yield selenenic acid **7** accompanied by disulfide formation. (Scheme 1.7, Cycle A). The catalytic cycle is completed by the reaction of the selenenic acid **7** with the thiol to afford the key intermediate selenenyl sulfide **4**.

Scheme 1.7 Alternative Catalytic Cycles of Ebselen[62,63]
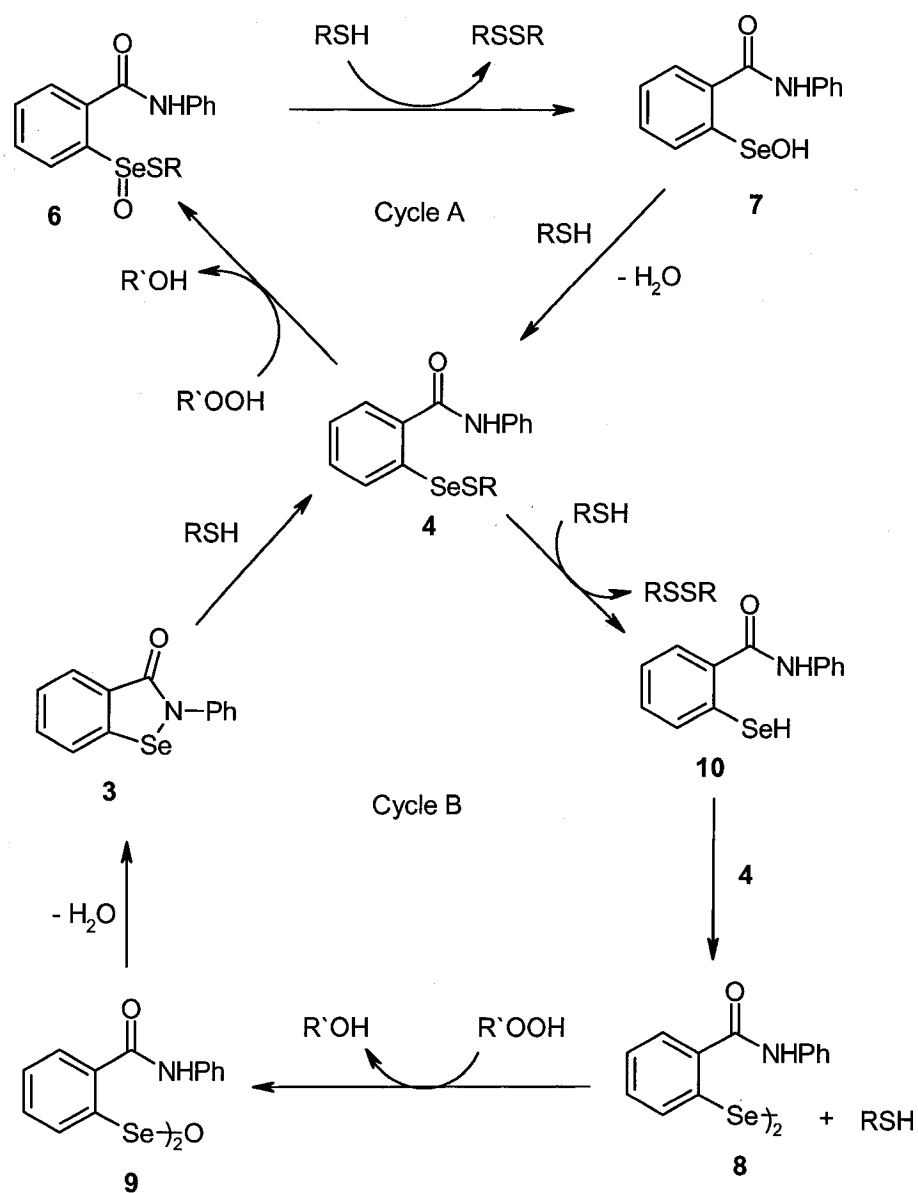
Haenan and coworkers suggested instead that the selenenyl sulfide reacts directly with the thiol to form selenol **10** and the disulfide. The selenol then reacts with the selenenyl sulfide **4** to generate diselenide **8** which, after oxidation, yields ebselen (**3**) through selenenic anhydride **9** (Scheme 1.7, Cycle B).

Ebselen has been known since 1924, when it was synthesized by Lesser and Weiss[64] from anthranilic acid **11** according to Scheme 1.8.

Scheme 1.8 Synthesis of Ebselen[64]
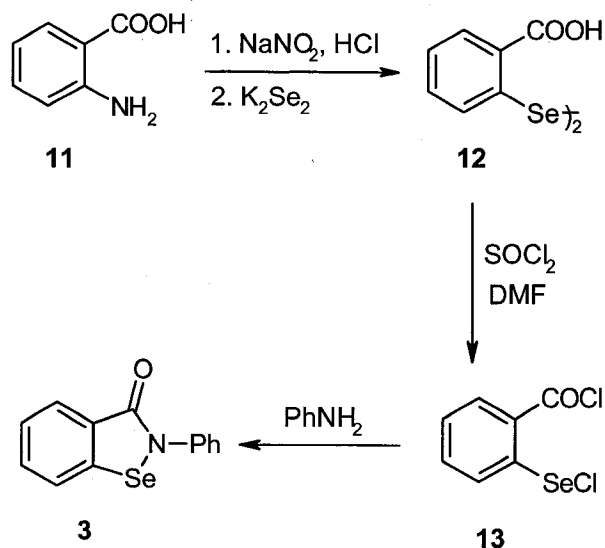
Ebselen (**3**) which was needed in large amounts for further pharmacological studies was prepared in one pot using a procedure reported by Engman.[65] Starting from the commercially available benzanilide (**14**) and elemental selenium, **3** was synthesized in 68% yield via *ortho*-lithiation of **14** with LDA and *n*-BuLi, followed by insertion of Se and CuBr$_2$-mediated cyclization of the lithiated product **15** (Scheme 1.9). A similar approach has been employed to prepare labelled ebselen enriched with ^{77}Se.[66]
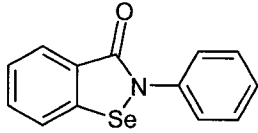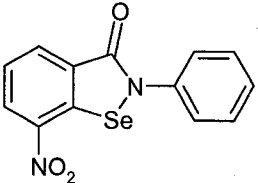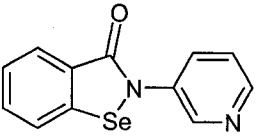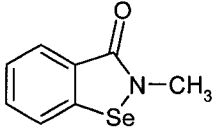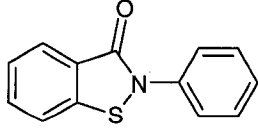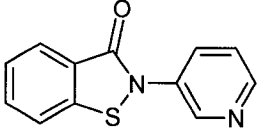
Scheme 1.9 Engman's Synthesis of Ebselen[65]
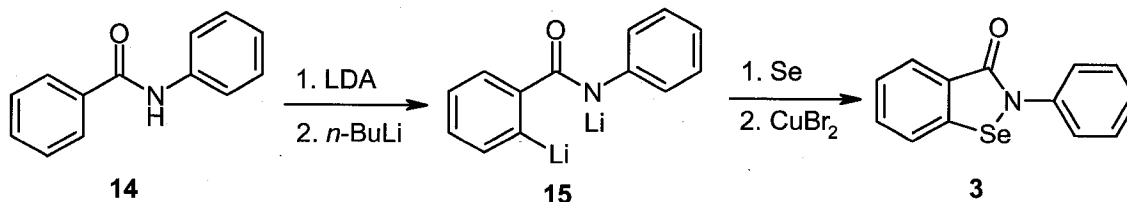
Recently, Fong and Schiesser[67] reported a free radical synthesis of ebselen via intramolecular homolytic substitution with amidyl radicals.

Due to the low toxicity of ebselen, a host of other GPx mimetics were designed by modifying its core structure. Substitution of the hydrogen atom *ortho* to selenium with a nitro group resulted in significantly increased catalytic activity compared to ebselen,[68] while maintaining its relatively low toxicity. Replacement of the phenyl group on the nitrogen with a pyridyl group slightly increased catalytic activity without increasing acute toxicity. The corresponding *N*-methyl derivative appears to be 30 times more toxic than ebselen. Sulfur analogues of ebselen do not display any GPx-like activity. (Table 1.2)

Table 1.2 GPx-like Activity and Toxicity of Some Ebselen Derivatives[68]

	Compound	GPx activity[a] at 30 μmol/L	LD$_{50}$ mouse (mg/kg, p.o.)
	Ebselen RP 60931	100	>6810
	RP 63600	928	4128
	RP 61605	148	>4640
	NAT 02-677	122	260
	RP 62373	0	3220
	RP 63165	0	556

[a] All compounds related to ebselen at 100%

Reich and Jasperse[69] investigated the catalytic activity of selenenamide **16**, which served as a model system for the hypothesis that the enzyme's selenocysteine residue in its oxidized form may have a similar cyclic selenenamide structure. It was proved that compound **16** pursues a similar catalytic pathway as the one reported for the GPx enzyme. Moreover, observations of these authors suggested that the presence of a basic amino group might enhance the catalytic activity of GPx mimetics by facilitating the formation of thiolate anion, which is more reactive towards electrophilic selenium than the original thiol. This prompted an investigation of catalysts containing basic amino groups.
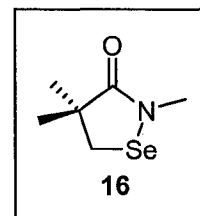
Chaudière and colleagues[70] prepared GPx mimetics in which the carbonyl group of ebselen was replaced by a quartenary tetrahedral carbon atom (Figure 1.5). The *N*-ethyl derivative **18** is about three times less active than the parent compound **17** and compounds **19** and **20** are almost inactive. Nitro derivatives **21** and **22** exhibit slightly lower catalytic activity than the unsubstituted selenazoline **17**. In 1994, Chaudière extended his selenazoline series by homologation of **17** to form the six-membered ring of **23**.[71] The activity of the selenazine **23** was more than three times higher than that of parent compound **17**. Presently, compound **23** (ALT-2074) is being evaluated by the HaptoGuard Co. (U.S.A) and is in Phase II clinical trials as an orally-active compound with potent glutathione peroxidase activity, for acute cardiovascular indications. Substitution of the hydrogen atom *para* to the selenium atom by an electron-donating *p*-methoxy group (**24**) did not improve the catalytic activity of this compound.

Figure 1.5 Examples of Selenazoline and Selenazine Derivatives Exhibiting GPx-like Activity

17 R=H
18 R=Et
19 R=CH₃CO

20

21

22

23

24
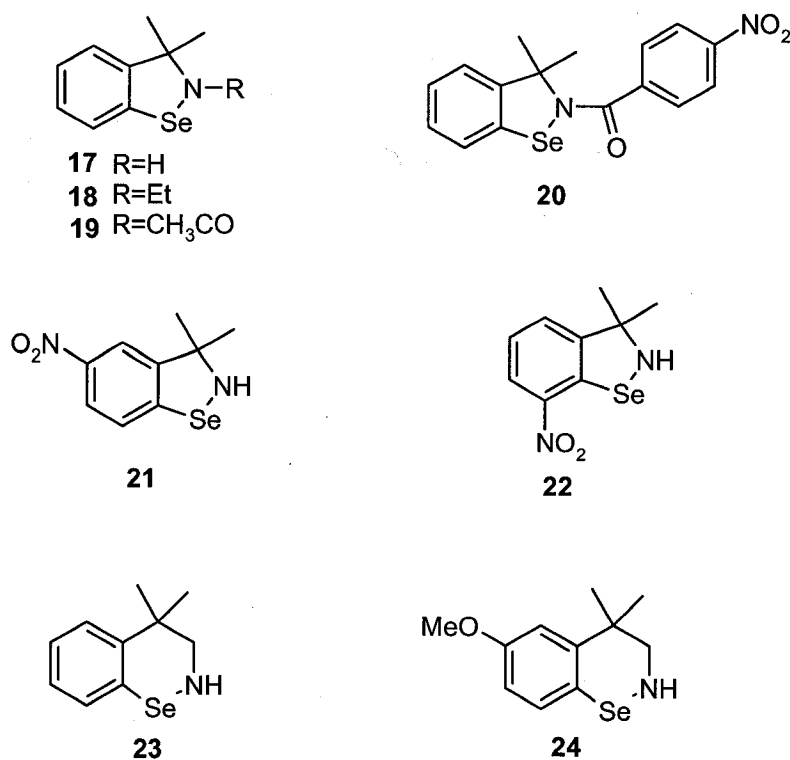
Back and Dyck[72] prepared a camphor-derived cyclic selenenamide **25**, which displays activity ca. 2.5 times higher than that of ebselen. It was established that selenenyl sulfide **26**, formed after a rapid reaction of **25** with benzyl thiol acts as the true catalyst, providing entry to the same catalytic mechanism as that for GPx (Figure 1.6). Benzyl thiol was used as a surrogate for glutathione in these experiments.

Figure 1.6 Camphor-derived Cyclic Selenenamide Exhibiting GPx Activity

25

26
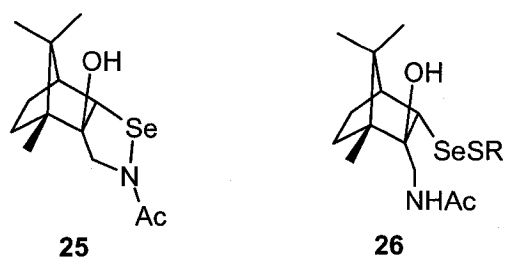
Aromatic diselenides have also attracted attention, even though the Se-Se bond is nonpolar and therefore entry into the catalytic mechanism via the reaction of the diselenide with a thiol is retarded. This reaction usually proceeds only in the presence of a significant excess of dithiols (more than 10 fold).[73] According to Singh and Whitesides,[74] monothiols do not reduce diselenides at all. However, catalytic action can be initiated by prior oxidation of diselenides. Thus, a series of aromatic diselenides **27-37** containing substituents at various locations have been prepared to date (Figure 1.7).

Figure 1.7 Diselenides with GPx-like Activity
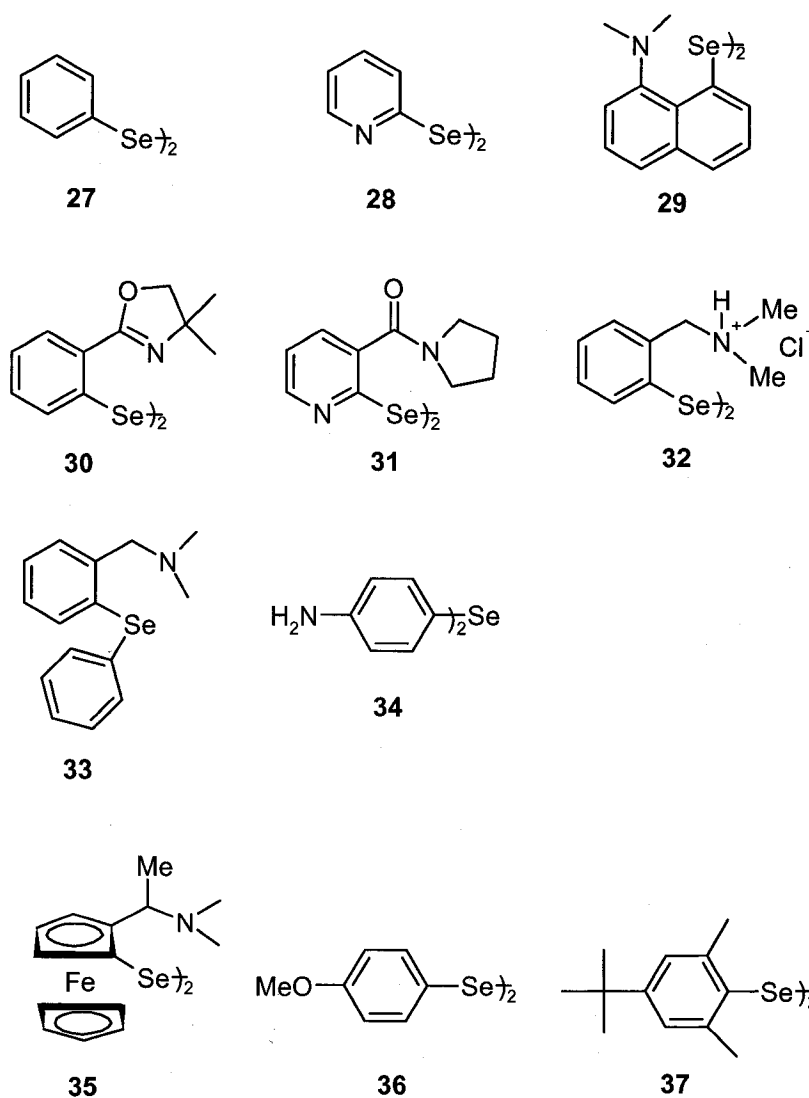
Surprisingly, Wilson's group[75] demonstrated that simple diphenyl diselenide **27** has greater catalytic activity than ebselen. Additionally, compound **32**, which possesses a side chain with a tertiary amino group capable of coordinating, in the form of its free base, with the selenium atom, exhibited 10 times higher catalytic activity when compared to ebselen. Interestingly, selenides **33** and **34** didn't exhibit any catalytic activity. Moreover, compounds **29** and **30**, also displaying strong Se...N interactions, did not show any significant catalytic activity.[76] Furthermore, the electron-withdrawing nature of the pyridine ring in compounds **28** and **31** lowers the nucleophilic character of the selenium atom, resulting in inactive compounds. Mugesh, Singh and their coworkers[76,77] reported that diferrocenyl diselenide (**35**) is a very active catalyst, displaying ca. 900 fold enhancement in catalytic activity when compared to diphenyl diselenide **27**. This activity is attributed to the synergistic effect of the redox-active ferrocenyl moiety and an internally chelating amino group. Other diferrocenyl diselenides without the amino group display catalytic activity only ca. 6 times higher than that of diphenyl diselenide **27** under the same conditions. Diselenide **36**,[78] with the electron-donating methoxy group in *para* position, shows high catalytic activity. Conversely, the hindered diselenide **37** does not exhibit any noticeable activity.[76]

As the results from the nitrogen-containing GPx mimetics indicated, close proximity of this heteroatom to the selenium atom can significantly influence their catalytic activity. In an attempt to gain further insight into the effect of an amino group on the antioxidant activity of GPx mimetics, Tomoda and Iwaoka[79] investigated diselenide **38** in a GPx-like model assay.
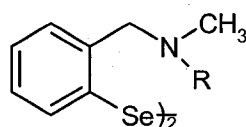
38

R = cyclohexyl

According to their observations, initiation of the catalytic activity is represented by the reaction of the diselenide **38** with benzenethiol to form the corresponding selenol **39** and selenenyl sulfide **41**, both of which play an active role in the catalytic cycle (Scheme 1.10). Furthermore, ^{1}H NMR experiments provided evidence that supports the formation of a nitrogen-stabilized zwitterionic form of the corresponding selenol **39**, which is activated toward subsequent oxidation. Oxidation of the selenol **39** results in a highly reactive intermediate, selenenic acid **40**, which undergoes a rapid bimolecular displacement at the selenium atom with benzenethiol to form the selenenyl sulfide **41**.

Scheme 1.10 Role of the Nitrogen Stabilized Zwitterionic Form of a Selenol
in the GPx-like Activity

R = cyclohexyl
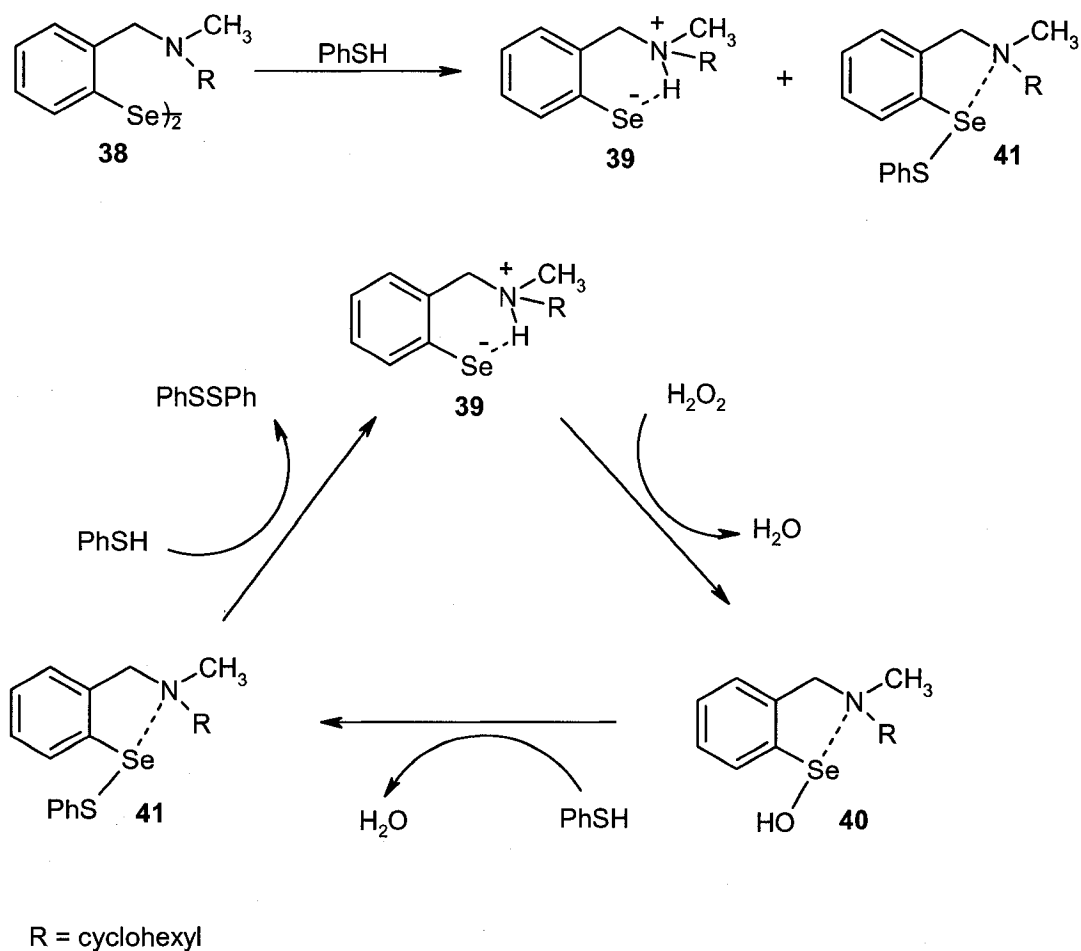
The subsequent re-formation of **39** from the selenenyl sulfide **41** via a facile bimolecular displacement by the thiol occurs preferentially at the sulfur atom due to the hypervalent Se...N interaction. Further studies of the intramolecular selenium-nitrogen nonbonded interactions on a series of 2-selenobenzylamines **42** using ^{1}H, ^{77}Se and ^{15}N NMR spectroscopy, and *ab initio* MO calculations by the same authors,[80] indicated that there is electron delocalization from the nitrogen lone pair (n_N) to the low-lying antibonding orbital of the Se-X bond (σ^*_{Se-X}) and the strength of this interaction was evaluated to be on the order of 7.7 to 18.8 kcal/mol. (Figure 1.8)

Figure 1.8 Intramolecular Selenium-Nitrogen Nonbonded Interaction

42
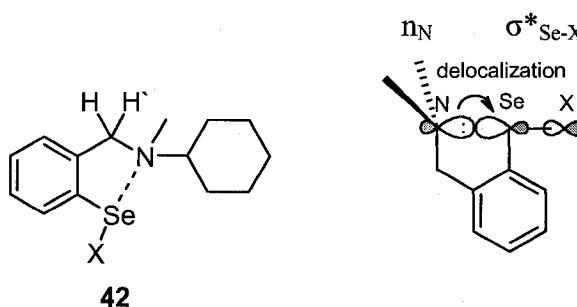
X=Br, Cl, OAc, CN, SPh, SeAr, Me

This electron delocalization causes thermodynamic stabilization of the X-Se...N system as well as weakening of the Se-X bond, which may result in improved GPx activity of such systems. Further studies[81] indicated that the strength of the interactions decreases in the order Se...N>Se...O>Se...F as the electron-donating ability of the second-row atom decreases. Nevertheless, the possibility of an oxygen atom having an intramolecular interaction with the selenium atom has become a topic for investigation by our group and that of Wirth et. al.,[82] who prepared diselenides shown in Figure 1.9.

Figure 1.9 GPx Mimetics possessing Se...O Interactions

43   **44**
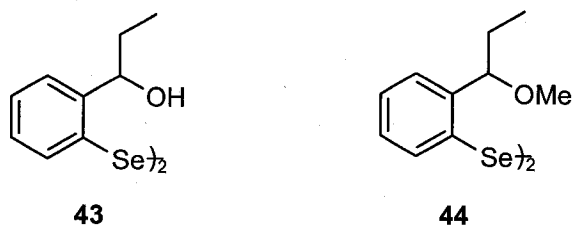
Compounds **43** and **44**[78] were prepared by *ortho*-lithiation of the corresponding substituted benzyl alcohol or ether, and insertion of selenium into the lithiated intermediate, followed by acidification and oxidation of the resulting selenol to the corresponding diselenide (Scheme 1.11).[82] Their GPx activity was investigated, showing that diselenide **44** containing a methoxy group, exhibits 50% of the activity of diselenide **43** with a free hydroxyl group.

Scheme 1.11 Synthesis of Aromatic Diselenides via *Ortho*-directed Lithiation.
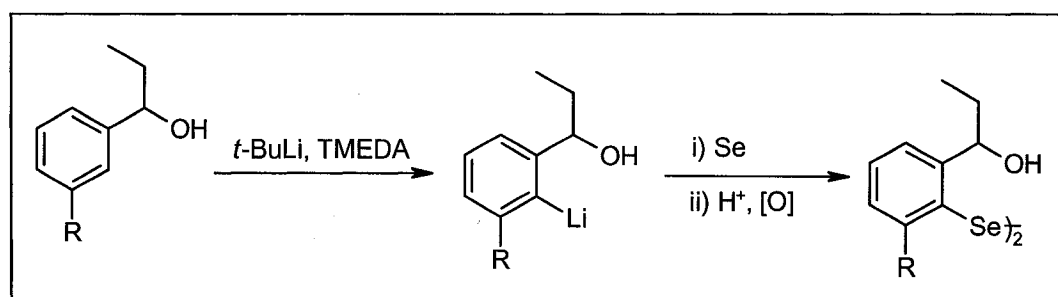
Our group was interested in studying the effect of a proximate oxygen atom on the catalytic activity of various types of organoselenium compounds, and therefore a series of alkyl diselenides[83] was prepared and their catalytic activity studied.
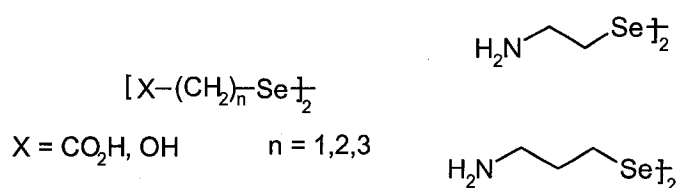
All of them proved to be poor catalysts for the reduction of peroxides in the presence of thiols. Amino diselenides were prepared for comparison and these displayed considerably higher catalytic activity than their oxygen-containing counterparts.

In 2002, our group reported that allyl 3-hydroxypropyl selenide (**45**) undergoes a series of very rapid steps upon oxidation with *t*-butyl hydroperoxide (TBHP), resulting in the generation of the novel cyclic seleninate ester **46**.[83,84] The product **46** can be isolated quantitatively by treating **45** with excess *t*-butyl hydroperoxide.

Figure 1.10 Novel Aliphatic GPx Mimetics

45   **46**
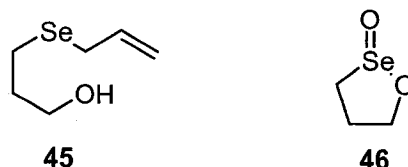
This reaction is depicted in Scheme 1.12 and goes through a cascade of oxidation steps to form allyl selenoxide **47**, followed by its [2,3]sigmatropic rearrangement to intermediate **48**, a second oxidation to **49** and finally cyclization to **46**. Allyl 3-hydroxypropyl selenide **45** exhibits 10 times higher catalytic activity than ebselen (**3**), when tested in an assay with 90% *tert*-butyl hydroperoxide as the oxidant and benzyl thiol as the corresponding reducing agent, in the presence of 10 mol% of catalyst. The rationale for this choice of assay in our laboratory will be explained in Section 2.2.

Scheme 1.12 Cascade Mechanism of the Cyclic Seleninate Ester **46** Synthesis[84]
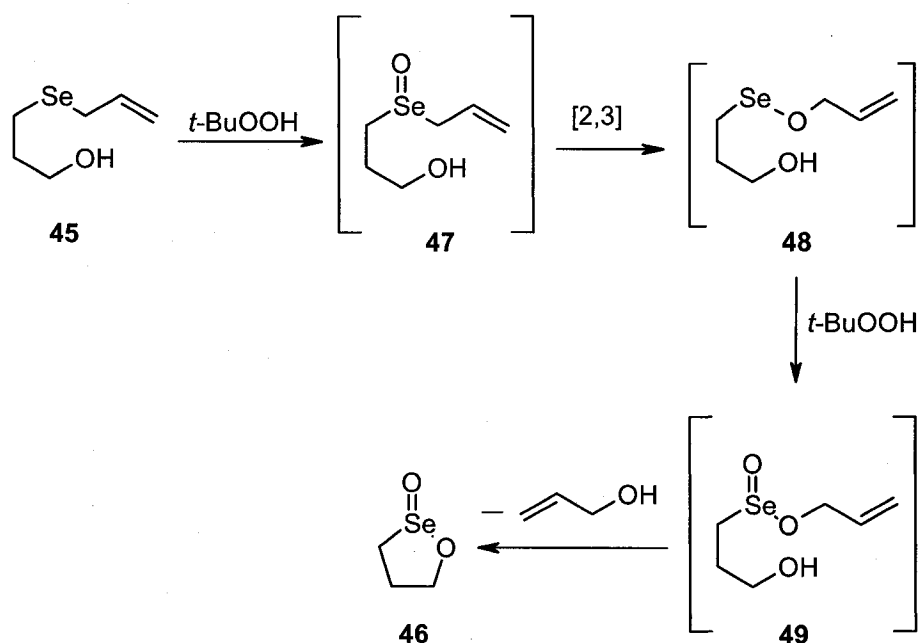
Interestingly, the cyclic seleninate ester **46** displays even higher catalytic activity, with a half-life for the oxidation of benzyl thiol ($t_{1/2}$, time required for 50% conversion of benzyl thiol to benzyl disulfide) equal to 2.5 h in comparison to allyl selenide **45** with $t_{1/2}$ of 4.8 h, ebselen (**3**) with $t_{1/2}$ equal to 42 h and a control experiment with no selenium-containing catalyst with $t_{1/2}$ >300 hours, respectively. The catalytic mechanism of the cyclic seleninate ester proved to be significantly different from that of GPx and is depicted in Scheme 1.13. Based on mechanistic studies, cyclic seleninate ester **46** reacts with benzyl thiol to produce thioseleninate **50**, which after further thiolysis affords the selenenic acid **51** and dibenzyl disulfide. Oxidation and cyclization of **51** consequently regenerates the cyclic seleninate ester **46**. In the absence of peroxide, selenenic acid **51** reacts with a third equivalent of benzyl thiol, forming selenenyl sulfide **52**.

Scheme 1.13 Catalytic Mechanism of the Cyclic Seleninate Ester **46**[84]
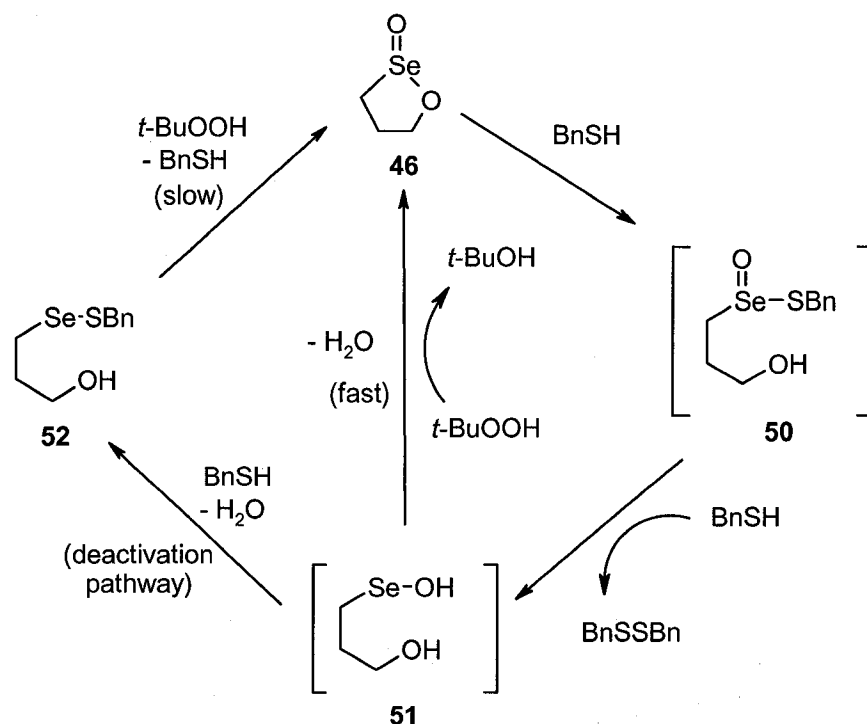
It will be recalled that similar selenenyl sulfides play an essential role in the catalytic mechanism of GPx and many GPx mimetics such as ebselen. However, in this case,

formation of the selenenyl sulfide **52** proved to be a deactivation pathway of the catalytic cycle. It was independently prepared and tested for GPx-like behaviour, exhibiting considerably lower catalytic activity ($t_{1/2}$ = 35 h) than **46**. Homologues of **46** with bigger or smaller ring sizes were synthesized as well, displaying lower catalytic activity, which suggested that the optimum ring size is that of **46**.

Additionally, the novel spirodioxyselenuranes **53** and **54**[85] were discovered to display exceptional potency towards peroxide reduction in the presence of thiols. They exhibit $t_{1/2}$ of 2.5 h and 5.1 h, respectively, under the conditions of the same assay as previously described by our group.

Figure 1.11 Novel Spirodioxyselenuranes with GPx-like Activity

53   **54**
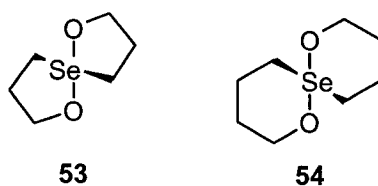
The proposed catalytic mechanism again differs from that reported for GPx and is illustrated in Scheme 1.14. Spirodioxyselenurane **53** enters the catalytic cycle by substitution of one alkoxy group with a benzylthio group to form intermediate **55**, which undergoes reductive elimination with a second equivalent of benzyl thiol to generate selenide **56** and benzyl disulfide. Subsequently, **56** is oxidized by *t*-butyl hydroperoxide to the transient selenoxide **57**, which after cyclization regenerates the spirodioxyselenurane **53**. At high concentrations of thiol, this catalyst exists in form of selenide **56** and under high peroxide concentration conditions, in the form of spirodioxyselenurane **53**.

Scheme 1.14 Mechanism for Catalysis by the Spirodioxyselenurane 53[85]
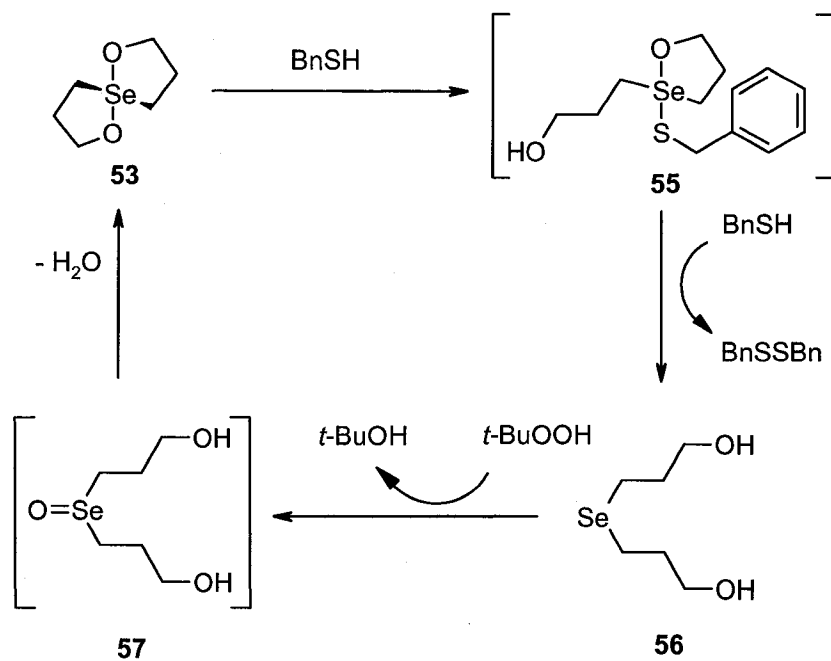
Cotgreave and colleagues[86] studied the catalytic activity of the α-(phenylseleno)ketones 58-60, which exhibit their catalytic activity by cleavage of the Se-C bond after reacting with GSH. The selenolate anion PhSe⁻ then serves as the active catalytic species. The catalytic activity is decreased after instalment of the electron-donating methoxy group in compound 58, while the electron-withdrawing nitro substituent increases its catalytic activity.

Figure 1.12 α-(Phenylseleno)ketones as GPx Mimetics[87]

R = H, OCH₃, NO₂
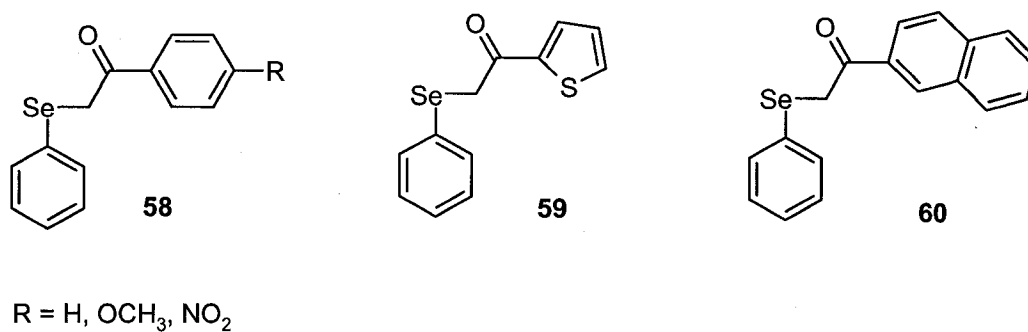
Another approach to the GPx mimetics can be found in the selenium analogues **61** and **62** of the antitumor alkaloid ellipticine, which show catalytic activity in the reduction of peroxides as well.[88] Aromatization in **62** caused a decrease in the activity of this compound relative to **61** (Figure 1.13).

Figure 1.13 Carbazole-based GPx Mimetics

61 **62**
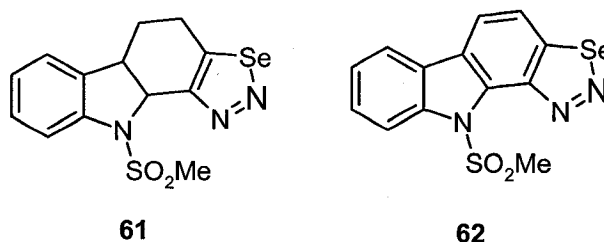
1.2.4 Tellurium Compounds as GPx mimetics

Even though the toxicity and other biological properties of tellurium compounds have been much less studied than those of analogous selenium derivatives, a few organotellurium compounds have been investigated as potential GPx mimetics. The tellurium atom is even more readily oxidized from the divalent to the tetravalent state than is selenium. This property makes organotellurium compounds potential scavengers of reactive oxygen species. Diaryl tellurides **63-67**, portrayed in Figure 1.14, were extensively studied by Andersson[89] and showed up to 900% higher catalytic activity than ebselen. A catalytic mechanism for the reduction of peroxides in the presence of thiols and tellurides, depicted on Scheme 1.15, was suggested by Detty and Gibson[90] and later proposed by Engman.[91] According to this mechanism, the tellurium atom undergoes rapid cycling between oxidation states II and IV.

Scheme 1.15 Catalytic Mechanism of Aromatic Tellurides
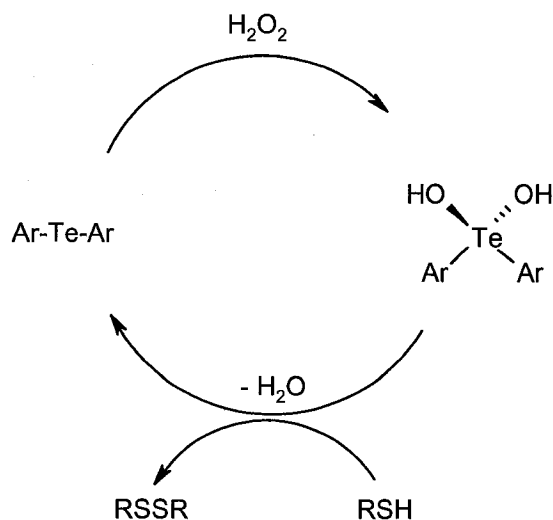
Engman and collaborators[91] studied the influence of substitution in the catalyst upon the rate of the reaction of hydrogen peroxide with thiols. Their work indicated that introduction of conjugatively electron-donating substituents (OH, NH_2, NMe_2, NHPh) reduces the time required to reduce the thiol concentrations in their studies by 50% ($t_{1/2}$) in comparison to the unsubstituted compound. In contrast, the electron-withdrawing group CF_3 had the reverse effect. Additionally, 2,2'-disubstituted organotellurides **64** were less active catalysts compared to 4,4'-disubstituted organotellurides **63** due to increased steric hindrance around the tellurium atom, which prevents it from interacting with the peroxide. Compound **65** showed very low catalytic activity because of the same reason. On the other hand, compounds **66** and **67**, containing phenolic substituents, proved to be more potent antioxidants. Compound **67** was shown to protect against *tert*-butyl hydroperoxide-induced cell death in lung fibroblast cultures and to protect rat kidney tissue against oxidative damage by anoxia or reoxygenation.[92]

Figure 1.14 Aromatic Tellurides as GPx Mimetics
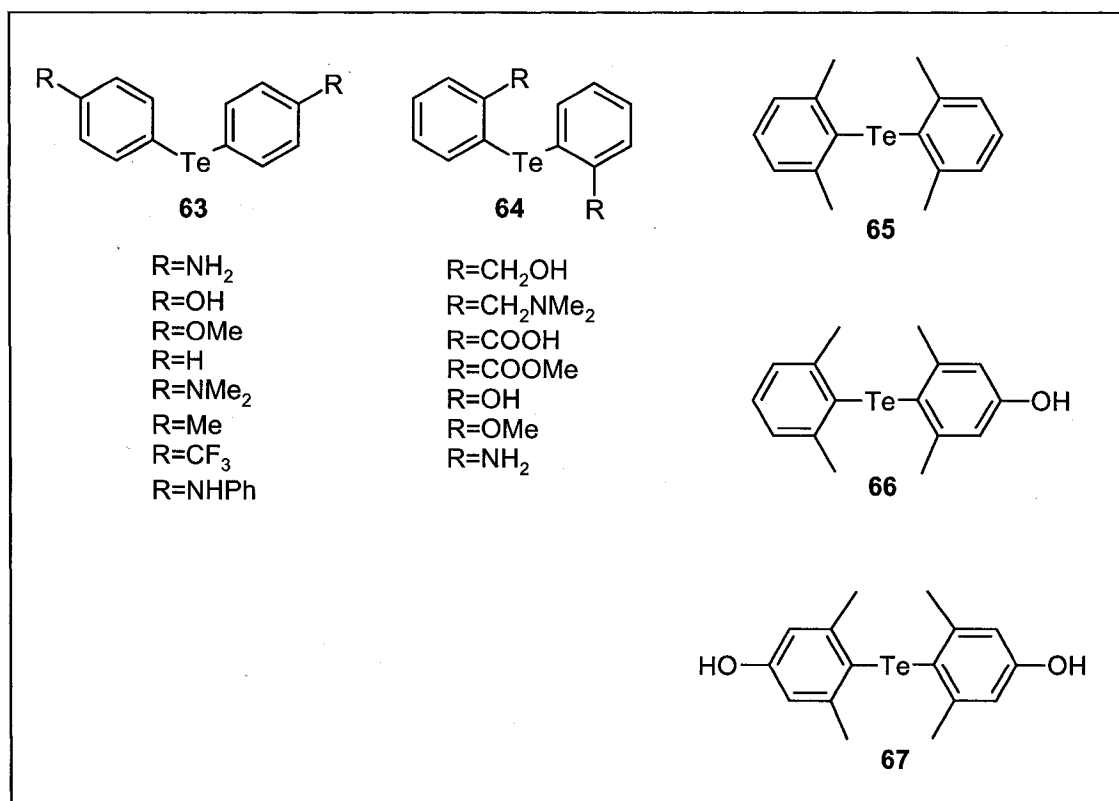
Furthermore, Engman prepared water-soluble organotellurium compounds **68-70**[93] (Figure 1.15), which were screened as antioxidants. Compound **68a** displayed significant activity towards hydrogen peroxide, peroxynitrite, and the hydrogen peroxide-induced hydroxyl radical in cortical synaptosomal systems of gerbil brain. Likewise, it prevented neuronal death caused by ONOO$^-$.[94]

Figure 1.15 Organotellurides with GPx-like Behaviour
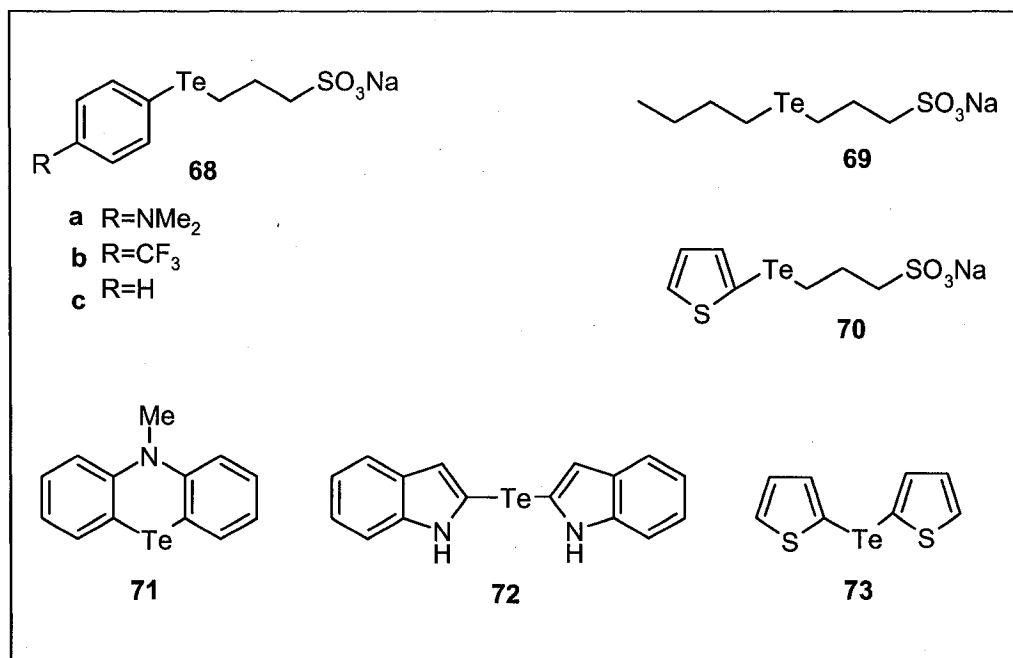
Additionally, heterocyclic and heteroaryl organotellurides **71-73** were studied[91] and exhibited no significant catalytic activity.

1.2.5 Other Biological Importance of Organoselenium Compounds[34,95,96]

Besides the glutathione peroxidase-like activity and antioxidant activity described in preceding sections, organoselenium compounds possess a wide variety of biological activities. Some organoselenium compounds exhibit antiinflammatory activity because they inhibit the activity of enzymes such as nitric oxide synthase (NOS), lipoxygenases (LOX), and protein kinase C (PKC), which are implicated in inflammatory processes.[97] Many organoselenium compounds display strong anticarcinogenic activity. In the early stages of the development of the antitumor organoselenium compounds, they were mostly represented by analogues of sulfur compounds with similar known activity. A good

example is 6-selenoguanine.[98] Another major class of organoselenium compounds exhibiting anticarcinogenic activity are the benzylic selenocyanates (Figure 1.16). Compound **74** was found to inhibit the action of 4-(methylnitrosoamino)-1-(3-pyridyl)-1-butanone (NNK), which is a compound found in tobacco smoke and is implicated in lung cancer.[99] Compound **75** substantially inhibits the growth of P388 mouse leukemia without exhibiting significant toxicity.[100] Some derivatives of 1,3-selenazole act as antiproliferative agents.[101] Selenazofurin **76** displays antiviral activity against a wide range of viruses, including type I herpes simplex virus, type 3 parainfluenza virus, and type 13 rhinovirus.[102] The α- and β- anomers of oxaselenolane nucleosides **77** act against HIV and hepatitis B viruses.[103,104]

Figure 1.16 Examples of Organoselenium Compounds with Anticarcinogenic and Antiviral Activity

74	**75**	**76**	**77**
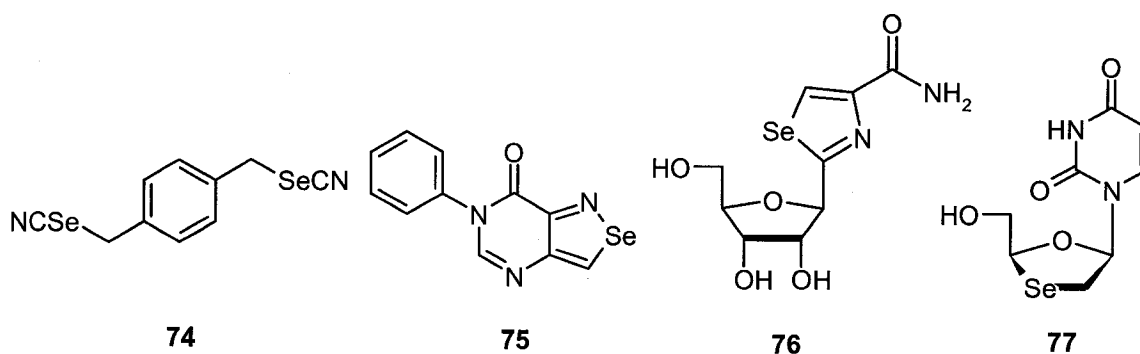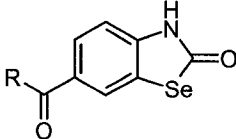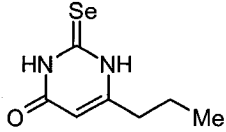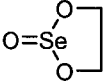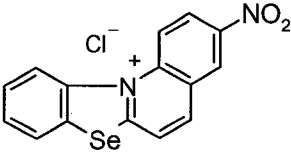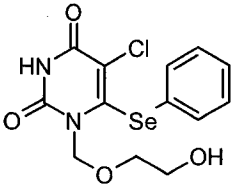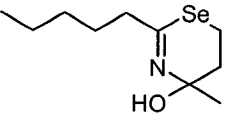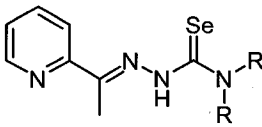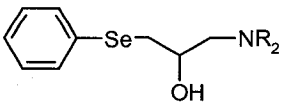
The observation that the intake of inorganic selenium and β-carotene has an inhibitory effect on carcinogenesis in rats[105] has led to the development of synthetic selenocarotenoids such as **78** (see Figure 1.17). Selenium analogues of the antibacterial penicillins, such as **79**, have been reported.[106] Despite their higher activity, they haven't been commercialized due to their high toxicity. Compound **80**,[107] a selenium analogue of glutathione, exhibits antioxidant activity comparable to that of other diselenides. Water-soluble porphyrin analogues such as **81**[108] act as sensitizers in photodynamic therapy (PDT) and might be potentionally used for treatment of certain types of cancer. Selenosugars **82** that are designed to act as D-glucose cellular transport blockers were developed by Schiesser et. al.[109]

Figure 1.17 Examples of Novel Classes of Organoselenium Compounds[34]
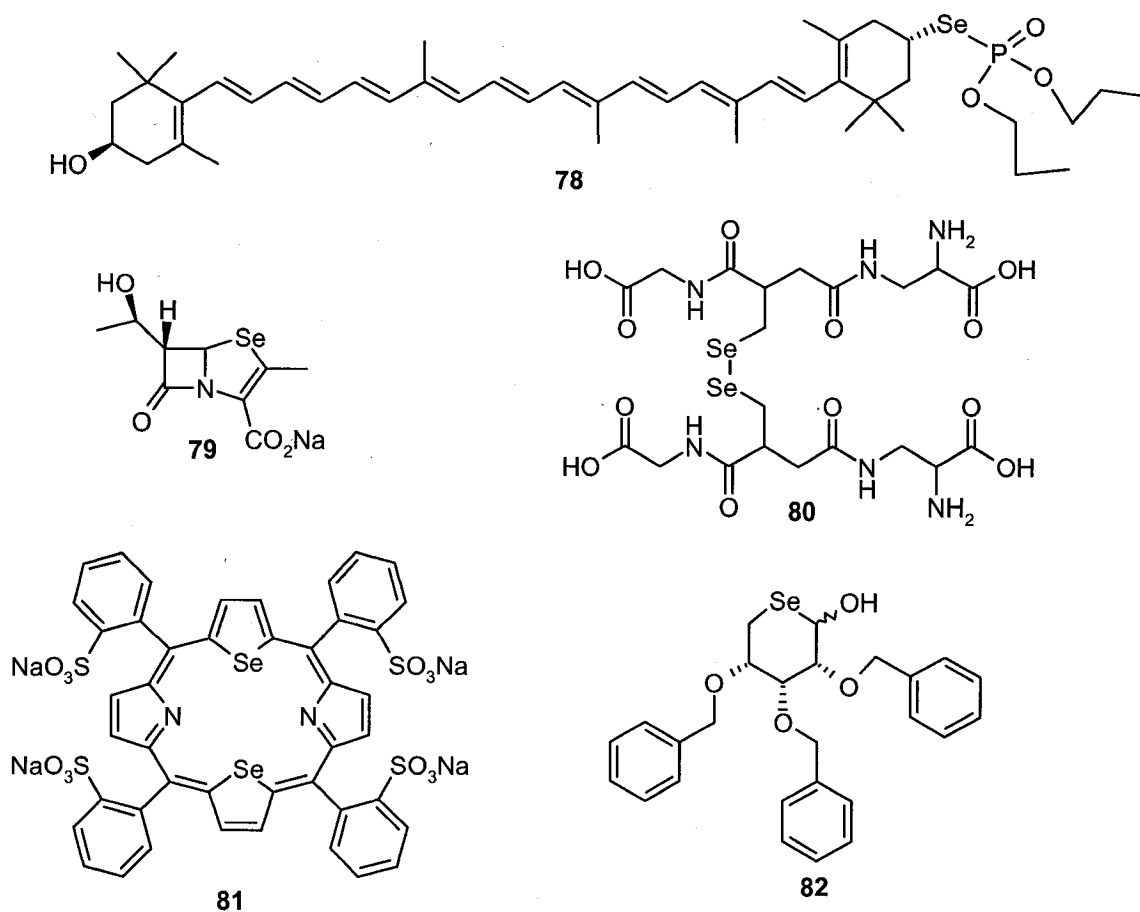
One of the major uses of organoselenium compounds in relation to biology is the utility of their ^{75}Se labelled derivatives as radioimaging agents. They have several advantages over other types of radioimaging compounds, such as a relatively long half-life, stability in vivo and ease of incorporation of ^{75}Se into these compounds. Good examples are 19-selenocholesterol and 17α-selenoethynylestradiol.[103] Some other examples of biologically active organoselenium compounds are presented in Table 1.3.

Table 1.3 Examples of Other Biologically Active Organoselenium Compounds[34,96]

Major indication	Structure (example)	Claimed activity
Enzyme inhibitor		lipoxygenases inhibitor
		type I iodothyronine deiodinase inhibitor
Anti-cancer		antineoplastic
		cytotoxic, anti-tumor, antiviral
Antiviral		anti HIV-1 (strain LAV)
Anti-infective		antibacterial activity against E. coli, S. aureus
		antimalarial, antileukemic
Cardiovascular		antiarrhythmic, negative ionotropic, antioxidative

1.2.6 Pharmacology of Organotellurium Compounds[95]

There is not much known about the pharmacology of organotellurium compounds and data published to date differ significantly. Since the tellurium atom has a similar electronic configuration to selenium, both these atoms share certain chemical properties. In general, the weaker C-Te bond compared to the C-Se bond makes organotellurium compounds less stable than structurally related selenium compounds. So far, no natural biological function has been described for tellurium. Besides the previously mentioned glutathione peroxidase-like activity, organotellurium compounds exhibit other interesting properties. Ammonium trichloro(dioxoethylene-O,O′-)tellurate (**83**) shows antitumor effects,[110] stimulates proliferation of lymphokines by human lymphoid cells,[111] and protects mice from ionizing radiation.[112] Compounds **84** and **85** act as potent inhibitors of thioredoxin reductase and inhibit cancer cell growth.[113] Telluranthren **86** possesses bacterial toxicity and is capable of inducing apoptotic cell death in eukaryotic HL-60 cells.[114] The lipophilic chalcogenopyrylium dye **87** acts as a photochemotherapeutic agent (sensitizer in photodynamic therapy) that has potential applications in the treatment of certain cancers.[115]
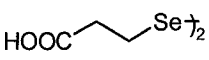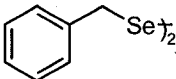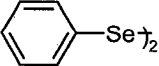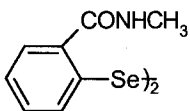
Figure 1.18 Examples of Biologically Active Organotellurium Compounds
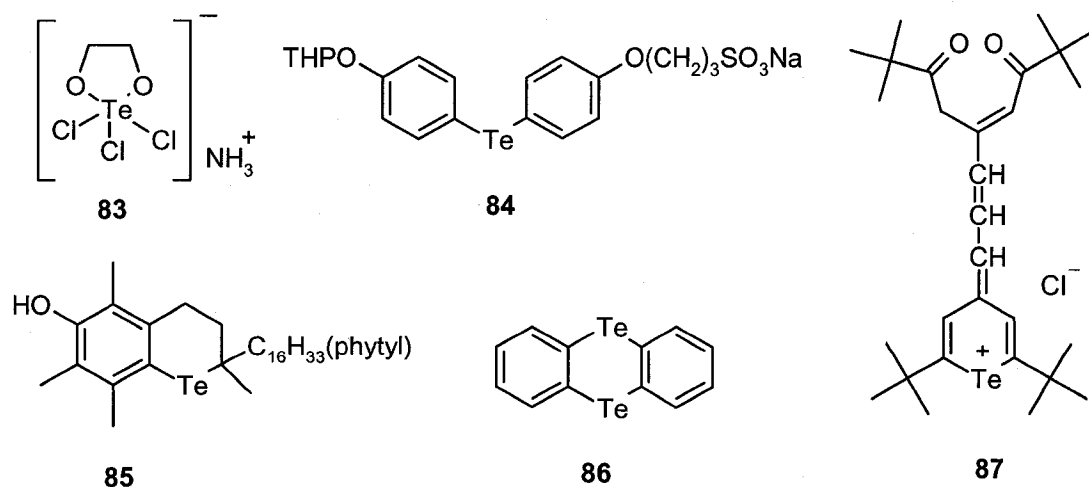
1.2.7 Toxicology of Organoselenium Compounds

Interest in the utility of organoselenium compounds in medicine was strongly attenuated by the experience with inorganic selenium compounds, which display high toxicity in mammalian organisms. Elemental selenium is not particularly irritating to the body and is not well absorbed. On the other hand, inorganic selenium compounds such as selenium dioxide (SeO_2), selenate (SeO_4^{2-}), selenite (SeO_3^{2-}), selenium oxychloride ($SeOCl_2$), selenium chloride ($SeCl_2$) and hydrogen selenide (H_2Se) are strong irritants and cause severe damage to exposed tissues. Exposure to high concentrations of these forms of selenium can lead to selenium toxicosis (selenosis).[116] It is a rare form of poisoning and is caused by the ingestion of selenium accumulator plants or by accidental over-supplementation. It is characterized by "garlic breath", hair loss and neurological abnormalities. The toxicity of organoselenium compounds depends on several factors such as the chemical form and quantity of the element, animal species, age, physiological state, nutrition and dietary interactions, and the route of administration.[117] In general, toxicity of organoselenium compounds in vivo is dependent on the stability of the carbon-selenium bond. The C_{sp3}-Se bond is weaker than the C_{sp2}-Se bond, resulting in alkyl selenides and diselenides being more toxic compared to their aryl derivatives, since they are more easily metabolized by C-Se cleavage and oxidation to the more highly toxic inorganic species. (Table 1.4)

Table 1.4 Comparison of Toxicity of Organic Diselenides[96]

diselenide	LD_0 (mg/kg, mouse, p.o.)
HOOC~~~Se⅟₂	67
phenyl-CH₂-Se⅟₂	25
aryl-Se⅟₂	230
aryl(CONHCH₃)-Se⅟₂	651

LD_0 = maximal non-lethal dose

In 1941, Painter suggested that the toxicity of inorganic selenium might be associated with the oxidation of biologically important thiols, including glutathione (GSH), cysteine, dihydrolipoic acid, and coenzyme A.[118] This was later confirmed when the severe loss of GSH from the blood and organs of animals with selenite-induced poisoning was observed.[119] In the late 1990s, Seko's and later Spallholz's work suggested that thiols react with sodium selenite and selenocysteine, producing reactive superoxide and hydroperoxide species.[120,121] It was proposed that much of the cytotoxicity of organoselenium compounds might arise from their ability to reduce dioxygen, thus initiating the uncontrolled production of free radical species. This process is called glutathione oxidase activity. It is interesting and somewhat ironic that selenium compounds can act as protective agents against oxidative stress under some circumstances, but can also contribute to the production of ROS in others. As a result, the toxicity of organoselenium compounds depends on the balance between generated reactive oxygen species and antioxidant defenses. Several studies of organoselenium compounds, such as ebselen,[122] diaryl diselenides,[78] selenocystine[123] and selenocystamine,[124] show the ease of one-electron transfer from RSe⁻ to a variety of reducible substrates (Scheme 1.16). Selenocystamine was shown to catalyze the oxygen-mediated oxidation of excess GSH to glutathione disulfide at neutral pH and ambient oxygen pressure.[125]

Scheme 1.16 Glutathione Oxidase Activity of Organoselenium Compounds[125]
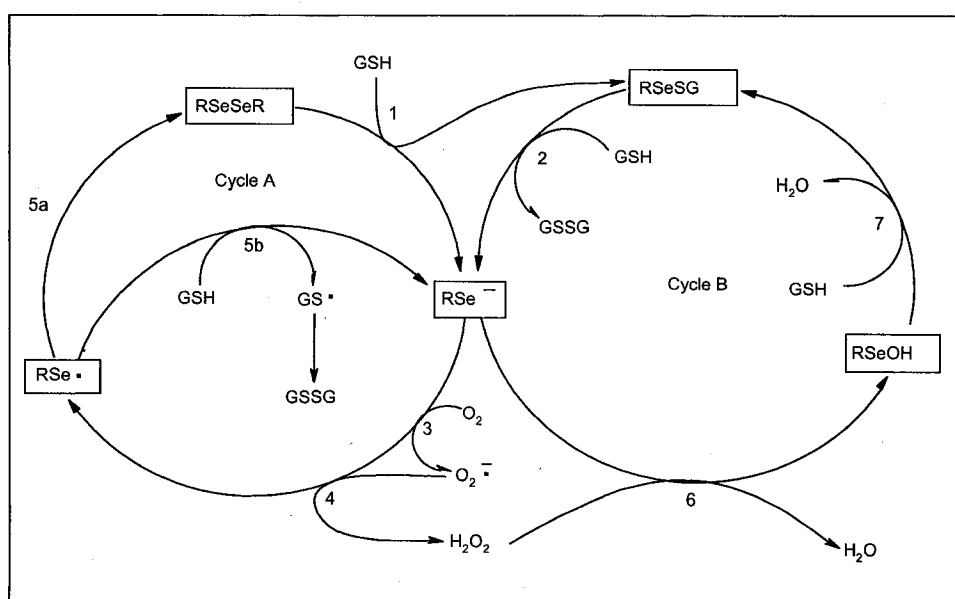
In this glutathione oxidase cycle, heterolytic reduction of the diselenide leads to two equivalents of selenolate ion (RSe⁻) via the formation of the selenenyl sulfide intermediate (step 1 and 2). Selenolate ion is further involved in the three-step reduction of oxygen to water. The first step is a one-electron transfer from RSe⁻ to dioxygen yielding superoxide (O_2^-) (step 3) and selenyl radical RSe·, which decays rapidly into diselenide RSeSeR (step 5a) or can be trapped by excess GSH to form glutathione radical GS· (step 5b) which forms GSSG subsequently. The next step involves reduction of the superoxide to hydrogen peroxide by the selenolate RSe⁻ by a rapid one-electron transfer mechanism (step 4). The third step is a two-electron transfer from RSe⁻, which resulted in the production of the selenenyl sulfide RSeSG (step 6) via a selenenic acid (RSeOH) intermediate (step 7). Even though the glutathione oxidase activity is only minor compared to the glutathione peroxidase activity, this study explained the toxicity of organodiselenides, selenenyl sulfides and selenols, which also serve as the key intermediates in the catalytic cycles of the majority of GPx mimetics.

In terms of toxicity of the organoselenium compounds, several studies suggested that the brain is a potential target for lipophilic organoselenium compounds. Diphenyl diselenide crosses the blood-brain barrier fairly easily. Reportedly, after exposure for 2 months to high doses of diphenyl diselenide, the total selenium content in the brain of mice increased three-fold.[126] Diphenyl diselenide has been demonstrated to be highly toxic to the central nervous system of rodents,[127] because it is a potent inhibitor of squalene monooxygenase (SMO), a key enzyme in the synthesis of cholesterol. Thus, it causes a dramatic decrease in the rate of cholesterol biosynthesis in Schwann cells, which consequently leads to degradation of the myelin sheath and transient demyelination of peripheral nerves.[128] Exposure to high doses of diphenyl diselenide has proven to have an inhibitory effect on glutamate uptake by rat synaptosomes and synaptic vesicles.[129] Glutamate is the major excitatory amino acid transmitter in the human CNS and is believed to play an important role in several physiological and pathological processes.[130] Additionally, diphenyl diselenide inhibits ^{45}Ca flux into synaptosomes, which can disrupt

a variety of neurophysiological processes, causing high neurotoxicity of this compound.[131]

1.2.8 Toxicology of Organotellurium compounds

To date, data on the toxicology of organotellurium compounds has been sparse in the literature. The toxicity of organotellurium compounds compared to their selenium analogues is in many cases questionable and hard to predict, because it depends on many factors such as the species of animal being tested and the route of administration.[132] Inorganic tellurium (IV) compounds are metabolized in a similar way as selenium (IV) species. However, methylated tellurium products are more toxic to mammals.[133] Similarly to their selenium analogues, organotellurides dramatically reduce biosynthesis of cholesterol by reacting with vicinal cysteine sulfhydryl groups on the squalene monooxygenase (SMO) enzyme. Hydrophobic compounds were found to be less toxic because the enzyme-inhibitor interaction is decreased. As a result of inhibition of SMO, organotellurium compounds have neurotoxic effects. Diorganyl ditellurides are stronger inhibitors than their selenium counterparts of glutamate uptake by brain synaptosomes.[134] Similarly to organic diselenides, neurotoxicity of organic ditellurides can be attributed to their ability to affect ^{45}Ca flux into brain synaptosomes.[135] Nogueira and coworkers demonstrated high liver and renal toxicity of diphenyl ditelluride.[136] According to their study, this compound is highly toxic with an LD_{50} of < 1 μmol/kg in rats.

1.2.9 The Design of New Efficient GPx Mimetics

As a result of the earlier investigations described in preceding sections, one can predict some characteristics of a good GPx mimetic. One can anticipate superior catalytic activity in molecules having (a) a hydrogen bond between a selenol moiety and proximate amino/imino/ether/alcohol group to promote dissociation of the selenol, (b) strong Se....N or Se...O interactions in the selenenic acid in order to increase the electrophilic nature of the selenium atom resulting in its enhanced reactivity with thiols,

thus also suppressing overoxidation to selenium IV species, (c) amino/imino/ether/hydroxyl groups that can interact with sulfur in the selenenyl sulfide intermediate causing kinetic activation of Se-S bond.[53] From the studies of previously reported GPx mimetics, Se...N and Se....O interactions are advantageous since they activate the Se-Se bond toward oxidative cleavage in diselenides. On the other hand, strong Se...N interactions in selenenyl sulfides were reported to deactivate the catalyst.[77] Moreover, one should bear in mind that aromatic organoselenium compounds are in general less toxic than aliphatic ones. Additionally, diselenides and selenenyl sulfides have the ability to enter into the glutathione oxidase cycle, which increases the toxicity of these compounds.

1.2.10 Objectives

In continuation of the studies previously done by our research group in the area of glutathione peroxidase mimetics, we focused on the synthesis and exploration of the catalytic activity of new derivatives of the novel cyclic seleninate ester **46** and spirodioxyselenurane **53**. Despite the exceptional catalytic activity of these compounds, their prospects to become drug candidates is diminished by their expected high toxicity, which is characteristic of aliphatic organoselenium compounds in general. The focus of the present work is therefore on the preparation of aromatic derivatives of the cyclic seleninate ester and spirodioxyselenurane, which are potentially less toxic than their parent compounds and more likely to become pharmacologically interesting. Additionally, we desired to investigate the effects of substitution on the catalytic activity of the aromatic derivatives, as well as to determine the relative activity of the corresponding tellurium analogues.

Chapter Two

Synthesis and Glutathione Peroxidase-like Activity of Aromatic Derivatives and Tellurium Analogues of Cyclic Seleninate Esters and Spirodioxyselenuranes

2.1 Introduction

With the discovery of the essential role played by the selenium atom in the active site of GPx and several other enzymes, an augmented interest in the small-molecule selenium compounds that mimic the activity of these enzymes was initiated. The success of ebselen as an anti-inflammatory agent/antioxidant further provoked the search for improved GPx mimetics. The additional realization of more facile redox chemistry displayed by organotellurium compounds led to the expansion of the search for GPx mimetics to this element. Recently, Back and Moussa reported the novel cyclic seleninate ester **46**[84] and spirodioxyselenurane **53**[85] that acted as exceptionally potent catalysts in the destruction of *tert*-butyl hydroperoxide in the presence of benzyl thiol. We wished to compare the catalytic activity of **46** and **53** with their novel aromatic derivatives and tellurium analogues in order to devise compounds with the optimum balance of high catalytic activity and low toxicity. The comparison of catalytic activity was performed using the model assay developed in our group, which is described in the following section.

2.2 Assessment of the GPx-like Catalytic Activity by a Standard Assay

The assessment of the GPx-like properties of organoselenium compounds required the development of an experimental assay, which could be applied as a model of the GPx-GSH system. Several groups involved in research on GPx mimetics have employed different assays and methods for the evaluation of GPx-like activity based on a variety of NMR,[62] enzymatic[75] and UV[79, 137] techniques. In the present study, a method developed by Back and Dyck,[72] which utilizes HPLC analysis to follow the progress of a

model reaction, was used. In this model reaction, 56% *tert*-butyl hydroperoxide (0.038 M) or 29% hydrogen peroxide (0.040 M), which were titrated prior to use, served as oxidizing agents, while redistilled benzyl thiol (0.031 M) was used as a sacrificial stoichiometric reductant. The evaluated GPx mimetics were employed as 10 mol % catalysts (0.0031 M) with respect to benzyl thiol. In the overall reaction, two molecules of benzyl thiol are oxidized to dibenzyl disulfide and one molecule of *tert*-butyl hydroperoxide or hydrogen peroxide is reduced to *tert*-butanol or water respectively (see Scheme 2.1).

Scheme 2.1 Model Reaction

$$
2\ BnSH + ROOH \xrightarrow[\substack{CH_2Cl_2:MeOH\ (95:5) \\ 18\,^{\circ}C \\ naphthalene}]{10\ mol\%\ catalyst} BnSSBn + ROH + H_2O
$$
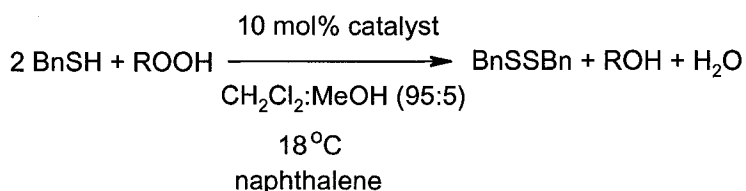
R = *t*-Bu or H

Our assays were typically run in dichloromethane/methanol (95:5) mixture because this solvent system can dissolve the thiol, peroxide, as well as the majority of the investigated polar GPx mimetics. Experiments were performed in a water bath at 18 °C in order to monitor the faster reactions without overly retarding the rates of the slower ones. The progress of the reaction was conveniently followed by HPLC, using a UV absorbance detector (λ 254 nm) and an acetonitrile/water mixture, in a gradient mode, as the mobile phase (tables of gradients are listed in Appendix A). For convenient analysis of the reaction mixture, naphthalene was used as an internal standard. Benzyl thiol and its corresponding disulfide were chosen in this protocol because they contain chromophores that make their concentrations easy to monitor by HPLC during the course of each reaction. Moreover, their methylene groups provide convenient NMR signals for further investigations of possible intermediates. The catalytic activities of the GPx mimetics were compared by means of the half-lives of the reactions ($t_{1/2}$), which represent the time

required to oxidize 50% of the thiol to its disulfide. This choice for expressing the catalytic activity possesses advantages over measuring the rate constants, because the kinetic profiles of some GPx mimetics include irregularities such as induction periods during the initial oxidation step or unusually rapid early stage kinetics (presumably due to the rapid conversion of the catalyst to an intermediate that then reacts more slowly in a subsequent step). For comparison, a control reaction was performed in the absence of any catalyst. Figure 2.1 shows an HPLC plot of the control experiment, where well-resolved peaks for benzyl thiol (retention time = 3.69 min), naphthalene (retention time = 5.68 min) and dibenzyl disulfide (retention time = 10.35 min) are shown.

Figure 2.1 HPLC Plot of the Control Experiment
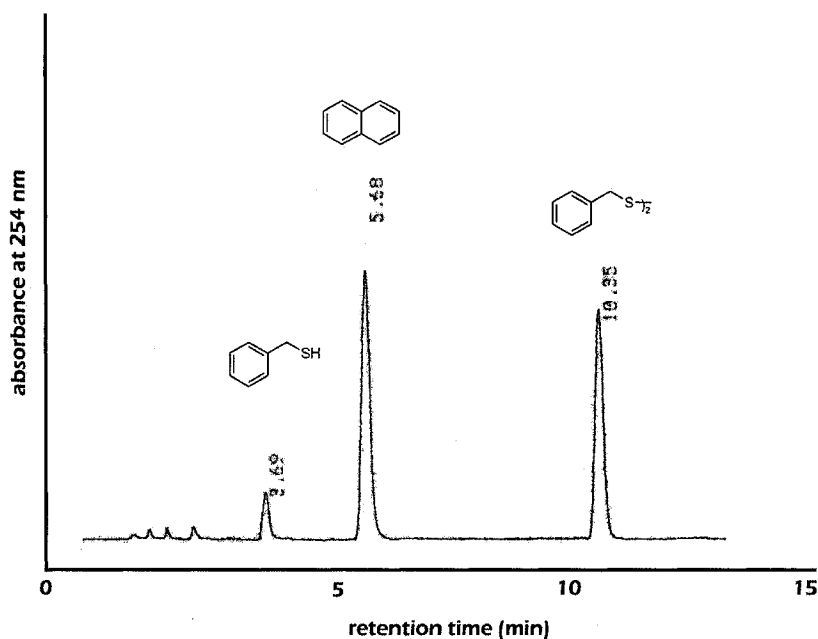
Integrated areas of the corresponding peaks were compared to the internal standard and the progress of each reaction was portrayed as a plot of the yield of dibenzyl disulfide (%) versus time (h) (see Appendix B). Relative response factors of dibenzyl disulfide were based on a calibration plot, in which the concentration of naphthalene remained constant, while concentration of the disulfide was varied (see Appendix C).

2.3 Synthesis of Ebselen and Evaluation of Its Catalytic Activity

In order to compare the catalytic activities of newly prepared GPx mimetics to that of a broadly known and well-studied organoselenium compound, which exhibits glutathione peroxidase-like behaviour, we decided to synthesize ebselen (3), and study its catalytic activity in our model assay. Ebselen was prepared from benzanilide using Engman's procedure[65] (Scheme 1.9) and subsequently subjected to the model assay. Formerly, Back and Moussa reported that in the presence of 90% *tert*-butyl hydroperoxide (0.061 M), ebselen produced a half-life of the model reaction, $t_{1/2}$, of 42 hours.[84] We expanded this work and studied ebselen in the presence of various concentrations of peroxides or different types of oxidants, respectively. From Figure 2.2, it is seen that in the presence of 58% *tert*-butyl hydroperoxide (0.039 M) ebselen exhibits lower catalytic activity ($t_{1/2}$ of 62 hours) than with 90% *tert*-butyl hydroperoxide. This observation suggests the dependence of the catalytic activity of ebselen on the concentration of *tert*-butyl hydroperoxide. Moreover, investigation with 32% hydrogen peroxide (0.040 M) revealed a three-fold increase in the rate of the destruction of this peroxide ($t_{1/2}$ = 20 hours), when compared to *tert*-butyl hydroperoxide at a similar concentration. The observed dependence of the catalytic activity of ebselen on the identity of the oxidant is apparently a consequence of the different rates of the oxidation of the selenium atom during the course of the reaction. For clarification, we will return to this topic in Section 2.10. In the uncatalyzed reaction, the time required to convert 50% of benzyl thiol to dibenzyl disulfide was measured to be greater than 300 h with all investigated concentrations of *tert*-butyl hydroperoxide and 116 hours in the case of 29% hydrogen peroxide, respectively.

Figure 2.2 Catalytic Activity of Ebselen and Control in the Presence of Different Oxidants
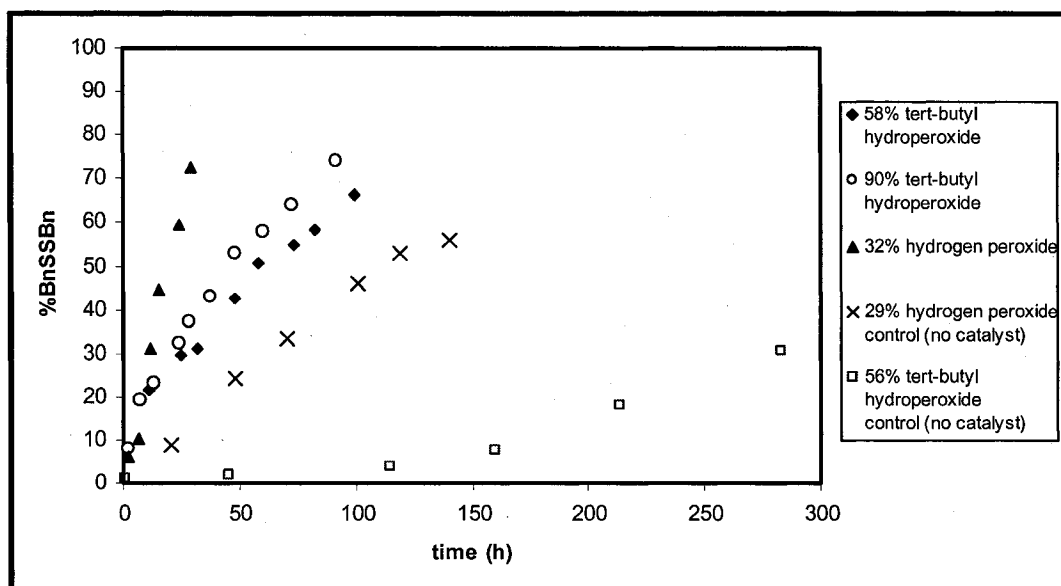
As previously mentioned in Chapter 1.2.3, the catalytic mechanism of ebselen is dependent on various factors including the concentrations of thiol and peroxide, and the conditions and solvents used during each study. Our observations showed that after treating the dichloromethane/methanol (95:5) solution of ebselen with excess of either *tert*-butyl hydroperoxide or hydrogen peroxide, followed by benzyl thiol, the reaction mixture instantaneously changed its colour from clear to yellow after the addition of the thiol, and immediate analysis by HPLC revealed the formation of the selenenyl sulfide **88**. It was independently prepared by the reaction of ebselen with three moles of benzyl thiol, and in the corresponding HPLC plot (Figure 2.3) is observed as a peak with a retention time of 9.00 min. The rapid formation of this selenenyl sulfide **88** and the fact that its concentration does not change over the course of the reaction suggests a key role of the selenenyl sulfide in the catalytic mechanism of ebselen under the conditions of our assay.
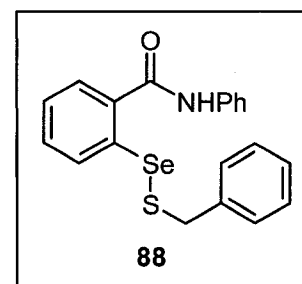
Figure 2.3 HPLC Plot of the Model GPx Assay in the Presence of 10% Ebselen and 58% *tert*-Butyl Hydroperoxide at 73 Hours
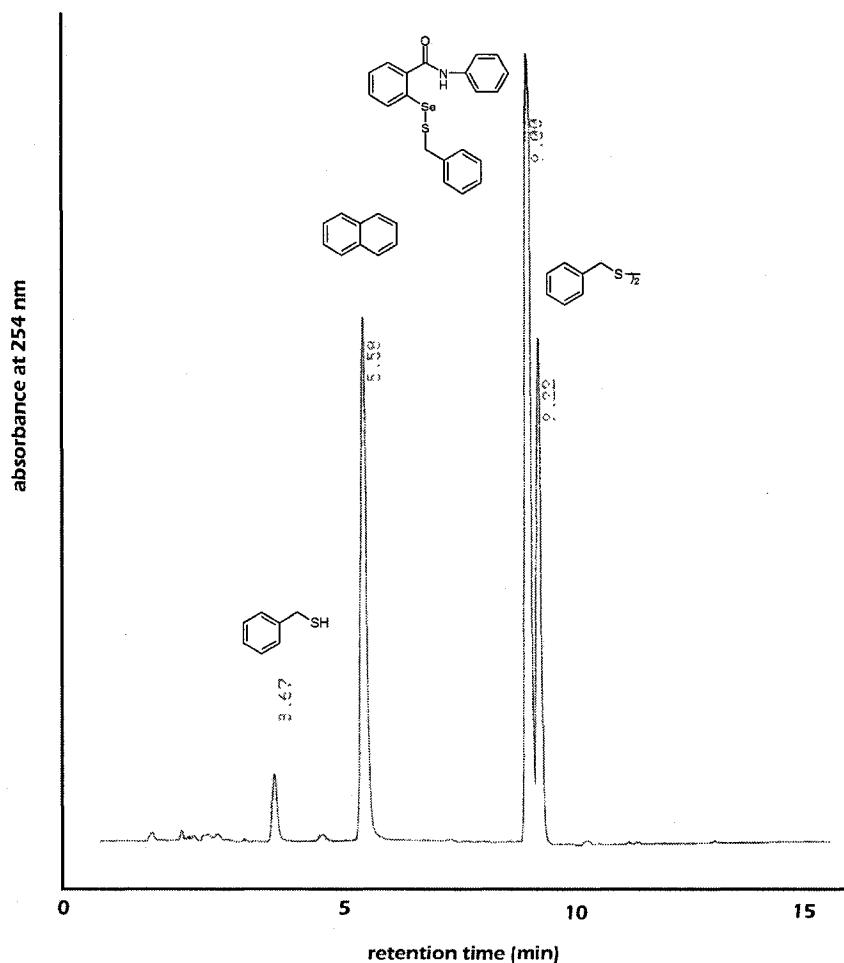
2.4 Aromatic Cyclic Seleninate Esters as GPx Mimetics

On account of the high catalytic activity expressed by aliphatic cyclic seleninate ester **46**, we proceeded in the synthesis and investigation of the GPx-like behaviour of the series of its aromatic derivatives **89**, **90**, **91**, **92** and **93** (Figure 2.4), since they are expected to have lower toxicity than their aliphatic counterparts. All these compounds are novel and possess features that might help us better understand the mechanism by which they catalyze peroxide destruction in the presence of thiols. The first logical step was synthesis of the unsubstituted aromatic seleninate **89** followed by the cyclic seleninate **90**, which was prepared in order to study the consequence of the electron-withdrawing

carbonyl group on the catalytic activity of cyclic seleninates. Similarly, the electron-donating methoxy group as well as the electron-withdrawing nitro and fluoro substituents were introduced into the aromatic ring of **89** with the aim of investigating their effects on the catalytic activity.

Figure 2.4 Novel Cyclic Seleninate Esters
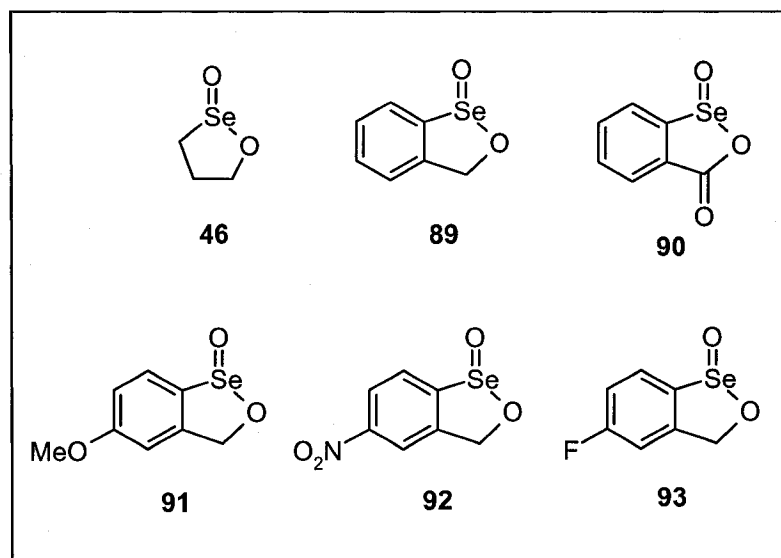
Syntheses of novel cyclic seleninates **89**, **90**, **91**, **92** and **93** are described in Sections 2.4.1 to 2.4.5 and the evaluation of their catalytic activity will be discussed in Section 2.5.

2.4.1 Synthesis of Benzo-1,2-oxaselenolane *Se*-Oxide (89)

Our initial attention was turned to benzo-1,2-oxaselenolane *Se*-oxide (**89**), which was synthesized in 39% overall yield in three steps from commercially available anthranilic acid (**11**) (Scheme 2.2). In the first step, 2,2`-diselenobis(benzoic acid) (**12**) was prepared by one of the oldest yet most reliable methods for the preparation of aromatic diselenides, namely the reaction of alkali diselenides with diazonium salts of substituted anilines.[138] The diazonium salt of anthranilic acid (**11**) was reacted with potassium diselenide (K_2Se_2), which was prepared by melting selenium powder with potassium hydroxide at 140 °C.[138] An interesting feature of this reaction is that it can be

performed in the presence of air in spite of the general low stability of inorganic diselenides toward air oxidation. Diselenide **12** prepared by this procedure contained ca. 5-10% of the corresponding selenide and was used without any further purification. Subsequently, the reduction of the diselenide and carboxylic acid moieties with excess lithium aluminum hydride, followed by nucleophilic displacement of iodide from allyl iodide with the resulting selenolate, afforded allyl (2-hydroxymethyl)phenyl selenide (**94**) in 50% yield in a one-pot reaction. Cyclization to the final product **89** was performed with excess *tert*-butyl hydroperoxide in 88% yield via the sequence of oxidation of the allyl selenide **94**, [2,3]sigmatropic rearrangement, a second oxidation and cyclization with displacement of allyl alcohol as previously portrayed in Scheme 1.12.

Scheme 2.2 Synthesis of Benzo-1,2-oxaselenolane *Se*-Oxide (**89**)
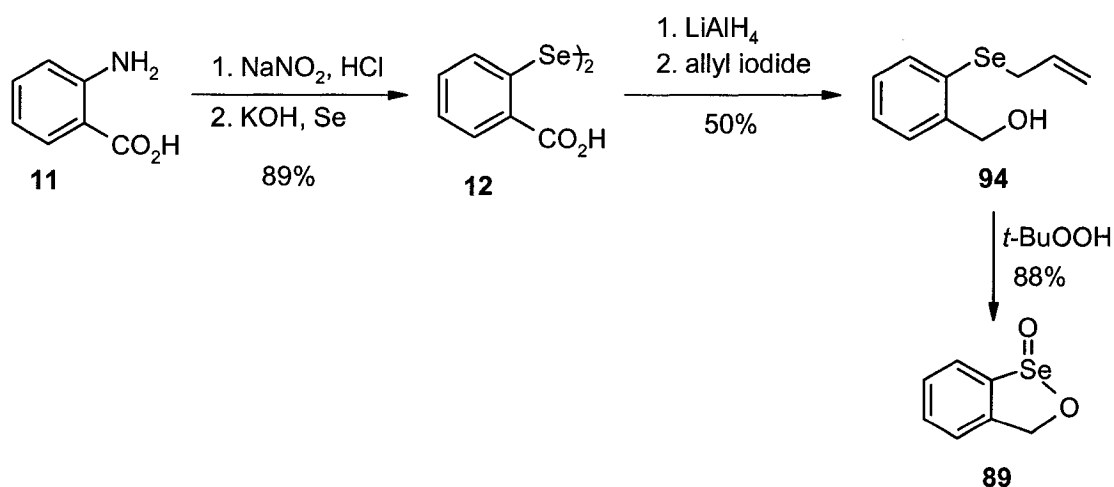
Cyclic seleninate **89** proved to be stable for several months when kept at room temperature, even in the presence of light. Its IR, ^{1}H, ^{13}C, ^{77}Se NMR and mass spectra were consistent with the proposed structure. A satisfactory elemental analysis served as the evidence of its purity. The proton NMR spectrum is depicted in Figure 2.5 and shows a downfield shift of the proton in the *ortho* position relative to selenium (doublet with chemical shift of 7.81 ppm). Diastereotopic methylene protons (CH$_2$O), which appear as a pair of doublets at δ 5.97 and 5.61 ppm with a coupling constant $J = 13.8$ Hz, are a result of the selenium atom being a chiral centre. The ^{77}Se NMR spectrum shows a signal

at δ 1349.1 ppm, which is comparable to the previously reported chemical shift of 1340.9 ppm of the aliphatic cyclic seleninate ester **46**.[84]

Figure 2.5 The ^{1}H NMR Spectrum of **89**
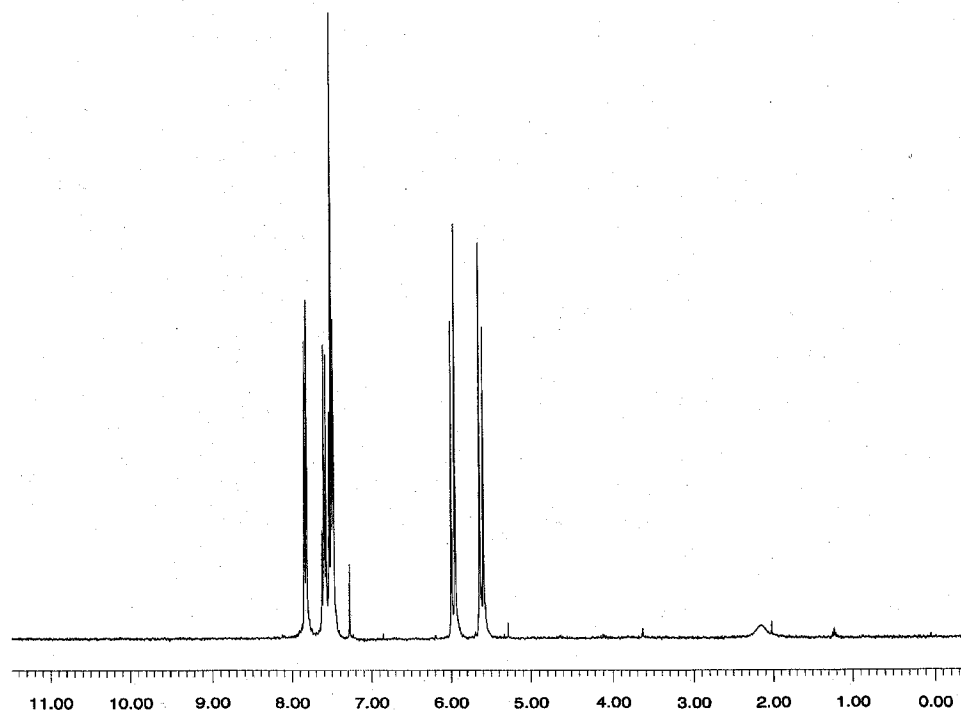
2.4.2 Synthesis of Benzo-3-oxo-1,2-oxaselenolane *Se*-Oxide (90)

The synthesis of benzo-3-oxo-1,2-oxaselenolane *Se*-oxide (**90**) is depicted in Scheme 2.3. Reduction of the previously prepared 2,2'-diselenobis(benzoic acid) (**12**) to the selenolate anion was performed with sodium borohydride in order to avoid reduction of the carboxylic acid moiety present in the molecule. Subsequent allylation of the corresponding selenolate anion with allyl iodide afforded allyl 2-carboxyphenyl selenide (**95**) in 67% yield. Its oxidation with *tert*-butyl hydroperoxide followed by cyclization led to our target compound **90** in 74% yield. This method proved superior to the direct

oxidation of diselenide **12** with hydrogen peroxide, which yielded only an intractable, highly polar brown material of presumably polymeric nature.

Scheme 2.3 Synthesis of Benzo-3-oxo-1,2-oxaselenolane *Se*-Oxide (**90**)
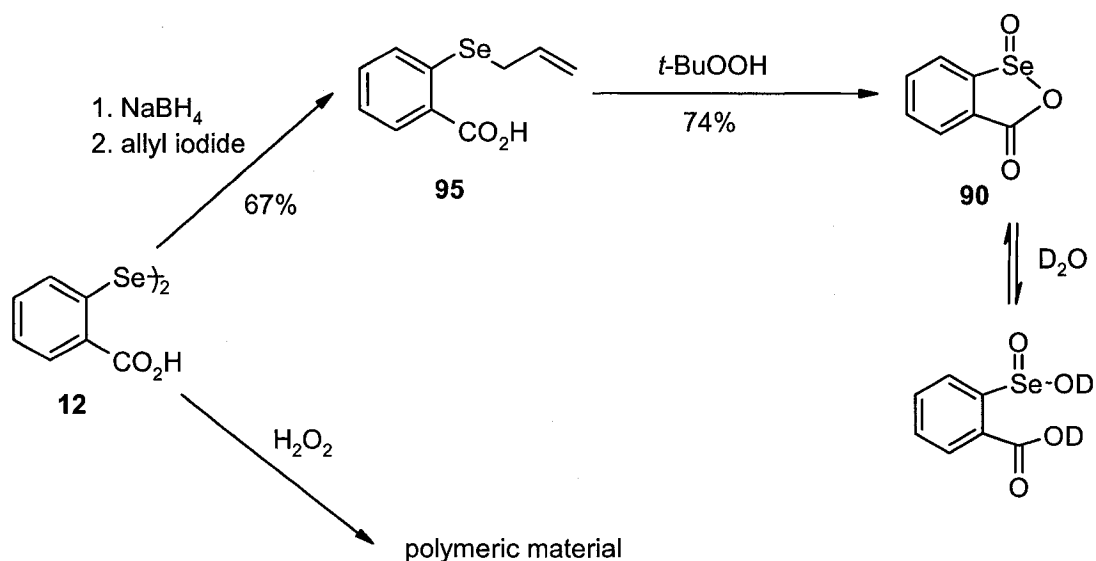
Compound **90** is extremely polar and its purification using column chromatography was not successful. A spectroscopically pure sample was acquired by recrystallization from acetonitrile, but a satisfactory elemental analysis could not be obtained. Although **90** is fairly stable and does not exhibit decomposition in its crystalline state, obtaining a ^{13}C NMR spectrum of this compound was challenging. Due to its very high polarity, the use of spectroscopic solvents was limited to DMSO-d_6 and methanol-d_4. Unfortunately, in both these solvents, cyclic seleninate **90** decomposed before a reasonable ^{13}C NMR spectrum could be obtained. It was finally acquired in D_2O at 340 K, conditions under which it is soluble yet stable (Figure 2.6). The IR spectrum shows a characteristic C=O absorption at 1653 cm^{-1} while the ^{77}Se NMR spectrum shows a peak at δ 1022.3 ppm, which is considerably upfield compared to the benzo analogue **89**. This can be because of in situ conversion to the corresponding seleninic acid as shown in Scheme 2.3.

Figure 2.6 The ^{13}C NMR Spectrum of **90**
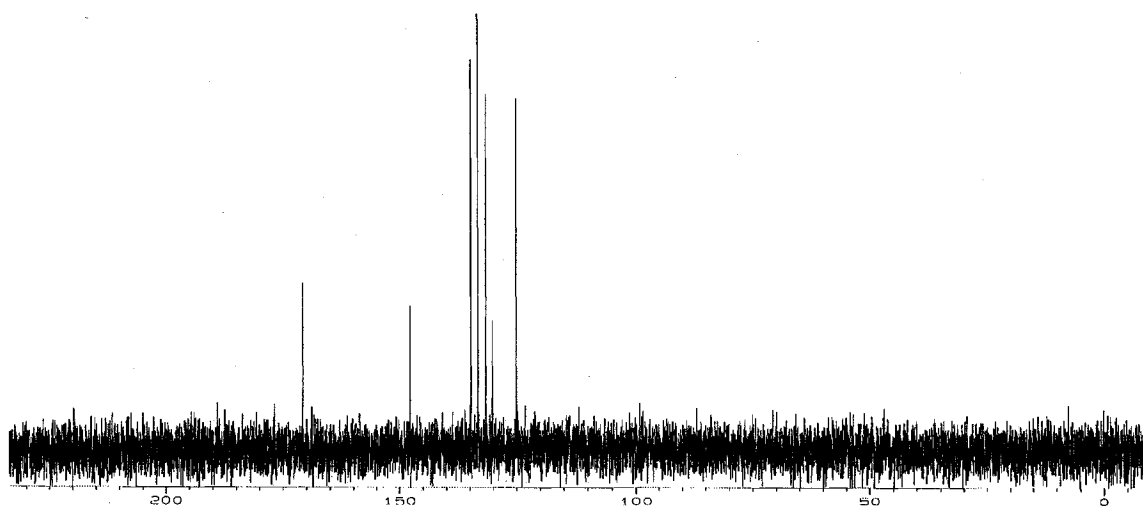
2.4.3 Synthesis of *p*-Methoxybenzo-1,2-oxaselenolane *Se*-Oxide (91)

The synthetic pathway to *p*-methoxybenzo-1,2-oxaselenolane *Se*-oxide (**91**) is depicted in Scheme 2.4. It was prepared in overall yield of 23% starting from commercially available *m*-anisaldehyde (**96**). First, **96** was brominated by refluxing with bromine in chloroform,[139] followed by the reduction of the aldehyde moiety in **97** with sodium borohydride.[140] This sequence of reactions afforded 2-bromo-5-methoxybenzyl alcohol (**98**) in 73% overall yield. 2, 2`-Diselenobis(5-methoxybenzyl alcohol) (**100**) was prepared by a halogen-lithium exchange reaction of **98** with *tert*-butyllithium via intermediate **99**, followed by selenium insertion and air oxidation. Three equivalents of *tert*-butyllithium and excess selenium gave optimum yields. The reaction mixture was warmed to room temperature in order to allow selenium insertion into the lithiated product **99**, as this process occurs at temperatures above 0 °C.[141] Tetrahydrofuran proved to be the best solvent of several investigated, despite its reactivity toward *tert*-butyllithium at temperatures above 0 °C.[141] In our case, no selenium insertion was observed when dry diethyl ether was used as the solvent. Diselenide **100** was then converted to allyl selenide **101** by reduction of the diselenide using sodium borohydride,

and subsequent reaction of the resulting selenolate with allyl iodide. Finally, oxidation of **101** with excess *tert*-butyl hydroperoxide afforded *p*-methoxybenzo-1,2-oxaselenolane *Se*-oxide (**91**) in 81% yield. Attempted direct oxidation of diselenide **100** again resulted in a polymeric product.

Scheme 2.4 Synthesis of *p*-Methoxybenzo-1,2-oxaselenolane *Se*-Oxide (**91**)
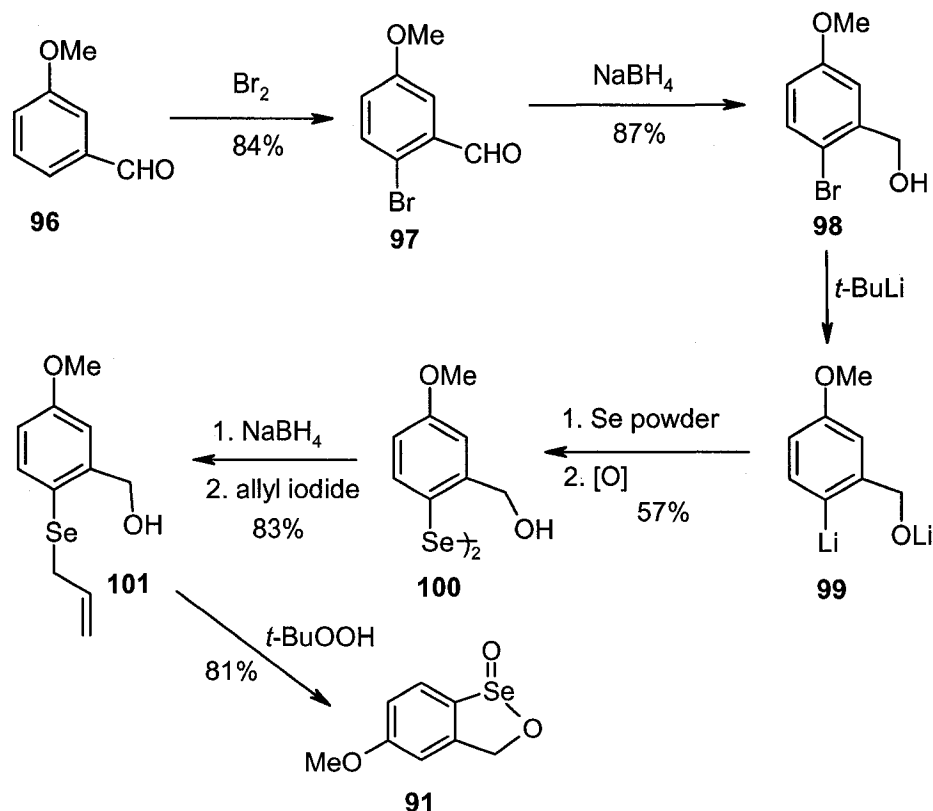
The identity of **91** was confirmed by its IR, ^{1}H NMR, ^{13}C NMR, mass and ^{77}Se NMR spectra. Its proton spectrum is shown in Figure 2.7. Interestingly, the ^{77}Se NMR spectrum of **91** showed a peak at δ 1348.8 ppm, similar in value to that of the unsubstituted cyclic seleninate **89**, when obtained in the same solvent, deuterated chloroform.

Figure 2.7 The ^{1}H NMR Spectrum of 91
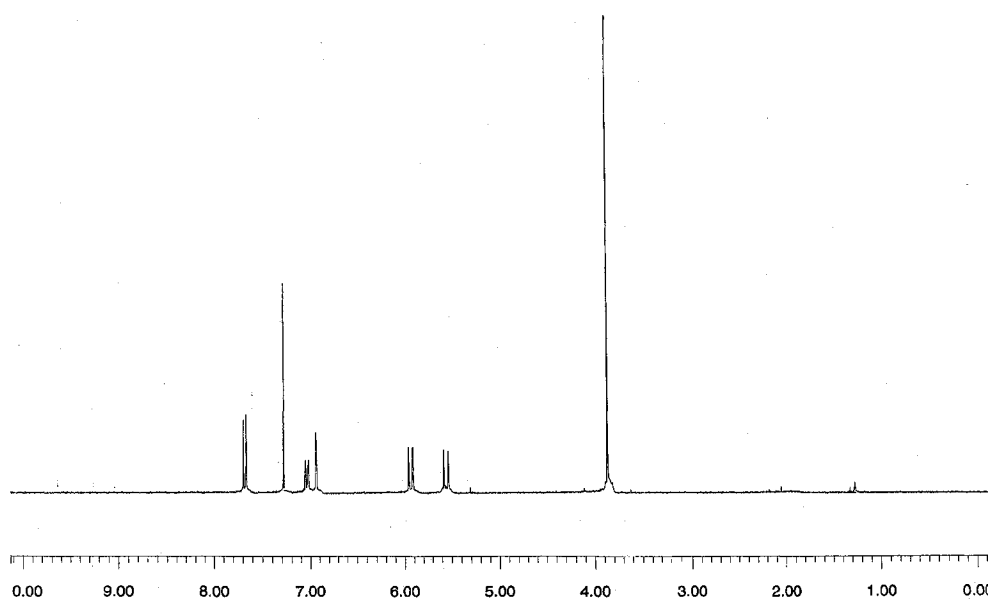
2.4.4 Attempted Preparation of p-Nitrobenzo-1,2-oxaselenolane Se-Oxide (92)

The nitro derivative 92 was chosen as an example of an aromatic cyclic seleninate containing an electron-withdrawing substituent. Attempted ortho-lithiation of 3-nitrobenzyl alcohol (102) using excess n-butyllithium in refluxing hexane, followed by the addition of elemental selenium, failed to give any reaction (Scheme 2.5).

Scheme 2.5
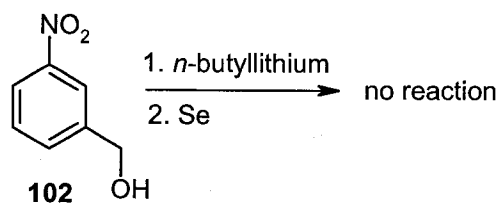
Lithium-halogen exchange of a suitable aromatic halide, with subsequent reaction of the lithiated product with selenium was the second option to be investigated. Synthesis

of 2-bromo-5-nitrobenzyl alcohol (106), an aromatic halide essential for the lithium-halogen exchange, is depicted in Scheme 2.6. First, commercially available *o*-bromobenzoic acid (103) was nitrated with nitric acid/sulfuric acid solution (3:1) according to a previously reported literature procedure,[142] to give 2-bromo-5-nitrobenzoic acid (104) in 62 % yield. Reduction of the carboxylic acid moiety in the presence of the nitro group is a challenging undertaking and is not possible using strong reducing reagents such as lithium aluminum hydride or borane-THF. Therefore, carboxylic acid 104 was converted to the corresponding methyl ester 105, which was then reduced by sodium borohydride to give alcohol 106. In general, sodium borohydride does not reduce carboxylic acid esters. However, rare precedents in the literature indicate that the reduction of some esters with $NaBH_4$ is possible when 7-10 equivalents are used in polar solvents such as water or dioxane.[143]

Scheme 2.6
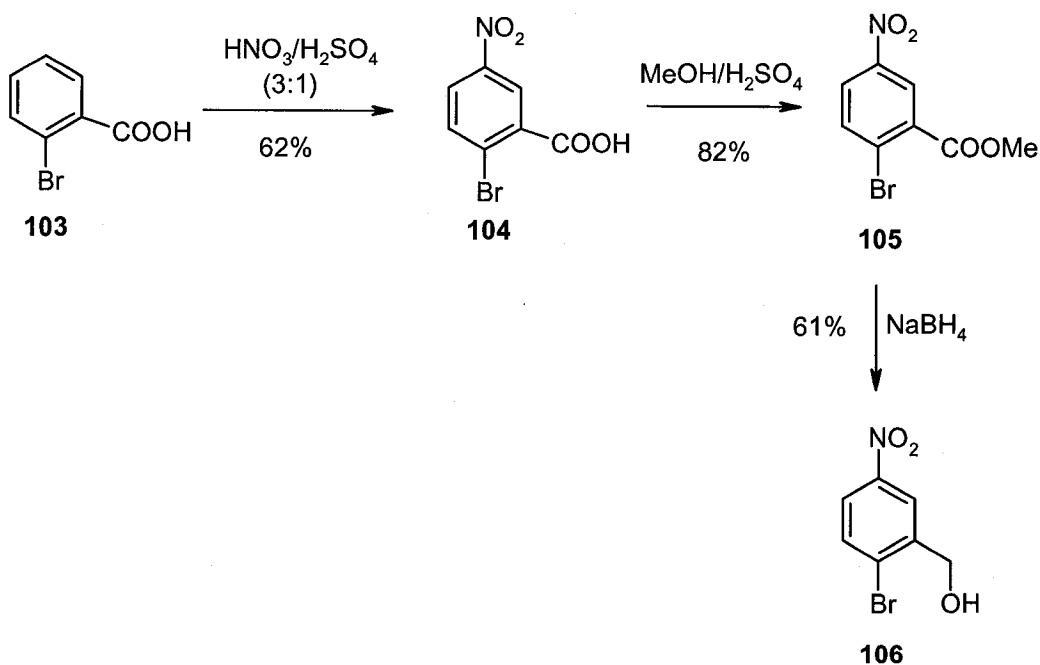
2-Bromo-5-nitrobenzyl alcohol (106) was then subjected to lithium-halogen exchange using *tert*-butyllithium (Scheme 2.7). Unfortunately, this reaction led to extensive decomposition right after the addition of *tert*-butyllithium to the solution of 106

in either dry tetrahydrofuran or diethyl ether at -78°C. When alcohol **106** was protected with the methoxymethyl (MOM) group to give **107**, its reaction with *tert*-butyllithium yet again resulted in decomposition. To confirm that the bromine atom does indeed exchange with *tert*-butyllithium, the reaction mixture was quenched with deuterium oxide. However, this led to decomposition as well and therefore the lithium-halogen exchange reaction was ruled out as a useful synthetic pathway to prepare our desired product.

Scheme 2.7

$$\xrightarrow[\text{2. Se or D}_2\text{O}]{\text{1. }\textit{tert}\text{-butyllithium}} \text{decomposition products}$$

106 R = H

107 R = CH$_2$OCH$_3$
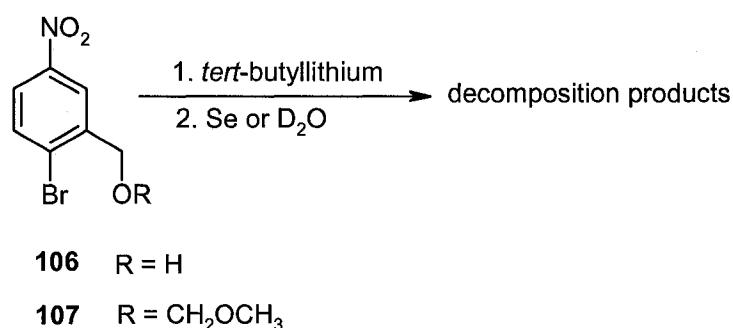
It has been reported that electron-deficient aromatic halides undergo substitution with alkali selenides and diselenides via an addition-elimination mechanism. This reaction was therefore attempted with **106** using different alkali diselenides, ranging from lithium diselenide to potassium diselenide, in polar solvents such as water, dimethylformamide (DMF) or hexamethylphosphoric triamide (HMPA) (Scheme 2.8). None of these reactions led to the formation of the expected diselenide and the only isolable material was unreacted **106**.

Scheme 2.8

Li$_2$Se$_2$/THF

Na$_2$Se$_2$/DMF

Na$_2$Se$_2$/HMPA

K$_2$Se$_2$/H$_2$O

K$_2$Se$_2$/H$_2$O, Cu

no reaction

106
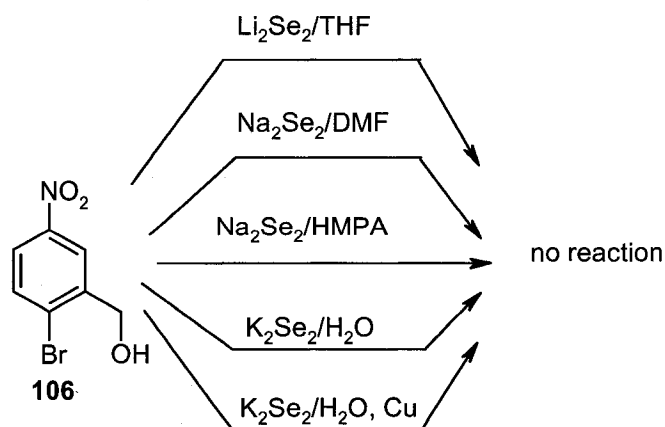
Refluxing alcohol **106** with potassium selenocyanate with copper in dioxane over a period of twelve hours, as reported in the literature for similar systems,[144] also failed and the starting material was recovered (Scheme 2.9).

Scheme 2.9
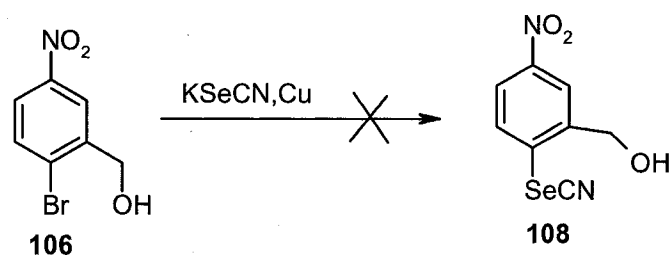
The preceding strategy therefore had to be re-evaluated and, in a different approach, one could envision the preparation of 2-amino-5-nitrobenzyl alcohol (**109**), followed by diazotation and reaction with potassium diselenide to form **110**, as shown in Scheme 2.10. Nevertheless, attempts to convert **106** to **109** were not successful.

Scheme 2.10
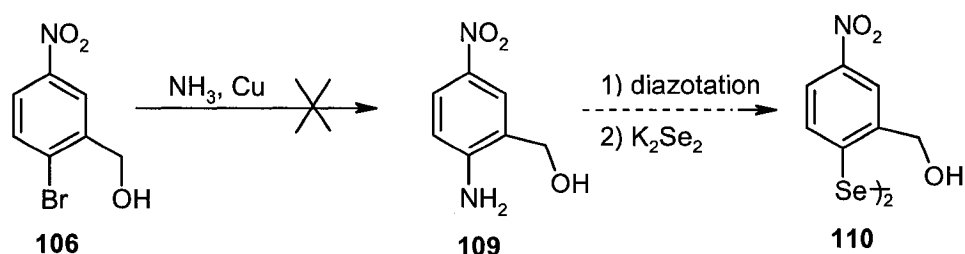
On the other hand, the aromatic nucleophilic substitution of 2-bromo-5-nitrobenzoic acid (**104**) with aqueous ammonia in the presence of copper by a modified literature procedure[145] afforded 5-nitroanthranilic acid (**111**) in 74% yield (see Scheme 2.11). We attempted to reduce the carboxylic acid in the presence of the nitro group, as described previously for **104** (Scheme 2.6), by converting the acid to its methyl ester **112** and treating it with sodium borohydride. Unfortunately, the reduction failed even when

up to 20 equivalents of sodium borohydride were used in refluxing water/dioxane for several hours.

Scheme 2.11
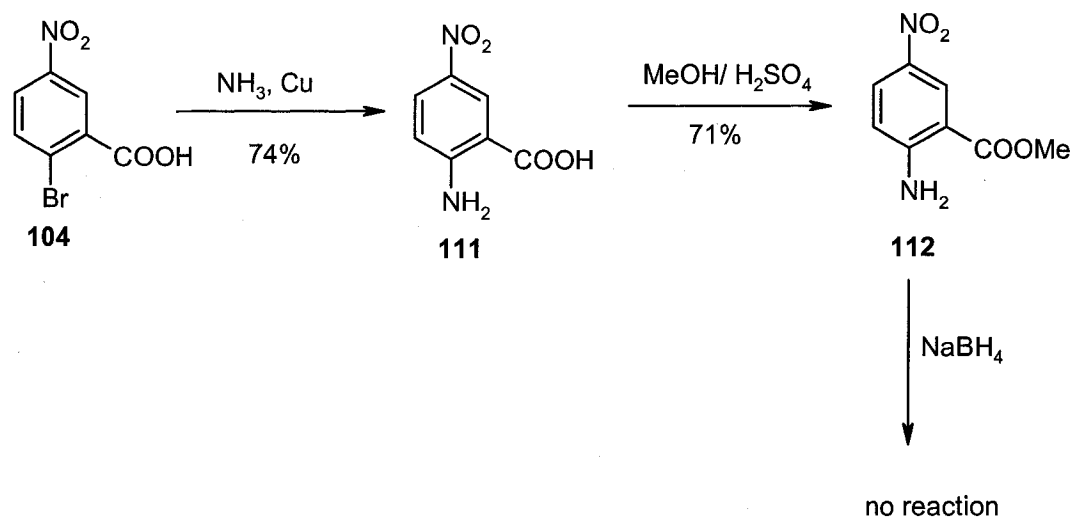
The difficult reduction of ester **112** was circumvented by the use of zinc borohydride, which is capable of reducing esters[146] and in some cases even carboxylic acids[147] (Scheme 2.12). Amino alcohol **109** was thus prepared and diazotized in the usual manner. Due to its very low solubility in water, diazotation was carried out in dioxane/water solution with subsequent reaction of **113** with potassium diselenide. Unfortunately, this reaction sequence failed to provide the desired diselenide **110**. Its synthesis was finally achieved by the preparation of selenocyanate **108**, which was then reduced using sodium borohydride, followed by acidification and aerial oxidation. The synthesis of seleninate ester **92** was accomplished via allyl selenide **114**, even though only in an NMR tube.

Scheme 2.12
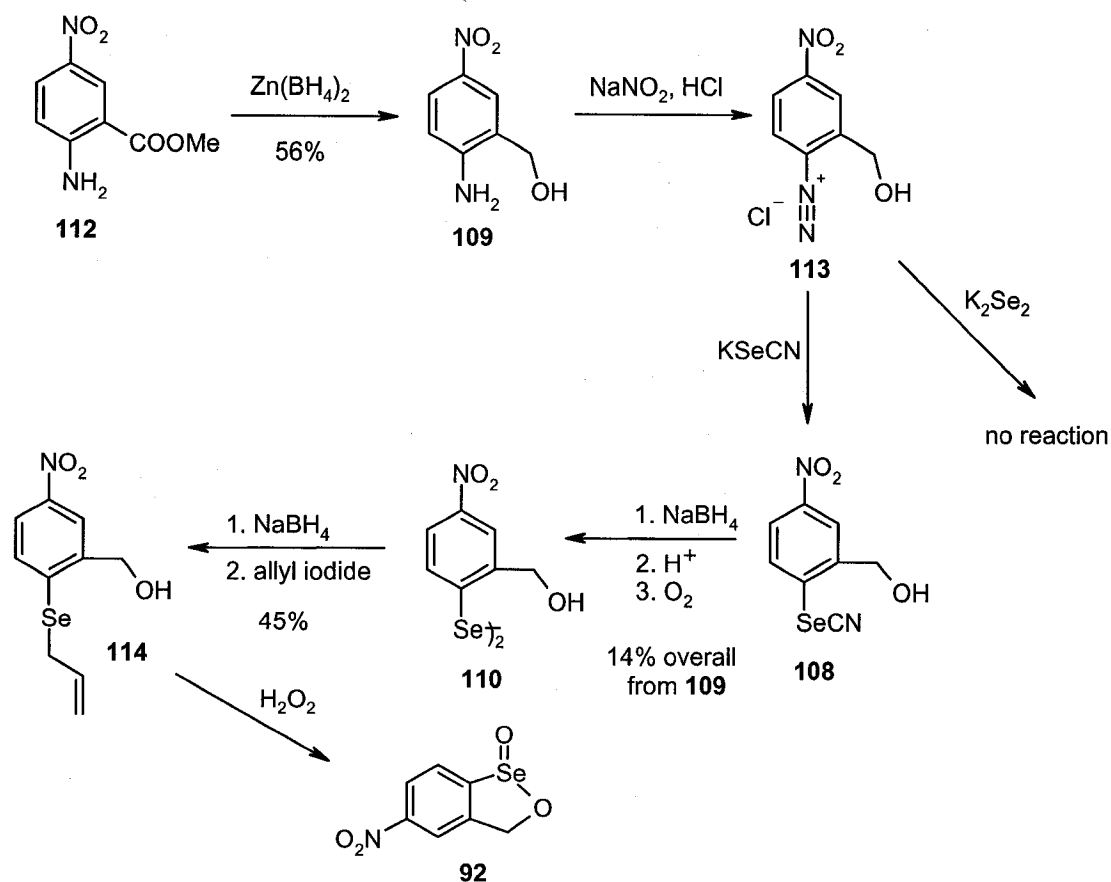
Conversion of the amino alcohol **109** to diselenide **110** was thus accomplished in a poor yield of 14 %. Moreover, the inability to prepare the corresponding selenide, which could be used later for the synthesis of spirodioxyselenuranes (see Section 2.7), prevented this synthetic route from being useful. We therefore decided to prepare the corresponding *p*-fluoro derivative instead, as the representative cyclic seleninate ester with an electron-withdrawing moiety.

2.4.5 Preparation of *p*-Fluorobenzo-1,2-oxaselenolane *Se*-Oxide (93)

The synthesis of **93** followed an identical path to that of the unsubstituted cyclic seleninate ester **89**, and is shown in Scheme 2.13. Starting from commercially available 5-fluoroanthranilic acid (**115**), 2,2`-diselenobis(5-fluorobenzoic acid) (**116**) was prepared

in 88% yield via a diazotation reaction, followed by introduction of potassium diselenide prepared in the usual manner. Subsequent reduction of the carboxylic acid and diselenide moieties using lithium aluminum hydride, and allylation provided the allyl selenide **117**. Finally, *p*-fluorobenzo-1,2-oxaselenolane *Se*-oxide (**93**) was prepared in 78 % yield by oxidation of **117** with excess *tert*-butyl hydroperoxide.

Scheme 2.13
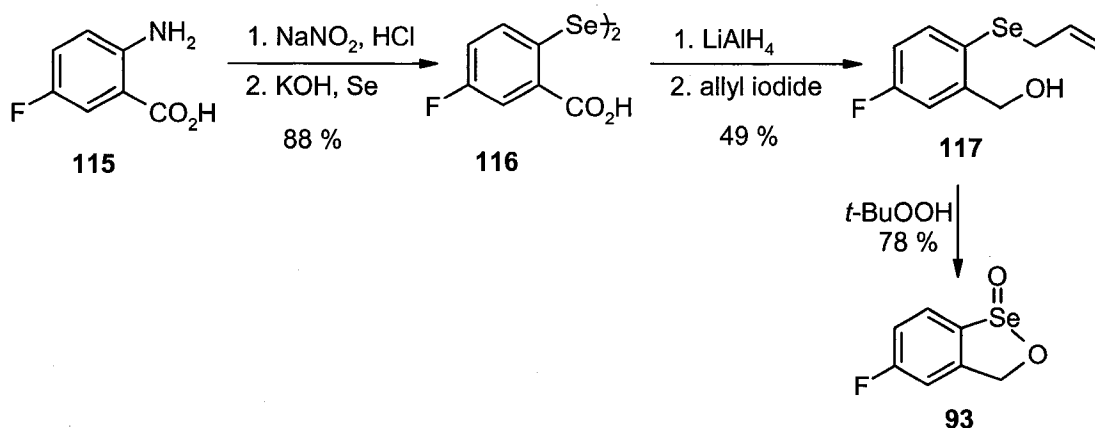
Recrystallization from ethyl acetate afforded a sample with an acceptable elemental analysis. The proton and ^{13}C NMR spectra of **93** are presented in Figure 2.8. The fluorine atom with its spin of ½ and high natural abundance, as well as high sensitivity, couples to both protons and ^{13}C nuclei. When observing the proton spectrum, fluorine couples to all aromatic protons of **93**. Thus, ^{1}H-^{19}F coupling constants for protons *ortho* and *meta* to the fluorine substituent were determined to be 6.8 Hz and 5.0 Hz, respectively, which are values in good agreement with the literature.[148] Diastereotopic protons of the methylene group can be seen as two doublets at δ 5.88 and 5.53 ppm, both with a coupling constant of 14.4 Hz. Coupling of the fluorine atom to ^{13}C nuclei was also observed in the carbon NMR spectrum, including a one-bond coupling of 251.7 Hz. In the ^{77}Se NMR spectrum, the selenium atom appears with a chemical shift of 1358.9 ppm.
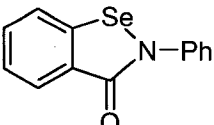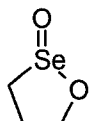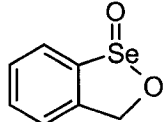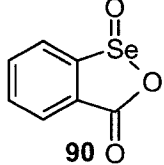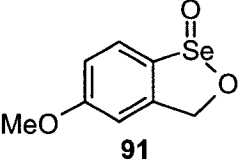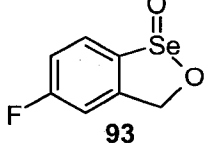
Figure 2.8 The ^{1}H NMR and ^{13}CNMR Spectra of **93**
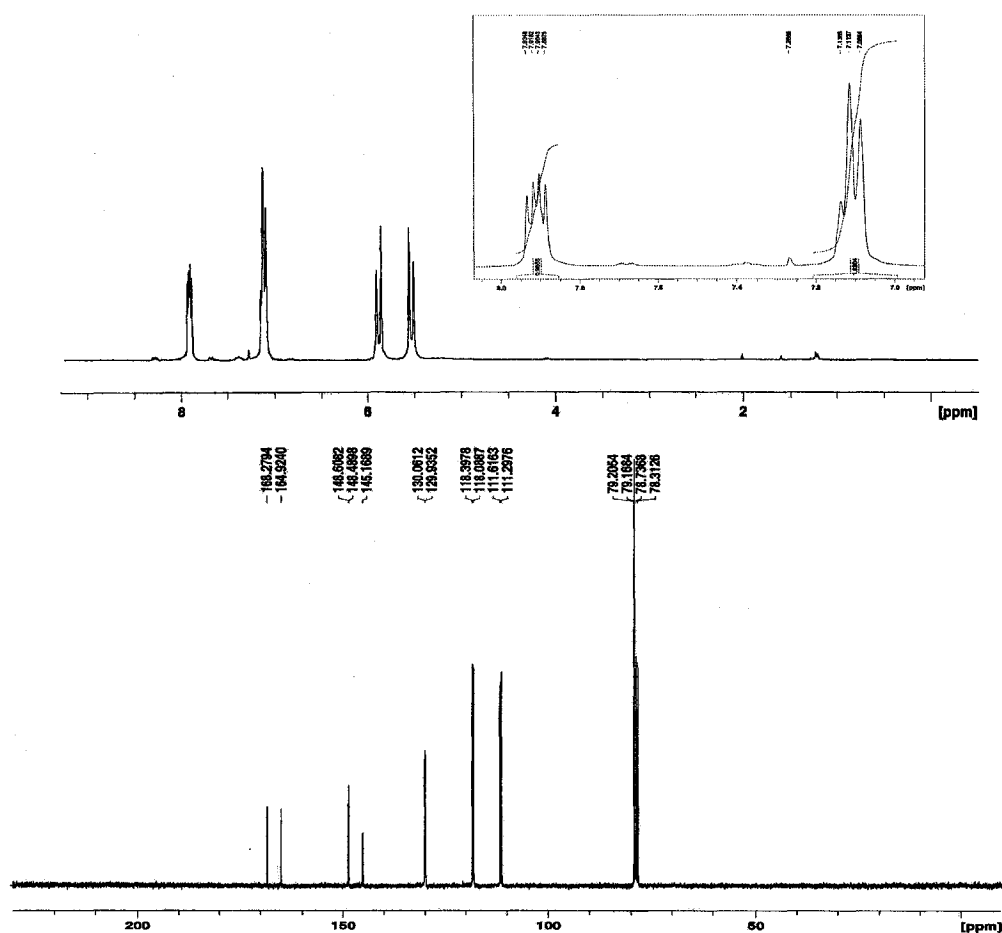
2.5 Catalytic Activity of Cyclic Seleninate Esters

Results of the measured catalytic activity of cyclic seleninate esters are presented in Table 2.1. Control experiments, which were performed in the absence of any catalyst, showed an extremely slow rate of reaction with half-lives of over 300 hours for *tert*-butyl hydroperoxide and 116 hours for 29% hydrogen peroxide respectively (entries 1-3). As discussed in Section 2.3, and presented in entries 4-6, concentration and type of oxidant play a role in the rate of the catalytic reduction of peroxides in the presence of ebselen. Thus, the catalytic activity of the aliphatic cyclic seleninate **46** was re-investigated and our results (entries 7-9) show that decreased concentration of *tert*-butyl hydroperoxide

dramatically increased $t_{1/2}$ of the model reaction from 2.5 h[84] for 90% *tert*-butyl hydroperoxide to 167 hours for 38% *tert*-butyl hydroperoxide. We also discovered that the $t_{1/2}$ for the reduction of hydrogen peroxide by **46** was 18 hours, which is considerably lower than with *tert*-butyl hydroperoxide of comparable concentration. Investigation of the aromatic cyclic seleninates revealed their generally diminished ability to reduce *tert*-butyl peroxide when compared to the aliphatic analogue. Unsubstituted cyclic seleninate ester **89** displayed $t_{1/2}$ of 162 hours in the presence of 56% *tert*-butyl hydroperoxide (entry 11), while the rate of reduction of 29% hydrogen peroxide in its presence was the same as in the case of **46** ($t_{1/2}$ = 18 hours, entries 10 and 12). Introduction of the electron–withdrawing carbonyl group into the seleninate ring further decreased the catalytic activity of **90** (entries 13 and 14). Moreover, our measurements show that the electron-donating methoxy group in **91** increased the catalytic activity in the reduction of 56% *tert*-butyl hydroperoxide relative to the unsubstituted analogue **89** (entries 11 and 15). In contrast to this finding, reduction of 32% hydrogen peroxide was slower when compared to **89** (entries 12 and 16). Similarly to **90**, the seleninate **93**, containing an electron-withdrawing fluoro substituent, proved to be inferior in catalytic activity when compared to unsubstituted cyclic seleninate **89** (compare entries 11 and 12 with 17 and 18). It therefore appears that electron-withdrawing groups or substituents in **90**, and **93** retard the reduction of both *tert*-butyl hydroperoxide and hydrogen peroxide relative to the unsubstituted catalyst **89**, while the donating substituent in **91** accelerates this process only for *tert*-butyl hydroperoxide.

Table 2.1 Catalytic Activities of Cyclic Seleninates[a]

Entry	Catalyst	$t_{1/2}$ (h)	Oxidant
1	Control	>300	90% t-BuOOH[b]
2	(no catalyst)	>300	56% t-BuOOH
3		116	29% H_2O_2
4		42	90% t-BuOOH
5	ebselen (3)	62	58% t-BuOOH
6		20	32% H_2O_2
7		2.5	90% t-BuOOH[b]
8		90	56% t-BuOOH
9	46	167	38% t-BuOOH
10		18	29% H_2O_2
11	89	162	56% t-BuOOH
12		18	29% H_2O_2
13	90	252	56% t-BuOOH
14		73	29% H_2O_2
15	91	81	58% t-BuOOH
16		28	32% H_2O_2
17	93	238	58% t-BuOOH
18		39	32% H_2O_2

[a] Reactions were performed with BnSH (0.031 M), the catalyst (0.0031 M), and either 56% TBHP (0.038 M), 38% TBHP (0.023 M), or 29% H_2O_2 (0.040 M) in CH_2Cl_2-MeOH (95:5) at 18 °C, except for entries 13 and 14, where the solvent was CH_2Cl_2-MeOH (4:1). [b] Data taken from ref. 84

2.6 Exploration of the Catalytic Mechanism of Cyclic Seleninates

The diminished catalytic activity of **46** in the presence of lower concentrations of *tert*-butyl hydroperoxide led us to re-investigate its catalytic mechanism (see Scheme 1.13). This decrease can be attributed to the accumulation of the selenenyl sulfide **52** at lower hydroperoxide concentrations. It had previously been identified in the competing deactivation pathway in the catalytic cycle of **46**. The present results with lower concentrations of *tert*-butyl hydroperoxide are in contrast with the original measurements done by Back and Moussa, with 90% *tert*-butyl hydroperoxide, where selenenyl sulfide **52** was formed only as a minor product.[84] Clearly, the relative concentration of peroxide versus thiol is important in partitioning of the reaction between the normal pathway, favoured by high peroxide concentration, and the deactivation pathway, favoured by high thiol concentration. Moreover, when **46** was reacted with three moles of benzyl thiol (Scheme 2.14), it resulted in instant quantitative formation of **52**.

Scheme 2.14

46 + 3 BnSH → **52** + BnSSBn + H$_2$O
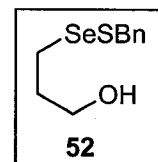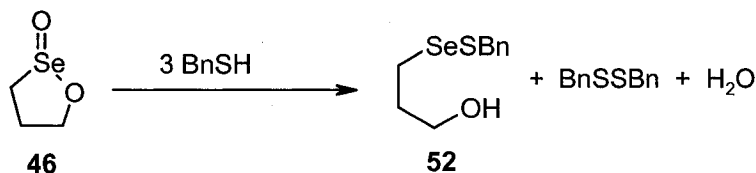
In order to rationalize the lower observed catalytic activity of the aromatic analogues of **46**, several control experiments with cyclic seleninate **89** were performed. They revealed that compound **89** reacted significantly with neither *tert*-butyl hydroperoxide nor hydrogen peroxide over a period of ten days (Scheme 2.15).

Scheme 2.15

89, 10 eq. *t*-BuOOH or H$_2$O$_2$, 10 days, CDCl$_3$ → no reaction
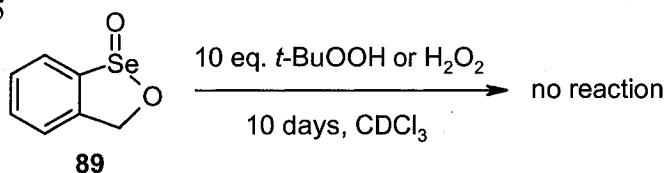
Conversely, **89** reacted rapidly with benzyl thiol in the absence of a peroxide, to form the selenenyl sulfide **118**, which was isolated in 86% yield (Scheme 2.16). Additionally, when the model reaction mixture was analyzed by HPLC immediately after its commencement, the initial consumption of three equivalents of benzyl thiol and the immediate appearance of selenenyl sulfide **118** was revealed.

Scheme 2.16
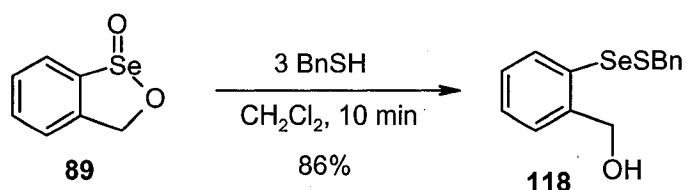
The selenenyl sulfide **118** proved to be considerably stable. Its role in the catalytic cycle was further investigated. Our control experiments showed that it acts as a poor catalyst for the reduction of peroxides in the presence of thiols and it produced a $t_{1/2}$ of 192 hours in the presence of 56% *tert*-butyl hydroperoxide. Moreover, when **118** was subjected to excess hydroperoxide, it very slowly reformed the cyclic seleninate ester **89**. This reaction presumably occurs via oxidation of the selenium atom to form thioseleninate **119** followed by cyclization (Scheme 2.17).

Scheme 2.17
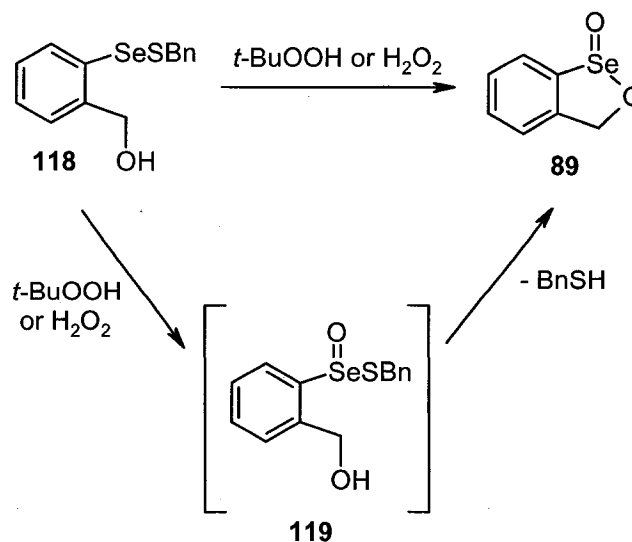
Additionally, no reaction between the selenenyl sulfide **118** and benzyl thiol was observed over a period of 10 days (Scheme 2.18).

Scheme 2.18
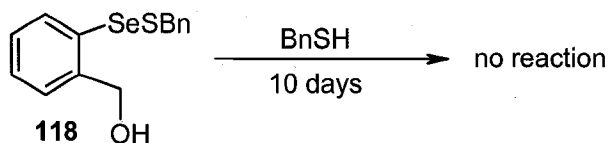
Closer analysis of the HPLC plot of the reaction mixture, where **89** was present as a catalyst (Figure 2.9), revealed the slow appearance of diselenide **120** (retention time = 2.24 min). Its formation presumably takes place by disproportiation of the selenenyl sulfide **118** (retention time = 5.00 min). After 213 hours no selenenyl sulfide was observed while a strong peak for the diselenide appeared (Figure 2.9, graph b).
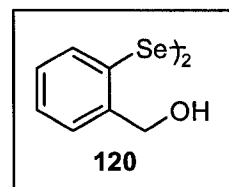
Figure 2.9 Model Reaction in the Presence of **89** and 56% *tert*-Butyl Hydroperoxide

(a) Injection after 89 hours

(b) Injection after 213 hours
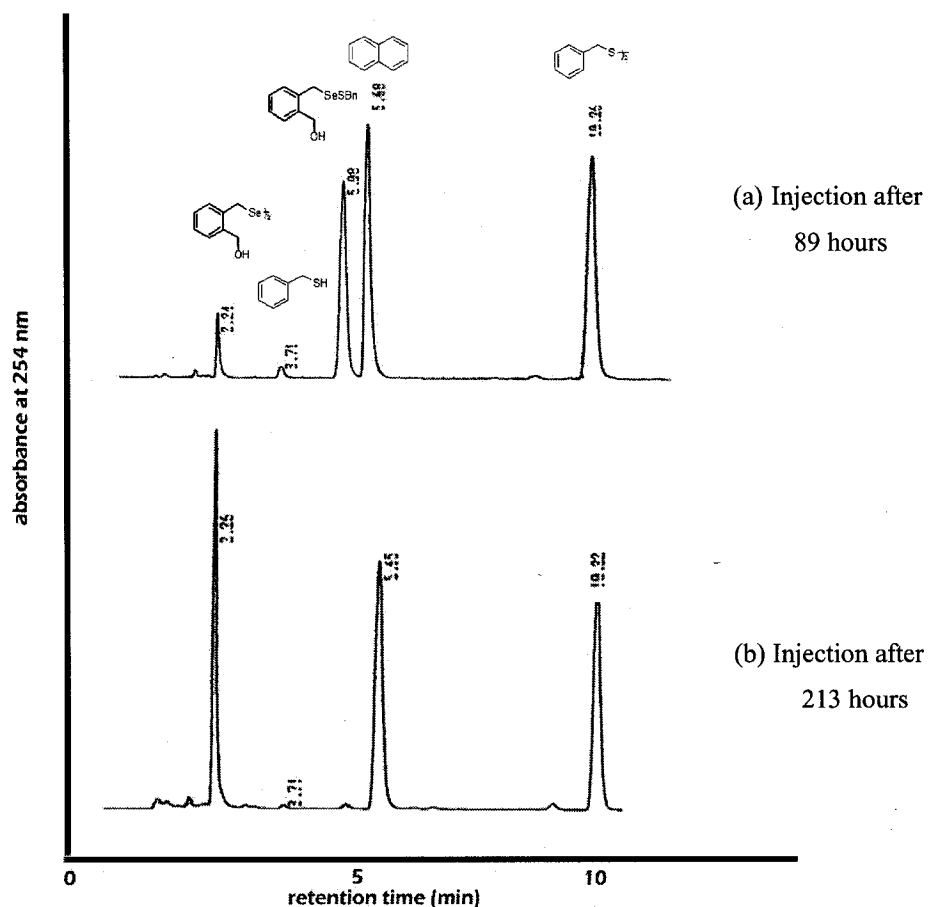
A further control experiment showed that diselenide **120** did not react with benzyl thiol; however, its very slow oxidation afforded the cyclic seleninate ester **89**, possibly via the anhydride **121** (Scheme 2.19).

Scheme 2.19
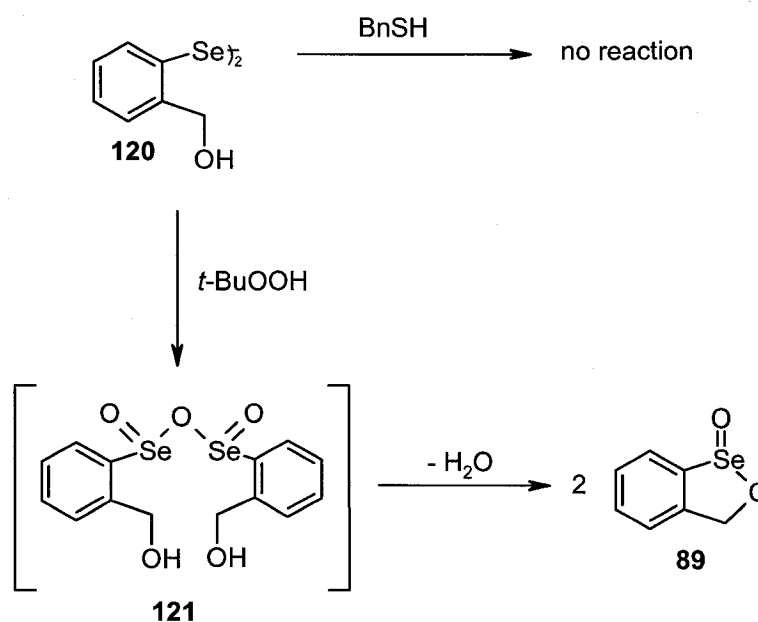
On the basis of the control experiments described above, the catalytic mechanism, shown in Scheme 2.20, can be proposed for the reduction of *tert*-butyl hydroperoxide by **89** in the presence of benzyl thiol. First, the cyclic seleninate **89** reacts instantly with benzyl thiol to form the thioseleninate ester **119**. Even though this reaction is very fast, formation of intermediate **119** is associated with the appearance of a transient blue colour, which disappears within five seconds after the addition of thiol. It was previously shown that other thioseleninate species are characterized by a similar blue colour.[149] Intermediate **119** then undergoes reaction with a second molecule of benzyl thiol to form selenenic acid **122** and a molecule of disulfide. In contrast to the case of aliphatic seleninate **46**, we postulate that selenenic acid **122** does not get oxidized by peroxide, but rather reacts with a third molecule of benzyl thiol to afford selenenyl sulfide **118**. Oxidation of **118** to **119** is the rate-limiting step in the catalytic cycle. Thioseleninate

ester **119** then returns to the catalytic cycle by reaction with more thiol. Disproportiation of **118** to diselenide **120** also takes place, but is an even slower process. Finally, diselenide **120** undergoes a very slow oxidation with *tert*-butyl hydroperoxide to reform the cyclic seleninate **89**.

Scheme 2.20 Proposed Catalytic Mechanism for Hydroperoxide Reduction by 89
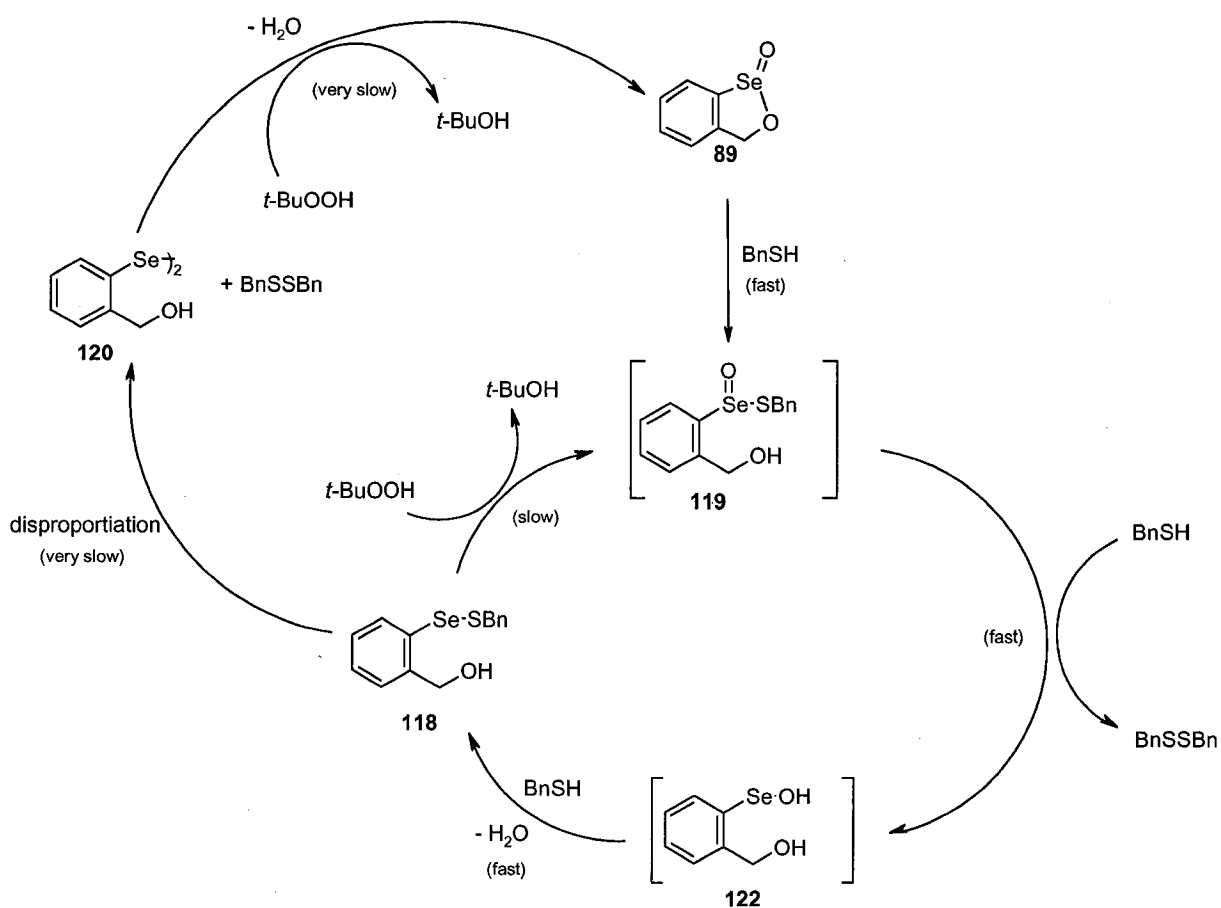
It therefore appears that the deactivation pathway involving the selenenyl sulfide **118**, and eventually the diselenide **120**, both of which are poor catalysts, is more dominant in the case of the benzo analogue **89** than in that of parent aliphatic cyclic seleninate **46**. This in turn results in a longer $t_{1/2}$ when **89** is used in the model assay compared to **46**.

In addition, examination of the benzoyl derivative **90** revealed decreased catalytic activity that can be attributed to the electron-withdrawing carbonyl moiety, which decreases electron density on the selenium atom. This in turn facilitates its reaction with the nucleophilic thiol and suppresses its reaction with peroxides. As a result, it ultimately leads to increased formation of the selenenyl sulfide **123** and diselenide **12**, both of which are relatively inert under the conditions of the model reaction. Hence, compound **123** was prepared independently by the reaction of **90** with benzyl thiol, and was fully characterized and examined in the model assay. It proved to be an extremely poor catalyst, where $t_{1/2}$ for the reduction of 56% *tert*-butyl hydroperoxide was over 300 hours and for 29% hydrogen peroxide was 89 hours, respectively. These values are very close to the ones obtained in the absence of any catalyst. As expected, **93** displayed lower catalytic activity than **89** due to the electron-withdrawing nature of the fluorine atom as in the previous case. 5-Methoxy derivative **91** proved to be superior in catalytic reduction of 58% *tert*-butyl hydroperoxide compared to unsubstituted derivative **89** because of the increased electron density on the selenium atom and therefore greater ease of oxidation of the corresponding selenenyl sulfide. A slower reduction of 32% hydrogen peroxide by **91** compared to **89** may be the result of a more rapid formation of the corresponding diselenide from the selenenyl sulfide, which further lowers catalytic activity of **91**. However, an unequivocal explanation for the relatively low activity of **91** toward hydrogen peroxide, as compared to **89**, is not available at this time.
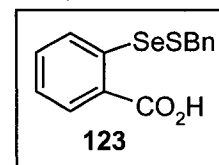
2.7 Aromatic Spirodioxyselenuranes as GPx Mimetics

Spirodioxyselenuranes are a novel class of organoselenium compounds and there are merely a handful of examples reported in the literature, of which just one is aromatic. A series of aliphatic spirodioxyselenuranes, prepared in our group, were screened for their glutathione peroxidase-like activity.[85] The novel spirodioxyselenurane **53** exhibited very strong catalytic activity in destroying hydroperoxides in the presence of thiols. The present work comprises an extension of this research and involves the preparation of a

series of aromatic derivatives of **53**. All the prepared aromatic spirodioxyselenuranes depicted in Figure 2.10 are novel compounds with the exception of **125**,[150] which is the only aromatic spirodioxyselenurane found in the literature to date. Besides studying the unsubstituted aromatic derivative **124**, we wished to synthesize compounds **125**, **126** and **127**, in order to evaluate their GPx-like activity with emphasis on establishing the effects of substituents. Additionally, the novel and unusual cyclic acylaminoselenonium salts **128** and **129** were prepared and investigated for glutathione peroxidase-like behaviour along with the synthesis of the unstable spirodiazaselenurane **130**.

Figure 2.10 The Novel Aromatic Derivatives of Spirodioxyselenurane **53**
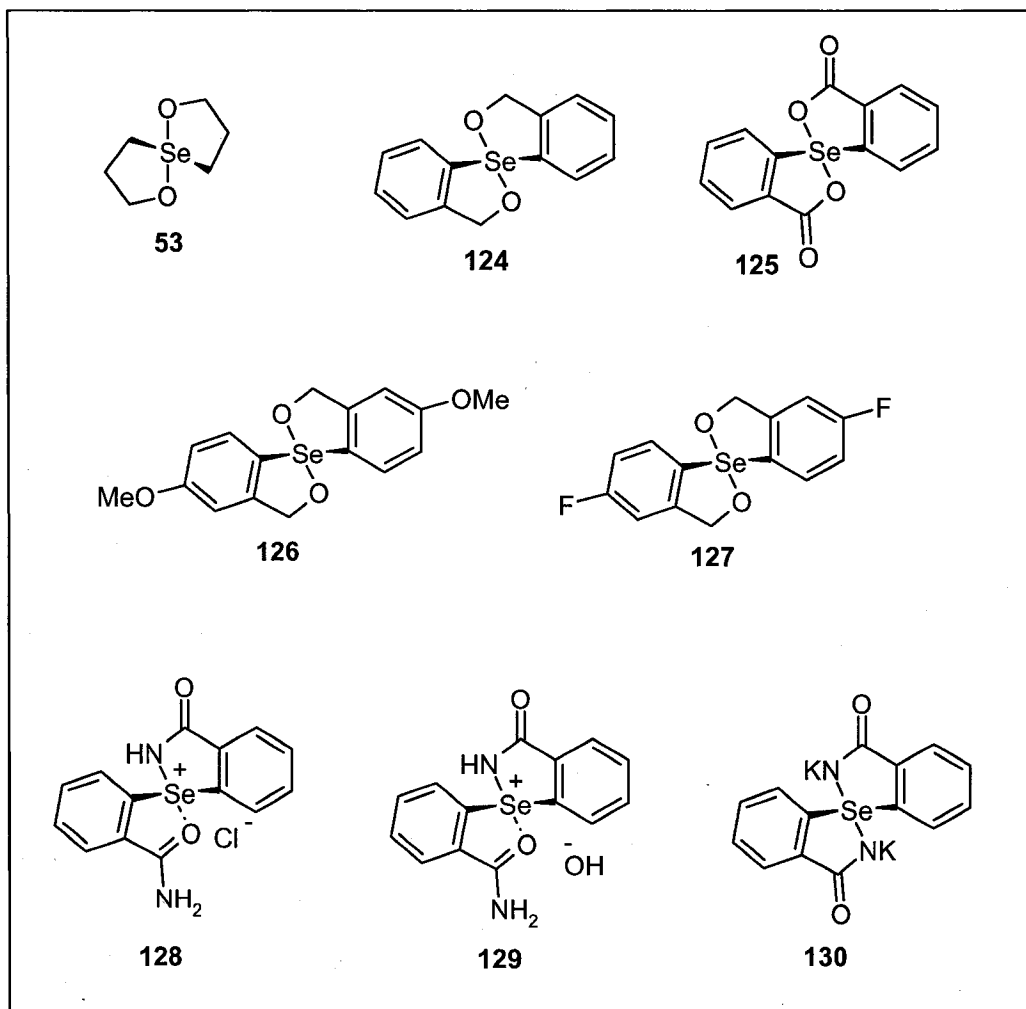
Syntheses of the above compounds will be described in Sections 2.7.1 to 2.7.5 and the evaluation of their catalytic activity, along with proposed mechanisms, will be discussed in Section 2.8 and 2.9, respectively.

2.7.1 Preparation of Spirodioxyselenurane 124

For the purpose of synthesizing spirodioxyselenurane **124** (Scheme 2.21), the previously prepared 2,2`-diselenobis(benzoic acid) **(12)** was converted to 2,2`-selenobis(benzoic acid) **(131)** by a modified procedure of that reported by Dáhlen and Lindgren.[150] Its reduction to 2,2`-selenobis(benzyl alcohol) **(132)** was accomplished in 53% yield by refluxing the diacid with three moles of lithium aluminum hydride in dry tetrahydrofuran for 90 minutes. Under these conditions, small amounts of diselenide **120** were isolated, which presumably forms via reductive cleavage of the selenium-carbon bond in selenide **132**, followed by aerial oxidation of the corresponding selenolate. When the reaction was continued for 3 hours, the major product was the diselenide **120**. Fortunately, separation of **132** from diselenide **120** could be achieved by a careful column chromatography. Subsequent oxidation of **132** with excess hydrogen peroxide yielded **124** in 98% yield.

Scheme 2.21 Synthesis of Spirodioxyselenurane **124**
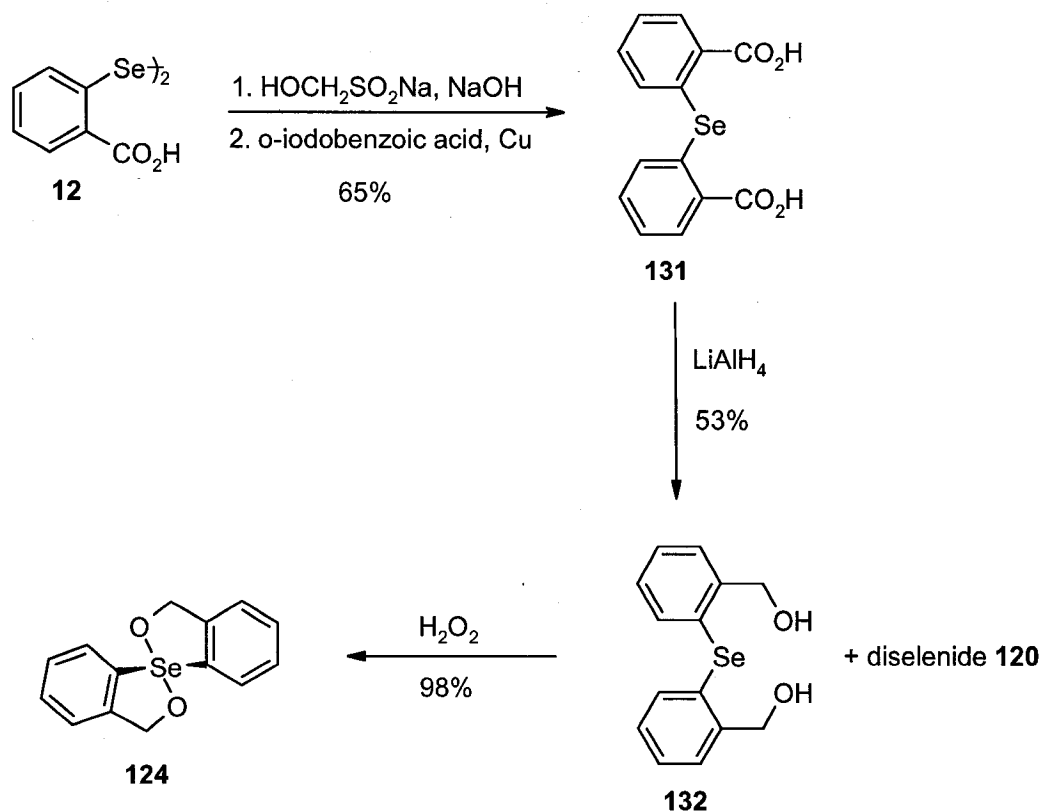
Spirodioxyselenurane **124** is a stable compound and may be stored at room temperature for a period of several months. The proton NMR spectrum of **124** is presented in Figure 2.11 and shows the signal from a proton in the *ortho* position to the selenium atom as a doublet with a chemical shift of δ 8.03 ppm as well as the two coincidentally equivalent methylene protons (CH_2O), occurring as a singlet at δ 5.3 ppm. As expected, the ^{13}C NMR spectrum of **124** exhibits equivalent peaks for the two benzyl systems. In the ^{77}Se NMR spectrum, a peak was observed at 802.4 ppm, with a significant upfield shift when compared to the aliphatic spirodioxyselenurane **53**.

Figure 2.11 The ^{1}H NMR Spectrum of **124**
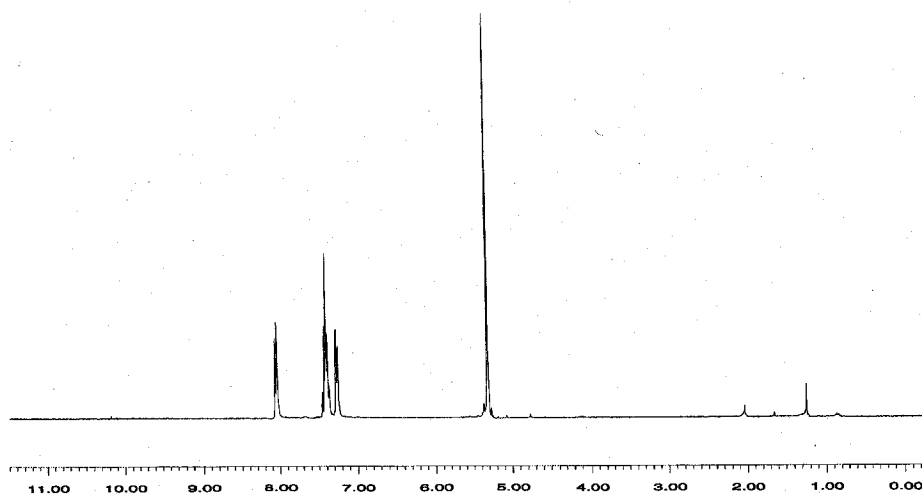
2.7.2 Preparation of Spirodioxyselenurane 125

Benzoyl derived spirodioxyselenurane **125** is a known compound and was prepared in 73% yield by a literature procedure,[150] whereby 2,2`-selenobis(benzoic acid) (**131**) was oxidized with hydrogen peroxide in acetic acid (Scheme 2.22).

Scheme 2.22 Synthesis of Spirodioxyselenurane **125**
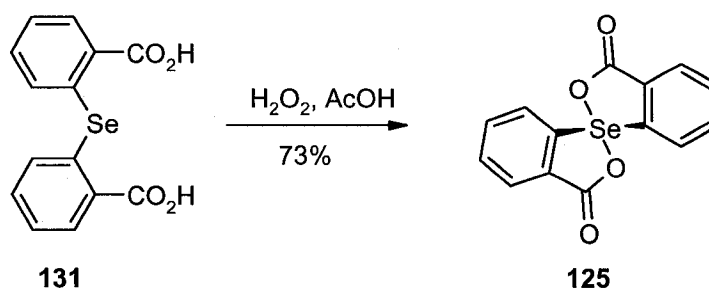
Compound **125** displayed high polarity and an extremely high melting point (326-328 °C). Its polarity and poor solubility in most solvents resulted in difficulties with its purification. The originally reported dissolution of the crude product in hot alkaline solution with charcoal, followed by filtration and acidification, did not provide a

spectroscopically pure product (mp 310-322 °C). Moreover, the presence of traces of base or acid during the kinetic measurements of catalytic activity strongly augmented the rate of the reaction and therefore they must not be present. Recrystallization from ethyl acetate provided **125** in pure form, which was confirmed by NMR spectroscopy and a satisfactory elemental analysis.

2.7.3 Preparation of Spirodioxyselenurane 126

The 4-methoxy-substituted spirodioxyselenurane **126** was synthesized using a lithium-halogen exchange reaction (Scheme 2.23). Previously prepared 2-bromo-5-methoxybenzyl alcohol **(98)** (for details see Scheme 2.4) was treated with three equivalents of *tert*-butyllithium in dry tetrahydrofuran at -78 °C to afford the lithiated product **99**, which was subjected to reaction with selenium (II) diethylthiocarbamate $(Se(dtc)_2)$. This compound is a source of electrophilic selenium and was prepared by a method reported by Foss.[151] The disadvantage of this reaction is the fairly quick decomposition of $Se(dtc)_2$ under the reaction conditions, which results in low yields (28%) of **133**. Its oxidation with *tert*-butyl hydroperoxide yielded spirodioxyslenurane **126** in 89% yield.

Scheme 2.23 Synthesis of Spirodioxyselenurane **126**
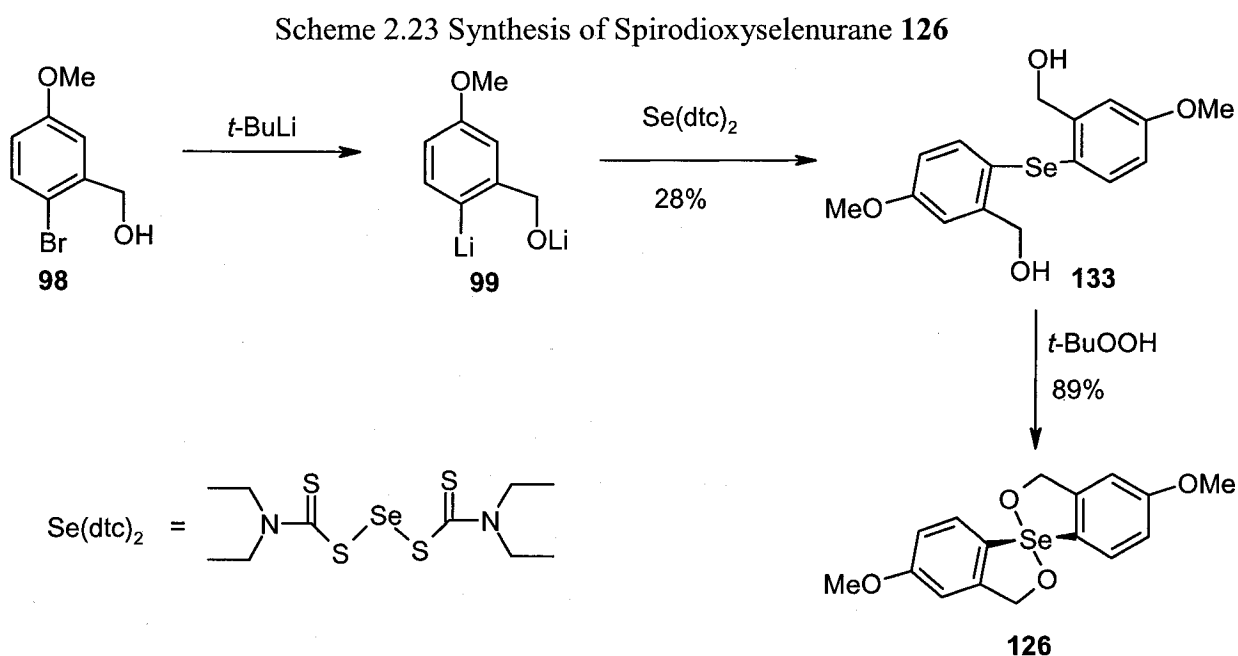
2.7.4 Preparation of Spirodioxyselenurane 127

The intended retrosynthetic pathway for preparing the *p*-fluoro-substituted spirodioxyselenurane **127** is depicted in Scheme 2.24. We envisioned its synthesis by oxidation of selenide **135**, which could be obtained after reduction of diacid **134**, prepared from commercially available 5-fluoroanthranilic acid (**115**).

Scheme 2.24 Retrosynthetic Pathway of **127**
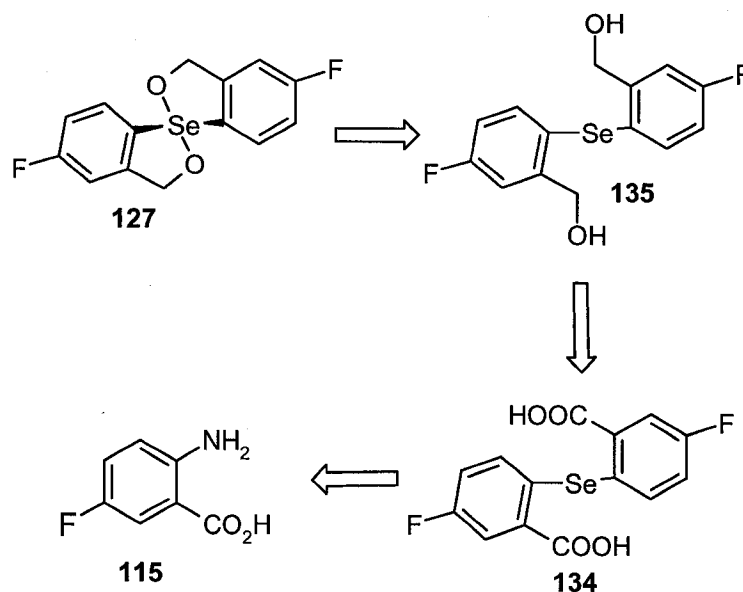
The attempted direct synthesis of **134** by diazotation of **115**, followed by substitution with sodium selenide was not successful (Scheme 2.25). When the diazonium salt of **115** was treated with sodium selenide, prepared by the reduction of selenium with sodium borohydride, only decomposition products were obtained. Additionally, the reaction of diazotized **115** with sodium selenide prepared by refluxing black selenium in alkaline rongalite C solution under an argon atmosphere led, surprisingly, only to the formation of diselenide **116**. The main reason for this negative outcome is probably the low stability of sodium selenide toward the acidic solution used to produce the diazonium salt. Efforts to succeed by adjusting the pH of the diazonium salt solution with sodium acetate were not successful. Our attention then turned to amino alcohol **136**, which was prepared using a literature procedure by reduction of **115** with

lithium aluminum hydride.[152] Unfortunately, **136** proved susceptible to the same problems as **115**.

Scheme 2.25
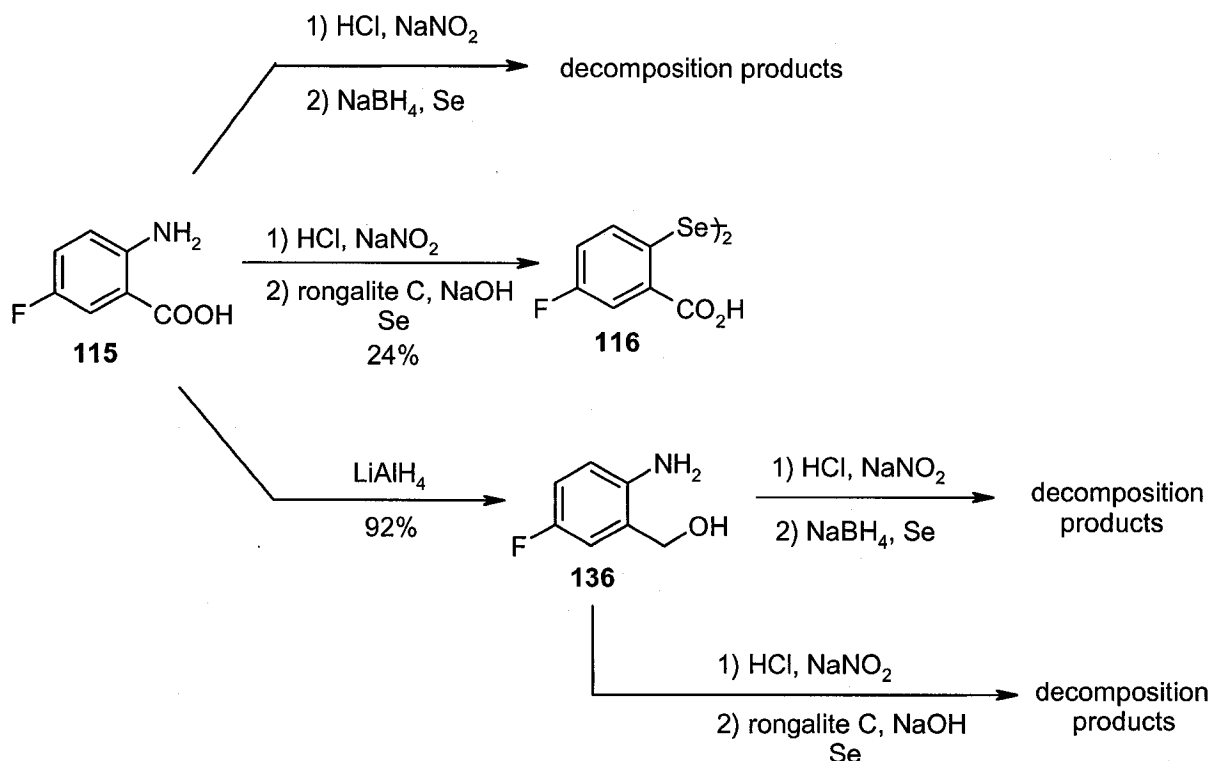
We next considered the reduction of diselenide **116** to the corresponding selenolate anion, which might then react with the appropriate diazonium salt. As shown in Scheme 2.26, the attempted reduction of **116** with sodium borohydride to the corresponding selenolate, followed by its reaction with the diazonium salt of **115**, resulted in isolation of the starting material. In a subsequent effort, diacid **116** was reduced to alcohol **137** in 42% yield using lithium aluminum hydride. Fortunately, its subsequent reduction with sodium borohydride and reaction of the formed selenolate ion with the diazonium salt of amino alcohol **136** yielded our desired product **135** in 34% yield. Importantly, this reaction was only successful in tetrahydrofuran-water (1:1)

solution, out of several solvents investigated. Oxidation of selenide **135** with hydrogen peroxide afforded our target compound **127**.

Scheme 2.26
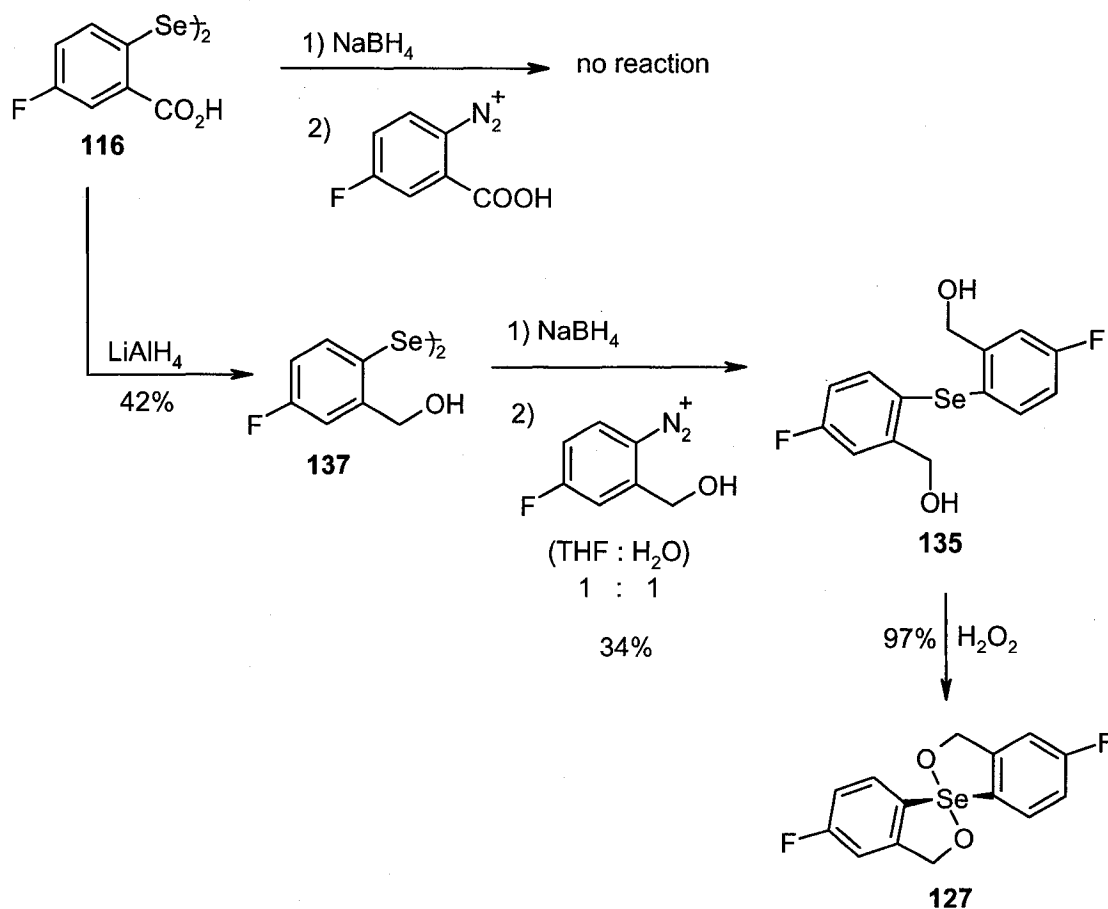
The ^{1}H NMR spectrum of **127** is depicted in Figure 2.12. The proton in the *ortho* position relative to the selenium atom appears as a doublet of doublets due to coupling to the neighbouring proton ($J = 3.7$ Hz) as well as the fluorine atom ($J = 2.5$ Hz). All the remaining aromatic protons are also coupled to the fluorine atom. The diastereotopic CH_2O protons appear as two doublets at δ 5.32 and 5.26 ppm respectively, with a coupling constant of 14.9 Hz. In the ^{13}C NMR spectrum, strong coupling to the fluorine atom can be observed, resulting in splitting of each ^{13}C signal. The ^{77}Se NMR spectrum shows a signal at 807.1 ppm.

Figure 2.12 Proton NMR and ^{13}C NMR Spectra of **127**
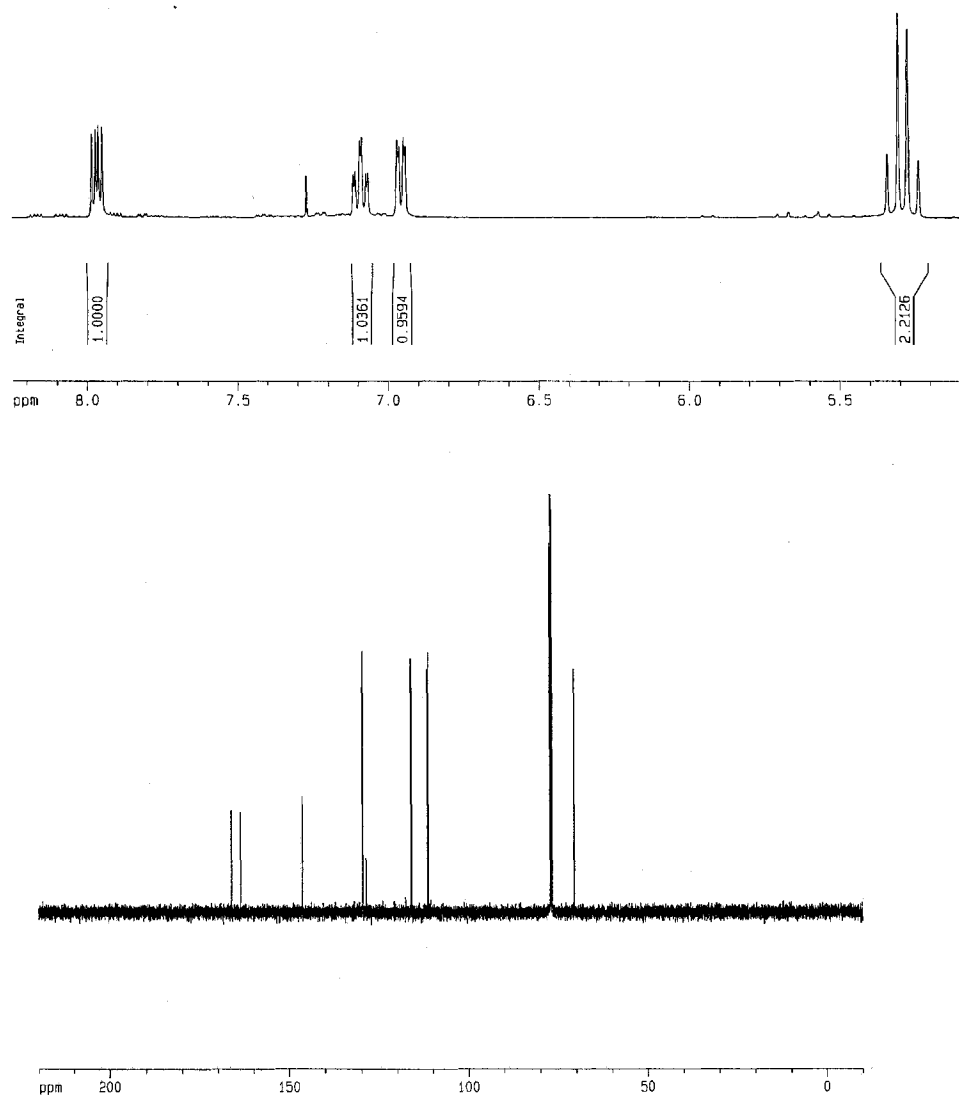
2.7.5 Preparation of Spirodiazaselenurane

An attractive idea that emerged during our work was the preparation of spirodiazaselenurane **138** (see Figure 2.13). There has been only one example of a tetracoordinated diazaselenurane **139**,[153] with two unsymmetrical apical ligands, reported to date.

Figure 2.13 Spirodiazaselenuranes

138   **139**
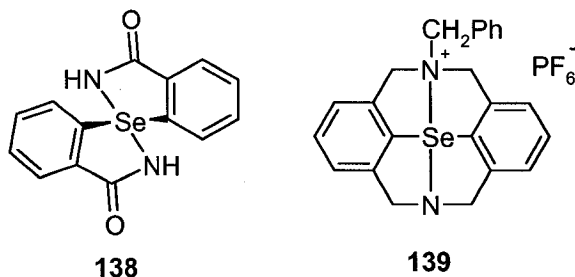
We commenced the synthesis of **138** by preparing 2,2'-selenobis(benzamide) (**141**) according to a modified procedure reported by Lesser[64] (Scheme 2.27).

Scheme 2.27

131   **140**   **141**

71% over 2 steps
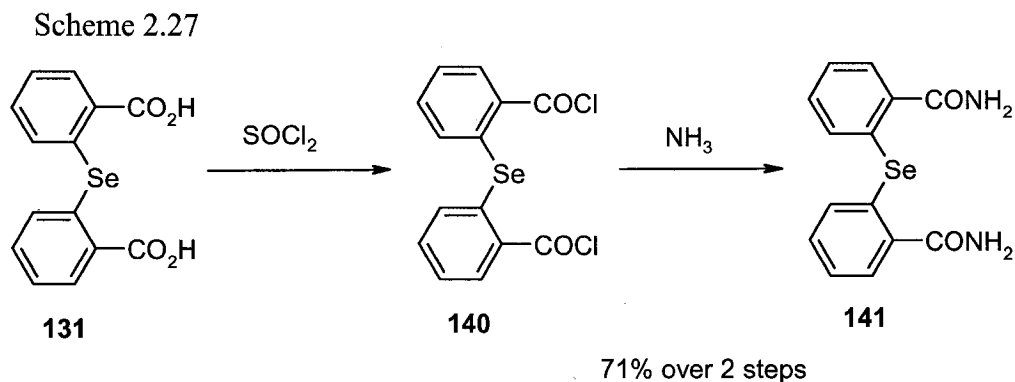
Oxidation of **141** with two equivalents of *N*-chlorosuccinimide (NCS) in methanol/dichloromethane (1:1), as shown in Scheme 2.28, didn't yield the desired product **138**, but rather an interesting compound with unexpectedly magnetically non-equivalent aromatic rings.

Scheme 2.28

141   **138**
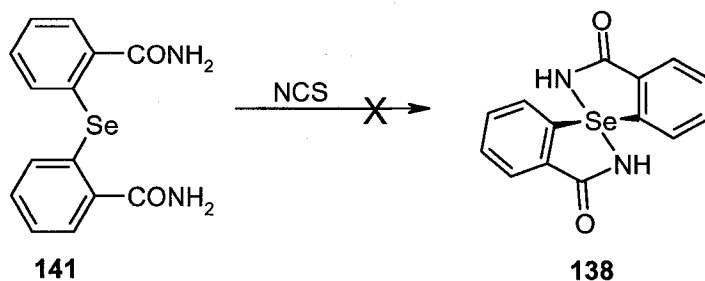
Both proton and ^{13}C NMR spectra of this product are portrayed in Figure 2.14, and based on this non-equivalence the expected structure of spirodiazaselenurane **138** was ruled out. The ^{1}H NMR spectrum shows three exchangeable protons, as confirmed by treatment with D$_2$O, as broad singlets with chemical shifts of δ 10.67 (peak A), 9.77 (peak B) and 9.33 (peak C) ppm. Additionally, a doublet with an integration of one appears at δ 8.42 ppm (peak D), suggesting a lack of symmetry. The ^{13}C NMR spectrum displays 14 separate peaks and the IR spectrum showed C=O stretching vibrations (amide I band) at 1665 cm^{-1} and N-H bending vibrations (amide II band) at 1595 and 1550 cm^{-1}.

Figure 2.14 ^{1}H and ^{13}C NMR Spectra of Oxidized Benzamide **141**
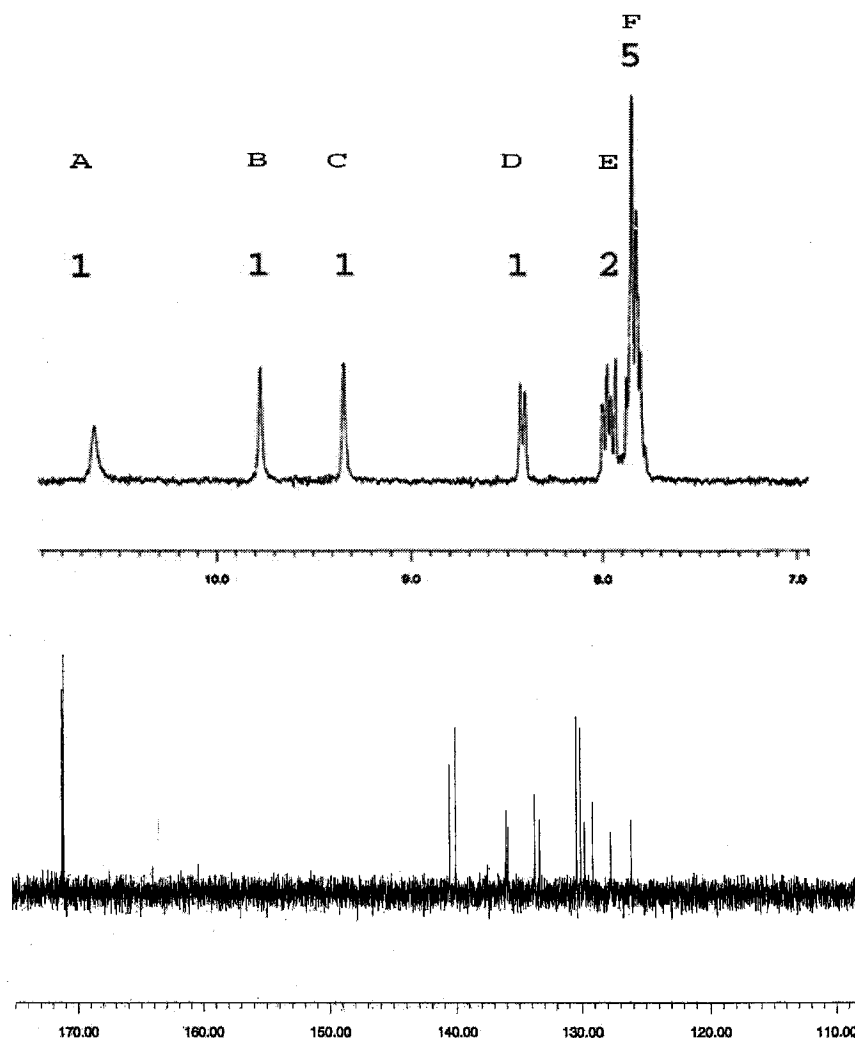
Additionally, 2D-NOE difference spectroscopy experiments suggested a strong through-space interaction of protons B and C, as well as of C and D. Based on the collected evidence, we propose the structure **128** for this compound, as presented in Figure 2.15. The atoms in **128** are numbered for convenience of discussion and are not based on IUPAC rules.

Figure 2.15 Proposed Structure of **128**
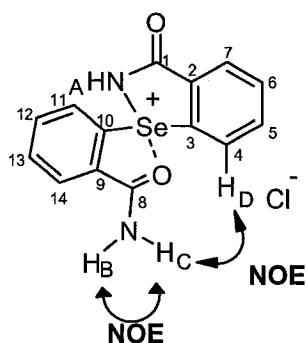
Two non-equivalent signals B and C belong to two protons in the free amido group (H_B and H_C). Their non-equivalence arises from the restricted rotation in the amido group. Exchangeable signal A belongs to the single proton (H_A) in the cyclized amido group. Proton H_D can be identified by its observed 2D-NOE effect with the free amido proton H_C. The difference in the chemical shifts of the protons in the *ortho* position (H-4 and H-11) relative to the selenium atom, arises from the non-equivalence of the two aromatic rings, as a consequence of the lack of symmetry. In the ^{77}Se NMR spectrum, a strongly downfield-shifted peak at δ 1658.5 ppm was observed. The mass spectrum of **128** could not be obtained using electron impact as the ionizing technique, because this method is not suitable for ionic structures. Therefore, electrospray ionization (ESI), a soft-ionizing method, was used. The spectrum was acquired using the positive mode in DMSO/water solution. In this solvent the ionic structure of **128** completely dissociates and therefore only ions with m/z = 319 and m/z = 341, which correspond to $[M-Cl+H]^+$ and $[M-Cl+Na]^+$, were found.

The proposed structure of **128** was confirmed by X-ray diffraction. Its ORTEP diagram is shown in Figure 2.16, and final atomic coordinates and the relevant geometric parameters are summarized in Tables 1-7 in Appendix D.

Figure 2.16 ORTEP Diagram of **128**
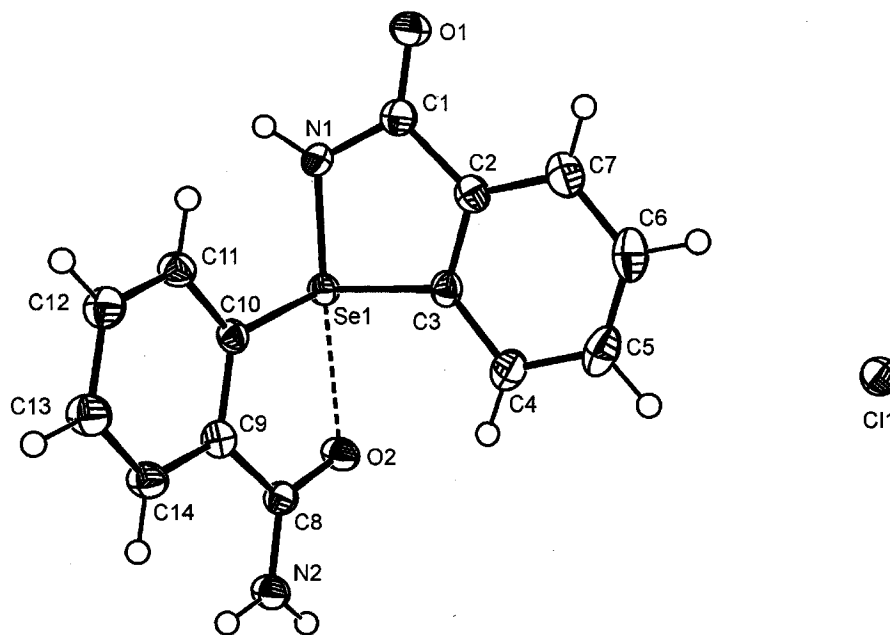
Diaryl(acylamino)selenonium salts have not been reported to date, but their sulfur analogues were studied in the past.[154] They are known to exhibit almost perfect trigonal bipyramidal geometry (TBP) around the sulfur atom. In our case, the electronegative oxygen (O2) and nitrogen (N1) atoms assume apical positions. The N1(axial)-Se1-O2(axial) axis is roughly linear with a bond angle of 169°, while the N1(axial)-Se1-C3(equatorial) angle is 85°. This slight deformation from the TBP geometry can be attributed to the arrangement around the central positively charged selenium atom, in which the free amido group is not in such close contact with the selenium atom. Consequently, the C10(equatorial)-Se1-O2(axial) bond of 78° differs from that of N1-Se1-C3. This results in a longer distance between the Se1 and O2 atoms

(2.312 Å) than for the Se1-N1 bond (1.828 Å). The sum of the covalent radii for a Se-O bond is 1.75 Å,[155] suggesting a weaker interaction between O2 and Se rather than a covalent bond. The Se1-N1 bond is comparable to the "normal" Se-N single bond (1.80 Å).[155] The Se1-C3 and Se-C10 bond lengths of 1.934 Å and 1.952 Å, respectively, are typical Se-C$_{aromatic}$ bonds.[156] As shown in the ORTEP diagram, one atom of chlorine is present in the molecule, which exhibits hydrogen bonding with the N1-H and N2-H hydrogens outside of the unit cell. Oxygen O1 serves similarly as a hydrogen bond acceptor for the N2-H hydrogen of a second molecule. These hydrogen bond lengths range from 2.05 to 2.59 Å, which are considered to be typical. Distances of hydrogens to their hydrogen bond donors were adjusted to the idealized distances (0.88 Å). Endocyclic torsion angles show that the free amido group is in one plane with the aromatic ring, with the N2-C8-C9-C10 torsion angle equal to 177.9° and Se1-O2-C8-N2 equal to 174.6°, respectively. The two aromatic rings are almost perpendicular to each other (101.39° angle for C3-Se1-C10) giving this molecule a "butterfly" shape. The packing of two molecules of **128** in a single unit cell is portrayed in Figure 2.17.

Figure 2.17 The Unit Cell of **128** Rendered Using Mercury 1.4.1 Software
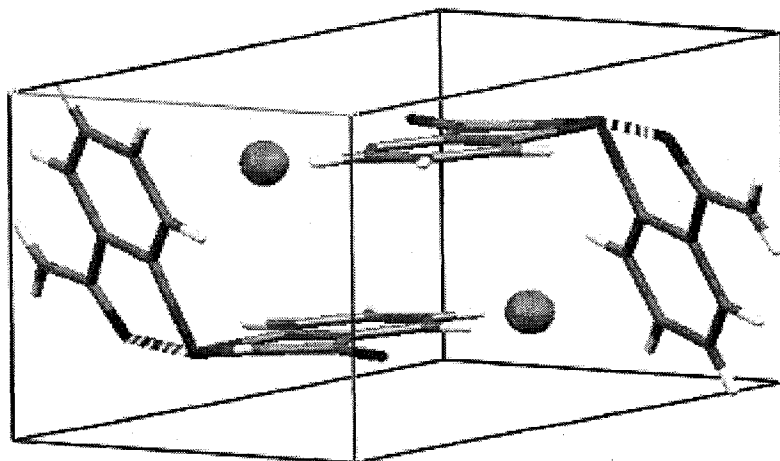
Compound **128** is a white solid with mp of 287 °C that can be recrystallized from glacial acetic acid. However, in aqueous acetic acid **128** hydrolyzed to **125** (Scheme 2.29).

Scheme 2.29
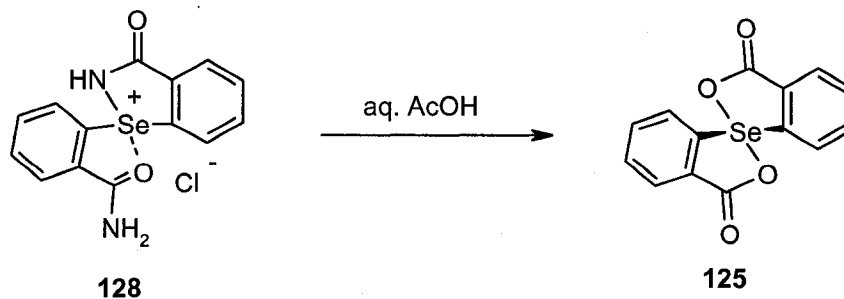
In a further attempt to prepare the symmetrical spirodiazaselenurane **138**, we dissolved amide **141** in acetone and treated this solution with 29% hydrogen peroxide (Scheme 2.30). After three days, fine white crystals were formed, but they proved to have similar NMR properties to those of **128**, clearly indicating two non-equivalent aromatic rings. The spectra and a satisfactory elemental analysis allowed us to propose the structure **129**, differing from **128** only with respect to the counterion.

Scheme 2.30
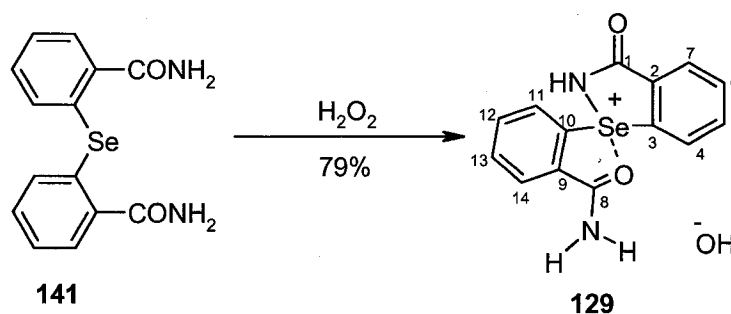
Interestingly, even though a satisfactory elemental analysis confirmed the correct molecular formula of **129**, one other possible structure could be that of **142**. This problem was solved by acquiring the mass spectrum of this compound using the electrospray ionization method. This analysis was carried out in methanol, in which **129** but not **142** should completely dissociate. Using the positive mode, ions with m/z = 319 and 341 were obtained. These ions correspond to [M-OH+H]$^+$ and [M-OH+Na]$^+$, respectively. If **142** was present, we would expect to see m/z =337 for [M+H]$^+$ in the case of the positive mode, or m/z = 335 for [M-H]$^-$ in the case of the negative mode. Additionally, X-ray diffraction of this material was performed. Albeit the quality of the crystal was poor, it resulted in a refined structure with a final R factor of 9.1 %. Based on this evidence we tentatively propose the structure of the above discussed material to be that of **129** rather than **142**.
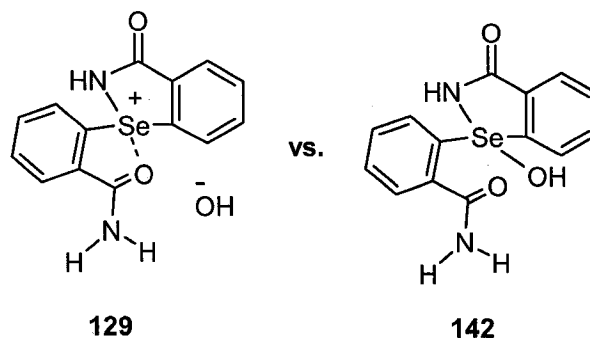
Our inability to obtain spirodiazaselenurane **138** appears to be caused by its very low stability toward water. Therefore, oxidation of selenide **141** was performed in dry deuterated solvents, using oxidizing agents such as bromine, iodine, *N*-methylmorpholine *N*-oxide (NMO), sodium periodate and sodium peroxide. Unfortunately, none of these reactions successfully produced the symmetrical spirodiazaselenurane **138**. We therefore tried to force the cyclization of **128** by means of the strong base, potassium hydride, under anhydrous conditions as shown in Scheme 2.31. This method proved to be successful in producing the dipotassium salt **130** of **138**.

Scheme 2.31 Preparation of Spirodiazaselenurane **130**

128

130
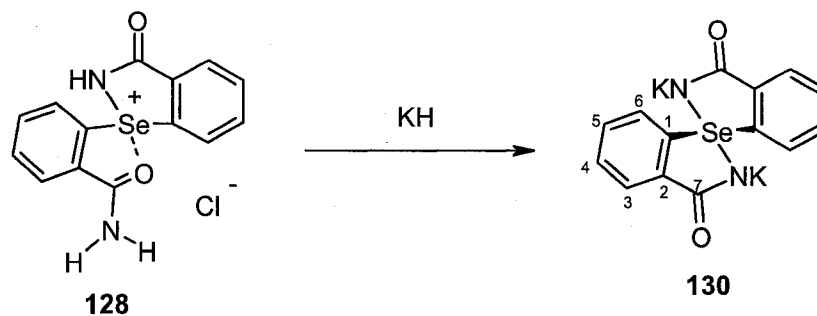
Its proton and ^{13}C NMR spectra are portrayed in Figure 2.18. The proton NMR spectrum shows doublets at δ 8.24 ppm and δ 7.73 ppm with coupling constants of 7.6 Hz and 7.2 Hz corresponding to either H-6 and H-3 or vice versa. Two triplets at δ 7.31 and 7.16 ppm both with coupling constants of 7.2 Hz are assigned to the H-5 and H-4 protons. In the ^{13}C NMR spectrum, only 7 peaks were observed, indicating the two halves of the molecule are indeed equivalent.

Figure 2.18 ^{1}H and ^{13}C NMR Spectra of **130**
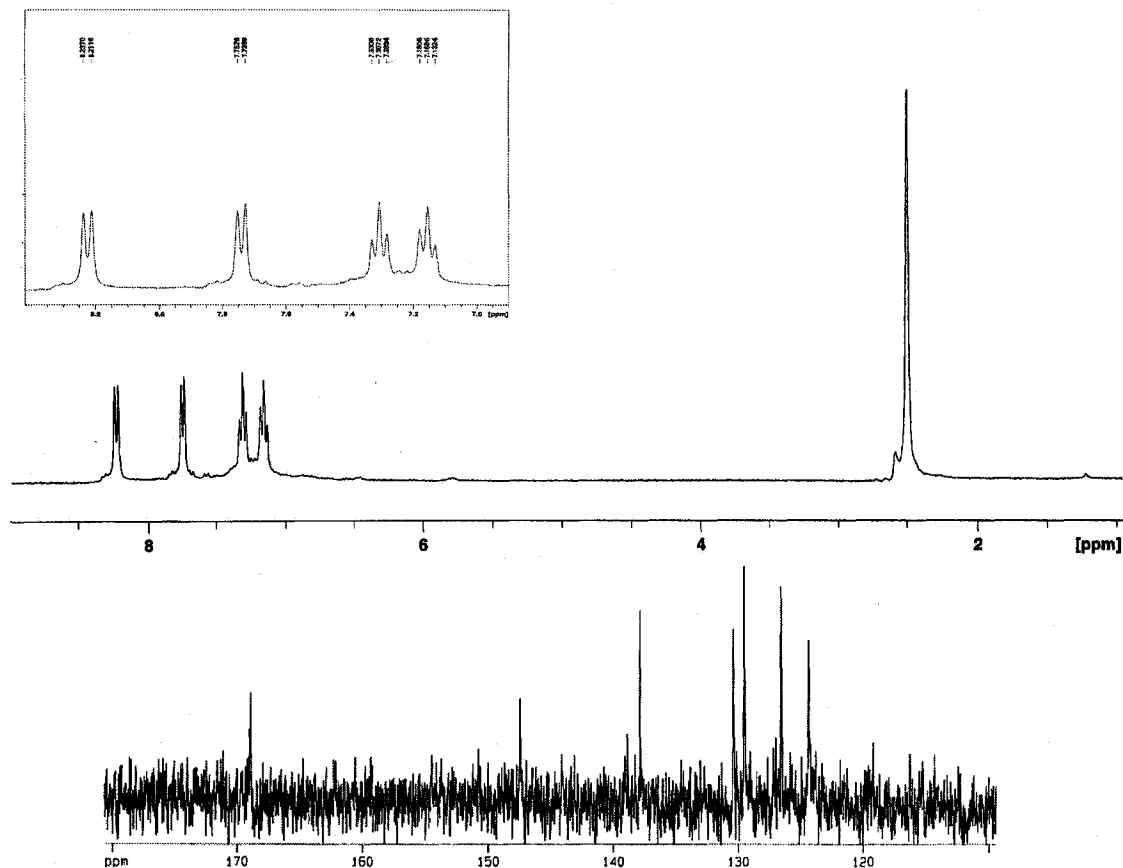
The structure of **130** was further confirmed by mass spectrometry, which was performed in dry dimethyl sulfoxide using the ESI method. An m/z of 395 was obtained in the positive mode, which corresponds to the ion $[M+H]^+$ of the proposed structure. If **138** was present then either m/z = 319 for $[M+H]^+$ or m/z = 341 for $[M+Na]^+$ or 359 for $[M+K]^+$ would be observed. Additionally, when the spectrum was acquired in negative mode, an m/z ratio of 317 was obtained, which corresponds to $[M-2K^+ + H^+]^-$.

As expected, exposure of **130** to air resulted in its quick hydrolysis to **129**, as seen in Scheme 2.32.

Scheme 2.32

130   **129**
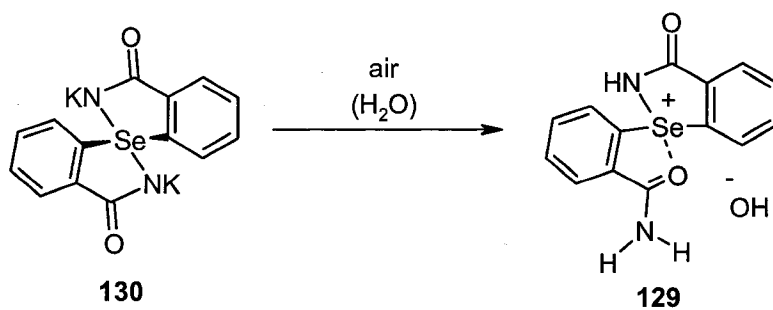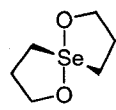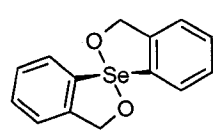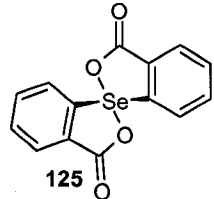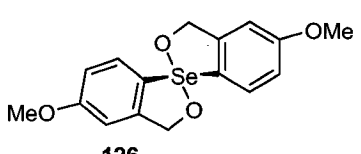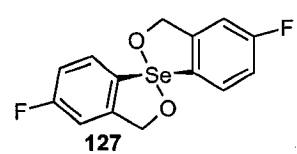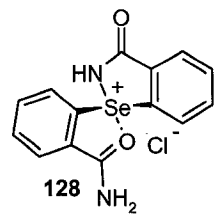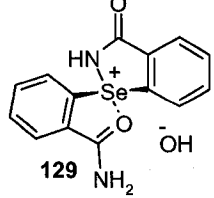
2.8 Catalytic Activity of Spirodioxyselenuranes

The series of novel spirodioxyselenuranes that we had prepared was then subjected to our GPx model assay. Their catalytic activities based on the half-lives of the reaction are summarized in Table 2.2. The previously reported aliphatic analogue **53** was synthesized according to the literature[85] procedure and its catalytic activity was re-evaluated with various concentrations of *tert*-butyl hydroperoxide and in the presence of 29% hydrogen peroxide. It displayed low sensitivity toward hydroperoxide concentration, expressing a strong, yet comparable catalytic activity in the presence of *tert*-butyl hydroperoxide with concentrations ranging from 90% to 38% (entries 1-3). The rate of catalytic reduction of 29% hydrogen peroxide was ca. 10 times more rapid than that of *tert*-butyl hydroperoxide (entry 4). The benzo analogue **124** showed an approximately 30-fold decrease in catalytic activity compared to **53** and the introduction of the electron-withdrawing carbonyl group in the benzoyl derivative **125**, further decreased the catalytic activity toward both peroxides (entries 5-8). This trend was additionally confirmed by investigating the *para* substituted derivatives. The electron-donating methoxy substituent, incorporated into the benzene ring in structure **126**, helped increase catalytic activity compared to the unsubstituted spirodioxyselenurane **124** by ca. 40%; conversely, the electron-withdrawing fluoro group decreased the catalytic activity by 3-fold (entries 9-12). The diaryl(acylamino)selenonium chloride **128** stands out from this series with the highest catalytic activity (entry 13-15) of all the aromatic GPx mimetics we prepared to date, while the hydroxide salt **129** displayed an average catalytic activity for reduction of *tert*-butyl hydroperoxide (comparable to spirodioxyselenurane **124**; $t_{1/2}$ = 62 h), but proved to be a poor catalyst for reduction of 32% hydrogen peroxide ($t_{1/2}$ = 17 h, entries 16 and 17). All of the studied spirodioxyselenuranes and acylaminoselenonium salts proved to be more active catalysts in the reduction of hydrogen peroxide than of *tert*-butyl hydroperoxide.

Table 2.2 Catalytic Activity of Spirodioxyselenuranes and Acylaminoselenonium Salts[a]

Entry	Catalyst	$t_{1/2}$ (h)	Oxidant
1		2.9	90% t-BuOOH[b]
2		1.9	56% t-BuOOH
3	**53**	2.1	38% t-BuOOH
4		0.2	29% H_2O_2
5		62	56% t-BuOOH
6	**124**	5.5	29% H_2O_2
7		113	56% t-BuOOH
8	**125**	35	29% H_2O_2
9		39	58% t-BuOOH
10	**126**	3.3	32% H_2O_2
11		181	58% t-BuOOH
12	**127**	16	32% H_2O_2
13		18	56% t-BuOOH
14		22	38% t-BuOOH
15	**128**	2.7	29% H_2O_2
16		62	56% t-BuOOH
17	**129**	17	32% H_2O_2

[a]Reactions were performed with BnSH (0.031 M), the catalyst (0.0031 M), and either 56% TBHP (0.038 M), 38% TBHP (0.023 M), or 29% H_2O_2 (0.040 M) in CH_2Cl_2-MeOH (95:5) at 18 °C, except for entries 13 to 17, where the solvent was CH_2Cl_2-MeOH (4:1). [b]Data taken from ref. 85

2.9 Catalytic Mechanism of Peroxide Reduction by Spirodioxyselenuranes

In order to rationalize our observations, the catalytic mechanism of the spirodioxyselenuranes was investigated further through a series of control reactions. First, the spirodioxyselenurane **124** was treated with 10 equivalents of *tert*-butyl hydroperoxide or hydrogen peroxide, respectively (Scheme 2.33). In both cases, no reaction was observed, even after 10 days, which suggests that the reaction of **124** with peroxides is not a feasible entry into the catalytic mechanism.

Scheme 2.33

124
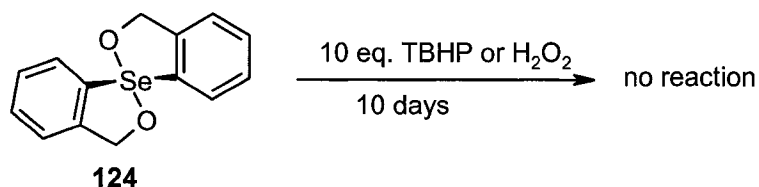
On the other hand, when **124** was subjected to reaction with excess thiol, the immediate formation of selenide **132**, along with the disulfide, was observed (Scheme 2.34). Therefore, this reaction represents the entry into the catalytic mechanism in the model assay reaction.

Scheme 2.34

124   **132**
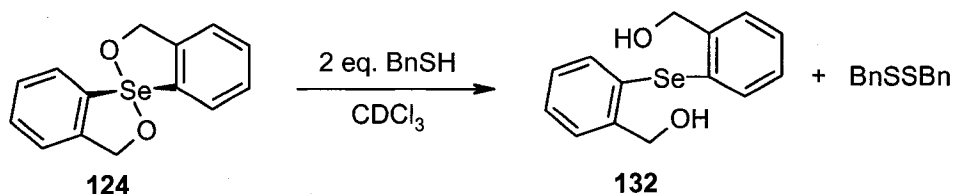
The proposed catalytic mechanism for the reduction of peroxides by **124** is depicted in Scheme 2.35. First, substitution of one alkoxy moiety of **124** by benzyl thiol occurs, resulting in the formation of intermediate **143**. This undergoes a reaction with second molecule of thiol, resulting in reductive elimination of dibenzyl disulfide, along

with the formation of **132**. This selenide is then oxidized with peroxide to the selenoxide intermediate **144**, which undergoes ring closure back to **124** accompanied by elimination of a molecule of water. However, catalysis of the peroxide reduction by the selenoxide intermediate **144**, via direct thiolysis to **143** without passing through spirodioxyselenurane **124**, cannot be ruled out. This mechanism is similar to that proposed earlier[85] for aliphatic spirodioxyselenurane **53** (Scheme 1.14).

Scheme 2.35 Catalytic Mechanism of Peroxide Reduction by **124**
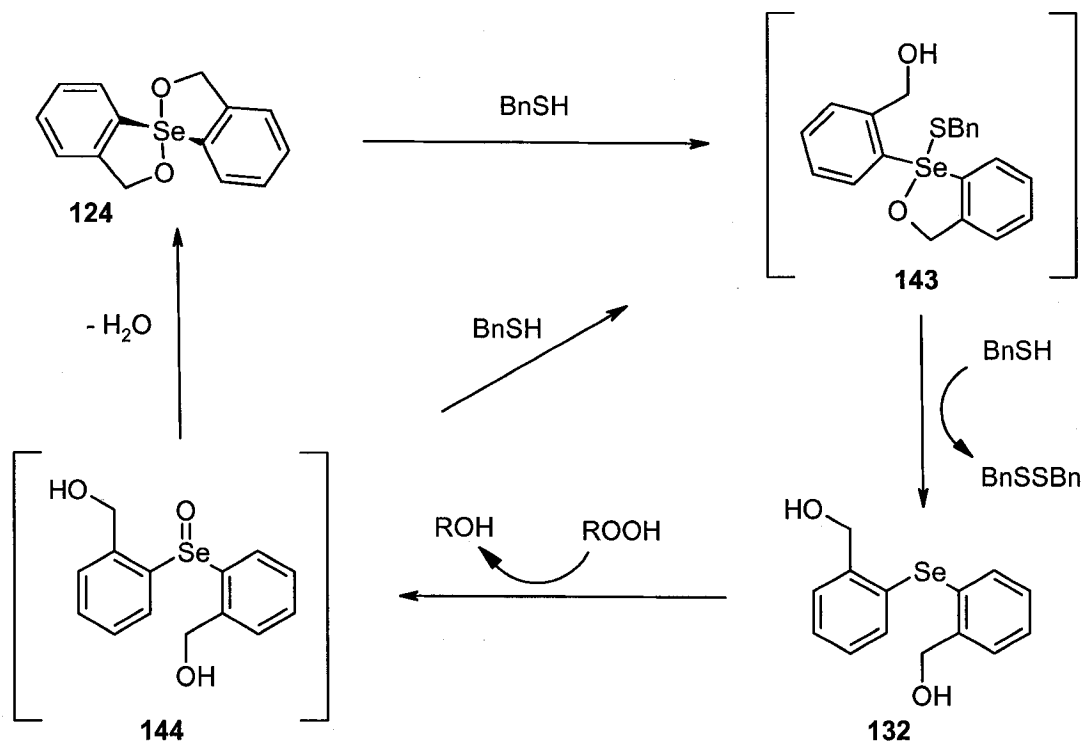
R = *t*-Bu or H

The above proposed mechanism is further endorsed by the recovery of spirodioxyselenurane **124** after the completion of the model assay, when all the thiol is oxidized to disulfide and where excess peroxide is still present. When the reaction was performed with an excess of thiol, selenide **132** was recovered. Therefore, depending on the concentration of the thiol and oxidant, either the spirodioxyselenurane **124** or selenide

132 can provide entry into the catalytic cycle. Examination of the HPLC chromatogram at the start of the assay and after 32 hours (see Fig. 2.19) shows no significant difference and indicates that the selenide **132** is the only selenium compound present. This in turn suggests that the oxidation of **132** to selenoxide **144** is the rate-limiting step in the catalytic mechanism, resulting in the build-up of the selenide **132** in the reaction mixture even in the presence of excess hydroperoxide.

Figure 2.19 The HPLC Plot of the Model Assay in the Presence of 10 mol %
of **124** and 56% *tert*-Butyl Hydroperoxide at 32 Hours
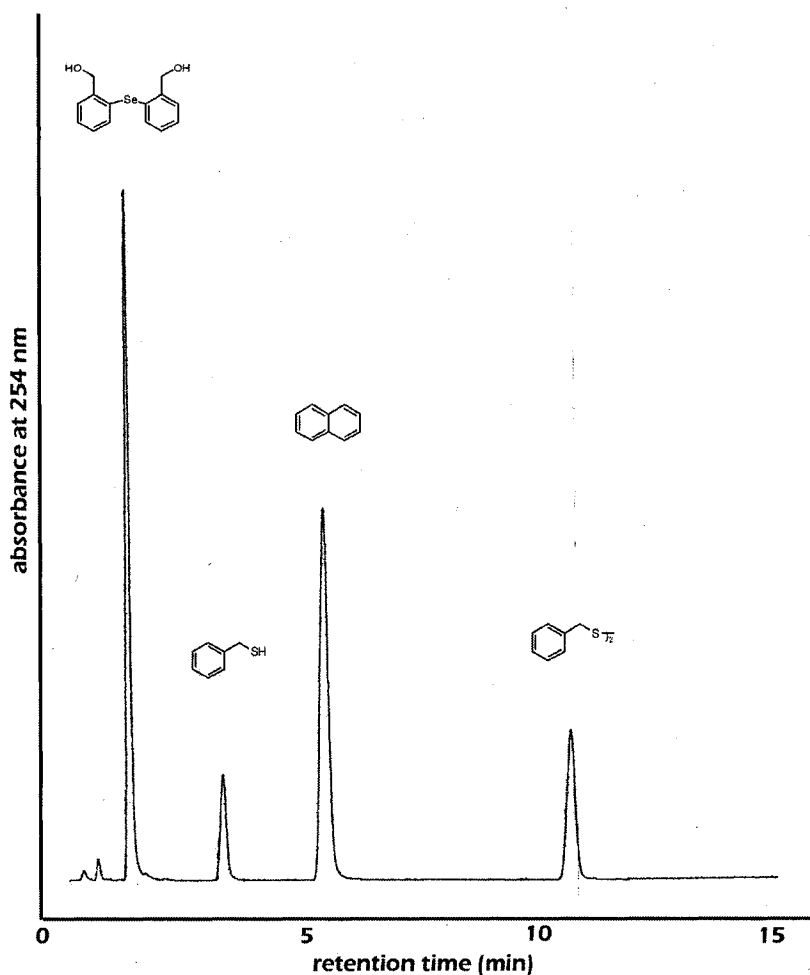
The low catalytic activity of the benzoyl analogue **125** toward both peroxides can be attributed to both a very slow oxidation of the corresponding selenide **131**, as well as slow reaction of **125** with benzyl thiol. This can be confirmed by a careful examination of the HPLC plot (Figure 2.20), in which even after five hours spirodioxyselenurane **125** is the only observable selenium compound, and formation of the corresponding selenide **131** is detected only after 26 hours.

Figure 2.20 HPLC Plot of the GPx Assay of **125** and 56% *tert*-Butyl Hydroperoxide
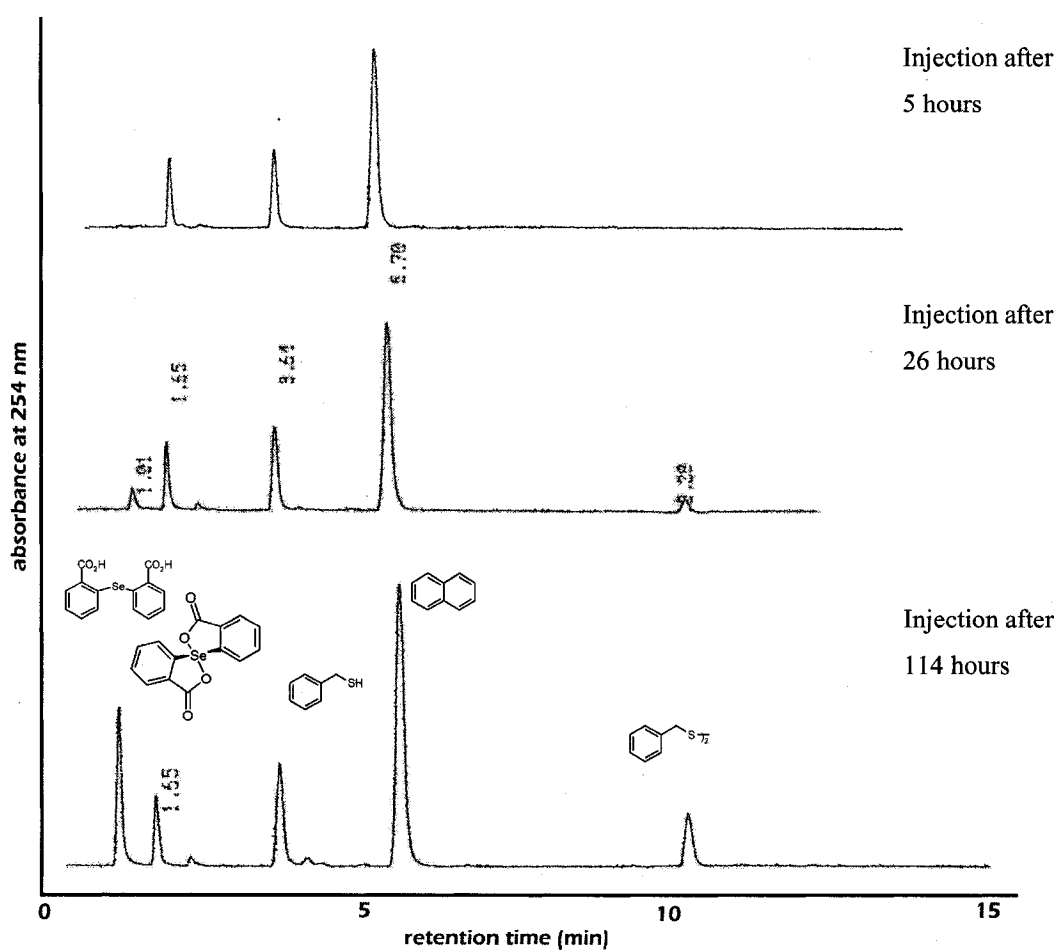
Cyclic acylaminoselenonium chloride **128** reacted immediately with the benzyl thiol in our model assay and was recovered after all the benzyl thiol was oxidized to its disulfide in the presence of excess oxidant.

2.10 Mechanism of Selenium Oxidation

Generally, the reaction of a selenide or related Se(II) species with hydrogen peroxide or a hydroperoxide is envisaged to proceed by a nucleophilic attack of the selenium atom upon a peroxide oxygen atom to afford an intermediate "hydroxyselenonium" species, which after rapid proton transfer forms the corresponding selenoxide (Scheme 2.36).

Scheme 2.36
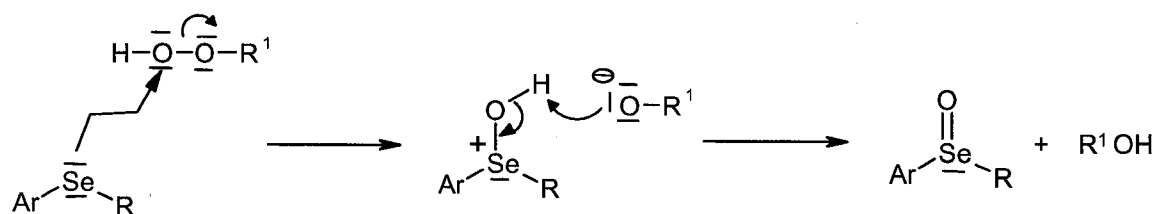
R^1 = t-Bu or H

This mechanism is consistent with two observations: (a) hydrogen peroxide is a better oxidant than *tert*-butyl hydroperoxide, which can be explained by the fact that the *tert*-butoxide anion is a poorer leaving group than hydroxide anion, since the *tert*-butyl group is more electron-donating than a hydrogen atom, and (b) electron-donating groups that increase electron density on the selenium atom, and therefore make it more nucleophilic, generally increase the catalytic activity of GPx mimetics, while electron-withdrawing groups, which decrease electron density on the central selenium atom, decrease the catalytic activity. These observations are also consistent with the oxidation of the selenium atom in both selenenyl sulfide and selenide intermediates being the rate-determining step in the catalytic mechanism of cyclic seleninate esters and spirodioxyselenuranes.

2.11 Tellurium Analogues of Cyclic Seleninate Esters and Spirodioxyselenuranes as GPx Mimetics

The more facile redox chemistry of the tellurium atom compared to selenium in organochalcogen compounds led us to investigate the tellurium analogues of our GPx mimetics. We synthesized the novel aliphatic organotellurium compounds **145** and **146**, depicted in Figure 2.21, in order to explore their ability to catalyze the reduction of peroxides in the presence of benzyl thiol and to compare them to their selenium counterparts.

Figure 2.21 Novel Tellurium-Based GPx Mimetics
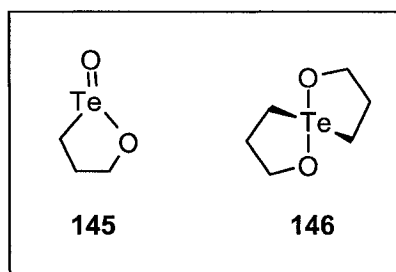
2.11.1 Preparation of 1,2-Oxatellurolane *Te*-Oxide (145)

Aliphatic organotellurium compounds are generally highly toxic and lack stability toward heat or light, and therefore our synthesis of such compounds was performed with great care. Starting from commercially available 3-bromopropan-1-ol (**147**), we prepared (3-hydroxypropyl)ditelluride (**148**) via a nucleophilic substitution of the bromide with sodium ditelluride (Scheme 2.37). The reagent Na_2Te_2 was prepared by reduction of tellurium powder with sodium borohydride in water under an argon atmosphere. Ditelluride **148** is a yellow oil sensitive to light, which results in the rapid extrusion of grey tellurium. It also decomposes within a few days when kept in the refrigerator in the absence of light. It was purified by flash column chromatography and was used immediately in the subsequent oxidation with *tert*-butyl hydroperoxide. The final product, 1,2-oxatellurolane *Te*-oxide (**145**) was obtained in overall 21 % yield and its identity was confirmed by spectroscopic analysis.

Scheme 2.37 Preparation of 1,2-Oxatellurolane *Te*-Oxide **145**
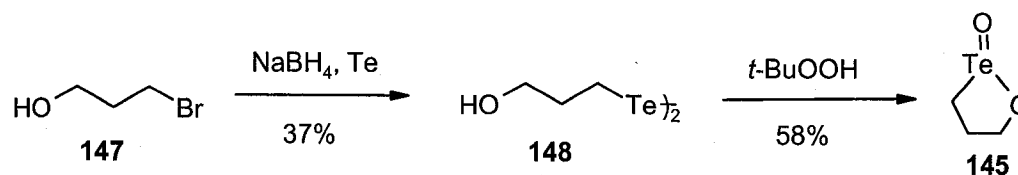
Proton and ^{13}C NMR spectra of **145** are portrayed in Figure 2.22. Similarly to the selenium analogues, the tellurium atom in **145** comprises a chiral centre. Therefore, each methylene unit in **145** is expected to consist of diastereotopic protons. However, the ^{1}H NMR spectrum showed only broadened peaks instead of clearly diastereotopic methylene groups, possibly because of the formation of hydrate **149** in the D$_2$O solvent that was employed. As expected, the ^{13}C NMR spectrum exhibits three signals with the OCH$_2$ carbon possessing a chemical shift of 70.2 ppm, while the TeCH$_2$ carbon appears at δ 46.9 ppm. The ^{125}Te NMR spectrum shows a peak at δ 1042.0 ppm. The extremely polar nature of **145** resulted in great difficulties with its purification and a satisfactory elemental analysis was not obtained. The spectroscopically pure product was produced by the precipitation of **145** from methanol with dichloromethane.
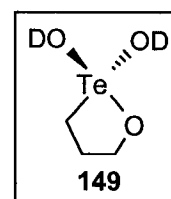
Figure 2.22 ^{1}H and ^{13}C NMR Spectra of **145**
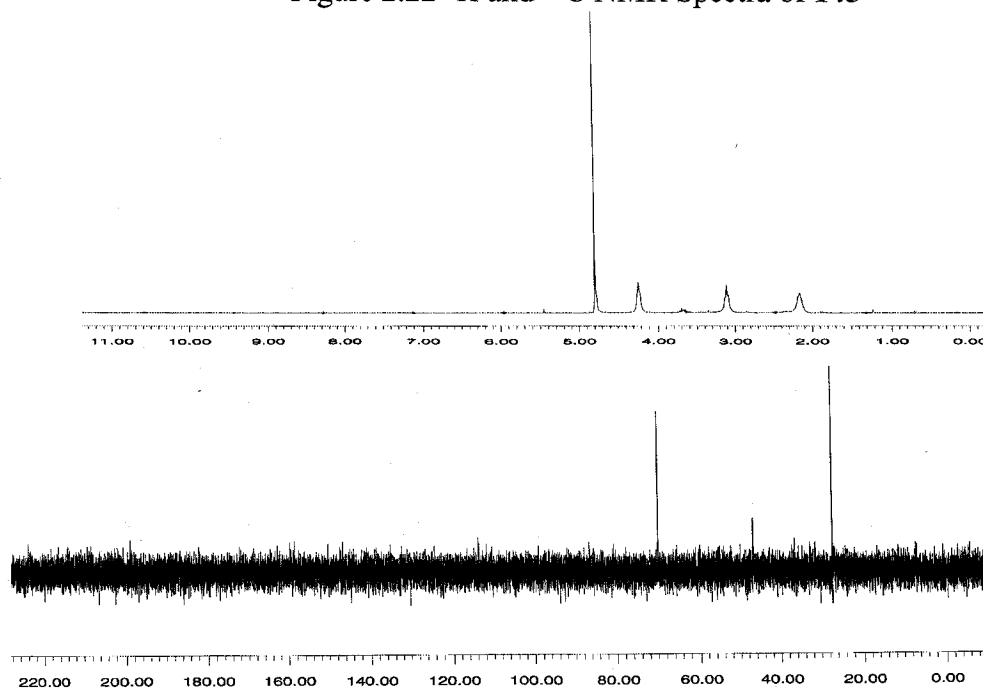
2.11.2 Preparation of Spirodioxytellurane 146

The tellurium analogue **146** of the spirodioxyselenurane **53** was prepared in two steps from commercially available 3-bromopropan-1-ol (**147**), as shown on Scheme 2.38.

<p align="center">Scheme 2.38 Synthesis of Spirodioxytellurane 146</p>
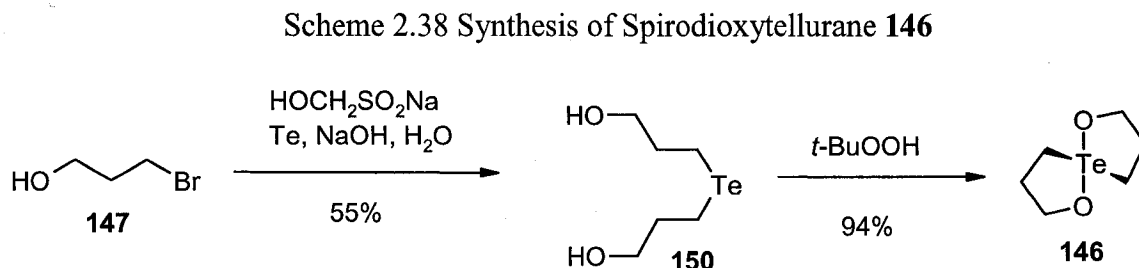
Originally, sodium telluride (Na_2Te) was prepared from tellurium powder using two equivalents of sodium borohydride. Unfortunatelly, this method led to the formation of sodium ditelluride (Na_2Te_2) as a by-product and subsequent difficulties in the separation of the resulting mixture of telluride **150** and ditelluride **148**. This problem was circumvented by utilizing Rongalite C (sodium sulfoxylate) in alkaline aqueous solution as the reducing agent. The formation of sodium telluride is indicated by dissolution of tellurium powder and the change of the solution from brown-red to clear pink after ca. 30 minutes of reflux. The nucleophilic addition of sodium telluride to 3-bromopropan-1-ol (**147**) yielded telluride **150** in 55% yield as a yellow oil after column chromatography. In contrast to the corresponding ditelluride, compound **150** was stable in the presence of light at room temperature for several weeks. Its oxidation with *tert*-butyl hydroperoxide, which occurs very rapidly (within ca. 2 minutes) and is indicated by discharge of the colour of the solution, yielded spirodioxytellurane **146** as a white waxy solid in 94% yield. It is also a stable compound and its identity was confirmed by IR, ^1H NMR, ^{13}C NMR spectroscopy, while its purity was verified by a satisfactory elemental analysis. The proton and ^{13}C NMR spectra are shown in Figure 2.23. The ^1H NMR spectrum shows three sets of signals for diastereotopic protons with OCH_2 protons appearing as two multiplets at δ 4.25-4.18 and 3.79-3.72 ppm, while the $TeCH_2$ protons appear as two overlapping multiplets at δ 2.90-2.73 ppm. The ^{13}C NMR spectrum shows three peaks as

expected, likewise one signal at δ 1097.0 ppm can be observed in the ^{125}Te NMR spectrum.

Figure 2.23 ^{1}H and ^{13}C NMR Spectra of **146**
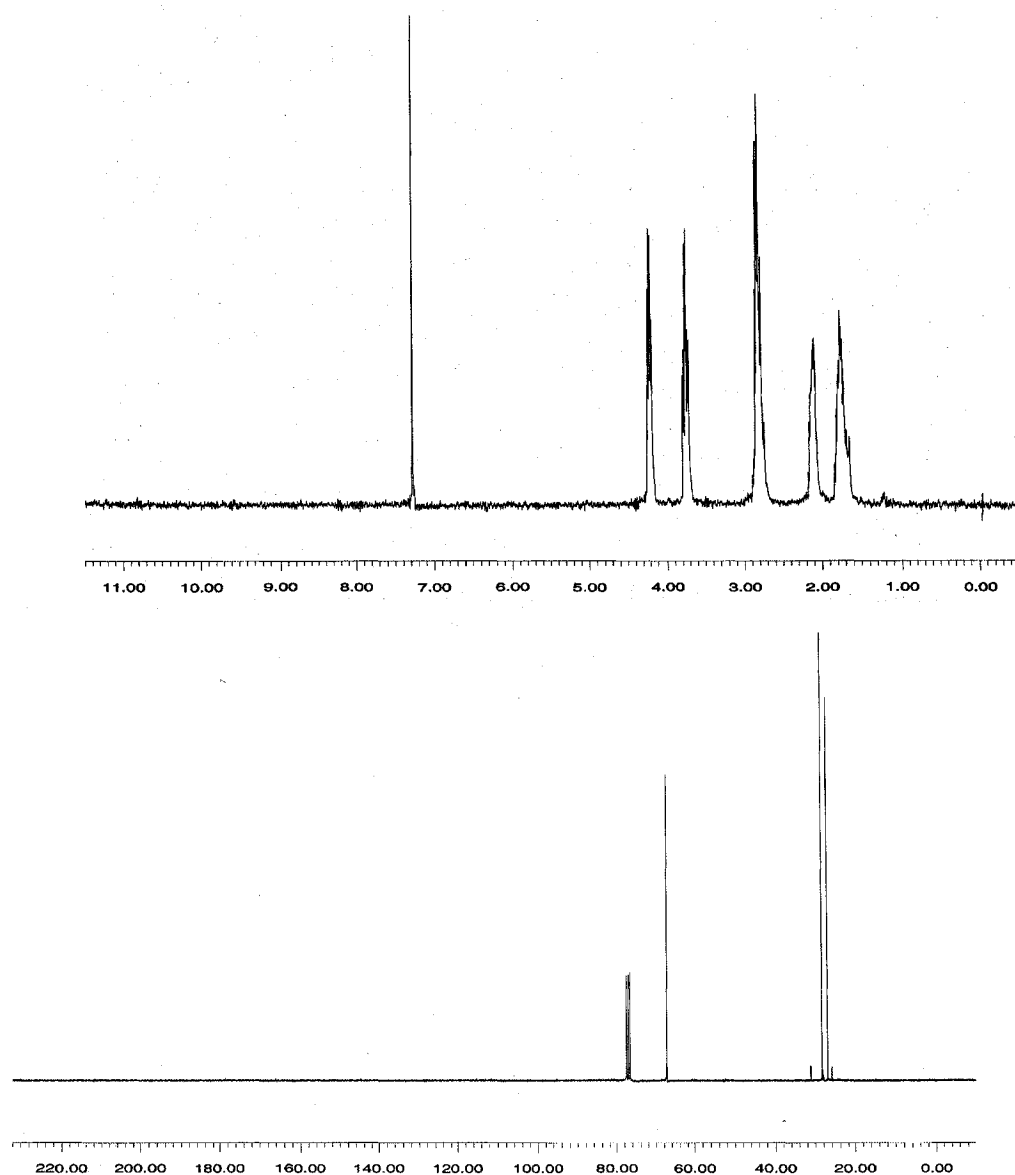
Interestingly, oxidation of telluride **150** with 29% hydrogen peroxide did not result in the formation of **146**, but rather unexpectedly afforded the bizarre peroxybis(tellurane) **151** (Scheme 2.39).

Scheme 2.39 Formation of Peroxybis(tellurane) **151**
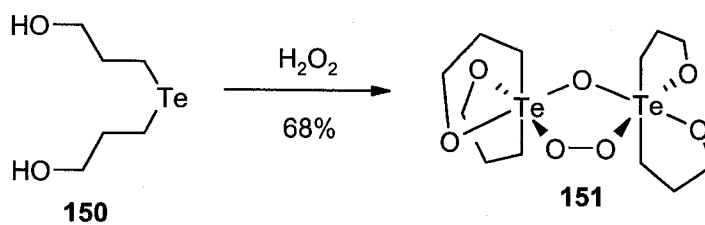
Its proton, ^{13}C NMR and ^{125}Te spectra are depicted in Figure 2.24. The ^{1}H NMR spectrum has a complicated pattern due to the number of diastereotopic protons in this molecule. The ^{13}C NMR spectrum shows two sets of three carbons, while the ^{125}Te NMR spectrum shows one signal at δ 1124.9 ppm, indicating equivalent tellurium atoms.

Figure 2.24 ^{1}H, ^{13}C and ^{125}Te NMR Spectra of **151**
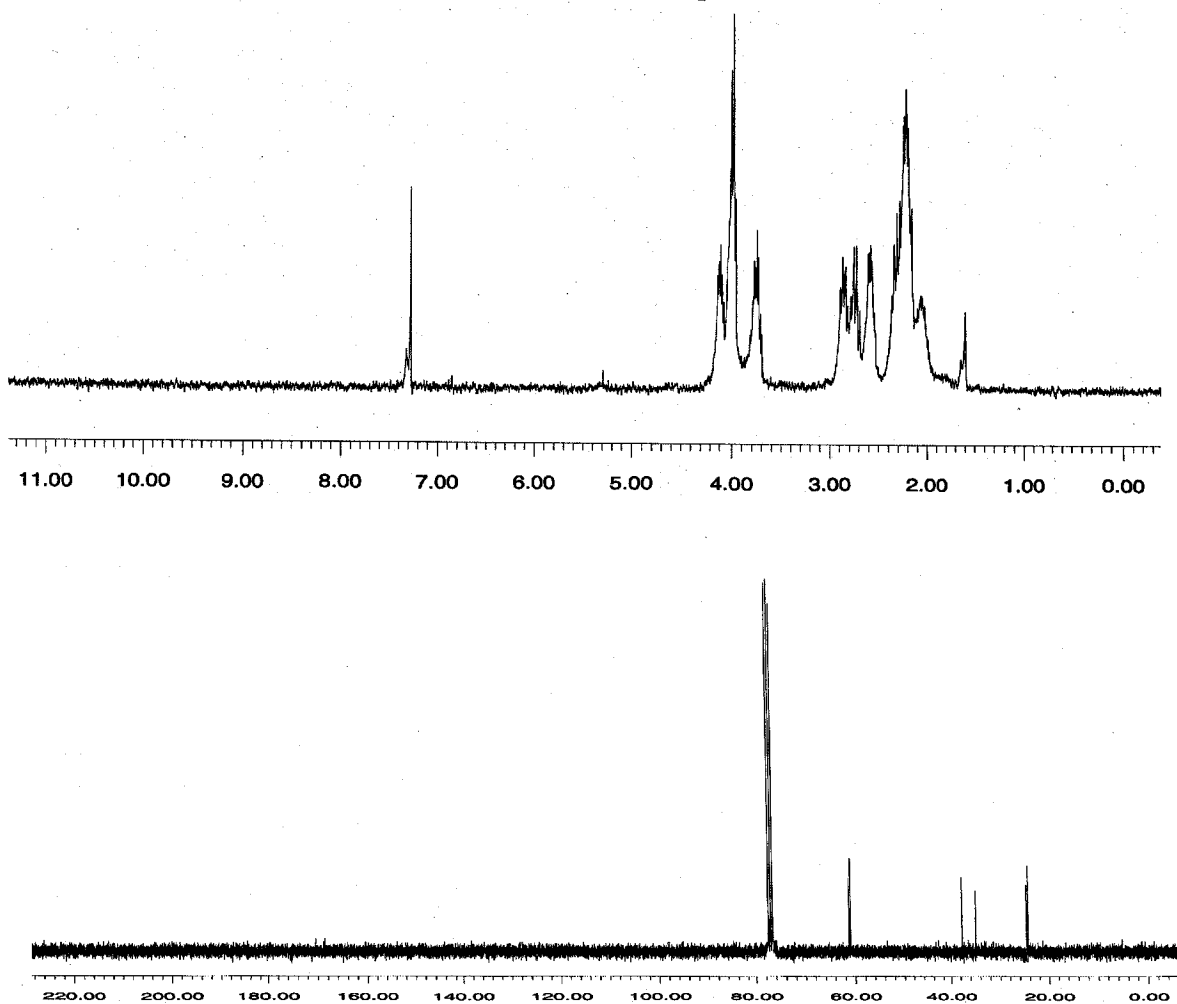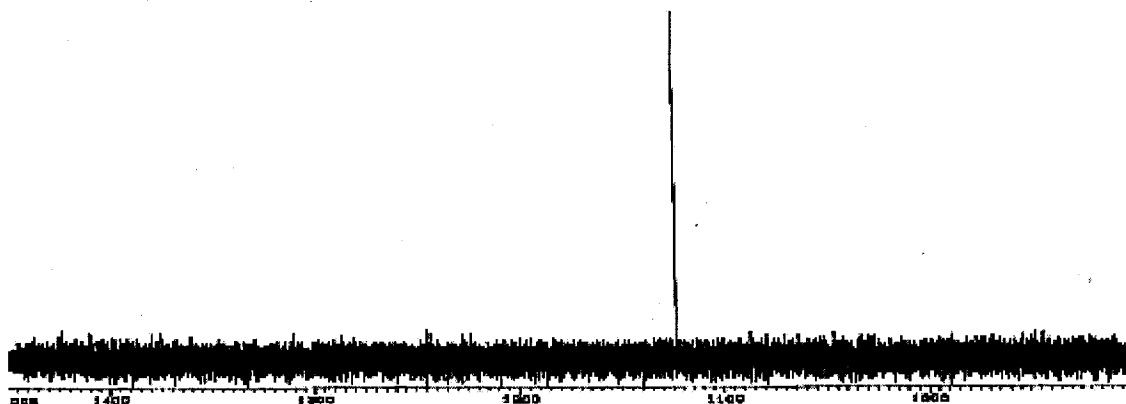
Compound **151** is unusually stable, considering that it possesses a peroxy bridge, which is usually associated with high reactivity, even explosiveness. Moreover, it is an aliphatic organotellurium compound, a class generally known to be relatively unstable. Peroxide **151** is a white solid with m.p. 211-213 °C. Its purity was confirmed by elemental analysis and its structure was solved using X-ray diffraction. The ORTEP diagram of this unusual peroxide is depicted in Figure 2.25. It has a dimeric structure, where each hypervalent tellurium atom occupies the center of a distorted octahedron bonded to four oxygen atoms in a roughly square planar arrangement. The O3-Te1-O1 angle is almost linear and equal to 175.02°. Similarly, the O2-Te1-O4 angle is 172.34°. The O2-Te1-O1 angle is close to a right angle with a value of 95.33°, indicating that the two tellurolane rings associated with each Te atom are almost perpendicular to each other. The tellurium-oxygen bonds in these tellurolane rings range from 1.968 Å to 1.993 Å, which is consistent with the sum of the covalent radii for Te and O atoms (2.00 Å).[155] The central ring comprises a 1,2,4-trioxa-3,5-ditellurolane moiety that includes the peroxide linkage. The Te1-O3-Te1* angle is equal to 121.2° and the distance between the tellurium atom and the peroxy oxygen (Te1-O4) is slightly elongated and equal to 2.032 Å. The peroxide bond (O4-O4*) is 1.477 Å long, which is a typical covalent oxygen-oxygen single bond. The torsion angle O3-T1-O4-O4* is 41.3°, while the O2-Te1-O3-

Te1* atoms lie almost in one plane (174.58°), suggesting a severe distortion of the O4 atom out of the plane of the 1,2,4-trioxa-3,5-ditellurolane ring.

Figure 2.25 ORTEP Diagram of **151**
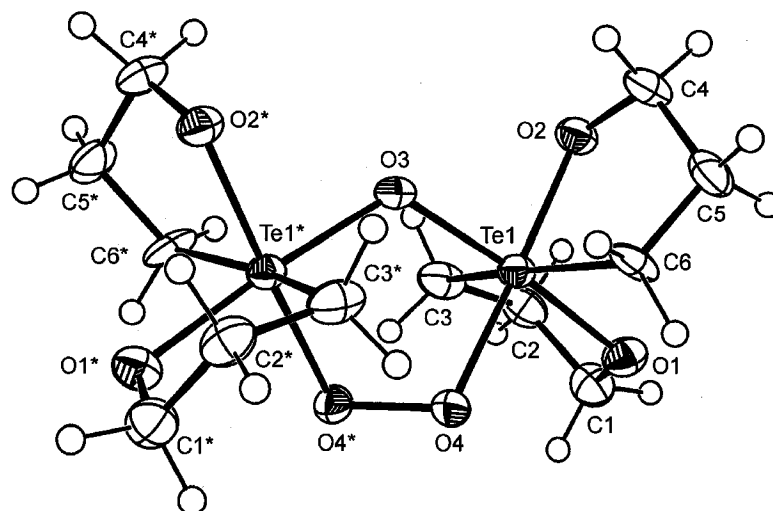
2.12 Catalytic Activity of 1,2-Oxatellurolane *Te*-oxide (145)

The novel tellurium compound **145** was independently investigated for its GPx-like behaviour. It exhibited catalytic activity with a $t_{1/2} < 5$ minutes in the case of both 56% *tert*-butyl hydroperoxide and 29% hydrogen peroxide in the presence of benzyl thiol. This represents an increase in the catalytic activity of **145** compared to its selenium analogue **46** of more than a thousand-fold with 56% *tert*-butyl hydroperoxide and more than 200-fold with 29% hydrogen peroxide. This reaction was too rapid for investigation of the intermediates or by-products by HPLC or NMR methods. The plot in Figure 2.26 shows the catalytic activity of **145** in the presence of both peroxides. Because of the rapidity of the reaction, each point in the graph represents a measurement performed on a separate reaction.

Figure 2.26 Plot of the Catalytic Activity of **145**
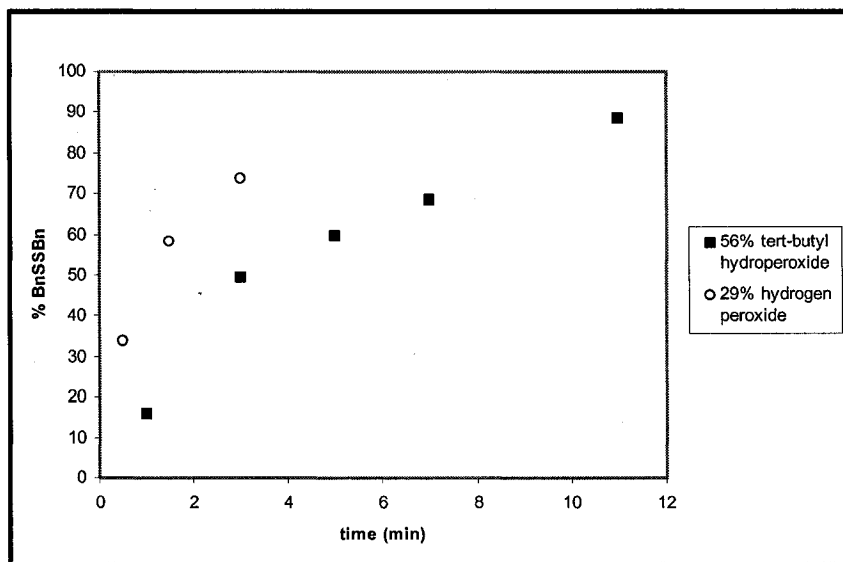
Our control experiments showed that **145** is inert to both 56% *tert*-butyl hydroperoxide and 29% hydrogen peroxide for at least several hours (Scheme 2.40), which rules out the entrance of **145** to the catalytic mechanism by further oxidation with peroxides. On the other hand, **145** reacted instantly with benzyl thiol, forming the mixture of tellurenyl sulfide **152** and ditelluride **148** along with dibenzyl disulfide. This control experiment was performed in deuterated chloroform and followed by proton NMR. Unfortunately, despite all attempts, tellurenyl sulfide **152** could not be obtained in spectroscopically pure form due to its low stability and rapid decomposition to ditelluride **148** and disulfide. Its identification therefore remains tentative.

Scheme 2.40
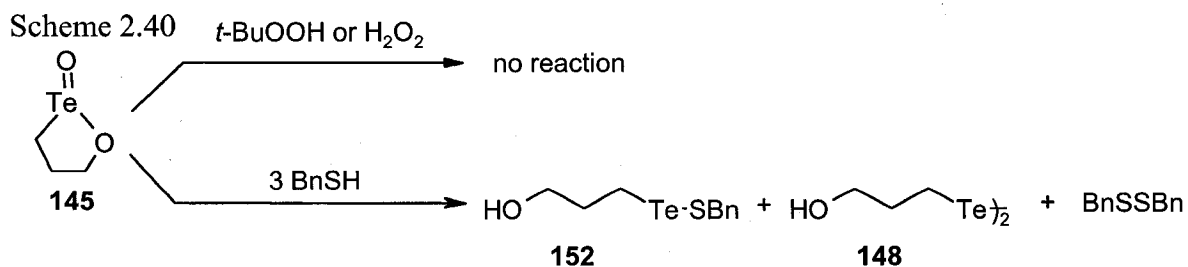
Formation of the suspected tellurenyl sulfide **152** was also observed in the HPLC plot of the model assay reaction as a peak with retention time of 3.41 minutes (Figure 2.27).

Interestingly, the concentration of the tellurenyl sulfide did not change over the entire course of the catalysis, suggesting that the tellurenyl sulfide plays the same key role in the catalytic mechanism as does the selenenyl sulfide in the case of the selenium analogue (see Section 2.6). Therefore, we tentatively propose the same catalytic mechanism as in the case of compound **89** (Section 2.6).

Figure 2.27 HPLC Plot of the Assay of **145**
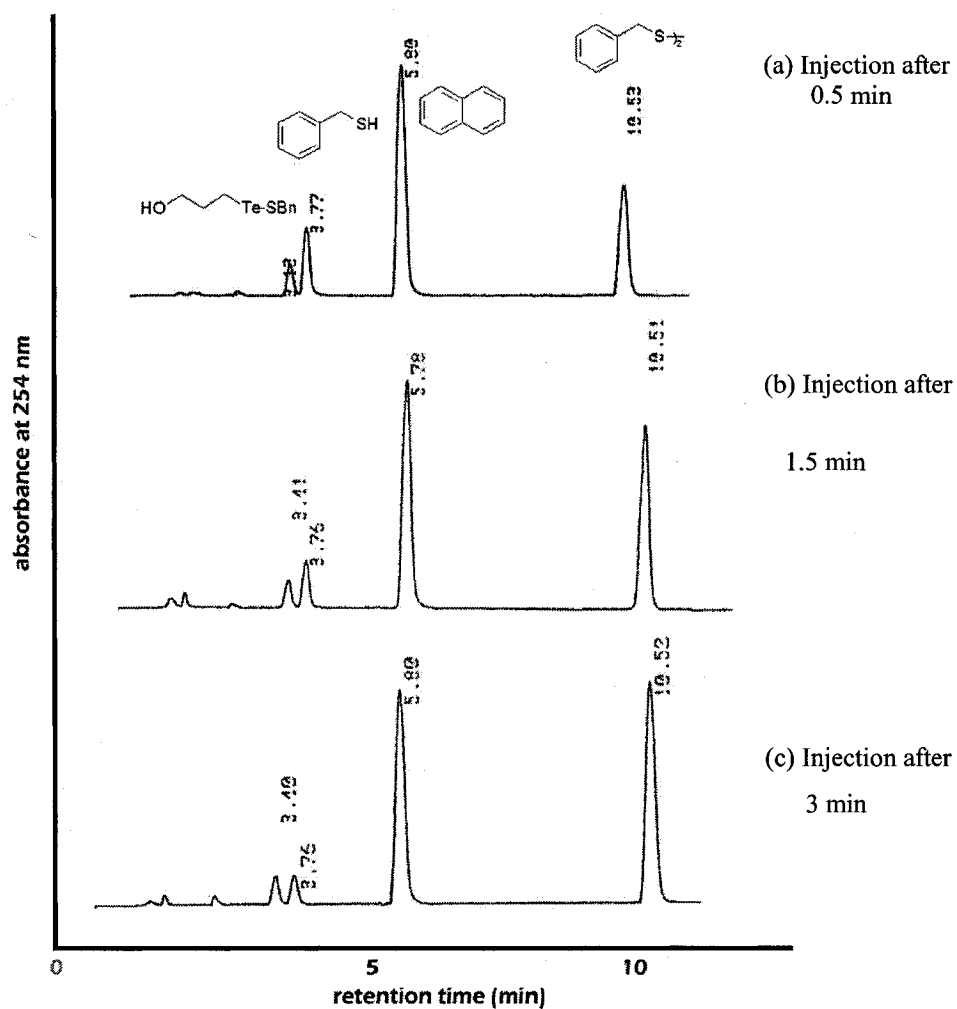
2.13 Catalytic Activity of Spirodioxytellurane 146

Spirodioxytellurane **146** also proved to be an exceptional catalyst for the reduction of peroxides in the presence of benzyl thiol, with $t_{1/2}$ values of ca. 4 minutes when evaluating 56% *tert*-butyl hydroperoxide and <6 minutes using 29% hydrogen peroxide. Thus, *tert*-butyl hydroperoxide seems to be reduced more easily than hydrogen peroxide in the presence of **146** and benzyl thiol. However, this apparent contrast to our previous observations could also be attributed to the error created by the rapidity of the reaction and an inability to perform the measurements at sufficiently close intervals. A plot of the catalytic activity of **146** is portrayed in Figure 2.28.

Figure 2.28 Plot of the Catalytic Activity of **146**
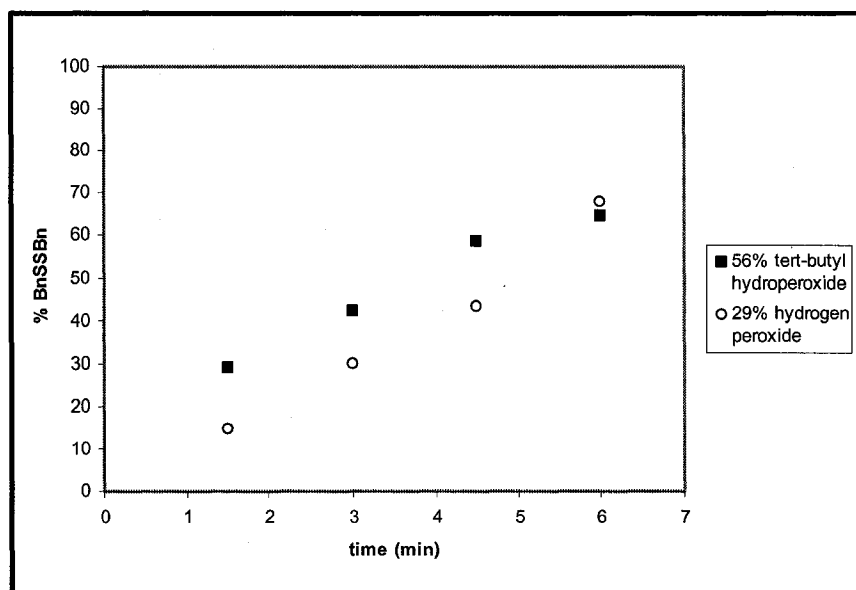
Control experiments were performed (Scheme 2.41) indicating that compound **146** does not react with 56% *tert*-butyl hydroperoxide but reacts rapidly with benzyl thiol, affording benzyl disulfide and telluride **150**. Therefore the catalytic mechanism is very likely the same as in the case of its selenium analogue.

Scheme 2.41
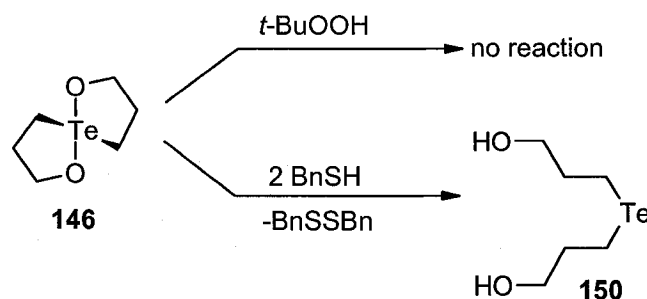
As shown in section 2.11.2, telluride **150** formed the unexpected peroxybis(tellurane) upon treatment with excess hydrogen peroxide. In our model assay, **151** also proved to be an excellent catalyst ($t_{1/2}$ <3 min) for the reduction of hydrogen peroxide in the presence of benzyl thiol. A question emerges whether **151** plays any direct role in the catalytic mechanism of reduction of hydrogen peroxide by **146**. This hypothesis was explored by a separate control experiment, which showed that the formation of peroxybis(tellurane) **151** from the oxidation of **150** with hydrogen peroxide is rather slow (ca. 50% complete after 6 hours). Therefore, **151** was ruled out as playing a direct role in the catalytic cycle of **146**. It probably serves as a procatalyst, generating **146** or another species that can be cycled repeatedly through the redox mechanism.

2.14 Summary and Conclusions

Chapter 2 described the synthesis of a series of glutathione peroxidase mimetics and the assessment of their catalytic activity in the reduction of peroxides with thiols. Additionally, the mechanism of catalysis of these compounds was investigated. We have found that aromatic derivatives of cyclic seleninate ester **46** are relatively poor catalysts. Their low catalytic activities, determined by long half-lifes in the oxidation of benzyl thiol (see Table 2.1), can be attributed to the accumulation of the corresponding selenenyl sulfides, in contrast to similar experiments with the aliphatic parent compound. After independent synthesis of selenenyl sulfides, such as **118** and **123**, measurement of their catalytic activity revealed their relatively unreactive nature toward the reduction of

peroxides. Additionally, we discovered that the catalytic reduction of peroxides is highly dependent on the type and, in some cases, concentration of these oxidants, where reduction of hydrogen peroxides proceeds more rapidly by up to an order of magnitude compared to that of *tert*-butyl hydroperoxide. We also prepared aromatic derivatives of spirodioxyselenurane **53**, which express generally higher catalytic activity than the corresponding aromatic seleninates. In addition, the novel cyclic acylaminoselenonium chloride **128** diplayed the highest catalytic activity of all of the aromatic organoselenium compounds we investigated. We also prepared the novel hydrolytically unstable symmetrical spirodiazaselenurane **130**. Moreover, we found that catalytic activity of our GPx mimetics is decreased when electron-withdrawing carbonyl groups are introduced into the cyclic seleninate or spirodioxyselenurane moiety. Further decrease in catalytic activity is caused by introduction of electron-withdrawing groups in the *para* position of the benzene ring relative to the selenium atom. Conversely, introduction of electron-donating substituents generally resulted in increased catalytic activity. Control experiments and the above substituent effects suggest that oxidation of Se(II) to Se(IV) is the rate-determining step in the catalytic cycles of these compounds. In addition to the above findings, we have prepared aliphatic tellurium analogues of the corresponding cyclic seleninate and spirodioxyselenurane, which are the most active catalysts studied in our laboratory to date. Lastly, we discovered the highly unusual peroxy-bridged dimer **151**, which also displayed exceptional catalytic activity.

2.15 Future work

As we have demonstrated, aromatic seleninate esters and spirodioxyselenuranes act as mimetics of the enzyme glutathione peroxidase. Their fairly low catalytic activity prompted us to investigate substituent effects as a possible means of enhancing their catalytic activity. The next step in this project is the synthesis and evaluation of a broader range of substituted compounds, such as the ones depicted in Figure 2.29. This may permit the construction of a Hammett plot, which might provide a better insight into the catalytic mechanism, as well as furnish opportunity to predict the activity of future

candidates for in vivo testing. Further, evaluation of the catalytic activity of these compounds might also be broadened by studying the dependence of the activity on pH. Additionally, aromatic tellurium analogues might be prepared in order to compare their activity to the aliphatic parent compounds.

Figure 2.29 Candidates for Future GPx Mimetics

X= Se or Te
R = Me, Cl, CN, COOH, COOR$_1$
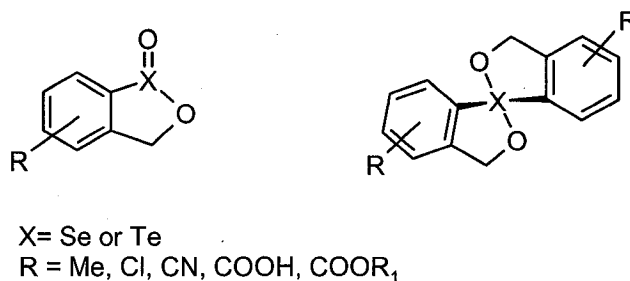
Finally, these compounds might be assessed as catalysts for oxidation reactions of sulfides to sulfoxides, cyclic ketones to lactones (Bayer-Villiger reaction) and epoxidations of alkenes. The scope of this chemistry could, in principle, be eventually expanded to asymmetric versions of the above reactions.

Chapter Three

Experimental Section

3.1 General Procedures

Melting points were obtained on an A. H. Thomas hot-stage apparatus and are uncorrected. IR Spectra were recorded on a Nicolet Nexus 470 FTIR ESP spectrophotometer, using thin films deposited from chloroform solution on NaCl or KBr plates, unless otherwise stated. ^{1}H and broad band decoupled ^{13}C NMR spectra were acquired on a Bruker UG 300, Bruker DMX 300, or a Bruker AMX 300 spectrometer (^{1}H, 300 MHz; ^{13}C, 75 MHz), or on a Bruker DRX 400 spectrometer (^{1}H, 400 MHz; ^{13}C, 100 MHz). Deuteriochloroform was employed as the solvent with either residual chloroform (^{1}H δ 7.27, ^{13}C δ 77.0 ppm) or tetramethylsilane (^{1}H δ 0.0 ppm) as the internal standard unless otherwise stated. All the ^{1}H NMR spectra listed have the following format: chemical shift δ (in ppm), multiplicity, coupling constant J (in Hz), integration, and assignment. The ^{13}C spectra have the following format: chemical shift δ (in ppm), assignment. ^{77}Se NMR spectra were acquired at 57 MHz on a Bruker AMX 300 spectrometer or at 76 MHz on a Bruker DRX 400 spectrometer with diphenyl diselenide in CDCl$_3$ (δ 461 ppm)[157] or selenium dioxide in D$_2$O (δ 1302.6 ppm)[158] as the standard, relative to dimethyl selenide (δ 0.0 ppm). ^{125}Te NMR spectra were acquired using a Bruker AMX 300 (95 MHz) or a Bruker DRX 400 (126 MHz) spectrometer with diphenyl ditelluride in CDCl$_3$ (δ 420.8 ppm)[159] as external standard and are reported relative to dimethyl telluride (δ 0.00). Low resolution mass spectra were obtained by either electron impact on a Micromass VG7070F spectrometer or electrospray ionization on a Bruker Esquire 3000 spectrometer, while high resolution mass spectra were obtained on a Kratos MS80 RFA mass spectrometer. All mass spectroscopic analyses were performed by Dr. Qiao Wu and Ms. Dorothy Fox at the University of Calgary. The data is listed as: mass (*m/z*), (relative intensity, assignment). Mass spetra of compounds containing selenium and tellurium displayed the characteristic isotopic distributions, but only masses based upon ^{80}Se and ^{130}Te are reported. Elemental analyses were performed by Ms. Roxanna Smith at the University of Calgary. HPLC measurements were

performed on a Waters 600 HPLC, equipped with a Novapak C_{18} 3.9 x 150 mm column and using a Waters 486 Tunable Absorbance Detector (λ 254 nm). Each assay was repeated at least three times and the range of values of data points was typically ± 10%. For further details see Appendices A and B. TLC was performed on aluminum sheets coated with 0.2 mm of silica gel and a fluorescent indicator (SG 60 F254, E. M. Merck), and the spots were visualized with UV light, or using iodine vapour. Flash chromatography was performed on silica gel, 230-400 mesh, and was carried out in the manner reported by Still et al.[160] The X-ray crystal structures of **128** and **151** were obtained by Dr. Masood Parvez, and the experimental details, along with atomic coordinates, bond lengths, and bond angles were provided by Dr. Parvez, or were calculated using Mercury 1.4.1 crystallographic software, and are presented in Appendices D and E, respectively. Additionally, the plots for the kinetic runs discussed in Sections 2.5 and 2.8 that were not presented in the text are shown in Appendix B.

All solvents used were reagent grade and were obtained from commercial sources; solvents were used without further purification, unless otherwise stated. THF was dried over lithium aluminum hydride and was distilled immediately prior to use. Reactions requiring anhydrous conditions were carried out under Ar or N_2, in flame or oven-dried glassware cooled under vacuum. Ice-water (0 °C), and acetone-dry ice (-78 °C) were used to maintain low temperature baths. Glassware for the kinetic experiments was rinsed with acetone and was flame-dried prior to use. Significant increase in catalytic activity was observed with traces of any kind of base. Benzyl thiol was distilled prior to use and the concentrations of *tert*-butyl hydroperoxide and hydrogen peroxide were determined by iodometric analysis.[161] Selenium (II) diethylthiocarbamate (Se(dtc)$_2$) was prepared by a method reported by Foss.[151] Organoselenium and tellurium compounds are highly toxic and therefore need extra caution during handling. Especially dangerous are reactions involving alkali metal selenides and diselenides, which are often accompanied by evolution of highly toxic hydrogen selenide gas if exposed to acidic solutions. Therefore, all reactions were performed in a fumehood. Compounds in this chapter are numbered for convenience and the numbering does not necessarily reflect IUPAC nomenclature.

3.2 Experiments related to Chapter Two

3.2.1 Preparation of ebselen (3)[65]
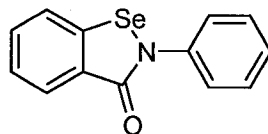
To a stirred solution of commercially available *N*-phenylbenzamide (736 mg, 3.73 mmol) in dry THF (35 mL) under an argon atmosphere, cooled to 0 °C, was added *n*-butyllithium (4.7 mL, 7.5 mmol). After 30 min, elemental selenium (296 mg, 3.75 mmol) was added to the resulting orange solution. It was stirred for 30 min, cooled to -78 °C and copper(II) bromide (1.68 g, 7.52 mmol) was added. The mixture was additionally stirred for 30 min at -78 °C and afterwards for 2 h at room temperature. The reaction mixture was poured into 80 mL of water containing 1 mL of acetic acid, filtered and extracted with dichloromethane. The resulting crude product was chromatographed (elution with dichloromethane) and recrystallized from ethanol to give 490 mg (48%) of the product with mp 178-179 °C (lit.[65] mp 180-181 °C); IR (KBr) 1595 (C=O), 1559, 1346, 1321, 1028, 757, 740 cm^{-1}; ^{1}H NMR (300 MHz) δ 8.17 (dd, J = 8.0 Hz, 0.9 Hz, 1 H, Ar-H), 7.74-7.62 (m, 4 H, Ar-H), 7.55-7.42 (m, 3 H, Ar-H), 7.35-7.24 (m, 1 H, Ar-H); ^{13}C NMR (75 MHz) δ 165.6 (C=O), 139.1, 137.6, 132.5, 129.4, 129.0, 127.5, 126.7, 126.5, 125.4, 123.7.

3.2.2 Preparation of 2,2`-diselenobisbenzoic acid (12)[138]
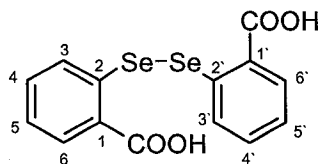
To a stirred solution containing 8.23 g (60.0 mmol) of o-aminobenzoic acid and 24 mL of concentrated hydrochloric acid in 24 mL of water cooled in an ice bath at 0 °C, were added dropwise 4.83 g (70.0 mmol) of sodium nitrite in 18 mL of water while the temperature was maintained below 5 °C. The resulting solution of the diazonium salt was stirred while a solution of potassium diselenide was prepared as follows. Selenium (9.6 g, 0.12 mol) and potassium hydroxide (27 g, 0.48 mol) were melted in a 500 mL round bottom flask. Cold water (80 mL) was added to the melt cooled to 100 °C in order to produce a red solution of potassium diselenide, which was subsequently cooled to 0 °C and treated dropwise with the solution of the diazonium salt. The resulting mixture was slowly warmed to 80 °C, cooled to room temperature and filtered to remove red selenium. The filtrate was acidified with 10% hydrochloric acid, yielding 10.7 g (89%) of a precipitated orange solid with mp 291-294 °C (lit.[138] mp 293 °C). This compound was used without any further purification; IR (KBr) 3400-2400 (broad, O-H stretch), 1669 (C=O), 1457, 1418, 1266, 1027, 736 cm^{-1}; ^{1}H NMR (300 MHz, DMSO-d$_6$) δ 13.73 (br s, 2 H, COOH), 8.05 (d, J = 8.0 Hz, 2 H, Ar-H), 7.69 (d, J = 8.0 Hz, 2 H, Ar-H), 7.51 (t, J = 7.2 Hz, 2 H, Ar-H), 7.39 (t, J = 7.2 Hz, 2 H, Ar-H).

3.2.3 Preparation of allyl (2-hydroxymethyl)phenyl selenide (94)
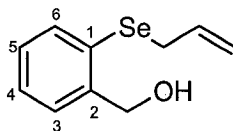
Diselenide **12** (1.43 g, 3.57 mmol) in 50 mL of dry THF was added dropwise to a stirred solution of 0.69 g (18 mmol) of lithium aluminum hydride in 20 mL of dry THF at 0 °C. After the initial vigorous reaction subsided, the mixture was warmed to room temperature, stirred for 6 h and treated with 0.7 mL (8 mmol) of allyl iodide. Stirring was continued overnight, the mixture was quenched with 100 mL of water, filtered and the residue was washed thoroughly with ether. The filtrate was extracted repeatedly with ether. The combined organic layers were dried and concentrated in vacuo. The crude product was chromatographed (elution with hexanes-ethyl acetate 3:2) to afford 816 mg (50%) of **94** as a yellow oil; IR (neat) 3350 (broad, O-H stretch), 1028, 750 cm^{-1}; ^{1}H NMR (300 MHz) δ 7.54 (dd, J = 7.4, 1.3 Hz, 1 H, H-6), 7.40 (dd, J = 7.4, 1.3 Hz, 1 H, H-3), 7.31–7.18 (m, 2 H, Ar-H), 6.00-5.86 (m, 1 H, C=CH), 4.99–4.92 (m, 2 H, C=CH$_2$), 4.76 (s, 2 H, OCH$_2$), 3.51 (d, J = 7.7 Hz, 2 H, SeCH$_2$), 2.40 (br s, 1 H, OH); ^{13}C NMR (75 MHz) δ 143.0, 134.8, 134.3, 129.7, 128.5, 128.4, 128.0, 117.3 (=CH$_2$), 65.6 (OCH$_2$), 31.1 (SeCH$_2$); mass spectrum, m/z (relative intensity) 228 (10, M$^+$), 187 (38, M$^+$ - C$_3$H$_5$), 157 (17), 129 (26), 105 (17), 78 (100). Exact mass calcd for C$_{10}$H$_{12}$O^{80}Se: 228.0053. Found: 228.0060.

3.2.4 Preparation of benzo-1,2-oxaselenolane *Se*-oxide (89)
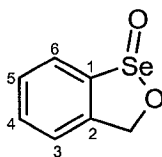
tert-Butyl hydroperoxide (0.96 mL of 38% aqueous solution, 3.9 mmol) was added to 448 mg (1.97 mmol) of allyl selenide **94** in 15 mL of dichloromethane. The mixture was stirred at room temperature overnight, concentrated *in vacuo* and chromatographed (elution with 20% methanol-ethyl acetate) to afford 351 mg (88%) of **89** as a white solid: mp 139-140 °C (from ethyl acetate); IR (KBr) 1462, 1260, 966 cm^{-1}; ^{1}H NMR (300 MHz) δ 7.81 (d, J = 7.7 Hz, 1 H, H-6), 7.61-7.47 (m, 3 H, Ar-H), 5.97 (d, J = 13.8 Hz, 1 H, OCHa), 5.61 (d, J = 13.6 Hz, 1 H, OCHb); ^{13}C NMR (75 MHz) δ 148.3, 143.7, 132.2, 129.3, 125.5, 122.9, 78.6 (OCH$_2$); ^{77}Se NMR (76 MHz) δ 1349.0; mass spectrum, *m/z* (relative intensity) 202 (30, M$^+$), 106 (74, M$^+$ - SeO), 78 (100). Exact mass calcd for C$_7$H$_6$O$_2$^{80}Se: 201.9533. Found: 201.9540. Analysis calcd for C$_7$H$_6$O$_2$Se: C, 41.81; H, 3.01. Found: C, 41.54; H 2.97.

3.2.5 Preparation of allyl 2-carboxyphenyl selenide (95)
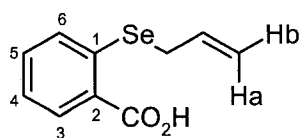
Sodium borohydride (0.59 g, 16 mmol) was added to diselenide **12** (1.24 g, 3.10 mmol) in 60 mL of dry THF. The stirred mixture was cooled to 0 °C and 50 mL of absolute ethanol was added dropwise. The mixture was warmed to room temperature and after 15 min, 1.13 mL (12.4 mmol) of allyl iodide was added. After 1 h, the mixture was acidified with 120 mL of 1 M HCl and extracted with ether. The combined organic

phases were washed with water, dried and concentrated in vacuo. The residue was chromatographed (elution with 30% dichloromethane-ethyl acetate) to give 998 mg (67%) of **95** as a white solid: mp 137-138 °C (from benzene-petroleum ether); IR (KBr) 3200-2300 (broad, O-H stretch), 1660 (C=O) cm^{-1}; ^{1}H NMR (300 MHz) δ 8.16 (d, J = 7.7 Hz, 1 H, H-3), 7.47-7.43 (m, 2 H, Ar-H), 7.29-7.23 (m, 1 H, Ar-H), 6.07-5.96 (m, 1 H, CH=C), 5.39 (dd, J = 16.9, 1.3 Hz, 1 H, C=CHa), 5.15 (d, J = 10.0 Hz, 1 H, C=CHb), 3.59 (d, J = 7.2 Hz, 2 H, SeCH$_2$); ^{13}C NMR (75 MHz) δ 172.0 (COOH), 139.3, 133.4, 133.3, 132.8, 128.3, 127.4, 124.9, 118.5, 28.4 (SeCH$_2$); mass spectrum, m/z (relative intensity) 242 (19, M$^+$), 201 (100, M$^+$ - C$_3$H$_5$). Exact mass calcd for C$_{10}$H$_{10}$O$_2{}^{80}$Se: 241.9846. Found: 241.9832. Analysis calcd for C$_{10}$H$_{10}$O$_2$Se: C, 49.81; H, 4.18. Found: C, 49.72; H, 3.91.

3.2.6 Preparation of benzo-3-oxo-1,2-oxaselenolane *Se*-oxide (90)
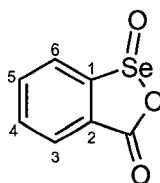
tert-Butyl hydroperoxide (0.65 mL of 56% aqueous solution, 3.8 mmol) was added to 322 mg (1.33 mmol) of allyl selenide **95** in 40 mL of dichloromethane. The mixture was stirred at room temperature for 14 h, concentrated in vacuo and recrystallized from acetonitrile to provide 212 mg (74%) of **90** as a white solid with mp 226-227 °C (from water); IR (KBr) 1653 (C=O), 1583, 1276 cm^{-1}; ^{1}H NMR (300 MHz, CD$_3$OD) δ 8.23 (dd, J = 7.7, 1.0 Hz, 1 H, H-3), 8.11 (dd, J = 7.4 Hz, 1.3 Hz, 1 H, H-6), 7.85-7.80 (m, 1 H, H-4), 7.69-7.65 (m, 1 H, H-5); ^{13}C NMR (100 MHz, D$_2$O, 340 K) δ 170.8 (C=O), 147.8, 134.8, 133.3, 131.6, 130.3, 125.1; ^{77}Se NMR (57 MHz) δ 1022.3; mass spectrum, m/z (relative intensity) 216 (9, M$^+$), 200 (28, M$^+$ - O), 120 (100, M$^+$ - SeO). Exact mass calcd for C$_7$H$_4$O$_3{}^{80}$Se: 215.9326. Found: 215.9309.

3.2.7 Preparation of 2-bromo-5-methoxybenzaldehyde (97)[139]
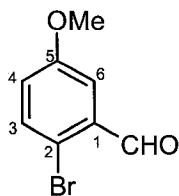
m-Anisaldehyde (96) (1.1 mL, 9.0 mmol) dissolved in 50 mL of chloroform was treated with bromine (2.9 g, 18 mmol) and the mixture was refluxed for 23 h. After the solvent was evaporated, the reddish solid was dissolved in hot hexane, treated with charcoal, and filtered through a Celite plug. After cooling the filtrate, 1.63 g (84%) of white product precipitated with mp 72-74 °C (from hexanes) lit[139] mp 73 °C; IR (KBr) 1675 (C=O), 1597, 1570, 1278, 1060, 1015, 820, 755 cm^{-1}; ^{1}H NMR (300 MHz) δ 10.31 (br s, 1 H, CHO), 7.52 (d, $J = 8.8$ Hz, 1 H, H-3), 7.41 (d, $J = 3.2$ Hz, 1 H, H-6), 7.03 (dd, $J = 8.8$ Hz, 3.2 Hz, 1 H, H-4), 3.81 (s, 3 H, OCH$_3$); ^{13}C NMR (75 MHz) δ 191.7 (C=O), 159.2 (C-5), 134.5, 133.9, 123.0, 117.9, 112.7, 55.7 (OCH$_3$).

3.2.8 Preparation of 2-bromo-5-methoxybenzyl alcohol (98)[140]
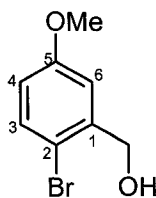
2-Bromo-5-methoxybenzaldehyde (97) (8.3 g, 39 mmol) was dissolved in 150 mL of methanol, cooled to 0 °C and with vigorous stirring, was cautiously treated with sodium borohydride (5.8 g, 0.15 mol). After the initial vigorous reaction subsided (ca. 15 min), the cooling bath was removed and the reaction mixture was stirred at room temperature. After 18 h, the solution was cooled to 0 °C, treated with 1 M hydrochloric acid (20 mL), concentrated to minimal volume, saturated with ammonium chloride solution and extracted with diethyl ether. After pooling the organic layers, drying with

anhydrous magnesium sulfate and concentration, the product was chromatographed (80% hexanes – ethyl acetate) to give 6.18 g (74%) of a white fluffy solid with mp 46-47 °C (from hexanes), lit[140] mp 49 °C; IR (KBr) 3270 (broad, O-H stretch), 1593 (C=C), 1572, 1297, 1270, 1218, 1160, 1056, 1013, 854, 808 cm^{-1}; ^{1}H NMR (300 MHz) δ 7.39 (d, J = 8.7 Hz, 1 H, H-3), 7.04 (d, J = 3.1 Hz, 1 H, H-6), 6.69 (dd, J = 8.7 Hz, 3.1 Hz, 1 H, H-4), 4.67 (s, 2 H, OCH$_2$), 3.79 (s, 3 H, OCH$_3$), 2.54 (br s, 1 H, OH); ^{13}C NMR (75 MHz) δ 159.4 (C-5), 140.9, 133.2, 114.8, 114.3, 112.6, 65.0 (OCH$_2$), 55.6 (OCH$_3$); mass spectrum, m/z (relative intensity) 216 (78, M$^+$), 201 (8, M$^+$ - CH$_3$), 137 (39), 109 (100), 94 (83), 77 (99), 63 (98), 51 (56), 39 (59). Exact mass calcd for C$_8$H$_9$O$_2$^{79}Br: 215.9786. Found: 215.9798.

3.2.9 Preparation of 2, 2`-diselenobis(5-methoxybenzyl) alcohol (100)
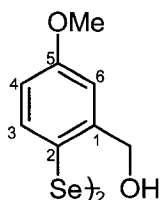
In a flame-dried 100 mL round bottom flask, 300 mg (1.38 mmol) of 2-bromo-5-methoxybenzyl alcohol (98) was dissolved in 15 mL of dry THF, cooled to – 78 °C under a nitrogen atmosphere and treated with *tert*-butyllithium (2.5 mL, 4.2 mmol). After being stirred for 40 min, selenium powder (0.33 g, 4.2 mmol) was added and the cooling bath was removed. The mixture was stirred for 5 h under nitrogen at room temperature to dissolve the selenium, forming a red solution. The flask was opened and the mixture was stirred overnight in the presence of air, followed by quenching with 1 M hydrochloric acid (8 mL), extraction with diethyl ether, washing with saturated ammonium chloride, drying and concentration in vacuo. The final product was chromatographed (50% hexane - ethyl acetate) to give 173 mg (58%) of yellow oil, which solidified upon standing with mp 103-104 °C (from ethanol/hexane); IR (KBr) 3337 (broad, O-H stretch), 1585 (C=C),

1566, 1294, 1222, 1163, 1056, 1014, 815, 795 cm^{-1}; ^{1}H NMR (300 MHz) δ 7.47 (d, J = 8.7 Hz, 2 H, H-3), 7.04 (d, J = 3.1 Hz, 2 H, H-6), 6.74 (dd, J = 8.7 Hz, 3.1 Hz, 2 H, H-4), 4.65 (s, 4 H, OCH$_2$), 3.84 (s, 6 H, OCH$_3$), 2.05 (br s, 2 H, OH); ^{13}C NMR (75 MHz) δ 161.3 (C-5), 145.7,139.1, 120.5, 114.2, 114.0, 65.6 (OCH$_2$), 55.5 (OCH$_3$); ^{77}Se NMR (76 MHz) δ 452.6; mass spectrum, m/z (relative intensity) 432 (8, M$^+$), 405 (16), 256 (18), 200 (58), 108 (100), 71 (55), 57 (93), 43 (69). Exact mass calcd for C$_{16}$H$_{18}$O$_4$^{80}Se$_2$: 433.9536. Found: 433.9517.

3.2.10 Preparation of allyl (2-hydroxymethyl)-4-methoxyphenyl selenide (101)
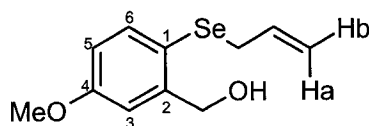
Diselenide **100** (176 mg, 405 μmol) was dissolved in 10 mL of dry THF, cooled to 0 °C and treated with sodium borohydride (77 mg, 2.0 mmol). Then, 2 mL of absolute ethanol were added dropwise to aid dissolution of the sodium borohydride and promote the reaction. After the vigorous reaction and evolution of hydrogen gas subsided, the solution was stirred under a nitrogen atmosphere until it turned pale yellow (ca. 5 min), indicating the formation of the selenolate ion. Following the addition of the allyl iodide (74 μL, 0.81 mmol), the mixture was stirred at room temperature for 1.5 h. Then, 1 M hydrochloric acid (5 mL) was added and the mixture was extracted with diethyl ether, dried, concentrated and chromatographed (elution with 40% ethyl acetate-hexanes) to give 171 mg (83%) of a clear oil; IR (neat) 3371 (broad, O-H stretch), 1591, 1293, 1234, 1053, 1018, 914, 813 cm^{-1}; ^{1}H NMR (300 MHz) δ 7.49 (d, J = 8.7 Hz, 1 H, H-6), 7.00 (d, J = 2.6 Hz, 1 H, H-3), 6.75 (dd, J = 7.2 Hz, 3.1 Hz, 1 H, H-5), 5.94-5.86 (m, 1 H, C=CH), 4.90 (dd, J = 10.3 Hz, 1.6 Hz, 1 H, C=CHb), 4.81 (dd, J = 15.4 Hz, 1.6 Hz, 1 H, C=CHa), 4.76 (d, J = 6.2 Hz, 2 H, OCH$_2$), 3.81 (s, 3 H, OCH$_3$), 3.40 (d, J = 7.2 Hz, 2 H, SeCH$_2$),

2.48 (t, J = 6.2 Hz, 1 H, OH); ^{13}C NMR (75 MHz) δ 160.2 (C-4), 145.6, 138.3, 134.5, 118.9, 116.9, 114.1, 114.0, 65.8 (OCH$_2$), 55.4 (OCH$_3$), 31.1 (SeCH$_2$); mass spectrum, m/z (relative intensity) 258 (16, M$^+$), 217 (12, M$^+$ - C$_3$H$_5$), 136 (17), 108 (100), 39 (21). Exact mass calcd for C$_{11}$H$_{14}$O$_2$^{80}Se: 258.0159. Found: 258.0140

3.2.11 Preparation of p-methoxybenzo-1,2-oxaselenolane Se-oxide (91)
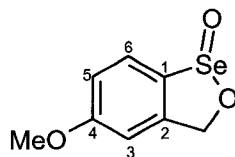
Cyclic seleninate **91** was prepared as in the case of **89**, by oxidation of allyl selenide **101** (137 mg, 0.534 mmol) with 58% tert-butyl hydroperoxide (430 μL, 2.7 mmol), in 81% (101 mg) yield as a fine white powder with mp 169-170 °C after recrystallization from ethyl acetate; IR (KBr) 1600, 1280, 1239, 1152, 1049, 983, 830 cm^{-1}; ^{1}H NMR (300 MHz) δ 7.67 (d, J = 8.7 Hz, 1 H, H-6), 7.04 (dd, J = 8.7 Hz, 2.0 Hz, 1 H, H-5), 6.94 (d, J = 2.0 Hz, 1 H, H-3), 5.93 (d, J = 13.8 Hz, 1 H, OCHa), 5.55 (d, J = 13.8 Hz, 1 H, OCHb), 3.88 (s, 3 H, OCH$_3$); ^{13}C NMR (75 MHz) δ 163.0 (C-4), 146.6, 139.8, 126.6, 115.9, 107.3, 78.2 (OCH$_2$), 55.9 (OCH$_3$); ^{77}Se NMR (57 MHz) δ 1348.8; mass spectrum, m/z (relative intensity) 232 (5, M$^+$), 216 (11, M$^+$ - O), 136 (84, M$^+$ - SeO), 108 (41), 43 (100). Exact mass calcd for C$_8$H$_8$O$_3$^{80}Se: 231.9639. Found: 231.9965. Analysis calcd for C$_7$H$_6$O$_2$Se: C, 41.58; H, 3.49. Found: C, 41.61; H 3.60.

3.2.12 Preparation of 2, 2`-diselenobis(5-fluorobenzoic acid) (116)
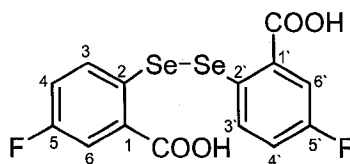
To a stirred solution containing 5.0 g (32 mmol) of 2-amino-5-fluorobenzoic acid (115) and 4.8 mL of concentrated hydrochloric acid in 50 mL of water cooled in an ice bath were added dropwise 2.36 g (34.2 mmol) of sodium nitrite in 30 mL of water while the temperature was maintained below 5 °C. The resulting solution of the diazonium salt was stirred for 20 min while a solution of potassium diselenide was prepared in the following fashion. Selenium (5.1 g, 65 mmol) and potassium hydroxide (16 g, 40 mmol) were melted in a 500 mL round bottom flask. Cold water (80 mL) was added to the hot melt to produce a red aqueous solution of potassium diselenide, which was subsequently cooled to 0 °C. The pH of the diazonium salt solution was adjusted to 6 with solid sodium acetate and this mixture was added dropwise to the potassium diselenide solution. The resulting mixture was stirred for 0.5 h at room temperature, then slowly warmed to 80 °C, cooled to room temperature and filtered to remove red selenium. The filtrate was acidified with concentrated hydrochloric acid, yielding 5.95 g (85%) of a precipitated orange solid with mp 263-266 °C. This compound was used without any further purification; IR (KBr) 3421-2550 (broad, O-H), 1675 (C=O), 1257, 1202, 824, 762 cm^{-1}; ^{1}H NMR (300 MHz, Acetone-d$_6$) δ 7.87 (dd, J = 9.2 Hz, 3.1 Hz, 1H, H-3), 7.79 (dd, J = 8.7 Hz, 5.1 Hz, 1 H, H-6), 6.74 (dt, J = 8.2 Hz, 3.1 Hz, 1 H, H-4); ^{13}C NMR (75 MHz, Acetone-d$_6$) δ 168.2 (COOH), 162.4 (d, J = 243.2 Hz, C-5,5`), 132.8 (d, $J$ = 6.7 Hz, C-3,3`), 131.2 (C-2,2`), 129.7 (C-1,1`), 121.4 (d, J = 21.2 Hz, C-4,4`), 118.8 (d, $J$ = 23.0 Hz, C-6,6`); mass spectrum, m/z (relative intensity) 438 (8, M$^+$), 358 (21), 219 (54), 202 (100), 174 (94), 131 (49), 71 (10). Exact mass calcd for C$_{14}$H$_8$O$_4$F$_2$^{80}Se$_2$: 437.8721. Found: 437.8736.

3.2.13 Preparation of allyl 4-fluoro-(2-hydroxymethyl)phenyl selenide (117)
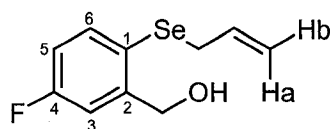
Compound **117** was prepared in 49% yield (223 mg) by the method described earlier for the preparation of **94**, by the reduction of diacid **116** (400 mg, 0.9 mmol) with lithium aluminum hydride (174 mg, 4.59 mmol), followed by alkylation with allyl iodide (170 µL, 1.9 mmol). The product was chromatographed (elution with 40% ethyl acetate-hexanes) to afford yellow oil; IR (neat, NaCl) 3304 (broad, O-H stretch), 1626, 1600 (C=C), 1579, 1464, 1268, 1226, 1146, 1104, 1028, 986, 917, 873, 813 cm^{-1}; ^{1}H NMR (300 MHz) δ 7.52 (dd, J = 8.4 Hz, 5.8 Hz, 1 H, H-6), 7.20 (dd, J = 9.5 Hz, 2.7 Hz, 1 H, H-3), 6.89 (dt, J = 8.3 Hz, 2.8 Hz, 1 H, H-5), 5.96-5.82 (m, 1 H, C=CH), 4.91 (d, J = 9.9 Hz, 1 H, C=CHb), 4.83 (d, J = 17.1 Hz, 1 H, C=CHa), 4.76 (d, J = 5.8 Hz, 2 H, OCH$_2$), 3.44 (d, J = 7.6 Hz, 2 H, SeCH$_2$), 2.39 (t, J = 5.9 Hz, 1 H, OH); ^{13}C NMR (75 MHz) δ 164.6 (d, J = 246.6 Hz, C-4), 147.8 (d, J = 7.1 Hz, C-5), 139.4 (d, J = 7.7 Hz, C-3), 135.6 (=CH$_2$), 124.5 (d, J = 3.3 Hz, C-1), 118.8 (CH), 116.8 (d, J = 6.4 Hz, C-6), 116.5 (d, J = 5.1 Hz, C-2), 66.6 (d, J = 1.2 Hz, OCH$_2$), 33.2 (SeCH$_2$); ^{77}Se NMR (57 MHz) δ 262.9; mass spectrum, m/z (relative intensity) 246 (24, M$^+$), 205 (31, M$^+$ - C$_3$H$_5$), 177 (9), 147 (14), 123 (10), 96 (100), 75 (10), 41 (37). Exact mass calcd forC$_{10}$H$_{11}$OF^{80}Se: 245.9959. Found: 245.9941. Analysis calcd for C$_{10}$H$_{11}$FOSe: C, 48.99; H, 4.52. Found: C, 48.89; H, 4.77.

3.2.14 Preparation of *p*-fluorobenzo-1,2-oxaselenolane *Se*-oxide (93)
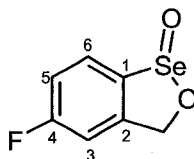
Compound **93** was prepared by oxidation of allyl selenide **117** (530 mg, 2.2 mmol) with 65% *tert*-butyl hydroperoxide (1.6 mL, 11 mmol) in dichloromethane (15 mL) as in the case of the preparation of **90**. After evaporation of the solvent and recrystallization of the crude product from ethyl acetate, **93** was obtained as a fine white powder in 78% yield (373 mg) with mp 141-142 °C; IR (KBr) 3073, 1579, 1250, 1231, 1134, 989, 927, 861, 830, 795 cm^{-1}; ^{1}H NMR (300 MHz) δ 7.91 (dd, J = 9.2 Hz, 5.0 Hz, 1 H, H-6), 7.27-7.09 (m, 2 H, Ar-H), 5.88 (d, J = 14.1 Hz, 1 H, OCHa), 5.53 (d, J = 14.1 Hz, 1 H, OCHb); ^{13}C NMR (75 MHz) δ 166.6 (d, J = 251.7 Hz, C-4), 148.5 (d, J = 8.9 Hz, C-2), 145.2 (C-1), 130.0 (d, J = 9.5 Hz, C-6), 118.2 (d, J = 23.2 Hz, C-3), 111.5 (d, J = 23.9 Hz, C-5), 79.2 (OCH$_2$); ^{77}Se NMR (76 MHz, Acetone-d$_6$) δ 1358.9; mass spectrum, *m/z* (relative intensity) 220 (12, M$^+$), 201 (3, M$^+$ - F), 124 (51), 96 (100), 50 (21). Exact mass calcd for C$_7$H$_5$O$_2$F^{80}Se: 219.9439. Found: 219.9455. Analysis calcd for C$_7$H$_5$O$_2$FSe: C, 38.38; H, 2.30. Found: C, 37.57; H, 2.58.

3.2.15 Preparation of selenenyl sulfide 118
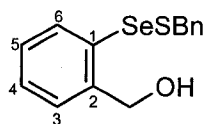
Cyclic seleninate ester **89** (115 mg, 0.572 mmol) was dissolved in 40 mL of dichloromethane and cooled in an ice-bath. Benzyl thiol (202 µL, 1.72 mmol) was added and stirring was continued for 10 min. The solution turned dark violet and then yellow. The solvent was evaporated and the crude product was chromatographed (elution with 15% ethyl acetate-hexanes) to afford 153 mg (86%) of **118** as a pale yellow oil, which

was stored in the refrigerator; IR (neat) 3356 (broad O-H stretch), 1258, 1198, 1023, 755, 695; ^{1}H NMR (300 MHz) δ 7.75 (d, J = 6.7 Hz, 1 H, H-6), 7.37-7.12 (m, 8 H, Ar-H), 4.77 (s, 2 H, OCH$_2$), 4.04 (s, 2 H, SCH$_2$), 1.96 (br s, 1 H, OH); ^{13}C NMR (75 MHz) δ 140.9, 137.8, 132.2, 131.8, 129.3, 128.7, 128.6, 128.5, 128.0, 127.6, 65.5 (OCH$_2$), 42.3 (SCH$_2$); ^{77}Se NMR (76 MHz) δ 440.2; mass spectrum, m/z (relative intensity) 310 (8, M$^+$), 186 (18, M$^+$ - SBn), 91 (100, Bn). Exact mass calcd for C$_{14}$H$_{14}$OS^{80}Se: 309.9931. Found: 309.9954. Analysis calcd for C$_{14}$H$_{14}$OSSe: C, 54.37; H, 4.56. Found: C, 54.58; H, 4.81.

3.2.16 Preparation of selenenyl sulfide 123
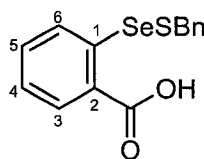
Cyclic seleninate ester **90** (22 mg, 0.10 mmol) was dissolved in 10 mL of methanol. Benzyl thiol (32 μL, 0.27 mmol) was added and the mixture was stirred for 1 h at room temperature. The product was concentrated in vacuo and recrystallized from ethyl acetate-hexanes to afford 23 mg (73%) of **123** as a white solid, mp 153-155 °C; IR (KBr) 3300-2300 (broad, O-H stretch), 1660 (C=O), 1266, 1027, 736; ^{1}H NMR (300 MHz) δ 8.19-8.10 (m, 2 H, Ar-H), 7.52-7.46 (m, 1 H, Ar-H), 7.47-7.18 (m, 6 H, Ar-H), 4.04 (s, 2 H, SCH$_2$); ^{13}C NMR (75 MHz) δ 172.2 (COOH), 139.0, 138.2, 134.0, 132.6, 129.1, 128.7, 127.6, 126.3, 125.9, 42.3 (SCH$_2$); ^{77}Se NMR (57 MHz) δ 566.8; mass spectrum, m/z (relative intensity) 324 (2, M$^+$), 200 (7), 91 (100). Analysis calcd for C$_{14}$H$_{12}$O$_2$SSe: C, 52.02; H, 3.74. Found: C, 51.86; H, 3.74.

3.2.17 Preparation of 2,2`-selenobisbenzoic acid (131)[150]
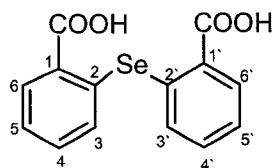
Hydroxymethanesulfinic acid monosodium salt dihydrate (Rongalite C, 0.95 g, 6.2 mmol) was added to 1.9 g (4.8 mmol) of diselenide 12 in 100 mL of 5% sodium hydroxide solution, which resulted in a discharge of the colour of this solution. To this stirred mixture, 2.36 g (9.51 mmol) of o-iodobenzoic acid dissolved in 50 mL of 5% sodium hydroxide solution and 0.60 g (9.5 mmol) of copper powder were added. The reaction mixture was refluxed for 11 h, after which black selenium was filtered and the filtrate was acidified with concentrated hydrochloric acid. The precipitated product was filtered and recrystallized from acetic acid to yield 1.97 g (65%) of 131 as yellow needles with mp 231-232 °C (lit.[150] mp 232 °C); IR (KBr) 3400-2300 (broad, O-H stretch), 1684 (C=O), 1554, 1255, 1028, 925, 802, 743cm^{-1}; ^{1}H NMR (300 MHz, DMSO-d$_6$) δ 13.26 (br s, 2 H, COOH), 7.89 (m, 2 H, H-6), 7.47-7.39 (m, 4 H, Ar-H), 7.30 (m, 2 H, H-4).

3.2.18 Preparation of di(2-hydroxymethyl)phenyl selenide (132)
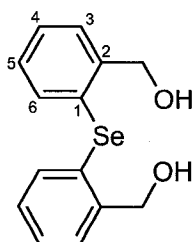
Diacid 131 (360 mg, 1.12 mmol) in 15 mL of dry THF was added dropwise to a refluxing solution of 128 mg (3.36 mmol) of lithium aluminum hydride in 20 mL of dry THF under an argon atmosphere. The resulting white slurry was refluxed for an additional 90 min, cooled to room temperature and quenched cautiously with 50 mL of

cold water. The mixture was filtered, the residue was washed thoroughly with ether and the filtrate was extracted repeatedly with ether. The combined organic layers were washed with saturated NaCl and water, dried and concentrated in vacuo. The product was chromatographed (elution with dichloromethane-ethyl acetate 3:1) to give 174 mg (53%) of **132** as a clear oil, which solidified upon standing: mp 84-86 °C (from dichloromethane-hexanes); IR (neat) 3300 (broad, O-H stretch), 1006, 733 cm^{-1}; ^{1}H NMR (300 MHz) δ 7.47 (dd, J = 6.9, 1.5 Hz, 2 H, H-6), 7.35-7.27 (m, 4 H, Ar-H), 7.21-7.15 (m, 2 H, Ar-H), 4.77 (s, 4 H, OCH$_2$), 1.89 (br s, 2 H, OH); ^{13}C NMR (75 MHz) δ 142.2, 134.6, 130.6, 129.0, 128.9, 128.5, 65.5 (OCH$_2$); ^{77}Se NMR (76 MHz) δ 316.5; mass spectrum, m/z (relative intensity) 294 (40, M$^+$), 292 (20), 246 (20), 228 (14), 195 (72), 91 (79), 77 (100). Exact mass calcd for C$_{14}$H$_{14}$O$_2$^{80}Se: 294.0159. Found: 294.0139.

3.2.19 Preparation of spirodioxyselenurane 124
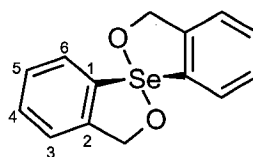
Selenide **126** (114 mg, 0.389 mmol) was dissolved in 15 mL of dichloromethane and 80 μL (0.7 mmol) of 29% aqueous hydrogen peroxide was added. The mixture was stirred for 8 h at room temperature, the solvent was evaporated and the crude product was chromatographed (elution with 75% ethyl acetate – hexanes) to afford 80 mg (71%) of **124** as a white solid: mp 171-173 °C (from ethyl acetate); IR (KBr) 2798, 1441, 1201, 1008 cm^{-1}; ^{1}H NMR (300 MHz) δ 8.03 (d, J = 7.2 Hz, 2 H, H-6), 7.41-7.34 (m, 4 H, Ar-H), 7.26–7.23 (m, 2 H, Ar-H), 5.32 (s, 4 H, OCH$_2$); ^{13}C NMR (75 MHz) δ 143.8, 134.1, 131.1, 128.2, 127.9, 124.3, 71.0 (OCH$_2$); ^{77}Se NMR (76 MHz) δ 804.4; mass spectrum, m/z (relative intensity) 292 (20, M$^+$), 291 (47), 263 (68), 77 (100). Analysis calcd for C$_{14}$H$_{12}$O$_2$Se: C, 57.74; H, 4.15. Found: C, 57.57; H, 4.18.

3.2.20 Preparation of spirodioxyselenurane 125[150]
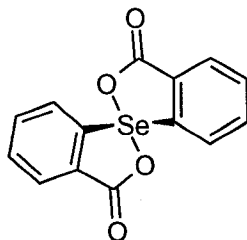
The product was obtained in 73% yield by oxidation of selenide **131** with hydrogen peroxide as described in the literature;[150] mp 326-328 °C (from ethyl acetate); lit.[150] mp 310-322 °C; IR (KBr) 1695 (C=O), 1269, 1104, 831, 743 cm^{-1}, ^{1}H NMR (300 MHz,) δ 8.25-8.10 (m, 4 H, Ar-H), 7.90-7.75 (m, 4 H, Ar-H); ^{13}C NMR (75 MHz, DMSO-d$_6$) δ 169.8 (C=O), 142.7, 136.2, 133.9, 130.4, 130.2, 127.1. Analysis calcd for C$_{14}$H$_8$O$_4$Se: C, 52.68; H, 2.53. Found: C, 52.25; H 2.43.

3.2.21 Preparation of 2,2`-selenobis(5-methoxybenzyl alcohol) (133)
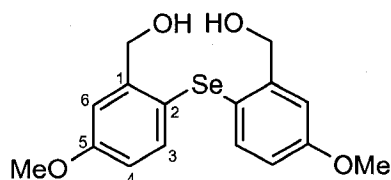
In a flame-dried 50 mL round bottom flask, 700 mg (3.22 mmol) of of 2-bromo-5-methoxybenzyl alcohol (**98**) were dissolved in 10 mL of dry THF, cooled to -78 °C under a nitrogen atmosphere and slowly treated with *tert*-butyllithium (4.0 mL, 6.8 mmol). After stirring the mixture at -78 °C for 40 min, it was slowly treated with selenium (II) diethylthiocarbamate (Se(dtc)$_2$)[151] (1.36 g, 3.64 mmol) dissolved in 15 mL of dry THF. The mixture was stirred at room temperature for 6 h and quenched with 1 M hydrochloric acid (15 mL). After washing with brine, extracting with ethyl acetate, drying and concentrating, the product was chromatographed (elution with 50% hexane - ethyl acetate) to give 208 mg (37%) of a clear solid with mp 77-78 °C; IR (neat) 3355

(broad, O-H stretch), 1591, 1472, 1234, 1051, 1016, 859, 734 cm^{-1}; ^{1}H NMR (300 MHz) δ 7.27 (d, $J = 10.8$ Hz, 2 H, H-3), 7.02 (d, $J = 2.6$ Hz, 2 H, H-6), 6.70 (dd, $J = 8.7$ Hz, 3.1 Hz, 2 H, H-4), 4.66 (s, 4 H, OCH$_2$), 3.79 (s, 6 H, OCH$_3$), 2.52 (br s, 2 H, OH); ^{13}C NMR (75 MHz) δ 159.9 (C-5), 143.8, 135.9, 120.6, 114.4, 114.3, 65.3 (OCH$_2$), 55.5 (OCH$_3$); mass spectrum, m/z (relative intensity) 354 (61, M$^+$), 256 (47), 214 (37), 200 (25), 135 (44), 121 (87), 108 (100), 77 (47). Exact mass calcd for C$_{16}$H$_{16}$O$_4$^{80}Se: 354.0370. Found: 354.0366.

3.2.22 Preparation of spirodioxyselenurane 126
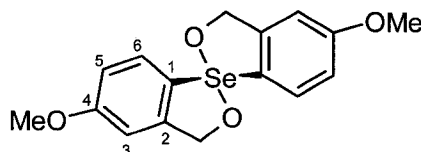
Compound **126** was obtained in 89% yield (182 mg), by oxidation of selenide **133** (206 mg, 0.582 mmol) with 65% *tert*-butyl hydroperoxide (0.80 mL, 8.6 mmol) in dichloromethane (20 mL), after recrystallization from ethyl acetate-hexanes (1:1) as a white powder with mp 171-173 °C; IR (KBr) 1581, 1276, 1234, 1027, 902, 872, 796 cm^{-}^{1}; ^{1}H NMR (300 MHz) δ 7.89 (d, $J = 8.7$ Hz, 2 H, H-6), 6.92 (dd, $J = 8.2$ Hz, 2.0 Hz, 2 H, H-5), 6.76 (d, $J = 2.0$ Hz, 2 H, H-3), 5.31 (d, $J = 14.4$ Hz, 2 H, OCHa), 5.26 (d, $J = 14.4$ Hz, 2 H, OCHb) 3.81 (s, 6 H, OCH$_3$); ^{13}C NMR (75 MHz) δ 163.9 (C-4), 147.5, 130.4, 127.0, 115.9, 110.3, 72.4 (OCH$_2$), 57.2 (OCH$_3$); ^{77}Se NMR (57 MHz) δ 800.9; mass spectrum, m/z (relative intensity) 352 (37, M$^+$), 321 (11, M$^+$ - OCH$_3$), 305 (27), 214 (40), 135 (44), 108 (70), 77 (62), 63 (100). Exact mass calcd for C$_{16}$H$_{16}$O$_4$Se: 352.0214. Found: 352.0206. Analysis calcd for C$_{16}$H$_{16}$O$_4$Se: C, 54.71; H, 4.59. Found: C, 53.89; H, 4.48.

3.2.23 Preparation of 2-amino-5-fluorobenzyl alcohol (136)[152]
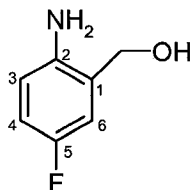
To lithium aluminum hydride (980 mg, 25.8 mmol) in 15 mL of dry THF, under an argon atmosphere and cooled to 0 °C, 5-fluoroanthranilic acid (115) (2.0 g, 13 mmol) dissolved in 15 mL of dry THF was added dropwise. The yellow-green solution was then stirred at room temperature for 2 h, quenched with 20 mL of water and 15 mL of 5% sodium hydroxide, filtered and extracted with ethyl acetate. After evaporation in vacuo, 1.68 g (92%) of 136 was obtained as yellow solid with mp 92-94 °C (lit[152] mp 103-108 °C); IR (KBr) 3384 (O-H stretch), 3195 (N-H), 1617, 1507, 1430, 1251, 1017, 883, 822, 715; ^{1}H NMR (200 MHz) δ 6.86 (m, 2 H, Ar-H), 6.64 (m, 1 H, Ar-H), 4.63 (s, 2 H, OCH$_2$), 4.04 (br s, 2 H, NH$_2$), 1.70 (br s, 1 H, OH).

3.2.24 Preparation of 2, 2`-diselenobis(5-fluorobenzyl alcohol) (137)
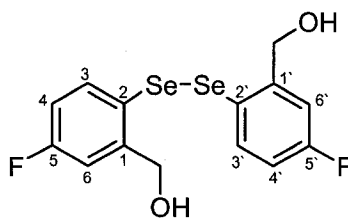
To lithium aluminum hydride (0.89 g, 23 mmol) in dry THF (20 mL) under an argon atmosphere at room temperature, 2, 2`-diselenobis(5-fluorobenzoic acid) (116) (2.05 g, 4.70 mmol) dissolved in 10 mL of dry THF was added dropwise. After refluxing for 50 min, the mixture was quenched with 20 mL of water and extracted with ethyl acetate. The aqueous solution was left sitting overnight with consequent precipitation of 815 mg (42%) of 137 as yellow needles with mp 112 °C; IR (KBr) 3214 (broad, O-H

stretch), 1577, 1016, 874, 814 cm^{-1}; ^{1}H NMR (300 MHz) δ 7.52 (dd, J = 8.2 Hz, 5.6 Hz, 2 H, H-3), 7.24 (dd, J = 9.8 Hz, 3.1 Hz, 2 H, H-6), 6.89 (dt, J = 8.2 Hz, 3.1 Hz, 2 H, H-4), 4.69 (s, 4 H, OCH$_2$), 2.06 (br s, 2 H, OH); ^{13}C NMR (75 MHz) δ 163.9 (d, J = 248.7 Hz, C-5,5'), 145.9 (d, J = 7.3 Hz, C-1,1'), 138.3 (d, J = 7.9 Hz, C-3, 3'), 124.2 (d, J = 3.7 Hz, C-2,2'), 115.6 (d, J = 12.1 Hz, C-4,4'), 115.3 (d, J = 13.4 Hz, C-6,6'), 64.9 (d, J = 1.2 Hz, OCH$_2$); ^{77}Se NMR (57 MHz) δ 441.8; mass spectrum, m/z (relative intensity) 410 (10, M$^+$), 188 (23), 123 (16), 96 (100), 75 (16). Exact mass calcd for C$_{14}$H$_{12}$O$_2$F$_2$^{80}Se$_2$: 409.9134. Found: 409.9132. Analysis calcd for C$_{14}$H$_{12}$O$_2$F$_2$Se$_2$: C, 41.20; H, 2.96. Found: C, 41.03; H, 2.83.

3.2.25 Preparation of 2,2'-selenobis(5-fluorobenzyl alcohol) (135)
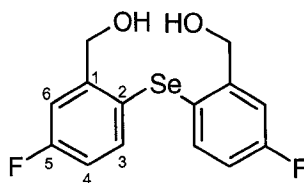
Amino alcohol **136** (90 mg, 0.64 mmol), suspended in 2 mL of water, was cooled to 0 °C and treated with 0.33 mL of concentrated hydrochloric acid, followed by dropwise addition of sodium nitrite (53 mg, 0.77 mmol) in one mL of water. The diazonium salt was stirred at 0 °C for 10 min. Meanwhile, diselenide **137** (104 mg, 0.254 mmol) was dissolved in 8 mL of THF-water (1:1), cooled to 0 °C under an argon atmosphere and treated with sodium borohydride (29 mg, 0.77 mmol). After the vigorous reaction subsided and formation of clear solution of the selenolate anion occured, the mixture was treated dropwise with the solution of the diazonium salt, the pH of which was adjusted to 5.5 with a saturated solution of sodium acetate. The addition of the diazonium salt was accompanied by a vigorous reaction. The reation mixture was then warmed to room temperature and stirred for 1 h, followed by the addition of ethyl acetate (10 mL) and saturated ammonium chloride (5 mL). The organic phase was separated,

dried and concentrated to give a red-brown oil, which was chromatographed (elution with 40% ethyl acetate-hexanes). The final product **135** (57 mg, 34%) was obtained as a pale yellow oil, which solidified upon standing (mp 109-111 °C); IR (neat, NaCl) 3291 (broad, O-H stretch), 1268, 1025, 813 cm^{-1}; ^{1}H NMR (300 MHz) δ 7.27-7.19 (m, 4 H, Ar-H), 6.87 (dt, J = 8.3 Hz, 2.9 Hz, 2 H, H-4), 4.68 (s, 4 H, OCH$_2$), 2.57 (br s, 2 H, OH); ^{13}C NMR (75 MHz) δ 164.6 (d, J = 246.8 Hz, C-5), 146.2 (d, J = 7.0 Hz, C-1), 137.5 (d, J = 7.7 Hz, C-3), 125.6 (d, J = 3.2 Hz, C-2), 117.3 (d, J = 7.6 Hz, C-4), 117.0 (d, J = 8.8 Hz, C-6), 66.1 (d, J = 1.1 Hz, OCH$_2$); ^{77}Se NMR (57 MHz) δ 300.3; mass spectrum, m/z (relative intensity) 330 (65, M$^+$), 281 (15, M$^+$ - CH$_2$OF), 232 (58, M+ - C$_2$H$_4$O$_2$F$_2$), 214 (29), 202 (45), 123 (39), 109 (73), 96 (100). Exact mass calcd for C$_{14}$H$_{12}$O$_2$F$_2$^{80}Se: 329.9971. Found: 329.9946. Analysis calcd for C$_{14}$H$_{12}$O$_2$F$_2$Se: C, 51.08; H, 3.67. Found: C, 50.45; H, 3.80. Analysis calcd for C$_{14}$H$_{12}$O$_2$F$_2$Se: C, 51.08; H, 3.67. Found: C, 50.46; H, 3.54.

3.2.26 Preparation of spirodioxyselenurane 127
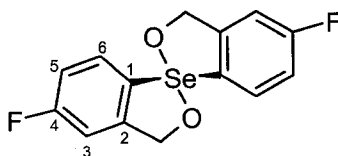
Compound **127** was prepared by oxidation of selenide **135** (63.3 mg, 0.192 mmol) with 32% hydrogen peroxide (0.14 mL, 1.3 mmol) in dichloromethane and recrystallized from ethyl acetate to afford a white powder with mp 189-191 °C in 97% (61.3 mg) yield; IR (KBr) 1581, 1250, 1026, 928, 860, 821, 759 cm^{-1}; ^{1}H NMR (400 MHz) δ 7.97 (dd, J = 8.8 Hz, 5.0 Hz, 2 H, H-6), 7.08 (dt, J = 8.6 Hz, 2.5 Hz, 2 H, H-5), 6.96 (dd, J = 8.3 Hz, 2.5 Hz, 2 H, H-3), 5.32 (d, J = 14.9 Hz, 2 H, OCHa), 5.26 (d, J = 14.9 Hz, 2 H, OCHb); ^{13}C NMR (100 MHz) δ 164.9 (d, J = 252.4 Hz, C-4), 146.2 (d, J = 8.2 Hz, C-6), 129.5 (d, J = 9.4 Hz, C-2), 128.6 (C-1), 115.8 (d, J = 23.4 Hz, C-5), 111.2 (d, J = 23.3 Hz, C-3), 70.5 (d, J = 2.2 Hz, OCH$_2$); ^{77}Se NMR (76 MHz) δ 808.98; mass spectrum, m/z (relative

intensity) 328 (3, M$^+$), 297 (25), 256 (11), 173 (9), 71 (44), 43 (100); Exact mass calcd for $C_{14}H_9O_2F_2{}^{80}Se$: 326.9736. Found: 326.9750.

3.2.27 Preparation of 2,2`-selenobisbenzamide (141)[162]
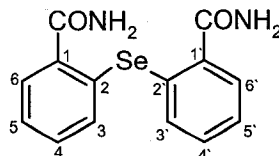
In a dry 250 mL round-bottom flask, diacid **125** (1.27 g, 3.95 mmol) was treated with 15.0 mL (206 mmol) of thionyl chloride and heated with a heat gun until all the acid had dissolved (ca. 5 min). The resulting acid chloride was concentrated and dried in vacuo. It was dissolved in dry benzene and anhydrous ammonia was bubbled through this solution for 10 min with concomitant precipitation of amide **141**. The volume of the mixture was decreased in vacuo and the product was filtered, followed by flash chromatography (elution with acetone), to give 636 mg (50%) of **141** as a white solid with mp 209-210 °C, lit[162] mp 212-213 °C. IR (KBr) 3444 (N-H stretch asym.), 3334 (N-H stretch sym.), 3205, 1653(C=O), 1602 (amide II band), 1381, 747 cm^{-1}; ^{1}H NMR (300 MHz, DMSO-d$_6$) δ 7.91 (br s, 2 H, NH), 7.59 (dd, J = 7.2 Hz, 1.8 Hz, 2 H, H-3), 7.47 (br s, 2 H, NH), 7.34-7.18 (m, 6 H, Ar-H); ^{13}C NMR (75 MHz) δ 170.8 (C=O), 139.3, 134.7, 133.5, 131.2, 128.7, 127.5; mass spectrum, m/z (relative intensity) 320 (19, M+), 200 (23, M$^+$ - C$_7$H$_2$NO), 138 (17), 50 (100).

3.2.28 Preparation of acylaminoselenonium chloride 128
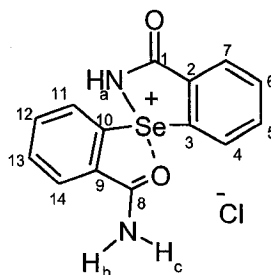
Amide **141** (178 mg, 0.558 mmol), dissolved in 30 mL of methanol-dichloromethane (1:1) solution and cooled in an ice-bath to 5 °C, was treated with 150 mg (1.12 mmol) of N-chlorosuccinimide dissolved in 5mL of methanol/dichloromethane (1:1). The mixture was stirred at room temperature for 5 h, concentrated and washed with ethyl acetate to give the crude product, which was recrystallized from glacial acetic acid to give 160 mg (81%) of a white solid with mp 286-287 °C; IR (KBr) 3268 (N-H stretch), 1665 (C=O), 1595 (amide II band), 1550 (amide II band), 1298, 743 cm^{-1}; ^{1}H NMR (300 MHz, DMSO-d$_6$) δ 10.67 (br s, 1 H, NHa), 9.77 (br s, 1 H, NHb), 9.33 (br s, 1 H, NHc), 8.42 (d, J = 6.9 Hz, 1 H, H-4), 8.43-7.78 (m, 7 H, Ar-H); ^{13}C NMR (75 MHz, DMSO-d$_6$) δ 171.1 (C=O), 170.0 (C=O), 140.5, 140.0, 136.0, 135.9, 133.8, 133.4, 130.4, 130.1, 129.8, 129.2, 127.8, 126.2; ^{77}Se NMR (57 MHz, DMSO-d$_6$) δ 1658.5; mass spectrum (ESI) 319 (M-Cl+H)$^+$, 341 (M-Cl+Na)$^+$; Analysis calcd for C$_{14}$H$_{11}$O$_2$N$_2$ClSe: C, 47.55; H, 3.14. Found: C, 46.79; H, 3.03. For the X-ray crystal structure of the product, see Figure 2.16 and Appendix D.

3.2.29 Preparation of acylaminoselenonium hydroxide 129
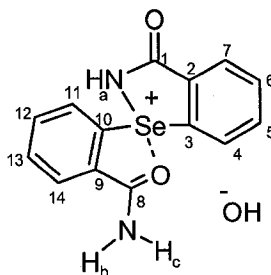
In a 20 mL vial, amide **141** (208 mg, 0.652 mmol) was dissolved in 15 mL of acetone and treated with 29% hydrogen peroxide (0.67 mL, 6.7 mmol). After three days of standing at room temperature, white crystals precipitated, which were filtered to afford 173 mg (79%) of **129** with mp 263-266 °C. IR (KBr) 3217 (N-H stretch), 1700 (C=O), 1676 (C=O), 1616, 1596 (amide II band), 1560 (amide II band), 1409, 1295, 745 cm^{-1}; ^{1}H NMR (300 MHz, DMSO-d$_6$) δ 8.90 (br s, 1 H, NHb), 8.47 (br s, 1 H, NHc), 8.15 (dd, $J =$ 7.2 Hz, 1.5 Hz, 1 H, H-4), 7.95 (d, $J =$ 7.2 Hz, 1 H, H-11), 7.81 (d, $J =$ 7.2 Hz, 1 H, Ar-H), 7.74-7.52 (m, 5 H, Ar-H); ^{13}C NMR (100 MHz, DMSO-d$_6$) δ 169.7, 133.8, 132.5, 132.3, 131.9, 130.8, 130.4, 128.3, 127.6, 126.8, 125.1; ^{77}Se NMR (57 MHz, DMSO-d$_6$) δ 2346.5; mass spectrum (ESI) 319 (M-OH+H)$^+$, 341 (M-OH+Na)$^+$; Analysis calcd for C$_{14}$H$_{12}$O$_3$N$_2$Se: C, 50.16; H, 3.61. Found: C, 49.98; H, 3.39.

3.2.30 Preparation of spirodiazaselenurane 130
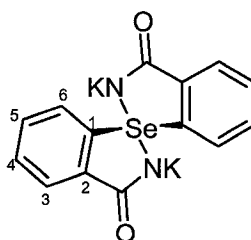
Acylaminoselenonium chloride **128** (7.8 mg, 0.02 mmol) dissolved in 0.5 mL of dry deuterated DMSO in a 5 mm NMR tube, was treated with solid potassium hydride (6.3 mg, 0.16 mmol). This reaction was performed in a glove bag under an argon

atmosphere. The reaction mixture turned yellow immediately and the NMR tube was purged with argon and capped. When kept under argon at room temperature, **130** survived unchanged for ca. 12 h. ^{1}H NMR (300 MHz, DMSO-d_6) δ 8.23 (d, J = 7.6 Hz, 2 H, H-6), 7.73 (d, J = 7.2 Hz, 2 H, H-3), 7.31 (t, J = 7.2 Hz, 2 H, Ar-H), 7.16 (t, J = 7.2 Hz, 2 H, Ar-H); ^{13}C NMR (100 MHz, DMSO-d_6) δ 168.9 (C=O), 147.4, 137.8, 130.4, 129.5, 126.5, 124.3; ^{77}Se NMR (57 MHz, DMSO-d_6) δ 723.09; mass spectrum (ESI) 395 (M+H)$^+$, 317 (M-2K+H$^+$)$^-$.

3.2.31 Preparation of di(3-hydroxypropyl) ditelluride (148)
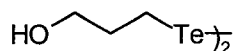
Water (30 mL) was added dropwise to 2.08 g (16.3 mmol) of tellurium powder and 0.62 g (16 mmol) of sodium borohydride under argon. The mixture was heated until the tellurium dissolved to afford a dark red solution. After it was cooled to room temperature, 2.27 g (16.3 mmol) of 3-bromopropan-1-ol (**147**) and 5 mL of water were added. The solution turned orange and was stirred for an additional 3 h. The mixture was extracted with ether, the combined organic phases were dried, concentrated in vacuo and chromatographed (elution with 60% ethyl acetate-hexanes) to give 1.14 g (37%) of **148** as a viscous red oil: IR (neat) 3230 (broad, O-H stretch), 1201 cm^{-1}; ^{1}H NMR (300 MHz) δ 3.71 (t, J = 6.1, 4 H, OCH$_2$), 3.20 (t, J = 7.2 Hz, 4 H, TeCH$_2$), 2.08-1.98 (quintet, J = 6.2 Hz, 4 H, CH$_2$), 1.86 (br s, 2 H, OH); ^{13}C NMR (75 MHz) δ 63.6 (OCH$_2$), 36.1 (CH$_2$), -0.2 (TeCH$_2$); ^{125}Te NMR (95 MHz) δ 120.0; mass spectrum, m/z (relative intensity) 378 (1, M$^+$), 256 (10, M$^+$ - Te), 171 (14), 130 (49), 39 (100). The deposition of tellurium from the product was observed within a few days even when the product was stored in a refrigerator. It was used without further purification.

3.2.32 Preparation of 1,2-oxatellurolane *Te*-oxide (145)

$$\underset{\substack{O \\ \| \\ Te \\ }}{}$$
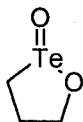
tert-Butyl hydroperoxide (750 µL of 56% solution, 4.5 mmol) was added to ditelluride **148** (241 mg, 0.646 mmol) in 35 mL of dichloromethane. The color of the ditelluride was discharged within 5 min. After an additional 30 min, the solution was concentrated *in vacuo* and the product was precipitated from methanol to afford 151 mg (58%) of **145** as a white solid: m.p. 257-260 °C; IR (KBr) 1033, 979, 664 cm^{-1}; ^{1}H NMR (300 MHz, D$_2$O) δ 4.23 (t, J = 5.3 Hz, 2 H, OCH$_2$), 3.11 (t, J = 6.7 Hz, 2 H, TeCH$_2$), 2.21-2.16 (m, 2 H, CH$_2$); ^{13}C NMR (100 MHz, D$_2$O) δ 70.2 (OCH$_2$), 46.9 (TeCH$_2$), 27.6 (CH$_2$); ^{125}Te NMR (95 MHz, D$_2$O) δ 1042.0; mass spectrum, *m/z* (relative intensity); mass spectrum, *m/z* (relative intensity) 204 (5, M$^+$), 188 (66, M$^+$ - O), 130 (100). Exact mass calcd for C$_3$H$_6$O$_2$^{130}Te: 203.9430. Found: 203.9418. Analysis calcd for C$_3$H$_6$O$_2$Te: C, 17.87; H, 3.00. Found: C, 18.19; H, 2.95.

3.2.33 Preparation of di(3-hydroxypropyl) telluride (150)

$$HO\diagdown\diagup\diagdown Te\diagdown\diagup\diagdown OH$$
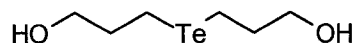
Hydroxymethanesulfinic acid monosodium salt dihydrate (3.0 g, 19 mmol) was added to 0.50 g (3.9 mmol) of tellurium powder and 2.5 g (63 mmol) of sodium hydroxide in 30 mL of water. The dark red mixture was refluxed under argon until it formed a pale pink solution (ca. 30 min). The solution was cooled to room temperature and 0.69 mL (7.6 mmol) of 3-bromopropan-1-ol (**147**) was added. The mixture turned yellow within 5 min and was stirred for an additional 30 min. The product was extracted with ether, dried, concentrated *in vacuo* and chromatographed (elution with ethyl acetate)

to give 0.51 g (55%) of **150** as a yellow oil: IR (neat) 3340 (broad, O-H stretch), 1221 cm^{-1}; ^{1}H NMR (300 MHz) δ 3.72 (t, J = 6.0 Hz, 4 H, OCH$_2$), 2.74 (t, J = 7.4 Hz, 4 H, TeCH$_2$), 2.07-1.98 (m, 4 H, CH$_2$), 1.80 (br s, 2 H, OH); ^{13}C NMR (75 MHz) δ 64.0 (OCH$_2$), 34.7 (CH$_2$), -1.4 (TeCH$_2$); ^{125}Te NMR (95 MHz) δ 228.5; mass spectrum, m/z (relative intensity) 248 (53, M$^+$), 189 (20, M$^+$ - C$_3$H$_7$O), 172 (53), 130 (26), 57 (56), 41 (100). Exact mass calcd for C$_6$H$_{14}$O$_2{}^{130}$Te: 248.0056. Found: 248.0044.

3.2.34 Preparation of spirodioxytellurane 146
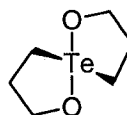
tert-Butyl hydroperoxide (550 μL of 38% solution, 2.2 mmol) was added to 524 mg (2.13 mmol) of telluride **150** in 15 mL of dichloromethane. The yellow mixture turned colourless and clear within 5 min and was stirred at room temperature for an additional 30 min. The solvent was evaporated under vacuum to give a colorless oil, which solidified upon standing to give 489 mg (94%) of **150** as a waxy solid; IR (neat) 1137, 1040, 982 cm^{-1}; ^{1}H NMR (300 MHz) δ 4.25-4.18 (m, 2 H, OCH$_2$), 3.79-3.72 (m, 2 H, OCH$_2$), 2.90-2.73 (m, 4 H, TeCH$_2$), 2.30-2.12 (m, 2 H, CH$_2$), 1.95-1.73 (m, 2 H, CH$_2$); ^{13}C NMR (75 MHz) δ 67.4 (OCH$_2$), 28.5, 27.2; ^{125}Te NMR (126 MHz) δ 1097.0; mass spectrum, m/z (relative intensity) 246 (1, M$^+$), 188 (42, M$^+$ - C$_3$H$_6$O), 130 (39), 43 (56). Exact mass calcd for C$_6$H$_{12}$O$_2{}^{130}$Te: 245.9900. Found: 245.9911. Analysis calcd for C$_6$H$_{12}$O$_2$Te: C, 29.56; H, 4.96. Found: C, 29.42; H, 5.05.

3.2.35 Preparation of peroxybis(tellurane) 151
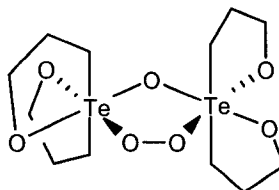
Di(3-hydroxypropyl) telluride **150** (170 mg, 0.693 mmol) was dissolved in 15 mL of dichloromethane and treated with hydrogen peroxide (150 µL of 29% solution, 1.4 mmol). The mixture turned clear within ca. 1 min and was then stirred for an additional 16 h at room temperature. The product was concentrated *in vacuo* to give 185 mg (100%) of a solid, which was recrystallized from ethanol to afford 126 mg (68%) of **151**, mp 211-213°C; IR (KBr) 1221, 1044, 989, 810 cm^{-1}; ^{1}H NMR (300 MHz) δ 4.20-4.08 (m, 2 H), 4.08-3.95 (m, 4 H), 3.84-3.70 (m, 2 H), 2.95-2.70 (m, 4 H), 2.68-2.53 (m, 2 H), 2.45-2.16 (m, 8 H), 2.16-1.95 (m, 2 H); ^{13}C NMR (75 MHz) δ 61.2 (OCH$_2$), 60.8 (OCH$_2$), 37.9 (TeCH$_2$), 35.1 (TeCH$_2$), 24.7 (CH$_2$), 24.5 (CH$_2$); ^{125}Te NMR (126 MHz) δ 1124.9. Analysis calcd for C$_{12}$H$_{24}$O$_7$Te$_2$: C, 26.91; H, 4.52. Found: C, 27.04; H, 4.37. For the X-ray crystal structure of the product, see Figure 2.25 and Appendix E.

3.2.36 General procedure for the oxidation of benzyl thiol with *tert*-butyl hydroperoxide in the presence of 10 mol % of catalyst

A solution containing 10 mol % of a catalyst (0.031 mmol) and naphthalene (10.3 mg, 0.08 mmol) as an internal standard in 10.5 mL of dichloromethane-methanol (95:5) solution was treated with aqueous *tert*-butyl hydroperoxide followed by addition of benzyl thiol (36 µL, 0.31 mmol). The mixture was stirred in a water bath at 18 °C and the progress of the reaction was monitored by HPLC. Aliquots of 2 µL were removed from the reaction and injected directly without quenching. Composition of the solvent mixture was gradually changed from 40:60 to 20:80 water/acetonitrile over the period of the first 15 min of each measurement (for gradients see Appendix A). The % yield of BnSSBn at

a given time was determined by using naphthalene as an internal standard according to the calibration plot shown in Appendix C. The reaction half-life ($t_{1/2}$) was determined by plotting the yield (%) of the product disulfide versus time and represents the time required for conversion of 50% of the thiol into its disulfide. A similar procedure was employed with hydrogen peroxide as the oxidant.

3.2.37 Fractional distillation of *tert*-butyl hydroperoxide[163]

A mixture of *tert*-butyl hydroperoxide, *tert*-butanol and water containing 17% *tert*-butyl hydroperoxide (150 mL) was introduced into a 250 mL round bottom flask fitted with a fractionation column. Pressure in the system was maintained at 91 mm Hg using a vacuum pump and manifold (water aspirator or house vacuum doesn't provide the stable vacuum necessary for this distillation). The distillation was undertaken behind a protective plastic shield. The mixture was slowly stirred and cautiously warmed using an oil bath until it reached 74 °C and the temperature at the still head was 59 °C. These conditions were maintained during the entire distillation to avoid overheating the mixture. Ca. 80 mL of distillate were collected, which separated into two cloudy layers and was left standing overnight until both layers turned clear. The top layer contained 66% *tert*-butyl hydroperoxide in *tert*-butanol.

3.2.38 Iodometric titration of *tert*-butyl hydroperoxide[161]

To a 250 mL round bottom flask fitted with a condenser and nitrogen line, 40 mL of isopropanol, 2 mL of glacial acetic acid and 2.00 mL of a mixture of *tert*-butyl hydroperoxide in isopropanol, with a maximum concentration of 2 mM, were introduced. This mixture was stirred and after being brought to a reflux, 10 mL of saturated sodium iodide in isporopanol solution was added through the condenser. This mixture was refluxed for 15 min and titrated immediately with a 0.1 N solution of sodium thiosulfate until a colourless solution persisted.

3.2.39 Iodometric titration of hydrogen peroxide[164]

A 1.00 mL sample of hydrogen peroxide was diluted to 100 mL with deionized water. Then, 10.0 mL of this solution were transferred to a 100 mL Erlenmeyer flask, together with approximately 30 mL of deionized water, 10 mL of 20% sulfuric acid, 10 mL of 1% w/v potassium iodide solution and 2 drops of the ammonium molybdate catalyst (prepared by dissolving 9 g of ammonium molybdate in 10 mL of 6 N ammonium hydroxide solution, and diluted to 100 mL with deionized water). This solution was then titrated with 0.1 N sodium thiosulfate solution until the colour was discharged. In order to avoid overtitration, a starch indicator was used. It was added only when a slightly pale yellow-coloured solution close to the titration point was present in order to avoid formation of an insoluble complex.

[1] Berzelius, J. J. *Acad. Handl. Stockholm* **1818**, *39*, 13.

[2] Mueller, F. J. *Physikalische Arbeiten der eintraechtigen Freunde in Wien*, **1783**, *1*, 63.

[3] Loewig, J. C. *Pogg. Ann.* **1836**, *37*, 552.

[4] Woehler, F. *Ann. Chem.* **1840**, *35*, 111.

[5] Siemens, C. *Ann. Chem.* **1847**, *61*, 360.

[6] Joy, C. A. *Ann. Chem.* **1853**, *86*, 35.

[7] Woehler, F.; Dean, J. *Ann. Chem.* **1857**, *97*, 1.

[8] Franke, K. W. *J. Nutr.* **1934**, *8*, 597.

[9] Pinsent, J. *Biochem. J.* **1954**, *57*, 10.

[10] Schwarz, K.; Foltz, C. M. *J. Am. Chem. Soc.* **1957**, *79*, 3292.

[11] Burk, R. F. (ed.) *Selenium in biology and human health*; Springer-Verlag: New York, 1993.

[12] Rotruck, J. T.; Pope, A. L.; Ganther, H. E.; Swanson, A. B.; Hafeman, D. G.; Hoekstra, W. G. *Science*, **1973**, *179*, 588.

[13] Klayman, D. L.; Günther, W. H. H. (ed.) *Organic selenium compounds: their chemistry and biology*; Wiley: New York, 1973.

[14] (a) Nicolau, K. C.; Petasis, N. A. *Selenium in natural products synthesis*; CIS: Philadelphia, 1984 (b) Paulmier, C. *Selenium reagents and intermediates in organic synthesis*, Pergamon Press: Oxford, 1986 (c) Patai, S.; Rappoport, Z. (ed.) *The chemistry of organic selenium and tellurium compounds*; Wiley: Chichester, 1986 and 1987; Vols. 1 and 2 (d) Liotta, D. (ed.) *Organoselenium chemistry*, John Wiley & Sons: Toronto, 1987 (e) Krief, A.; Hevesi, L. *Organoselenium chemistry I-Functional group transformations*, Springer-Verlag: New York, 1988 (f) Back, T. G. *Organoselenium chemistry. A practical approach*, Oxford University Press: New York, 1999 (g) Wirth, T. (ed.) *Organoselenium chemistry: modern developments in organic synthesis*; Springer-Verlag: Berlin, 2000.

[15] Petragnani, N. *Tellurium in organic synthesis*, Academic Press: London, 1994.

[16] Lee, H. K. (ed.) *Mitochondrial pathogenesis: from genes and apoptosis to aging and disease*, New York Academy of Sciences: New York, 2004.

[17] Cadenas, E.; Davies, K. J. *Free Radic. Biol. Med.* **2000**, *29*, 222.

[18] Kukin, M. L.; Fuster, V. in *Oxidative Stress and Cardiac Failure*, Futura Publishing Company, Inc.: Armonk, NY, 2003.

[19] Fitzpatrick, F.A. *Int. Imunopharmacol.* **2001**, *1*, 1651.

[20] Sanders, S. P.; Bassett, D. J. P.; Harrison, S. J.; Pearse, D.; Zweier, J. L.; Becker, P. M. *Lung* **2000**, *178*, 105.

[21] Bilenko, M. V. *Ischemia and reperfusion of various organs: injury, mechanisms, methods of prevention and treatment.* Nova Science Pub. Inc.: Huntington, NY, 2001.

[22] Kokaze, A.; Ishikawa, M.; Matsunaga, N.; Yoshida, M.; Sekine, Y.; Sekiguchi, K.; Satoh, M.; Harada, M.; Teruya, K.; Takeda, N.; Uchida, Y.; Takashima, Y. *Mech. Ageing Dev.* **2003**, *124*, 765.

[23] Taylor, E. W. *Journal of Orthomolecular Medicine* **1997**, *12*, 227.

[24] (a) Chance, B.; Sies, H.; Boveris, A. *Physiol. Rev.* **1979**, *59*, 527 (b) Boveris, A.; Chance, B. *Biochem. J.* **1973**, *134*, 707.

[25] Turrens, J. F.; Freeman, B. A.; Crapo, J. D. *Arch. Biochem. Biohys.* **1982**, *217*, 411.

[26] Balridge, C. W., Gerard, R. W. *Am. J. Physiol.* **1933**, *103*, 235.

[27] Vallyathan, V.; Castranova, V.; Shi, X. *Oxygen/nitrogen radicals-lung injury and disease*, Marcel Dekker, Inc.: New York, 2004, p. 1.

[28] Loschen, G.; Azzi, A.; Richter, C.; Flohe, L. *FEBS Lett.* **1974**, *42*, 68.

[29] Turrens, J. F.; McCord, J. M. *Mechanism and consequences of tissue injury.* In Zelenock, G. B.; D'Alecy, L. G.; Fantone, J. C. (ed.) *Clinical Ischemic Syndromes.* C. V. Mosby Co.: Dt. Louis, MO, 1990, p. 203.

[30] Cohen, G. *J. Neural. Transm. Suppl.* **1983**, *19*, 89.

[31] Clerch, L. B.; Massaro, D. J. *Oxygen, gene expression, and cellular function*, Marcel Dekker, Inc.: New York, 1997, p. 29.

[32] Hutchinson, F. *Radiat. Res.* **1957**, *7*, 473.

[33] Scandalios, J. G. *Oxidative stress and the molecular biology of antioxidant defenses*, CSHL Press: New York, 1997.

[34] Mugesh, G.; du Mont, W.-W.; Sies, H. *Chem. Rev.* **2001**, *101*, 2125.

[35] Wiseman, H.; Halliwell, B. *Biochem. J.* **1996**, *313*, 17.

[36] Harman, D. *J. Am. Geriatr. Soc.* **1972**, *20*, 145.

[37] Sies, H. *Oxidative Stress*, Academic Press: London, 1985, p.1.

[38] Sies, H. *Angew. Chem. Int. Ed. Engl.* **1986**, *25*, 1058.

[39] Diplock, A.T. *Antioxidants and free radical scavengers*. In *Free radical damage and its control*; Rice-Evans, C.A.; Burdon, R.H. (eds.); Elsevier: Amsterdam, 1994, p. 113.

[40] Fridovich, I.; Freeman, B. *Annu. Rev. Physiol.* **1986**, *48*, 693.

[41] McCord, J.M.; Fridovich, I. *J. Biol. Chem.* **1969**, *244*, 6049.

[42] Maddipati, K.R.; Marnett, L.J. *J. Biol. Chem.* **1987**, *262*, 17398.

[43] Schonbaum, G.; Chance, B. *Catalase* in Boyer, P. D. (ed.) *The Enzymes*, vol. 13, New York, Academic Press, 1976, p. 363.

[44] Ursini, F. in *Oxidative processes and antioxidants*, Paoletti, R., (ed.); Raven Press: New York, 1994, p. 25.

[45] Ursini, F.; Maiorino, M.; Brigelius-Flohe, R.; Aumann, K. D.; Roveri, A.; Schomburg, D.; Flohe, L., *Methods Enzymol.* **1995**, *252*, 38.

[46] Luo, G.-M.; Ren, X.-J.; Liu, J.-Q.; Mu, Y.; Shen, J.-C. *Curr. Med. Chem.* **2003**, *10*, 1151.

[47] Thomas, J.P.; Maiorino, M.; Ursini, F., and Girotti, A.W. *J. Biol. Chem.* **1990**, *265*, 454.

[48] Ren, B.; Huang W.; Åkesson, B; Ladenstein R. *J. Mol. Biol.* **1997**, *268*, 869.

[49] Flohe, L. in *Glutathione*, John Wiley & Sons: New York, 1989, p. 644.

[50] Epp, O.; Ladenstein, R.; Wendel. A. *Eur. J. Biochem.* **1983**, *133*, 51.

[51] Odom, J. D. *Struct. Bond.* **1983**, *54*, 1.

[52] Flohe, L.; Loschen, G; Guenzler, W.A., and Eichele, E. *Hoppe-Seyler's Z. Physiol. Chem.* **1972**, *353*, 987.

[53] Mugesh, G.; du Mont, W.-W. *Chem. Eur. J.* **2001**, *7*, 1365.

[54] Aumann, K.-D.; Bedorf, N.; Brigelius-Flohe, R.; Schomburg, D.; Flohe, L *Biomed. Environ. Sci.* **1997**, *10*, 136.

[55] Chaudière, J.; Courtin, O.; LeClaire, J. *Arch. Biochem. Biophys.* **1992**, *296*, 328.

[56] Wendel, A.; Fausel, M.; Safayhi, H.; Tiegs, G.; Otter, R. *Biochem. Pharmacol.* **1984**, *33*, 3241.

[57] Sies, H. *Free Radical Biol. Med.* **1993**, *14*, 313.

[58] Ziegler, D.M.; Graf, P.; Poulsen, L. L.; Stahl, W.; Sies, H. *Chem. Res. Toxicol.* **1992**, *5*, 163.

[59] Akerboom, T.P.M.; Sies, H.; Ziegler, D.M. *Arch. Biochem. Biophys.* **1995**, *316*, 220.

[60] Chen, G.-P.; Ziegler, D.M. *Arch. Biochem. Biophys.* **1994**, *312*, 566.

[61] Fischer, H.; Dereu, N. *Bull. Soc. Chim. Belg.* **1987**, *96*, 757.

[62] Engman, L.; Stern, D.; Cotgreave, I. A.; Andersson, C. M. *J. Am. Chem. Soc.* **1992**, *114*, 9737.

[63] Haenen, G. R. M. M.; De Rooji, B. M.; Vermeulen, N. P. E.; Bast, A. *Mol. Pharmacol.* **1990**, *37*, 412.

[64] Lesser, R.; Weiss, R. *Ber. Dtsch. Chem. Ges.* **1924**, *57*, 1077.

[65] Engman, L.; Hallberg A. *J. Org. Chem.* **1989**, *54*, 2964.

[66] Oppenheimer, J.; Silks, L.A. *J. Labeled Compd. Radiopharm.* **1986**, *23*, 59.

[67] Fong, M. C.; Schiesser, C. H. *J. Org. Chem.* **1997**, *62*, 3103.

[68] Parnham, M. J.; Biederman, J.; Bittner, C.; Dereu, N.; Leyck, S.; Wetzig, H. *Agents Actions* **1989**, *27*, 306.

[69] Reich, N. J.; Jasperse, C. P. *J. Am. Chem. Soc.* **1987**, *109*, 5549.

[70] Chaudière, J.; Erdelmeier, I.; Moutet, M.; Yadam, J.-C. *Phosphorus, Sulfur, Silicon Relat. Elem.* **1998**, *136, 137&138*, 467.

[71] Chaudière, J.; Yadan, J.-C.; Erdelmeier, I.; Tailhan-Lomont, C.; Moutet, M. in *Oxidative Processes and Antioxidants*; Paoletti, R. (ed.); Raven Press: New York, 1994; p. 165.

[72] Back, T. G.; Dyck, B. P. *J. Am. Chem. Soc.* **1997**, *119*, 2079.

[73] Guenther, W. H. H. *J. Org. Chem.* **1967**, *32*, 3931.

[74] Singh, R.; Whitesides, G. M. *J. Org. Chem.* **1991**, *56*, 6931.

[75] Wilson, S. R.; Zucker, P. A.; Huang, R.-R.; Spector, A. *J. Am. Chem. Soc.* **1989**, *111*, 5936.

[76] Mugesh, G.; Panda, A.; Singh, H. B.; Punekar, N. S.; Butcher, R. J. *J. Am. Chem. Soc.* **2001**, *123*, 839.

[77] Mugesh, G.; Panda, A.; Singh, H. B.; Punekar, N. S.; Butcher, R. J. *Chem. Commun.* **1998**, 2227.

[78] Wirth, T. *Molecules* **1998**, *3*, 164.

[79] Iwaoka, M.; Tomoda, S. *J. Am. Chem. Soc.* **1994**, *116*, 2557.

[80] Iwaoka, M.; Tomoda, S. *J. Am. Chem. Soc.* **1996**, *118*, 8077.

[81] (a) Burling, F. T.; Goldstein, B. M. J. *J. Am. Chem. Soc.* **1992**, *114*, 2313 (b) Barton, D. H. R.; Hall, M. B.; Lin, Z. Y.; Parekh, S. I.; Reibenspies, J. *J. Am. Chem. Soc.* **1993**, *115*, 5056 (c) Iwaoka, M.; Komatsu, H.; Katsuda, T.; Tomoda, S. *J. Am. Chem. Soc.* **2002**, *124*, 1902 (d) Iwaoka, M.; Katsuda, T.; Komatsu, H.; Tomoda, S. *J. Org. Chem.* **2005**, *70*, 321.

[82] Wirth, T.; Fragale, G. *Chem. Eur. J.* **1997**, *3*, 1894.

[83] Back, T. G.; Moussa, Z. *J. Am. Chem. Soc.* **2003**, *125*, 13455.

[84] Back, T. G.; Moussa, Z. *J. Am. Chem. Soc.* **2002**, *124*, 12104.

[85] Back, T. G.; Moussa, Z.; Parvez M. *Angew. Chem. Int. Ed.* **2004**, *43*, 1268.

[86] Engman, L.; Andersson, C.; Morgenstern, R.; Cotgreave, I. A.; Andersson, C.-M.; Hallberg, A. *Tetrahedron*, **1994**, *50*, 2929.

[87] Cotgreave, I. A.; Moldeus, P.; Brattsand, R.; Hallberg, A.; Andersson, C. M.; Engman, L. *Biochem. Pharmacol.* **1992**, *43*, 793.

[88] Ostrovidov, S; Franck, P.; Joseph, D.; Martarello, L.; Kirsch, G.; Belleville, F.; Nabet, P.; Dousset, B. *J. Med. Chem.* **2000**, *43*, 1762.

[89] Andersson, C.-M.; Hallberg, A.; Brattsand, R.; Cotgreave, I. A.; Engman, L.; Persson, J. *Bioorg. Med. Chem. Lett.* **1993**, *3*, 2553.

[90] Detty, M. R.; Gibson, S. L. *Organometallics* **1992**, *11*, 2147.

[91] Engman, L.; Stern, D, D.; Pelcman, M. *J. Org. Chem.* **1994**, *59*, 1973.

[92] Wieslander, E.; Engman, L.; Svensjö E.; Erlansson, M.; Johansson, U.; Linden, M.; Andersson, C.M.; Brattsand, R. *Biochem. Pharmacol.* **1998**, *55*, 573.

[93] Jacob, C.; Arteel, G. E.; Kanda, T.; Engman, L.; Sies, H. *Chem. Res. Toxicol.* **2000**, *13*, 3.

[94] Kanski, J.; Drake, J.; Aksenova, M.; Engman, L.; Butterfield, D. A. *Brain Res.* **2001**, *911*, 12.

[95] Nogueira, C. W., Zeni, G.; Rocha, J. B. T. *Chem. Rev.* **2004**, *104*, 6255.

[96] Parnham, M. J.; Graf, E. *Prog. Drug. Res.* **1991**, *36*, 9.

[97] Schewe, T. *Gen. Pharmacol.* **1995**, *36*, 1153.

[98] Mautner, H. G.; Chu, S. H.; Jaffe, J. J.; Sartorelli, A. C. *J. Med. Chem.* **1963**, *6*, 36.

[99] El-Bayoumy, K; Upadhyaya, P.; Desai, D. H.; Amin, S.; Hecht, S. S. *Carcinogenesis* **1993**, *14*, 1111.

[100] Ito, H.; Wang, J.-Z.; Shimura, K.; Sakakibara, J.; Ueda, T. *Anticancer Res.* **1990**, *10*, 891.

[101] Cho, S. I.; Koketsu, M.; Ishihara, H.; Matsushita, M.; Nairn, A. C.; Fukuzawa, H.; Uehara, Y. *Biochim. Biophys. Acta* **2000**, 1475, 207.

[102] Kirsi, J. J.; North, J. A.; McKernan, P. A.; Murray, B. K.; Canonico, P. G.; Huggins, J. W.; Srivastava, P. C.; Robins, R. K. *Antimicrob. Agents. Chemother.* **1983**, *24*, 353.

[103] Du, J.; Surzhykov, S.; Lin, J. S.; Newton, M. G.; Cheng, Y.-C.; Schinazi, R. F.; Chu, C. K. *J. Med. Chem.* **1997**, *40*, 2991.

[104] Chu, C. K.; Ma, L. ; Olgen, S.; Pierra, C.; Du, J.; Gumina, G.; Gullen, E.; Cheng, Y.-C.; Schinazi, R. F. *J. Med. Chem.* **2000**, *43*, 3906.

[105] Appel, M. J.; Roverts, G.; Woutersen, R. A. *Carcinogenesis* **1991**, *12*, 2157.

[106] Alpegiani, M.; Bedeschi, A.; Perrone, E.; Franceschi, G. *Tetrahedron Lett.* **1986**, *27*, 3041.

[107] Soda, K. *Phosphorus, Sulfur, Silicon and related elements* **1992**, *67*, 461.

[108] Stilts, C. E.; Nelen, M. I.; Hilmey, D. G.; Davies, S. R.; Gollnick, S. O.; Oseroff, A. R.; Gibson, S. L.; Hilf, R.; Detty, M. R. *J. Med. Chem.* **2000**, *43*, 2403.

[109] Schiesser, C. H.; Zheng, S.-L. *Tetrahedron Lett.* **1999**, *40*, 5095.

[110] Sredni, B.; Caspi, R. R.; Klein, A.; Kalechman, Y.; Danziger, Y.; Ben Ya`akov, M; Tamari, T.; Shalit, F.; Albeck, M. *Nature* **1987**, *330*, 173.

[111] Shani, A.; Tichler, T.; Catane, R.; Gurwith, M.; Rozenszajn, L. A.; Gezin, A.; Levi, E.; Schlesinger, M.; Kalechman, Y. Michlin, H.; Shalit, F.; Engelsman, E.; Farbstein, H, Farbstein, M.; Albeck, M.; Sredni, B. *Nat. Immun. Cell, Growth Regul.* **1990**, *9*, 182.

[112] Kalechman, Y.; Albeck, M.; Sredni, B. *Cell. Immunol.* **1992**, *143*, 143.

[113] Malmstroem, J.; Jonsson, M.; Cotgreave, I. A.; Hammarstroem, L.; Sjoedin, M.; Engman, L. *J. Am. Chem. Soc.* **2001**, *123*, 3434.

[114] Sailer, B. L.; Prow, T.; Dickerson, S.; Watson, J.; Liles, N.; Patel, S. J.; Fleet-Stalder, V. V.; Chasteen, T. G. *Environ. Toxicol. Chem.* **1999**, *18*, 2926.

[115] Detty, M. R.; Merkel, P. B.; Hilf, R.; Gibson, S.; Powers, S. K. *J. Med. Chem.* **1990**, *33*, 1108.

[116] Aitken, P. *Practice* **2001**, *23*, 286.

[117] Tinggi, U. *Toxicol. Lett.* **2003**, *137*, 103.

[118] Painter, E. P. *Chem. Rev.* **1941**, *28*, 179.

[119] Moxon, A. L.; Rhian, M. *Physiol. Rev.* **1943**, *23*, 305.

[120] Seko, Y.; Saito, Y.; Kitahara, J.; Imura, N. in *Selenium in biology and medicine*; Wendel, A.(ed.); Springer-Verlag: Berlin, 1989.

[121] Spallholz, J. E. *Free Radical Biol. Med.* **1994**, *17*, 45.

[122] Mueller, A.; Cadenas, E.; Graf, P.; Sies, H. *Biochem. Pharmacol.* **1984**, *33*, 3235.

[123] Dickson, R. C.; Tappel, A. L. *Arch. Biochem. Biophys.* **1969**, *130*, 547.

[124] Yasuda, K.; Watanabe, H.; Yamazaki, S.; Toda, S. *Biochem. Biophys. Res. Commun.* **1980**, *96*, 243.

[125] Chaudière, J.; Courtin, O.; Leclaire, J. *Arch. Biochem. Biophys.* **1992**, 296, 328.

[126] Maciel, E. N.; Flores, E. M.; Rocha, J. B. T.; Folmer, V. *Bull. Environ. Contam. Toxicol.* **2003**, *70*, 470.

[127] (a) Tsen, C.C., Tappel, A.L. *J. Biol. Chem.* **1958**, *233*, 1230 (b) Widy-Tysziewicz, E.; Piechal, A.; Gajkowska, B.; Smialek, M. *Toxicol. Lett.* **2002**, *131*, 203.

[128] Gupta, N., Porter, T.D. *J. Biochem. Mol. Toxicol.* **2001**, *16*, 18.

[129] Nogueira, C.W.; Rotta, L.N.; Zeni, G.; Rocha, J.B.T. *Neurochem. Res.* **2004**, *29*, 1505.

[130] Chapman, A. G. *Am. Soc. Nutr. Sci.* **2000**, 1043.

[131] Moretto, M.B.; Rossato, J.I.; Nogueira, C.W.; Zeni, G.; Rocha, J.B.T. *J. Biochem. Mol. Toxicol.* **2003**, *17*, 154.

[132] (a) Nogueira, C. W.; Meotti, F. C.; Curte, E.; Pilissao, C.; Zeni, G.; Rocha, J.B.T. *Toxicology* **2003**, *183*, 29 (b) Farina, M; Soares, F.A.; Zeni, G.; Souza, D.O.; Rocha, J.B.T. *Toxicol. Lett.* **2004**, *146*, 227.

[133] Laden, B.P.; Porter, T.D. *J. Lipid. Res.* **2001**, *42*, 235.

[134] Nogueira, C. W.; Rotta, L. N.; Perry, M. L.; Souza, D. O.; Rocha, J. B. T. *Brain Res.* **2001**, 906, 157.

[135] Moretto, M. B.; Rossato, J. I.; Nogueira, C. W.; Zeni, G.; Rocha, J. B. T. *J. Biochem. Mol. Toxicol.* **2003**, *17*, 154.

[136] Meotti, F.C.; Borges, V.C.; Zeni, G.; Rocha, J.B.T.; Nogueira, C.W. *Toxicol. Lett.* **2003**, *143*, 9.

[137] Bell, I. M.; Hilvert, D. *Biochemistry* **1993**, *32*, 13969.

[138] Lesser, R.; Weiss, R. *Ber. Dtsch. Chem. Ges.* **1913**, *46*, 2640.

[139] Esumi, T.; Wada, M.; Mizushima, E.; Sato, N.; Kodama, M.; Asakawa, Y.; Fukuyama, Y. *Tetrahedron Lett.* **2004**, *45*, 6941.

[140] Fukuyama, Y.; Yaso, H.; Nakamura, K.; Kodama, M. *Tetrahedron Lett.* **1999**, *40*, 105.

[141] Brandsma, L.; Verkrijsse, H. (eds.) *Metallated aromatic compounds* in *Preparative polar organometallic chemistry vol.1,* Springer-Verlag, Berlin, 1987.

[142] Huebner, B. *Chem. Ber.* **1875**, *8*, 560.

[143] Bianco, A.; Passacantilli, P.; Righi, G. *Synth. Commun.* **1988**, *18*, 1765.

[144] Berman, E.M.; Showalter, H.D.H. *J. Org. Chem.* **1989**, *54*, 5642.

[145] Zincke, T.; Rhalis, M. *Justus Liebigs Ann. Chem.* **1879**, *198*, 110.

[146] Yamakawa, T.; Masaki, M.; Nohira, H. *Bull. Chem. Soc. Jpn.* **1991**, *64*, 2730.

[147] Narasimhan, S.; Madhavan, S.; Ganeshwar Prasad, K. *J. Org. Chem.* **1995**, *60*, 5314.

[148] Silverstein, R. M.; Webster, F. X. *Spectroscopic identification of organic compounds,* Sixth Edition, John Wiley&Sons: New York, 1997.

[149] Glass, R. S.; Farooqui, F.; Sabahi, M.; Ehlar, K. W. *J. Org. Chem.* **1989**, *54*, 1092.

[150] Dahlén, B.; Lindgren, B. *Acta. Chem. Scand.* **1973**, *27*, 2218.

[151] Foss, O. *Inorg. Synth.* **1953**, *4*, 91.

[152] Torrens, A.; Mas, J.; Port, A.; Castrillo, J. A.; Sanfeliu, O.; Guitart, X.; Dordal, A.; Romero, G.; Fisas, M. A.; Sanchez, E.; Hernandez, E. *J. Med. Chem.* **2005**, *48*, 2080.

[153] Fujihara, H.; Mima, H, Erata, T.; Furukawa, N. *J. Am. Chem. Soc.* **1993**, *115*, 9826.

[154] Adzima, L.J.; Chiang, C.C.; Paul, I. C.; Martin, J. C. *J. Am. Chem. Soc.* **1978**, *100*, 953.

[155] Huheey, J. E. (ed.) Inorganic *Chemistry- principles of structure and reactivity*, Harper&Row: New York, 1975.

[156] Dahlén, B. *Acta Crystallogr. Sect. B* **1974**, *30*, 647.

[157] Duddeck, H. *Progr. NMR Spectrosc.* **1995**, *27*, 1.

[158] Pekonen, P.; Hiltunen, Y.; Laitinen, R. S.; Pakkanen, T. A. *Inorg. Chem.* **1990**, *29*, 2770.

[159] Granger, P.; Chapelle, S.; McWhinnie, W. R.; Al-Rubaie, A. *J. Organomet. Chem.* **1981**, *220*, 149.

[160] Still, W. C.; Kahn, M.; Mitara, A. *J. Org. Chem.* **1978**, *43*, 2923.

[161] Wagner, C.D.; Smith, R. H.; Peters, E. D. *Anal. Chem.* **1947**, *19*, 976.

[162] Lesser, R.; Weiss, R. *Ber. Dtsch. Chem. Ges.* **1914**, *47*, 2515.

[163] Chong, V. M. US Patent 5104493, 1992.

[164] Kolthoff, M. I. *Chem. Weekblad* **1920**, *17*, 197.

Appendix A

The HPLC Gradient Methods

	Time (min)	Flow (mL/min)	%A	%B
Gradient Method #1	Initial	0.90	40	60
	7.00	0.90	20	80
	9.00	0.90	20	80
	15.00	0.90	20	80
Gradient Method #2	Initial	0.90	40	60
	4.00	0.90	20	80
	5.00	0.90	0	100
	11.00	0.90	0	100
	15.00	0.90	0	100
Gradient Method #3	Initial	0.90	50	50
	4.00	0.90	20	80
	5.00	0.90	20	80
	6.00	0.90	20	80

Solvent A = water; **solvent B** = acetonitrile

Gradient Method #1 was used for evaluation of GPx-like activity of all studied compounds except for **3** and **93**

Gradient Method #2 was used for evaluation of GPx-like activity of **3**

Gradient Method #3 was used for evaluation of GPx-like activity of **93**

Appendix B

Rates of formation of BnSSBn from oxidation of BnSH (0.031 M) with *tert*-butyl hydroperoxide or hydrogen peroxide with various concentrations in the presence of various catalysts (0.0031 M) in CH_2Cl_2-MeOH (95:5) at 18 °C

Assay of 1,2-oxaselenolane *Se*-oxide (**46**)
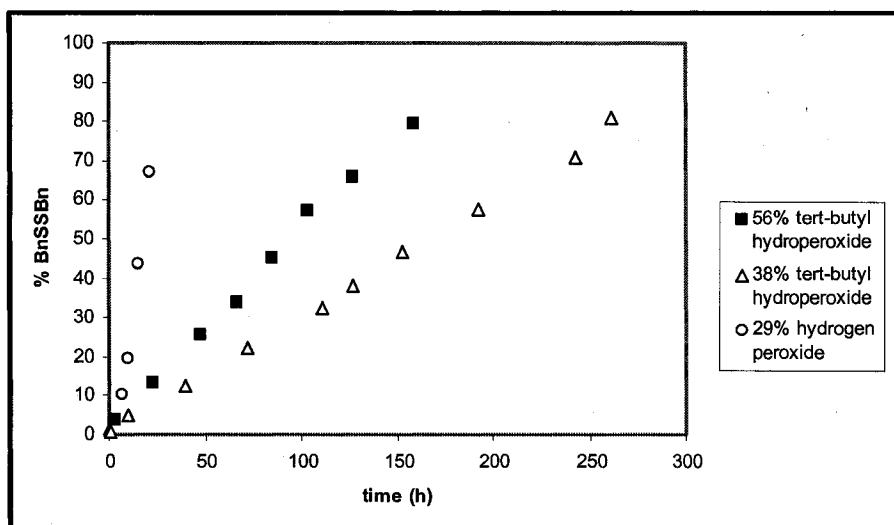
Assay of benzo-1,2-oxaselenolane *Se*-oxide (**89**)
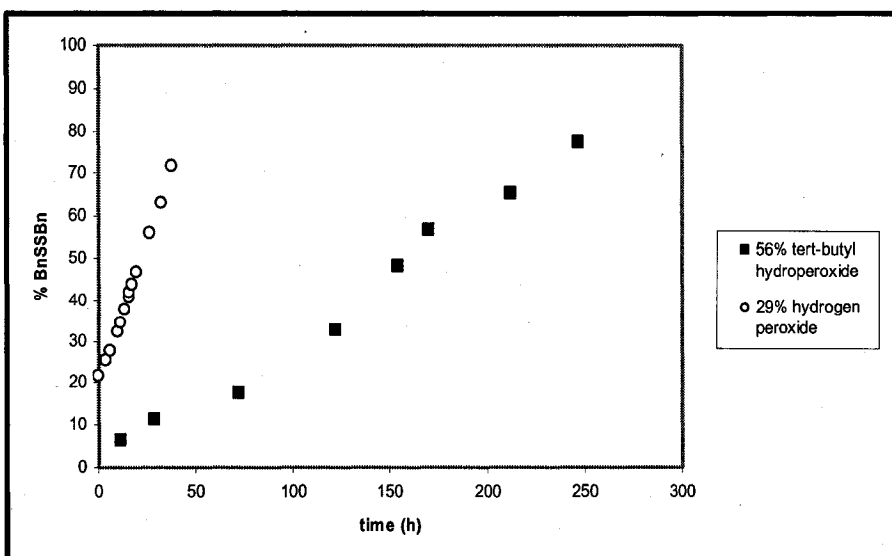
Assay of benzo-3-oxo-1,2-oxaselenolane *Se*-oxide (**90**)
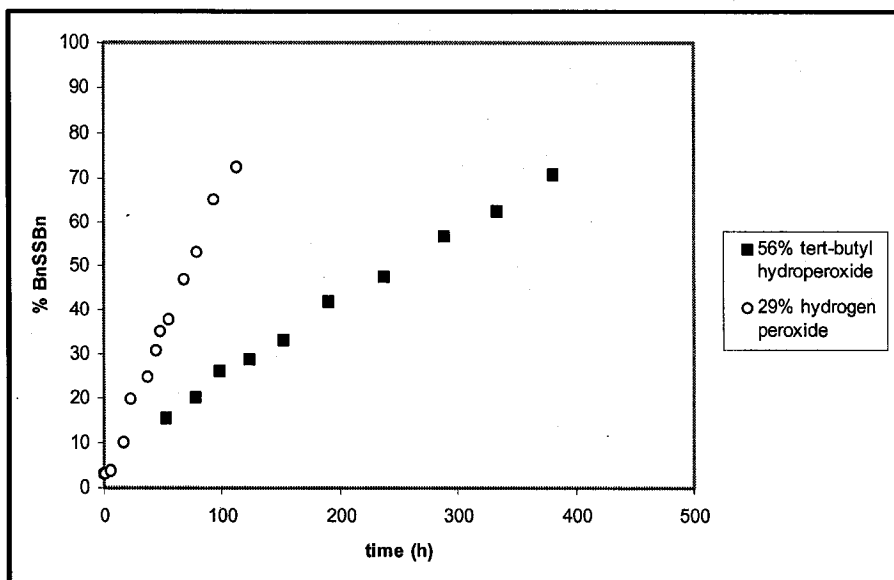
Assay of *p*-methoxybenzo-1,2-oxaselenolane *Se*-oxide (**91**)
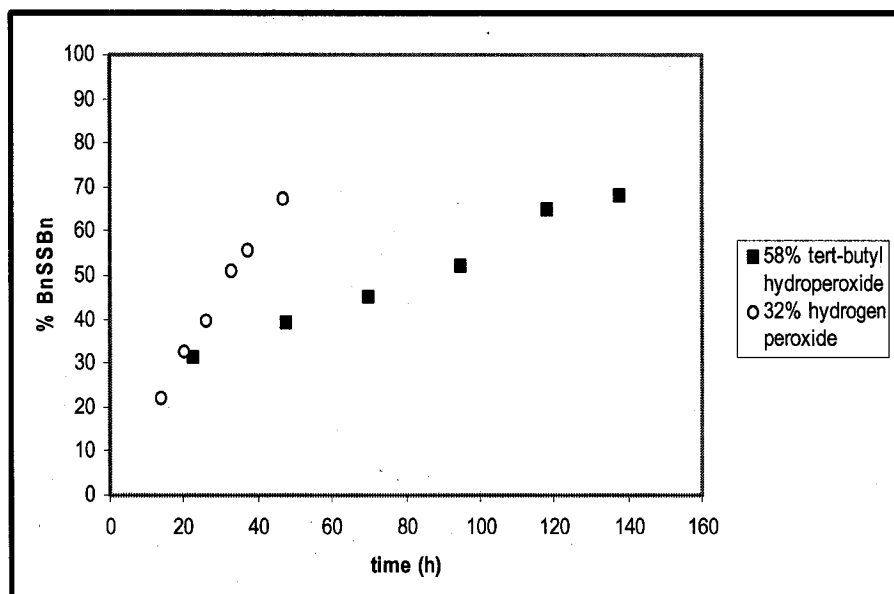
Assay of *p*-fluorobenzo-1,2-oxaselenolane *Se*-oxide (**93**)
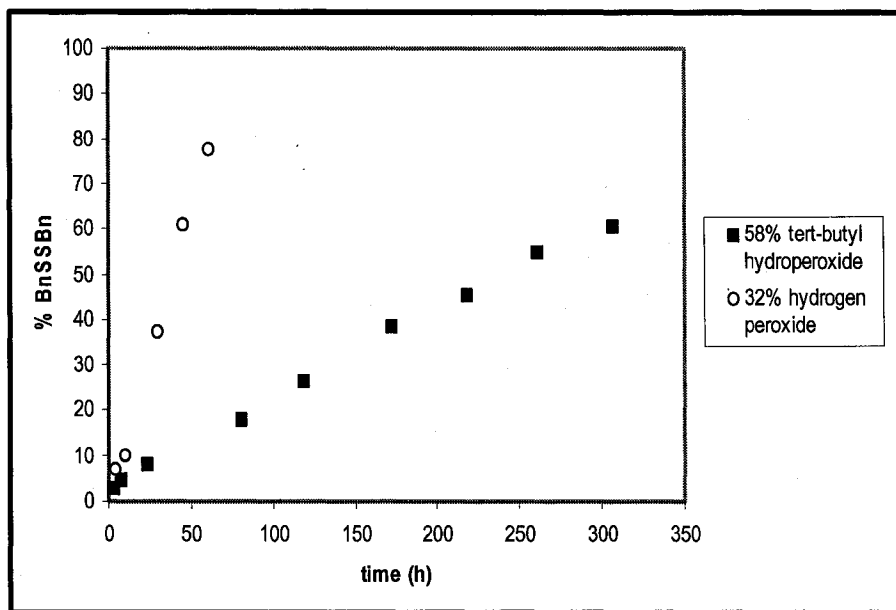
Assay of spirodioxyselenurane **53**
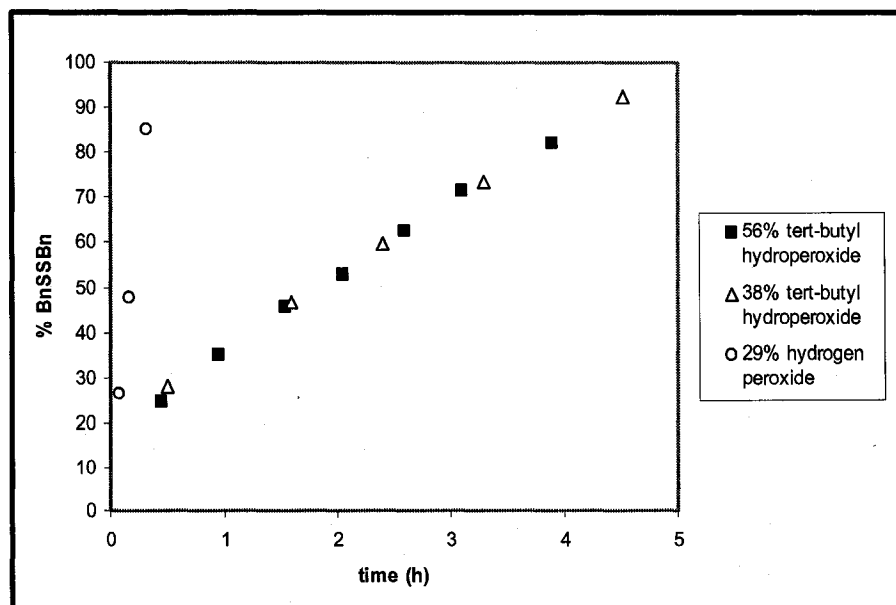
Assay of spirodioxyselenurane **124**
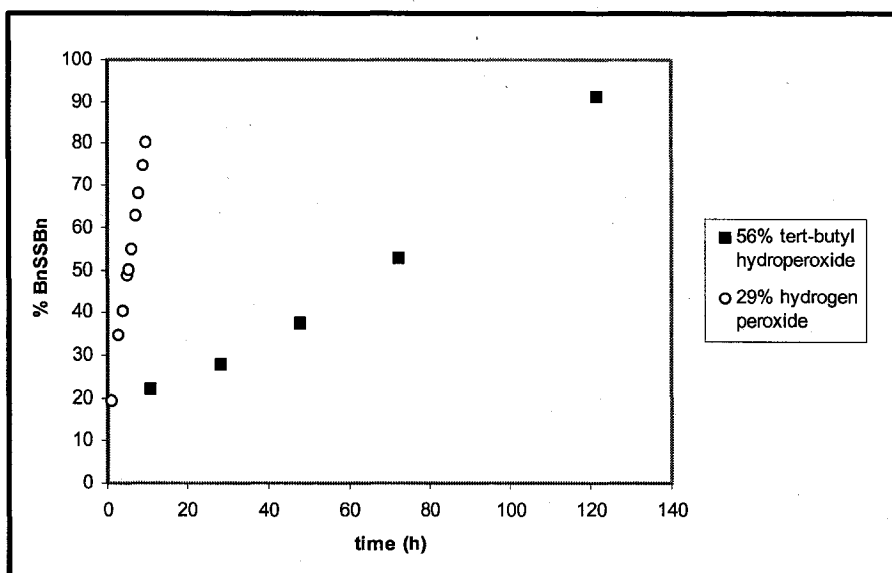
Assay of spirodioxyselenurane **125**
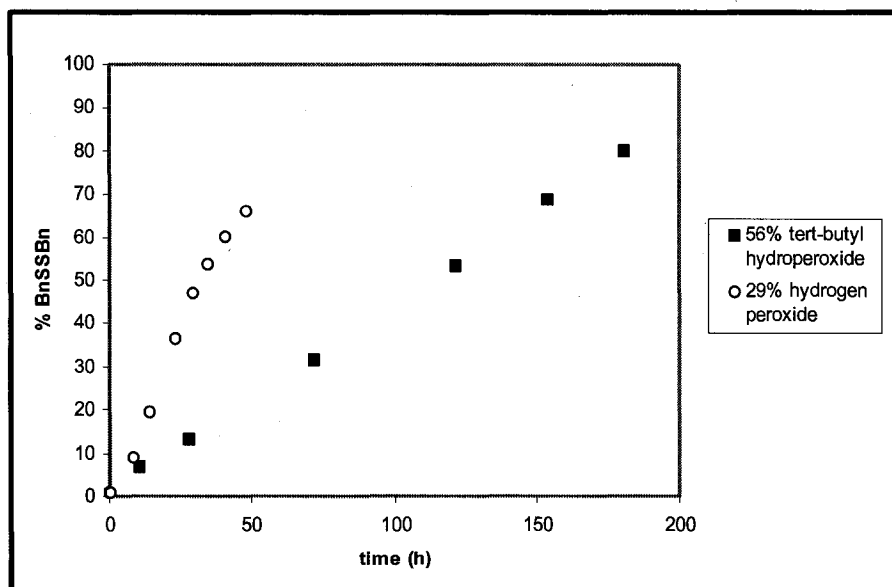
Assay of spirodioxyselenurane **126**
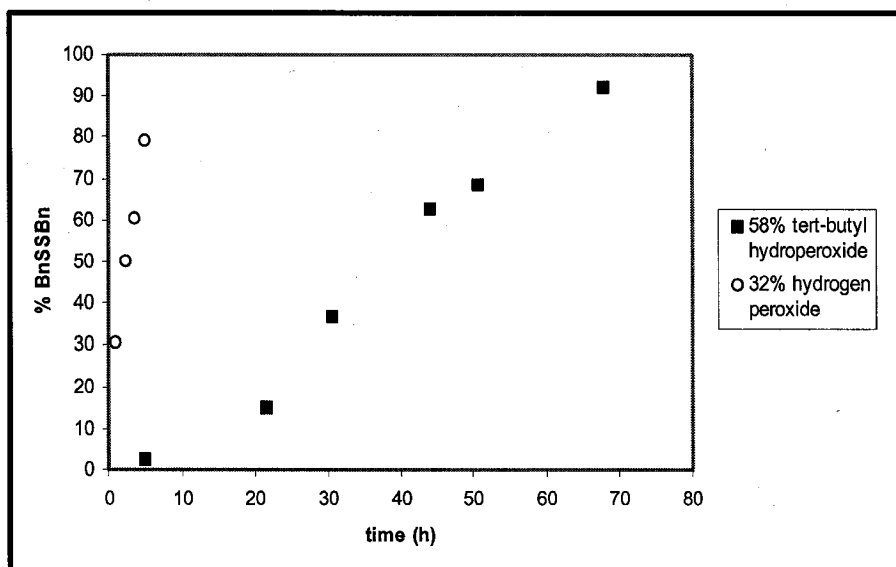
Assay of spirodioxyselenurane **127**
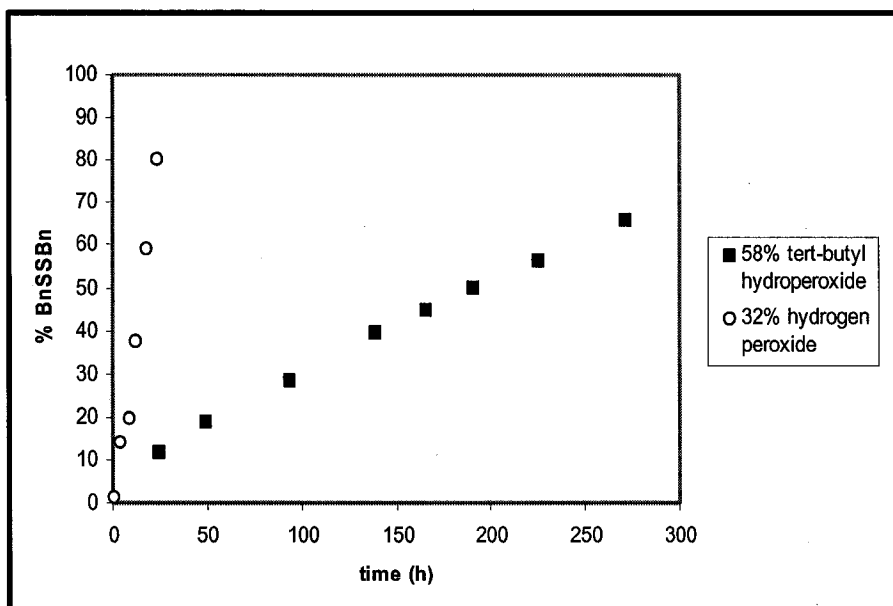
Assay of acylaminoselenonium chloride **128**
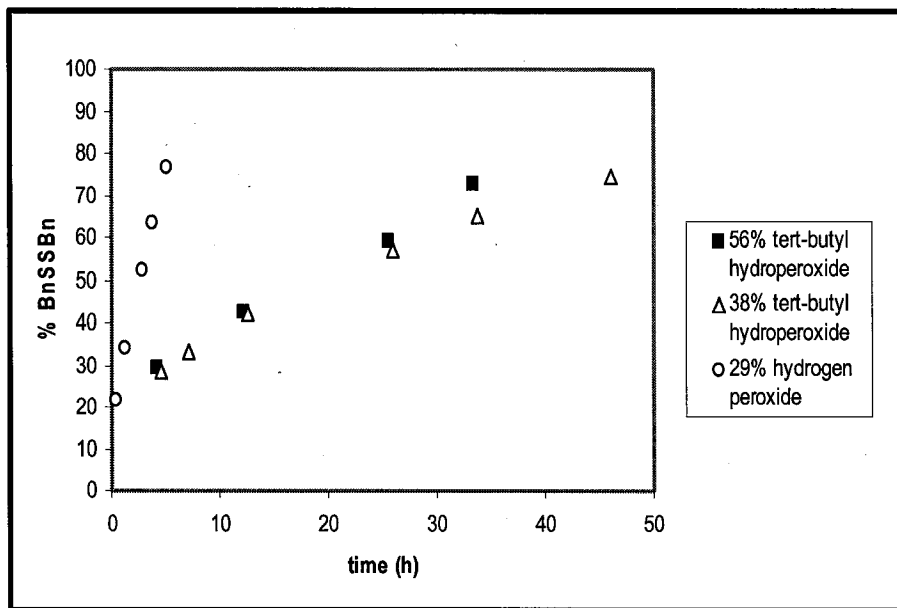
Assay of acylaminoselenonium hydroxide **129**
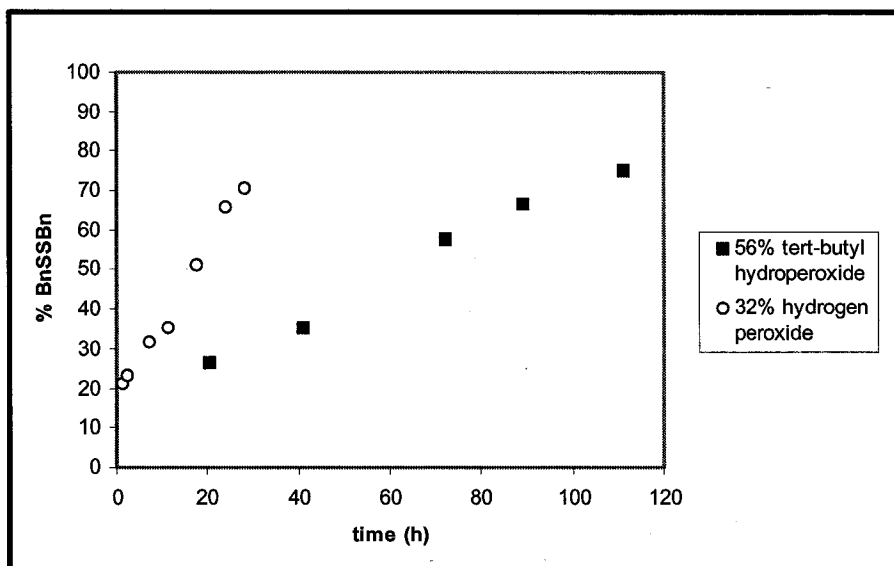
APPENDIX C

Calibration plot for dibenzyl disulfide[a,b]

$y = 0.036x$
$R^2 = 0.9995$
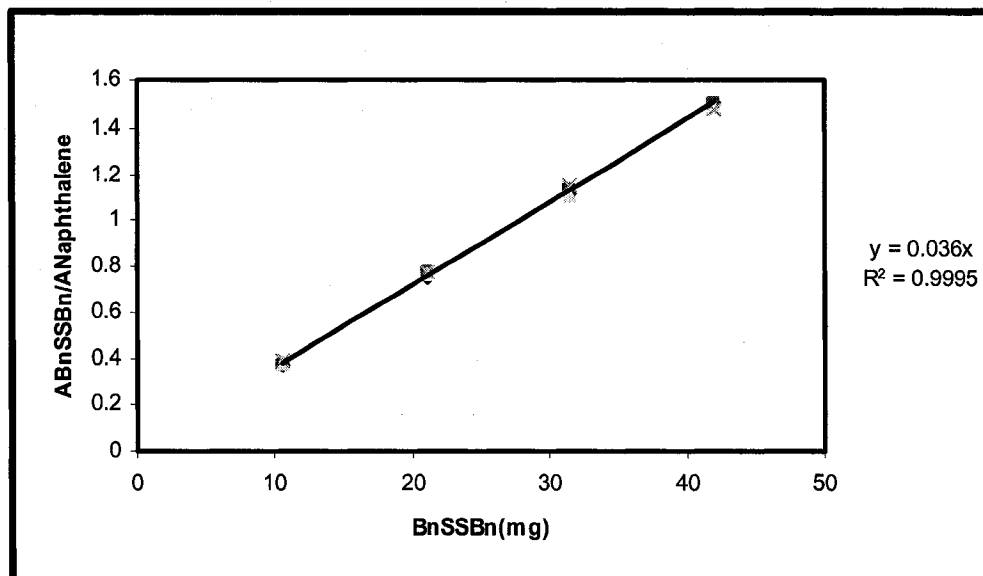
[a]Each data point represents an average of four measurements

[b]$A_{BnSSBn}/A_{naphthalene}$ represents the ratio of integrated areas of dibenzyl disulfide and naphthalene peaks, where 10.3 mg of naphthalene was used as the internal standard

Appendix D

X-ray Crystallographic Data for cyclic acylaminoselenonium chloride 128

ORTEP Diagram of **128**
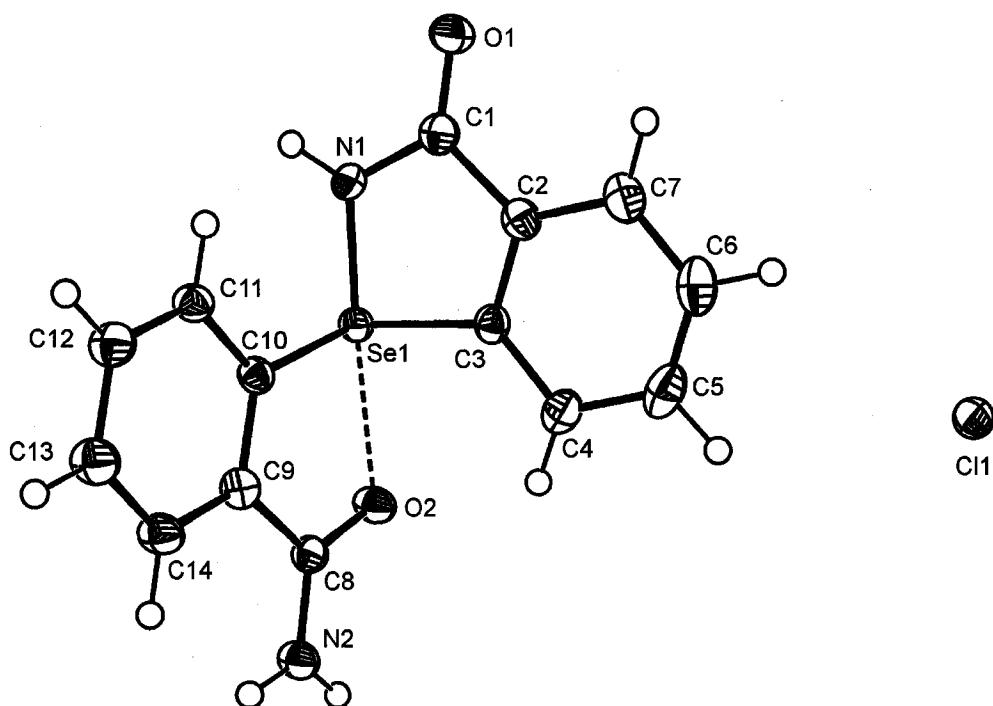
Experimental:

A colorless prismatic crystal of $C_{14}H_{13}ClN_2O_2Se$ was coated with Paratone 8277 oil (Exxon) and mounted on a glass fiber. All measurements were made on a Nonius KappaCCD diffractometer with graphite monochromated Mo-Kα radiation. Cell constants obtained from the refinement[1] of 6428 reflections in the range $3.8 < \theta < 27.4°$ corresponded to a primitive triclinic cell; details of crystal data and structure refinement have been provided in Table 1. The data were collected[2] at a temperature of 173(2) K using the ω and φ scans to a maximum θ value of 27.4°. The data were corrected for Lorentz and polarization effects and for absorption using multi-scan method[1]. Since the crystal did not show any sign of decay during data collection a decay correction was deemed unnecessary.

The structure was solved by the direct methods[3] and expanded using Fourier techniques[4]. The non-hydrogen atoms were refined anisotropically. A disordered water molecule was also located in the structure. Hydrogen atoms were located from a difference map, were included at geometrically idealized positions and were not refined; H-atoms of the disordered water of solvation were ignored. The final cycle of full-matrix least-squares refinement using SHELXL97[5] converged with unweighted and weighted agreement factors, R = 0.036 and wR = 0.084 (all data), respectively, and goodness of fit, S = 1.05. The weighting scheme was based on counting statistics and the final difference map was free of any chemically significant features. The figure was plotted with the aid of ORTEPII[6].

References:

1. Otwinowski, Z. & Minor, W. (1997). "Processing of X-ray Diffraction Data Collected in Oscillation Mode", *Methods in Enzymology,* Volume 276: Macromolecular Crystallograpy, part A, p. 307-326, C.W. Carter, Jr. & R.M. Sweet, Eds., Academic Press.

2. Hooft, R. (1998). *COLLECT*: Users Manual, Nonius B.V., Delft. The Netherlands.

3. Altomare, A., Cascarano, M., Giacovazzo, C.& Guagliardi, A. (1993). Completion and Refinement of Crystal Structures with *SIR92*. J. Appl. Cryst., **26**, 343-350.

4. Beurskens, P.T., Admiraal, G., Beurskens, G., Bosman, W.P., de Gelder, R., Israel, R. & Smits, J.M.M. (1994). The *DIRDIF-94* program system, Technical Report of the Crystallography Laboratory, University of Nijmegen, The Netherlands.

5. Sheldrick, G.M. (1997). *SHELXL97-* A Program for Refinement of Crystal Structures, University of Göttingen, Germany.

6. Johnson, C.K. (1976). *ORTEPII.* Report ORNL-5138. Oak Ridge National Laboratory, Tennessee, USA.

Table 1. Crystal data and structure refinement for $C_{14}H_{13}ClN_2O_2Se$.

Empirical formula	$C_{14}H_{13}ClN_2O_2Se$	
Formula weight	371.67	
Temperature	173(2) K	
Wavelength	0.71073 Å	
Crystal system	Triclinic	
Space group	P -1	
Unit cell dimensions	a = 7.9440(3) Å	α= 81.649(3)°.
	b = 9.7000(4) Å	β= 74.131(3)°.
	c = 11.0010(3) Å	γ = 67.2410(19)°.
Volume	751.16(5) Å^3	
Z	2	
Density (calculated)	1.643 Mg/m^3	
Absorption coefficient	2.688 mm^{-1}	
F(000)	372	
Crystal size	0.06 x 0.05 x 0.04 mm^3	
Theta range for data collection	3.8 to 27.4°.	
Index ranges	-10<=h<=10, -12<=k<=12, -14<=l<=14	
Reflections collected	6428	
Independent reflections	3416 [R(int) = 0.032]	
Completeness to theta = 27.4°	99.3 %	
Absorption correction	Multi-scan method	
Max. and min. transmission	0.900 and 0.855	
Refinement method	Full-matrix least-squares on F^2	
Data / restraints / parameters	3416 / 0 / 194	
Goodness-of-fit on F^2	1.05	
Final R indices [I>2sigma(I)]	R1 = 0.036, wR2 = 0.079	
R indices (all data)	R1 = 0.051, wR2 = 0.084	
Largest diff. peak and hole	0.50 and -0.54 e.Å^{-3}	

Table 2. Atomic coordinates (x 10^4) and equivalent isotropic displacement parameters ($\mathring{A}^2$x 10^3) for $C_{14}H_{13}ClN_2O_2Se$. U(eq) is defined as one third of the trace of the orthogonalized U^{ij} tensor.

Atom	x	y	z	U(eq)
Se(1)	2398(1)	3448(1)	8510(1)	20(1)
Cl(1)	1950(1)	4235(1)	1330(1)	25(1)
O(1)	2295(3)	7491(2)	7352(2)	33(1)
O(2)	2591(3)	1086(2)	8179(2)	26(1)
N(1)	2603(3)	5290(3)	8503(2)	23(1)
N(2)	4578(3)	-1311(3)	8212(2)	27(1)
C(1)	2457(4)	6181(3)	7434(3)	24(1)
C(2)	2520(4)	5331(3)	6394(3)	23(1)
C(3)	2551(4)	3889(3)	6720(2)	22(1)
C(4)	2566(4)	2967(4)	5852(3)	29(1)
C(5)	2540(5)	3570(4)	4627(3)	38(1)
C(6)	2506(5)	5008(4)	4288(3)	36(1)
C(7)	2512(4)	5898(4)	5161(3)	32(1)
C(8)	4167(4)	136(3)	8264(2)	21(1)
C(9)	5591(4)	700(3)	8423(2)	22(1)
C(10)	5015(4)	2243(3)	8511(2)	20(1)
C(11)	6222(4)	2886(3)	8656(3)	23(1)
C(12)	8047(4)	1968(3)	8693(3)	28(1)
C(13)	8650(4)	436(3)	8599(3)	31(1)
C(14)	7419(4)	-202(3)	8466(3)	27(1)
O(3A)	2791(17)	9546(11)	5082(10)	162(4)
O(3B)	730(20)	10190(18)	5084(15)	162(4)

Table 3. Bond lengths [Å] and angles [°] for C₁₄H₁₃ClN₂O₂Se.

Se(1)-N(1)	1.854(2)
Se(1)-C(3)	1.934(3)
Se(1)-C(10)	1.952(3)
Se(1)-O(2)	2.3124(19)
O(1)-C(1)	1.219(3)
O(2)-C(8)	1.253(3)
N(1)-C(1)	1.358(4)
N(1)-H(1)	0.8800
N(2)-C(8)	1.318(4)
N(2)-H(2A)	0.8800
N(2)-H(2B)	0.8800
C(1)-C(2)	1.484(4)
C(2)-C(3)	1.385(4)
C(2)-C(7)	1.389(4)
C(3)-C(4)	1.395(4)
C(4)-C(5)	1.391(4)
C(4)-H(4)	0.9599
C(5)-C(6)	1.382(5)
C(5)-H(5)	0.9600
C(6)-C(7)	1.383(5)
C(6)-H(6)	0.9601
C(7)-H(7)	0.9600
C(8)-C(9)	1.492(4)
C(9)-C(14)	1.385(4)
C(9)-C(10)	1.395(4)
C(10)-C(11)	1.382(4)
C(11)-C(12)	1.385(4)
C(11)-H(11)	0.9600
C(12)-C(13)	1.384(4)
C(12)-H(12)	0.9600
C(13)-C(14)	1.390(4)
C(13)-H(13)	0.9602
C(14)-H(14)	0.9599

O(3B)-O(3B)#1	1.41(3)
N(1)-Se(1)-C(3)	85.02(11)
N(1)-Se(1)-C(10)	96.20(11)
C(3)-Se(1)-C(10)	101.39(11)
N(1)-Se(1)-O(2)	169.26(9)
C(3)-Se(1)-O(2)	87.29(10)
C(10)-Se(1)-O(2)	77.97(9)
C(8)-O(2)-Se(1)	110.23(17)
C(1)-N(1)-Se(1)	117.17(18)
C(1)-N(1)-H(1)	121.4
Se(1)-N(1)-H(1)	121.4
C(8)-N(2)-H(2A)	120.0
C(8)-N(2)-H(2B)	120.0
H(2A)-N(2)-H(2B)	120.0
O(1)-C(1)-N(1)	124.3(3)
O(1)-C(1)-C(2)	125.4(3)
N(1)-C(1)-C(2)	110.3(2)
C(3)-C(2)-C(7)	119.7(3)
C(3)-C(2)-C(1)	115.8(2)
C(7)-C(2)-C(1)	124.4(3)
C(2)-C(3)-C(4)	122.4(3)
C(2)-C(3)-Se(1)	110.61(19)
C(4)-C(3)-Se(1)	126.8(2)
C(5)-C(4)-C(3)	116.6(3)
C(5)-C(4)-H(4)	123.5
C(3)-C(4)-H(4)	119.9
C(6)-C(5)-C(4)	121.7(3)
C(6)-C(5)-H(5)	118.6
C(4)-C(5)-H(5)	119.7
C(5)-C(6)-C(7)	120.8(3)
C(5)-C(6)-H(6)	120.4
C(7)-C(6)-H(6)	118.7
C(6)-C(7)-C(2)	118.8(3)
C(6)-C(7)-H(7)	121.4

C(2)-C(7)-H(7)	119.9
O(2)-C(8)-N(2)	122.1(3)
O(2)-C(8)-C(9)	117.5(2)
N(2)-C(8)-C(9)	120.5(2)
C(14)-C(9)-C(10)	119.2(3)
C(14)-C(9)-C(8)	124.2(3)
C(10)-C(9)-C(8)	116.5(2)
C(11)-C(10)-C(9)	121.4(3)
C(11)-C(10)-Se(1)	121.2(2)
C(9)-C(10)-Se(1)	117.4(2)
C(10)-C(11)-C(12)	118.6(3)
C(10)-C(11)-H(11)	119.9
C(12)-C(11)-H(11)	121.5
C(13)-C(12)-C(11)	120.9(3)
C(13)-C(12)-H(12)	119.2
C(11)-C(12)-H(12)	119.9
C(12)-C(13)-C(14)	120.0(3)
C(12)-C(13)-H(13)	120.2
C(14)-C(13)-H(13)	119.7
C(9)-C(14)-C(13)	119.8(3)
C(9)-C(14)-H(14)	119.5
C(13)-C(14)-H(14)	120.7

Symmetry transformations used to generate equivalent atoms:

#1 -x,-y+2,-z+1

Table 4. Anisotropic displacement parameters ($\text{Å}^2 \times 10^3$) for $C_{14}H_{13}ClN_2O_2Se$. The anisotropic displacement factor exponent takes the form:

$$-2\pi^2[\, h^2 a^{*2} U^{11} + \ldots + 2\, h\, k\, a^*\, b^*\, U^{12} \,]$$

Atom	U^{11}	U^{22}	U^{33}	U^{23}	U^{13}	U^{12}
Se(1)	17(1)	19(1)	23(1)	-1(1)	-7(1)	-6(1)
Cl(1)	24(1)	23(1)	26(1)	-2(1)	-9(1)	-4(1)
O(1)	38(1)	23(1)	46(1)	3(1)	-21(1)	-12(1)
O(2)	20(1)	20(1)	41(1)	0(1)	-12(1)	-7(1)
N(1)	25(1)	21(1)	27(1)	-2(1)	-13(1)	-8(1)
N(2)	21(1)	23(1)	39(1)	-1(1)	-11(1)	-7(1)
C(1)	17(1)	24(2)	33(2)	-1(1)	-10(1)	-7(1)
C(2)	20(1)	24(2)	25(1)	1(1)	-6(1)	-7(1)
C(3)	18(1)	24(2)	21(1)	-2(1)	-6(1)	-5(1)
C(4)	31(2)	32(2)	27(2)	-4(1)	-10(1)	-12(1)
C(5)	41(2)	49(2)	25(2)	-10(1)	-9(1)	-15(2)
C(6)	34(2)	50(2)	22(2)	4(1)	-9(1)	-16(2)
C(7)	32(2)	35(2)	30(2)	6(1)	-11(1)	-14(1)
C(8)	20(1)	21(1)	24(1)	-1(1)	-6(1)	-8(1)
C(9)	20(1)	24(1)	21(1)	-1(1)	-3(1)	-8(1)
C(10)	17(1)	20(1)	21(1)	0(1)	-6(1)	-6(1)
C(11)	22(1)	21(1)	28(1)	0(1)	-6(1)	-9(1)
C(12)	21(1)	30(2)	35(2)	-2(1)	-7(1)	-11(1)
C(13)	20(2)	28(2)	42(2)	-5(1)	-7(1)	-6(1)
C(14)	19(1)	23(2)	38(2)	-4(1)	-7(1)	-5(1)
O(3A)	184(10)	108(6)	170(7)	-20(5)	-43(8)	-22(6)
O(3B)	184(10)	108(6)	170(7)	-20(5)	-43(8)	-22(6)

Table 5. Hydrogen coordinates (x 10^4) and isotropic displacement parameters ($Å^2$x 10^3) for $C_{14}H_{13}ClN_2O_2Se$.

Atom	x	y	z	U(eq)
H(1)	2787	5575	9164	28
H(2A)	3733	-1636	8115	32
H(2B)	5697	-1951	8274	32
H(4)	2596	1971	6114	35
H(5)	2523	2987	4000	45
H(6)	2493	5403	3437	43
H(7)	2504	6894	4930	38
H(11)	5789	3949	8725	28
H(12)	8913	2395	8779	33
H(13)	9911	-192	8642	37
H(14)	7825	-1263	8399	32

Table 6. Torsion angles [°] for $C_{14}H_{13}ClN_2O_2Se$.

N(1)-Se(1)-O(2)-C(8)	63.7(5)
C(3)-Se(1)-O(2)-C(8)	108.02(19)
C(10)-Se(1)-O(2)-C(8)	5.77(18)
C(3)-Se(1)-N(1)-C(1)	10.1(2)
C(10)-Se(1)-N(1)-C(1)	111.1(2)
O(2)-Se(1)-N(1)-C(1)	54.6(5)
Se(1)-N(1)-C(1)-O(1)	169.1(2)
Se(1)-N(1)-C(1)-C(2)	-10.8(3)
O(1)-C(1)-C(2)-C(3)	-174.8(3)
N(1)-C(1)-C(2)-C(3)	5.1(3)
O(1)-C(1)-C(2)-C(7)	3.9(5)
N(1)-C(1)-C(2)-C(7)	-176.1(3)
C(7)-C(2)-C(3)-C(4)	-0.3(4)
C(1)-C(2)-C(3)-C(4)	178.5(3)
C(7)-C(2)-C(3)-Se(1)	-176.5(2)
C(1)-C(2)-C(3)-Se(1)	2.3(3)
N(1)-Se(1)-C(3)-C(2)	-6.4(2)
C(10)-Se(1)-C(3)-C(2)	-101.8(2)
O(2)-Se(1)-C(3)-C(2)	-178.9(2)
N(1)-Se(1)-C(3)-C(4)	177.6(3)
C(10)-Se(1)-C(3)-C(4)	82.3(3)
O(2)-Se(1)-C(3)-C(4)	5.1(3)
C(2)-C(3)-C(4)-C(5)	-0.3(4)
Se(1)-C(3)-C(4)-C(5)	175.2(2)
C(3)-C(4)-C(5)-C(6)	0.2(5)
C(4)-C(5)-C(6)-C(7)	0.5(5)
C(5)-C(6)-C(7)-C(2)	-1.1(5)
C(3)-C(2)-C(7)-C(6)	1.0(4)
C(1)-C(2)-C(7)-C(6)	-177.7(3)
Se(1)-O(2)-C(8)-N(2)	174.6(2)
Se(1)-O(2)-C(8)-C(9)	-5.6(3)
O(2)-C(8)-C(9)-C(14)	-176.6(3)
N(2)-C(8)-C(9)-C(14)	3.2(4)

O(2)-C(8)-C(9)-C(10)	2.3(4)
N(2)-C(8)-C(9)-C(10)	-177.9(2)
C(14)-C(9)-C(10)-C(11)	-0.9(4)
C(8)-C(9)-C(10)-C(11)	-179.8(2)
C(14)-C(9)-C(10)-Se(1)	-177.7(2)
C(8)-C(9)-C(10)-Se(1)	3.4(3)
N(1)-Se(1)-C(10)-C(11)	7.7(2)
C(3)-Se(1)-C(10)-C(11)	93.8(2)
O(2)-Se(1)-C(10)-C(11)	178.6(2)
N(1)-Se(1)-C(10)-C(9)	-175.5(2)
C(3)-Se(1)-C(10)-C(9)	-89.3(2)
O(2)-Se(1)-C(10)-C(9)	-4.62(19)
C(9)-C(10)-C(11)-C(12)	1.1(4)
Se(1)-C(10)-C(11)-C(12)	177.8(2)
C(10)-C(11)-C(12)-C(13)	-0.6(4)
C(11)-C(12)-C(13)-C(14)	-0.1(4)
C(10)-C(9)-C(14)-C(13)	0.2(4)
C(8)-C(9)-C(14)-C(13)	179.0(3)
C(12)-C(13)-C(14)-C(9)	0.3(4)

Table 7. Hydrogen bonds for $C_{14}H_{13}ClN_2O_2Se$ [Å and °].

D-H...A	d(D-H)	d(H...A)	d(D...A)	<(DHA)
N(1)-H(1)...Cl(1)#2	0.88	2.59	3.097(2)	117.5
N(2)-H(2A)...O(1)#3	0.88	2.05	2.902(3)	162.6
N(2)-H(2B)...Cl(1)#4	0.88	2.36	3.194(2)	159.0

Symmetry transformations used to generate equivalent atoms:
#1 -x,-y+2,-z+1   #2 x,y,z+1   #3 x,y-1,z   #4 -x+1,-y,-z+1

Appendix E

X-Ray Crystallographic Data for peroxybis(tellurane) 151

ORTEP Diagram of **151**
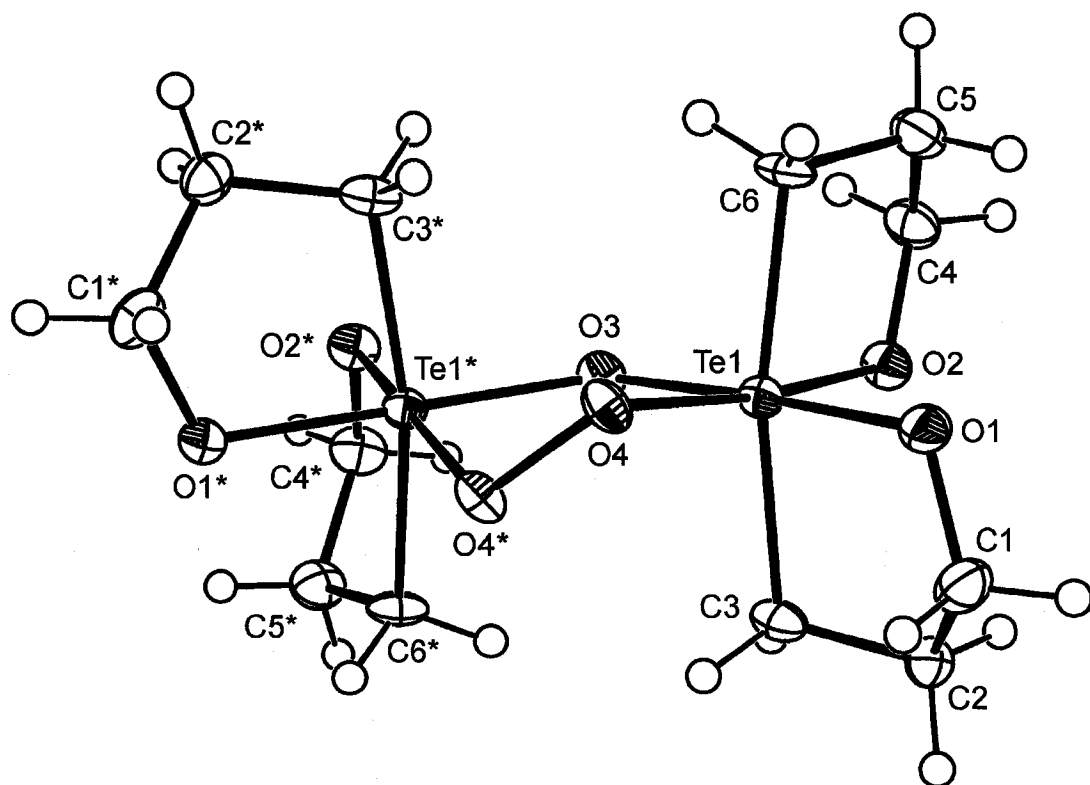
Experimental:

A colorless prismatic crystal of $C_{12}H_{24}O_7Te_2$ was coated with Paratone 8277 oil (Exxon) and mounted on a glass fiber. All measurements were made on a Nonius KappaCCD diffractometer with graphite monochromated Mo-Kα radiation. Cell constants obtained from the refinement[1] of 3421 reflections in the range $3.7 < \theta < 27.5°$ corresponded to a centered monoclinic cell; details of crystal data and structure refinement have been provided in Table 1. The space group was uniquely determined from the systematic absences. The data were collected[2] at a temperature of 173(2) K using the ω and φ scans to a maximum θ value of 27.5°. The data were corrected for Lorentz and polarization effects and for absorption using multi-scan method[1]. Since the crystal did not show any sign of decay during data collection a decay correction was deemed unnecessary.

The structure was solved by the direct methods[3] and expanded using Fourier techniques[4]. The non-hydrogen atoms were refined anisotropically. Hydrogen atoms were located from a difference map, were included at geometrically idealized positions and were not refined. The final cycle of full-matrix least-squares refinement using SHELXL97[5] converged (largest parameter shift was 0.00 times its esd) with unweighted and weighted agreement factors, R = 0.055 and wR = 0.147 (all data), respectively, and goodness of fit, S = 1.16. The weighting scheme was based on counting statistics and the final difference map was essentially free of any chemically significant features with the largest residual electron density within 1.5 Å from the metal atom. The figure was plotted with the aid of ORTEPII[6].

References:

1. Otwinowski, Z. & Minor, W. (1997). "Processing of X-ray Diffraction Data Collected in Oscillation Mode", *Methods in Enzymology,* Volume 276: Macromolecular Crystallograpy, part A, p. 307-326, C.W. Carter, Jr. & R.M. Sweet, Eds., Academic Press.

2. Hooft, R. (1998). *COLLECT*: Users Manual, Nonius B.V., Delft. The Netherlands.

3. Altomare, A., Cascarano, M., Giacovazzo, C.& Guagliardi, A. (1993). Completion and Refinement of Crystal Structures with *SIR92*. J. Appl. Cryst., **26**, 343-350.

4. Beurskens, P.T., Admiraal, G., Beurskens, G., Bosman, W.P., de Gelder, R., Israel, R. & Smits, J.M.M. (1994). The *DIRDIF-94* program system, Technical Report of the Crystallography Laboratory, University of Nijmegen, The Netherlands.

5. Sheldrick, G.M. (1997). *SHELXL97*- A Program for Refinement of Crystal Structures, University of Göttingen, Germany.

6. Johnson, C.K. (1976). *ORTEPII*. Report ORNL-5138. Oak Ridge National Laboratory, Tennessee, USA.

Table 1. Crystal data and structure refinement for $C_{12}H_{24}O_7Te_2$.

Empirical formula	$C_{12}H_{24}O_7Te_2$
Formula weight	535.51
Temperature	173(2) K
Wavelength	0.71073 Å
Crystal system	Monoclinic
Space group	C2/c
Unit cell dimensions	a = 20.345(9) Å $\quad$ $\alpha = 90°$.
	b = 10.237(4) Å $\quad$ $\beta = 107.27(2)°$.
	c = 8.191(3) Å $\quad$ $\gamma = 90°$.
Volume	1629.0(11) Å^3
Z	4
Density (calculated)	2.183 Mg/m^3
Absorption coefficient	3.61 mm^{-1}
F(000)	1024
Crystal size	0.10 x 0.06 x 0.04 mm^3
Theta range for data collection	3.7 to 27.5°.
Index ranges	-26<=h<=26, -13<=k<=12, -10<=l<=10
Reflections collected	3421
Independent reflections	1871 [R(int) = 0.037]
Completeness to theta = 27.5°	99.4 %
Absorption correction	Multi-scan method
Max. and min. transmission	0.869 and 0.714
Refinement method	Full-matrix least-squares on F^2
Data / restraints / parameters	1871 / 0 / 97
Goodness-of-fit on F^2	1.08
Final R indices [I>2sigma(I)]	R1 = 0.032, wR2 = 0.071
R indices (all data)	R1 = 0.043, wR2 = 0.076
Extinction coefficient	0.00135(17)
Largest diff. peak and hole	1.32 and -0.87 e.Å^{-3}

Table 2. Atomic coordinates (x 10^4) and equivalent isotropic displacement parameters (Å^2x 10^3) for $C_{12}H_{24}O_7Te_2$. U(eq) is defined as one third of the trace of the orthogonalized U^{ij} tensor.

Atom	x	y	z	U(eq)
Te(1)	811(1)	2108(1)	3924(1)	16(1)
O(1)	1599(2)	1013(3)	5249(4)	23(1)
O(2)	1298(2)	3798(3)	4531(4)	22(1)
O(3)	0	3052(4)	2500	21(1)
O(4)	209(2)	485(3)	3407(4)	20(1)
C(1)	2010(3)	538(5)	4227(6)	27(1)
C(2)	2001(2)	1510(5)	2802(6)	23(1)
C(3)	1260(3)	1886(5)	1906(6)	22(1)
C(4)	1169(3)	4406(5)	5972(6)	26(1)
C(5)	1066(3)	3360(5)	7240(6)	27(1)
C(6)	558(3)	2346(5)	6242(6)	22(1)

Table 3. Bond lengths [Å] and angles [°] for $C_{12}H_{24}O_7Te_2$.

Te(1)-O(3)	1.968(2)
Te(1)-O(2)	1.983(3)
Te(1)-O(1)	1.993(3)
Te(1)-O(4)	2.032(3)
Te(1)-C(6)	2.123(4)
Te(1)-C(3)	2.125(4)
O(1)-C(1)	1.433(5)
O(2)-C(4)	1.426(5)
O(3)-Te(1)*	1.968(2)
O(4)-O(4)*	1.477(6)
C(1)-C(2)	1.529(7)

C(2)-C(3)	1.516(7)
C(4)-C(5)	1.549(7)
C(5)-C(6)	1.521(7)
O(3)-Te(1)-O(2)	89.34(15)
O(3)-Te(1)-O(1)	175.02(14)
O(2)-Te(1)-O(1)	95.33(13)
O(3)-Te(1)-O(4)	86.06(14)
O(2)-Te(1)-O(4)	172.34(12)
O(1)-Te(1)-O(4)	89.47(13)
O(3)-Te(1)-C(6)	95.20(15)
O(2)-Te(1)-C(6)	84.93(15)
O(1)-Te(1)-C(6)	86.95(17)
O(4)-Te(1)-C(6)	89.38(15)
O(3)-Te(1)-C(3)	94.02(14)
O(2)-Te(1)-C(3)	89.41(16)
O(1)-Te(1)-C(3)	84.33(16)
O(4)-Te(1)-C(3)	97.01(16)
C(6)-Te(1)-C(3)	169.12(19)
C(1)-O(1)-Te(1)	112.8(3)
C(4)-O(2)-Te(1)	112.7(3)
Te(1)*-O(3)-Te(1)	121.2(2)
O(4)*-O(4)-Te(1)	109.95(15)
O(1)-C(1)-C(2)	110.4(4)
C(3)-C(2)-C(1)	108.6(4)
C(2)-C(3)-Te(1)	104.2(3)
O(2)-C(4)-C(5)	110.4(4)
C(6)-C(5)-C(4)	108.5(4)
C(5)-C(6)-Te(1)	104.6(3)

Symmetry transformations used to generate equivalent atoms:

#1 -x,y,-z+1/2

Table 4. Anisotropic displacement parameters ($\text{Å}^2 \times 10^3$) for $C_{12}H_{24}O_7Te_2$.
The anisotropic displacement factor exponent takes the form:

$$-2\pi^2[\, h^2 a^{*2} U^{11} + ... + 2\, h\, k\, a^*\, b^*\, U^{12}\,]$$

Atom	U^{11}	U^{22}	U^{33}	U^{23}	U^{13}	U^{12}
Te(1)	18(1)	15(1)	16(1)	0(1)	6(1)	-1(1)
O(1)	21(2)	28(2)	19(2)	2(1)	7(1)	3(1)
O(2)	25(2)	19(2)	22(2)	-1(1)	7(1)	-2(1)
O(3)	24(2)	18(2)	22(2)	0	5(2)	0
O(4)	24(2)	16(2)	15(2)	1(1)	1(1)	-1(1)
C(1)	22(2)	26(3)	34(3)	-4(2)	11(2)	2(2)
C(2)	19(2)	25(3)	24(2)	-3(2)	7(2)	-3(2)
C(3)	31(3)	22(2)	16(2)	-2(2)	11(2)	-4(2)
C(4)	32(3)	23(3)	23(2)	-6(2)	9(2)	-3(2)
C(5)	31(3)	31(3)	20(2)	-5(2)	8(2)	-4(2)
C(6)	33(3)	23(2)	15(2)	-4(2)	15(2)	-5(2)

Table 5. Hydrogen coordinates (x 10^4) and isotropic displacement parameters (Å^2x 10^3) for $C_{12}H_{24}O_7Te_2$.

Atom	x	y	z	U(eq)
H(1A)	1828	-315	3719	32
H(1B)	2489	407	4955	32
H(2A)	2271	2297	3290	27
H(2B)	2210	1108	1975	27
H(3A)	1024	1193	1103	26
H(3B)	1238	2714	1267	26
H(4A)	751	4957	5585	31
H(4B)	1562	4976	6554	31
H(5A)	1511	2938	7829	33
H(5B)	886	3773	8114	33
H(6A)	78	2657	6014	26
H(6B)	610	1511	6879	26

Table 6. Torsion angles [°] for $C_{12}H_{24}O_7Te_2$.

O(3)-Te(1)-O(1)-C(1)	65.3(11)
O(2)-Te(1)-O(1)-C(1)	-94.5(3)
O(4)-Te(1)-O(1)-C(1)	91.5(3)
C(6)-Te(1)-O(1)-C(1)	-179.1(3)
C(3)-Te(1)-O(1)-C(1)	-5.6(3)
O(3)-Te(1)-O(2)-C(4)	87.1(3)
O(1)-Te(1)-O(2)-C(4)	-94.7(3)
O(4)-Te(1)-O(2)-C(4)	34.0(10)
C(6)-Te(1)-O(2)-C(4)	-8.2(3)
C(3)-Te(1)-O(2)-C(4)	-178.9(3)

O(2)-Te(1)-O(3)-Te(1)*	174.58(9)
O(1)-Te(1)-O(3)-Te(1)*	14.7(10)
O(4)-Te(1)-O(3)-Te(1)*	-11.55(8)
C(6)-Te(1)-O(3)-Te(1)*	-100.57(13)
C(3)-Te(1)-O(3)-Te(1)*	85.22(13)
O(3)-Te(1)-O(4)-O(4)*	41.3(2)
O(2)-Te(1)-O(4)-O(4)*	94.6(9)
O(1)-Te(1)-O(4)-O(4)*	-136.5(3)
C(6)-Te(1)-O(4)-O(4)*	136.6(3)
C(3)-Te(1)-O(4)-O(4)*	-52.2(3)
Te(1)-O(1)-C(1)-C(2)	30.9(5)
O(1)-C(1)-C(2)-C(3)	-49.0(5)
C(1)-C(2)-C(3)-Te(1)	41.1(4)
O(3)-Te(1)-C(3)-C(2)	164.5(3)
O(2)-Te(1)-C(3)-C(2)	75.2(3)
O(1)-Te(1)-C(3)-C(2)	-20.2(3)
O(4)-Te(1)-C(3)-C(2)	-109.0(3)
C(6)-Te(1)-C(3)-C(2)	16.6(11)
Te(1)-O(2)-C(4)-C(5)	32.7(5)
O(2)-C(4)-C(5)-C(6)	-48.4(5)
C(4)-C(5)-C(6)-Te(1)	38.6(5)
O(3)-Te(1)-C(6)-C(5)	-106.7(3)
O(2)-Te(1)-C(6)-C(5)	-17.8(3)
O(1)-Te(1)-C(6)-C(5)	77.8(3)
O(4)-Te(1)-C(6)-C(5)	167.3(3)
C(3)-Te(1)-C(6)-C(5)	41.1(11)

Symmetry transformations used to generate equivalent atoms:

#1 -x,y,-z+1/2

APPENDIX F

Research Publications

Thomas G. Back, **Dušan Kuzma**, and Masood Parvez, "Aromatic Derivatives and Tellurium Analogs of Cyclic Seleninate Esters and Spirodioxyselenuranes that Act as Glutathione Peroxidase Mimetics." *J. Org. Chem.* **2005**, *70*, 9230. I completed all the research for this publication under the guidance of my supervisor, professor Thomas Back, and was responsible for writing the Experimental Section. The body of the manuscript was written by Dr. Back. Dr. Parvez provided the X-ray crystal structure.

Patents

Thomas G. Back, **Dušan Kuzma**, and Noah Berkowitz "Glutathione Peroxidase Mimetics and Uses Thereof." U.S. Provisional Patent Application, US60/723,930, filed on Oct. 06, 2005; conversion to U.S. and PCT patents filed on Oct. 06, 2006.

Presentations and Posters

Kuzma, D.; Back, T. G. "Organoselenium and Tellurium Compounds as Glutathione Peroxidase Mimetics." Oral presentation at the 2nd Banff Organic Symposium in Organic Chemistry in Banff, Alberta, Canada, **2005**. I completed all the research for this presentation under the guidance of my supervisor, professor Thomas Back, and was responsible for preparing the presentation.

Kuzma, D.; Kubicek, A.; Back, T. G. "Organoselenium Compounds as Glutathione Peroxidase Mimetics and Catalysts for Organic Transformations." Poster presented at the Canadian Society for Chemistry Conference in Saskatoon, Saskatchewan, Canada, **2005**. I completed part of the research for this poster under the guidance of my supervisor, professor Thomas Back, and collaborated on the making of the poster.